STATE ESTIMATION OF INTEGRATED POWER AND GAS DISTRIBUTION NETWORKS

A thesis submitted to Cardiff University
in candidature for the degree of
Doctor of Philosophy
by

Seyed Hamid Reza Hosseini

Institute of Energy, Cardiff School of Engineering
Cardiff University

March 2017

ACKNOWLEDGEMENTS

I would like to express my sincere gratitude to my dear supervisors Professor Nick Jenkins and Dr Meysam Qadrdan for their steady support, encouragement and guidance during the research. Thank you very much for considering your valuable time for this work and letting me have your precious comments and suggestions all the time to improve the research and the presentation of it.

I would like to thank Professor Jianzhong Wu for all his support and fruitful discussions on improvement of my work.

My sincere gratitude goes to all the members of the Energy Infrastructure research group and the CIREGS group within Institute of Energy at Cardiff School of Engineering for the engaging discussions on my work and hence helping me improve my research.

A very special thank you goes to my dearest family especially my mother for all their love, steady support and understanding throughout my candidacy. It would not have been possible without your support. Thank you.

DECLARATION

This work has not previously been accepted in substance for any degree and is not concurrently submitted in candidature for any degree.

Signed .... (candidate) Date ....

This thesis is being submitted in partial fulfilment of the requirements for the degree of PhD.

Signed .... (candidate) Date ....

This thesis is the result of my own independent work/investigation, except where otherwise stated. Other sources are acknowledged by explicit references.

Signed .... (candidate) Date ....

I hereby give consent for my thesis, if accepted, to be available for photocopying and for interlibrary loan, and for the title and summary to be made available to outside organisations.

Signed .... (candidate) Date ....

ABSTRACT

Future energy networks are likely to be highly integrated with several energy conversion utilities operating between them, which make the control and management of the whole system more complicated. Therefore, analysis of operation and management of the whole system needs to be performed in an integrated approach. In order to perform an effective control and management of the whole system, an accurate and reliable estimation of the state parameters and the energy flows within the integrated network is essential. In this research simulation and state estimation of integrated power and gas distribution networks with decentralised injection and generation in both networks was investigated. For this purpose, state estimation of individual networks was first reviewed. Afterwards, state estimation of integrated power and gas distribution networks was studied.

Firstly, an algorithm was developed for state estimation of power distribution networks, which was validated through a case study power distribution network. Afterwards, an algorithm for placement of additional measurements within power distribution networks for improvement of state estimation results was developed. The performance of the algorithm showed satisfactory results for placement of a given number of additional individual measurements and a given number of additional measurement units.

Secondly, an algorithm was developed for simulation of operation of gas distribution networks with decentralised injection, which was validated with the results of the commercial software Synergi Gas. Then, an algorithm was developed for the WLS state estimation of gas distribution networks with decentralised injection, which was validated on a case study gas distribution network. Afterwards, an algorithm was developed for placement of additional measurements within gas distribution networks with decentralised injection for improvement of estimation of the gas mixtures within the network, which showed satisfactory results on a case study gas distribution network.

Finally, an algorithm was developed for performing state estimation of power and gas distribution networks with decentralised injection and generation in both networks, which was validated on a case study power and gas distribution network. Afterwards, impact of deployment of smart meters on improvement of estimation of the state parameters of the other coupled network was investigated. It was observed that information from one of the energy networks has no significant impact on improvement of state estimation results of the other coupled network.

Table of Contents

List of Figures

List of Tables

Nomenclature

Abbreviations and Acronyms

abs	Absolute pressure
AGA	American Gas Association
ANN	Artificial Neural Network
$BCSE$	Branch Current State Estimation
BS	British Standard
DER	Distributed Energy Resource
DMS	Distribution Management System
DSE	Distribution State Estimator
$DSSE$	Distribution System State Estimation
GCV	Gross Calorific Value (kJ/m^3)
GHG	Green House Gas
HSE	Health and Safety Executive
IESM	Integrated Energy System Model
NREL	National Renewable Energy Laboratory
$NVSE$	Node Voltage State Estimation
$MAPE$	Mean Absolute Percentage Error
PDF	Probability Distribution Function
PMU	Phasor Measurement Unit
PoC	Point of Connection

$P2G$	Power to Gas unit
RTU	Remote Terminal Unit
sgn	Sign function
SE	State Estimation
STP	Standard Temperature and Pressure conditions
TBC	To Be Calculated
WF	Wind Farm
WLS	Weighted Least Squares

Greeks

α	Top portion of the reduced search space, which contains the problem solution
Δ	Difference between two values
ε	Acceptable tolerance
ϵ	Roughness (m)
θ	Voltage angle
μ	Dynamic viscosity (Pa.s)
π	Pi number (3.1415)
σ	Standard deviation
ν	Velocity of gas flow (m/s)
ρ	Density (kg/m^3)

η	Efficiency of energy conversion in a utility (between zero and one)
ψ	Mean value of a random variable
Z	Compressibility (dimensionless)

Parameters

a	Elements of state error covariance matrix
A	State error covariance matrix
AI	Accuracy Index
b	Susceptance of the series branch between two buses
B	Imaginary part of the complex bus admittance matrix
Br	Branch of a network
c	Summation factors (dimensionless)
C	Components of a gas mixture
CL	Confidence level
CLI	Confidence Level Inverse
d	Load in gas networks (kw)
D	Diameter (m)
DC	Device Cost
DS	Device Status (in service: $DS = 1$, not in service: $DS = 0$)
e	Error of a variable relative to true value
$E(\,)$	Expected value of a random variable

f	Friction factor (dimensionless)
$f(\ )$	Function (in general)
FM	Flow meter
g	Conductance of the series branch between two buses
$g(\ )$	First derivative of WLS objective function
G	Real part of the complex bus admittance matrix
$G(\ )$	Gain matrix of WLS state estimator
GC	Gas Chromatograph
GN	Gas network Node
h	Measurement function
H	Measurement Jacobian
i	Counter parameter
IP	Injection Power (kw)
J	Fitness function
j	Counter parameter
k	Counter parameter
L	Length (m)
$\mathcal{L}$	Log-likelihood function
m	Counter parameter
M	Molar mass (kg/kmol)
MD	Metering Device

MU	Money Unit
N	Number of a parameter
NM	Network Measurements
OB	Operator Budget
OF	Objective Function
p	Pressure (Pa)
P	Real power (the unit is specified upon use)
PB	Power Balance equation for the coupling components
PC	Package Cost
PM	Pressure meter
Pr	Probability
PS	Pressure squared (Pa^2)
PQ	Real and reactive power measurement
q	Volumetric flow (m^3/s)
Q	Reactive power (the unit is specified upon use)
r	Residual
R	Resistance (p.u.)
$\mathcal{R}$	Gas constant (J/kg.K)
Re	Reynolds number
S	Cross section area (m^2)
SA	Set of all possible locations

SD	Set of potential designs
SG	Specific Gravity (dimensionless)
SL	Set of potential locations
SP	State Parameters of the network
T	Temperature (K)
V	Voltage magnitude
W	Diagonal weights matrix
WI	Wobbe Index (kJ/m^3)
x	State vector of a system
X	Reactance (p.u.)
y	Molar fraction of a component (dimensionless)
z	Random variable (in general)
Z	Impedance of the branch (p.u.)

Subscripts

B	Buses of a power network
c	Refers to the state of all the molar fractions (except one) of the network
C	Components of gas flow
CC	Refers to the Coupling Components
cb	Referring to the connected branches to a node in a gas network
d	demand

e	Estimated value
f	Real and reactive power flow of a branch
g	Generation
GN	Refers to the Gas Network
GT	Gas Turbine
IM	Refers to the included meters in the measurement packages
inj	Refers to the injection in the power network
ip	Referring to power injection at a node in a gas network
j	Real and reactive power injection at a bus
$JPDF$	Joint Probability Density Function
K	Number of additional measurements
l	Referring to a load at a node in a gas network
m	measurements
mix	Refers to a gas mixture
MC	Monte Carlo simulation
MP	Measurement package
n	Refers to the STP conditions
N	Refers to the number of nodes of a gas network
p	Refers to the state of pressures (in accuracy index)
PN	Refers to the Power Network
PS	Problem Solution

r	Resistance component
s	Related to shunt branch
sp	Refers to the state parameters of a network
t	True value
V	Voltage magnitude
x	Reactance component

Superscripts

T	Transpose of a matrix
(k)	Value of a parameter at iteration k

SI units

h	Hour
J	Joule
K	Degrees Kelvin
kg	Kilogram
kV	kilo Volt
m	Meter
$mbar$	Millibar
mm	Millimetre

MJ	Mega Joule
MVA	Mega Volt Ampere
MW	Mega watt
N	Newton
Pa	Pascal (N/m^2)
$p.u.$	Per unit
s	Second

1 Introduction

1.1 Background

Future energy networks are likely to be highly integrated with several energy conversion utilities and coupling components operating between them. Individual parts of an integrated energy system are linked together. Hence, malfunctioning of each of them influences the operation and performance of the whole system. This makes the control and management of the whole integrated system more complicated. Therefore, planning, analysis of operation and management of the whole energy system needs to be performed in an integrated approach.

In this research, state estimation of integrated power and gas distribution networks is investigated. For this purpose, a brief overview of integrated analysis of energy systems including the benefits and challenges of integrated analysis and optimisation of operation of integrated energy systems is first presented. Then, the objectives of the research are described. Finally, the structure of the thesis and the sequence of the contents of the thesis are explained.

1.2 Integrated analysis of energy systems

1.2.1 System approach versus individual component approach

Figure 1.1 shows the schematic of two different approaches for planning, energy analysis and optimisation of operation of integrated energy systems.

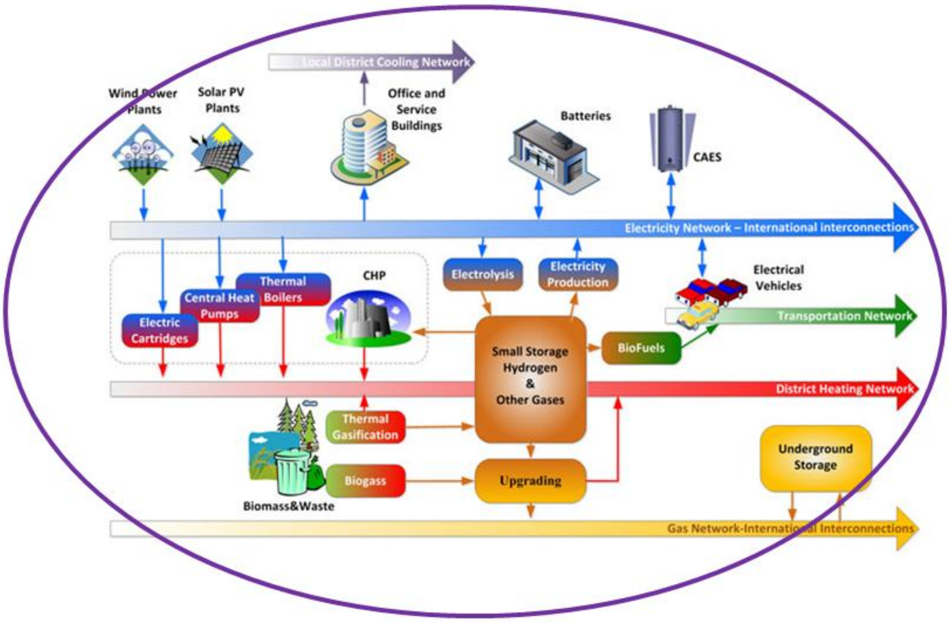

(a) System approach

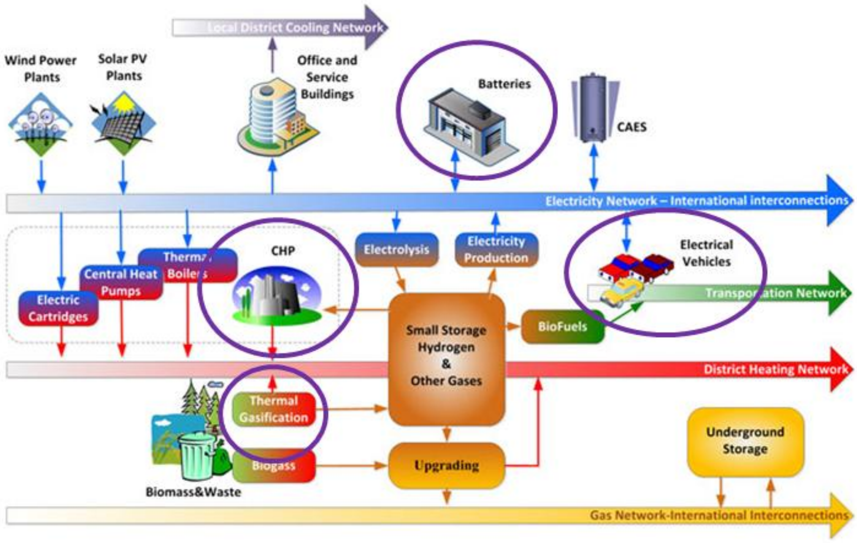

(b) Individual component approach

Figure 1.1: Schematic of possible approaches for studying the integrated energy systems[1]

The differences between these two approaches are summarised as follows:

- In the system approach (Figure 1.1(a)) all the individual components of the system as well as their interactions and inter-dependencies as a "whole" are considered for optimised design, planning and operation of the system. On the other hand, in the individual component approach (Figure 1.1(b)) design, planning and optimisation of operation of each individual component is carried

[1] Figure taken from: http://www.et.aau.dk/research-programmes/intelligent-energy-systems-and-active-networks/

out regardless of the whole system.

- In the system approach the operation of the whole system is optimised in terms of costs (operation and emissions); however, the operation of the components of the system may not be optimised, whereas, in the individual component approach the operation of each individual component may be optimised, but the operation of the whole system may not be optimised.

- In the system approach the operation of all the components does not have conflicts with one another. However, in the individual component approach optimised operation of each component may have conflicts with optimised operation of other components.

1.2.2 Overview

Systems approaches have begun to receive a great attention from different groups including governments, policy makers, academics and industry. UK Infrastructure Transitions Research Consortium (ITRC) has launched a project that carries the analysis and assessment of all the interdependent infrastructures of the UK including energy, transport, water, waste water and telecommunications through a system-of-systems approach (Hall et al. 2016). There are several challenges for developing a road map for the national infrastructure including the complexity, the uncertainties, multiple objective planning and across-various-sectors nature of the infrastructure. The work aims at developing concepts, methodologies, tools and models for decision-makers, academics and practitioners to develop and implement robust, sustainable and resilient strategies for the provision of national scale infrastructure.

National Renewable Energy Laboratory (NREL), which is a national laboratory of the US Department of Energy, has also launched a program to develop a system-of-systems approach for simulation and modeling of integrated energy systems (Mittal et al. 2015). They are “developing an Integrated Energy System Model (IESM) with an initial focus on the electricity system. The IESM can be used to understand and test the impact of new retail market structures and technologies such as Distributed Energy Resources

(DER), demand-response equipment and energy management systems on the ability of the system to provide reliable electricity to all customers” as they argue (Mittal et al. 2015).

A detailed review was fulfilled in academia on the benefits, analysis methods, research gaps and development opportunities of integrated energy systems of the UK (Abeysekera et al. 2016a). They have discussed “several drivers for integration between various energy systems including reduction of use of primary energy, provision of cost effective flexibility in the electrical power system and reduction or delay of capital expenditure”. They have also summarised the approaches taken for analysis of integrated energy systems as well as the advantages and challenges of integrated analysis and development of strategies for energy systems.

1.2.3 Benefits of integrated energy systems analysis and optimisation

There are several benefits associated with integrated analysis and optimisation of operation of energy systems, which are briefly summarised (Fiksel 2007; Eusgeld et al. 2011; Gabbar et al. 2014; Grisso et al. 2014; Hadian and Madani 2015; Mittal et al. 2015; Abeysekera 2016; Abeysekera et al. 2016a; Bai et al. 2016; Hall et al. 2016):

- The energy efficiency of the whole energy system is maximised while the energy waste, costs and emissions are all minimised.

- Demand-supply match and security of supply are guaranteed due to the flexibility for meeting the demand. Hence, the probability of outages is reduced while the reliability of energy supply is increased.

- Extraction of natural resources and hence carbon foot print of the whole system are reduced.

- Impact of poor operation of an individual component on operation of the whole system can be observed and alternative solutions can be evaluated since the inter-dependencies are observed and can be analysed and managed.

- It is possible to assess the impact of new energy technologies on operation of the whole system.

- It is possible to manage and control various prospective consumers.

- The existing assets are optimally and efficiently used.

- It is possible to increase the integration of distributed generation, intermittent renewable energy sources and energy storages in different forms.

- System approach is necessary for planning and operation of a sustainable system.

1.2.4 Challenges of integrated energy systems analysis and optimisation

In contrast to the benefits of integrated analysis and optimisation of operation of energy systems, there are several challenges that harden the implementation of integrated analysis and optimisation of the integrated energy systems. These challenges are summarised as follows (Fiksel 2007; Eusgeld et al. 2011; Gabbar et al. 2014; Grisso et al. 2014; Hadian and Madani 2015; Mittal et al. 2015; Abeysekera 2016; Abeysekera et al. 2016a; Bai et al. 2016; Hall et al. 2016):

- Integrated energy analysis and optimisation involves multi-objective decision making with trade-offs between conflicting targets of energy efficiency, cost and emission.

- The design and operation of the components of the system and matching the operation of them are very complicated.

- The time scale (granularity) of operation of the components of the energy system is different.

- Transient times in dynamic operation of the components of the energy system are different.

- The monitoring, control and management of the whole integrated energy system is difficult.

- No commercial tools have yet been developed for planning, design, operation analysis and management of the whole integrated energy system.

1.3 Research questions

UK Government has dedicated Carbon budgets in order to reduce GreenHouse Gas (GHG) emissions by at least 80% of 1990 levels by 2050 (Committee on Climate Change 2008). This might be achieved by integration of more renewables and consequently more integration of gas and electricity networks at both transmission and distribution levels through several coupling components. Also, UK Government has plans to deploy smart meters in all the country by 2020 (DECC 2012). Since the networks are expected to be more integrated (Figure 1.2) and investment on smart meters even in one of them is highly costly, the following main research question arises:

> "Investment in any distribution network needs great amount of money. If one of the networks, say the power network, is equipped with great deal of real time and hence more accurate measurements and the two networks are coupled at several points, is there any need to invest money on equipping the other coupled network, say the gas network, with real time measurements to obtain a suitable knowledge of the operation of it? In other words, in this case does the information (measurements data) from the equipped network (power network) transfer to the other coupled network (gas network) and help to understand the operation of it (gas network)?"

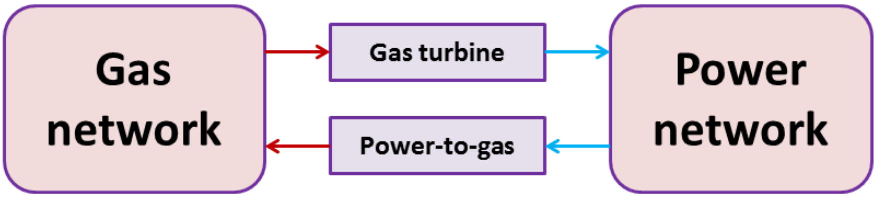

Figure 1.2: Schematic of a coupled gas and electricity distribution network

The above was the main research question and in fact the motivation behind the research in this thesis. In order to address this main research question, the following research questions were addressed first:

- How to estimate the state parameters and hence the operation of power distribution networks based on measurements taken from them?
- Since the measurements are the main inputs to the state estimation algorithm, where is the best location within a power distribution network to place additional measurements to obtain the best knowledge of the operation of the network?
- How to simulate operation of gas distribution networks with decentralised injection?
- How to estimate the state of gas distribution networks with decentralised injection based on the measurements?
- Where is the best location to place additional measurements within gas distribution networks with decentralised injection?
- How to simulate the operation of integrated power and gas distribution networks having several coupling components?
- How to estimate the state and hence the operation of integrated power and gas distribution networks based on all the measurements taken from both?

- If smart meters are deployed in one of the networks does it improve the state estimation of the other coupled network?

1.4 Research objectives

In order to study the systems approach to energy systems, analysis of integrated power and gas distribution networks was considered since integrated energy networks are substantial parts of energy systems. In order to develop and implement an efficient control and management tool for integrated power and gas distribution networks it is essential to have an appropriate knowledge of the operation of the integrated networks in terms of the values of the state parameters and energy flows throughout both networks.

Distribution networks lack sufficient real time measurements since they have great deal of branches and loads due to their root-tree-like structures. Hence, it is impossible for the operator of the integrated networks to equip the entire network with real time measurements of power or gas flow parameters. The operators usually have historical data, usually called pseudo measurements, of the loads at several nodes. Consequently, they need a "State Estimation" (SE) tool that is capable of aggregating all the information from few real time measurements and numerous pseudo measurements to obtain a reliable estimate of the state of the network. Once the state of the integrated network in terms of the values of the operation parameters and all the energy flows within the networks is known the operator is able to monitor, control and manage the networks efficiently and make the right decision at the right time.

The aim of this thesis was to investigate the transfer of information from one energy network for improvement of state estimation of the other coupled energy network through coupling components connected to both networks. In order to achieve this target several necessary steps were designed, which are depicted in Figure 1.3.

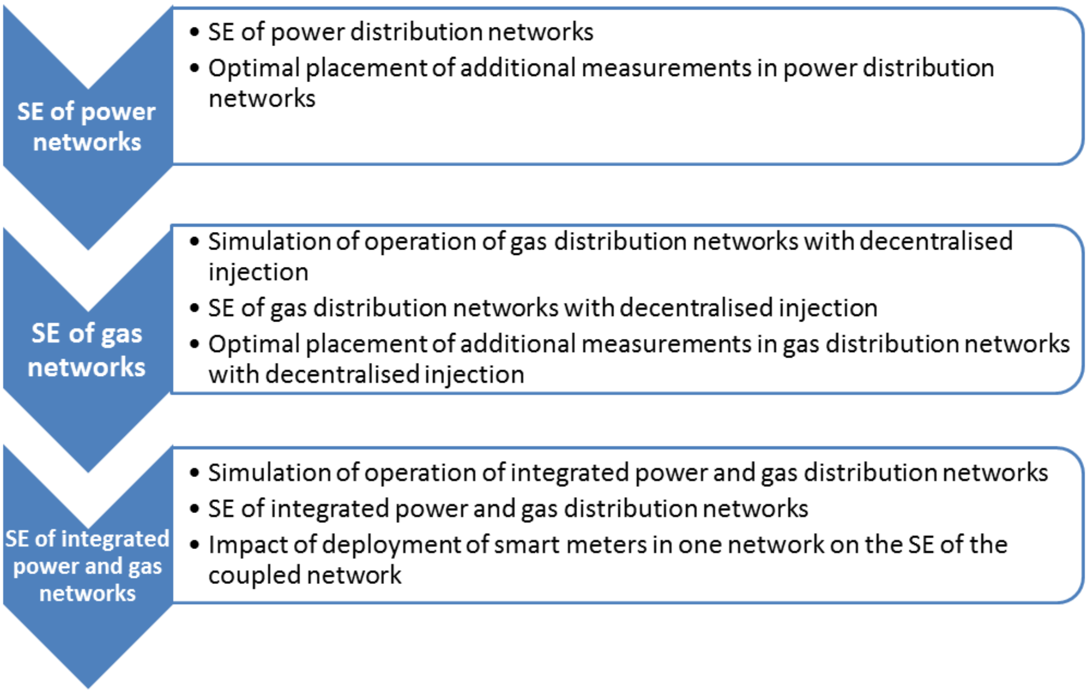

Figure 1.3: The flowchart of the contents of the thesis

According to Figure 1.3 the following research objectives were considered:

- To develop a state estimation algorithm for power distribution networks;
- To develop a method for optimal placement of additional measurements within power distribution networks for improved state estimation;
- To develop a method for simulation of operation of gas distribution networks with decentralised injection;
- To develop a method for state estimation of gas distribution networks with decentralised injection;
- To develop a method for optimal placement of additional measurements within gas distribution networks with decentralised injection for better state estimation results;
- To develop a method for state estimation of integrated power and gas distribution networks.

1.5 Thesis outline

This thesis consists of 8 Chapters in order to address state estimation of integrated power and gas distribution networks. For this purpose, state estimation of individual networks was first studied. Afterwards, state estimation of integrated power and gas distribution networks was investigated.

Chapter 1 presents a background on integrated energy systems analysis. The system approach for planning, energy analysis and optimisation of operation of integrated energy systems along with the benefits and challenges of the system approach is explained.

Chapter 2 contains the weighted least squares (WLS) state estimation of power distribution networks. A background and a literature review on state estimation of power networks are presented. Then, the maximum likelihood state estimation method and the measurement model and assumptions are explained. Afterwards, the formulation and the algorithm of the WLS state estimation of power distribution networks is presented. Finally, the performance of the algorithm on a case study, which is the UKGDS 95-bus test distribution network, is evaluated.

Chapter 3 describes the problem of optimal placement of additional measurements within power distribution networks. The Chapter starts with explanation of the importance of measurements in real time control and management of power distribution networks, which is followed by a literature review on the subject. Then, the formulation of the problem of placement of additional measurements within power distribution networks and the algorithm developed for this purpose are described. Afterwards, a case study, using the UKGDS 95-bus test distribution network, along with the assumptions of the algorithm is presented. Finally, application of the algorithm on the test network for placement of additional individual measurements and placement of additional measurement units is demonstrated.

Chapter 4 explains simulation of operation of gas distribution networks with decentralised injection. Firstly, an overview of the fundamentals of operation of gas networks and the advantages and challenges associated with decentralised injection of alternative gases in the gas networks are presented. Then, after a literature review on the subject formulation of the problem and the algorithm developed for simulation of operation of gas distribution networks with decentralised injection are explained. Afterwards, a case study gas distribution network is demonstrated. Finally, the validation of the simulation model developed based on the algorithm as well as the impact of decentralised injection on operation of the test network is described.

Chapter 5 presents state estimation of gas distribution networks with decentralised injection. The necessity of a tool capable of performing state estimation of gas distribution networks with decentralised injection for an efficient control and management of the network is first described, which is followed by a literature review on the subject. Then, the formulation and the algorithm developed for the problem of state estimation of gas distribution networks with decentralised injection based on the WLS estimation technique is described. Afterwards, a case study gas distribution network along with the assumptions of the algorithm is presented. Finally, the performance of the algorithm is evaluated through application of it on the case study.

Chapter 6 describes the problem of optimal placement of additional measurements within gas distribution networks with decentralised injection for improvement of estimation of the gas mixture within the networks. For this purpose, the necessity of a tool capable of placement of additional measurements within gas distribution networks is first explained. Then, after a literature review on the subject the formulation of the problem and the algorithm developed for placement of additional measurements within gas distribution networks with decentralised injection is presented. Afterwards, a case study gas distribution network along with the assumptions of the algorithm is demonstrated. Furthermore, impact of different types of measurements on the state estimation of gas distribution networks with decentralised injection is investigated. Finally, the results of optimal placement of additional measurements within gas distribution networks with decentralised injection as well as a sensitivity analysis are presented.

Chapter 7 explains state estimation of integrated power and gas distribution networks with decentralised injection and generation in both networks. The Chapter starts with a brief literature review on simulation of operation and state estimation of integrated power and gas distribution networks. Then, the formulations and the algorithms developed for simulation of operation and state estimation of integrated power and gas distribution networks are presented. Afterwards, a case study integrated power and gas distribution network along with the assumptions of the algorithms is demonstrated. Finally, after validation of the simulation model developed based on the algorithm for integrated state estimation of the integrated network impact of deployment of smart meters in one of the networks on improvement of the results of state estimation of the other coupled network is presented.

Chapter 8 summarises the conclusions of the research and the contributions of the thesis. Then, the future work is presented, which suggests further research for continuing the present work.

2 State estimation of power networks using the weighted least squares method

2.1 Introduction

In this Chapter a background on state estimation in power networks is presented, which is followed by a brief literature review on the topic. Then, the maximum likelihood estimation method and the weighted least squares technique are explained. Afterwards, the algorithm of a developed MATLAB simulation model, which performs state estimation of power networks using the WLS, is described. Finally, the performance of the simulation model is evaluated using a case study power distribution network.

2.1.1 Background

2.1.1.1 State estimation and state estimator

- Definition of “State” or “State parameter”

  “State”s or “State parameter”s of a system refer to the minimum parameters of that system that need to be determined in order to uniquely define all the characteristics of the system. For example, in a power network once the values of voltage magnitudes and voltage angles are defined, all the rest of the operation characteristics of the network including power flows and currents of the branches can be calculated. Therefore, in this case the state parameters of a power system are voltage magnitudes and voltage angles.

  As another example, in a gas network with injection of one type of gas, say natural gas, once the values of nodal pressures at all the nodes are defined, the values of gas flows within the branches and the values of gas flows at the nodes can uniquely be calculated. Therefore, the state parameters of this type of gas network are the values of nodal pressures.

  Hence, it can be concluded that in both of these examples the operation of the system is uniquely known once the values of the “state”s or “state parameter”s of the system are known.

- Definition of “State estimation” and “State estimator”

In order to obtain the values of the state parameters of a system, a number of measurements are taken from the system during which sometime redundancy in the measurements occur, which means several values for the same parameter are taken from several redundant sensors at the same location in the system. In this case, the problem is “over-determined”, which means the number of measurements is more than the number of the state parameters of the system.

In this case, where the problem is over-determined, a “state estimation” technique needs to be applied in order to obtain the values of the state parameters of the system based on all the available measurements from the system. For this purpose a model of the system is used in the “state estimator” so that all the parameters of the system are also considered along with the measurements in order to “estimate” the values of the “state parameters” of the system using a state estimation technique. The schematic of a state estimator is depicted in Figure 2.1 for a power system.

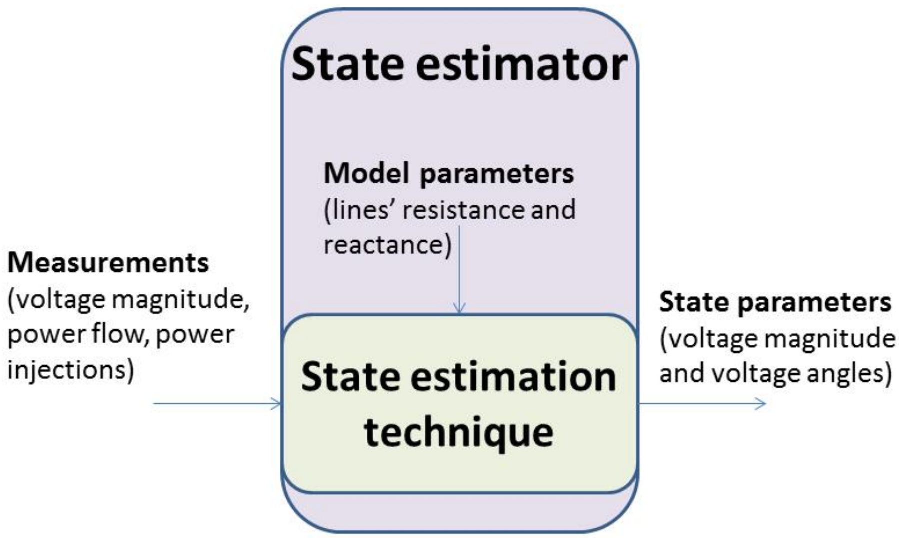

Figure 2.1: The schematic of a “state estimator”

As can be seen the “state estimator” takes the values of the measurements of the system and estimates the values of the state parameters of the system using the model of the system. In this process, the system needs to be over-determined, meaning the number of measurements are more than the number of the state parameters.[1]

2.1.1.2 State estimation of power systems

State estimation refers to the process of calculation of state parameters of a system using a number of measurements. The system needs to be over-determined, which means the number of measurements is greater than the number of state parameters. The control and management centre of an energy network, such as power, gas or district heating, needs to know the operating conditions of the network in real time in order to make the right decision at the right time. Therefore, the state parameters of the network are estimated using a state estimation technique. The technique is applicable to both transmission and distribution levels of power networks, however, control and management at distribution level is more challenging than the transmission level due to lack of real time measurements. Therefore, in a modern distribution management system (DMS), state estimation plays a critical role to estimate the real time system states that are unable to be obtained from the limited measuring instruments at the distribution system level (Lin and Teng 1996; Monticelli 2000; Deng et al. 2002).

With distribution system state estimation (DSSE), the operators can calculate power loss, perform voltage or power optimisation, implement network reconfiguration and prevent distribution lines from overloading. Therefore, the capability of monitoring, controlling and economically dispatching distribution systems, and the power quality and reliability of distribution systems can be improved. DSSE is a fundamental function in DMS (Lu et al. 1995; Deng et al. 2002).

State estimation in power systems has been investigated since the 1970s by developing algorithms to be applied to large scale power networks (Schweppe et al. 1970). Since then several areas have been defined so that development of a robust and effective state estimation algorithm needs to consider these areas thoroughly. The areas include real

[1] The interested readers are referred to (Abur and Exposito 2004) in order to learn some of the aspects of state estimation including network observability analysis, bad data detection and identification and robust state estimation.

time modelling of the network, network topology processor, observability analysis, bad data analysis and dynamic parameter estimation (Monticelli 2000).

State estimation algorithms work and produce results using several types of measurements as follows:

- Real time measurements:
  These measurements are collected via metering devices within the network in real time and their data is transferred to the control centre using telemetering communications often referred to as Remote Terminal Units (RTU). However, the number of these real time measurements is limited and some of them are missed at times due to telemetry communication problems. Therefore, there is a need for other kinds of measurements, so that state estimation module shall be able to run and estimate state parameters of the network. These additional types of measurements are pseudo measurements and virtual measurements.

- Pseudo measurements:
  Pseudo measurements are approximate values of parameters and in the field of analysis of power networks they refer to the approximate values of power consumption at load points, where real time measurements do not exist. Pseudo measurements are obtained based on historical data; hence, they may have large errors, as much as 50% relative to their true value, due to the fact that they are approximate values of loads. Consumption data are usually collected at load nodes; however, they are sent to the control centre with a delay and there they are dealt with as pseudo measurements. Therefore, large errors in this type of measurement are inevitable.

- Virtual measurements:
  A virtual measurement of energy flow at a point of the network refers to the zero value of power consumption at points within the network where there are not any power consumers or generators at those nodes. Therefore, it is assumed that a virtual measurement of load with a zero value reading is placed at these nodes.

2.1.2 Literature review

2.1.2.1 Transmission level SE

Since introduction of SE in 1970 and application of it to transmission power networks, several methods of SE were developed in order to improve it in terms of computation effort and also to make it more suitable for various applications and expectations. Additionally, improvements of the methods were necessitated due to differences in networks in terms of topology, configuration, loading and specifications of measurements. All these methods are classified in two main categories:

- Static state estimation:
  Static state estimation considers time invariance for the state parameters of the network. In other words, the network is analysed in separate snapshots and each time step is assumed to be independent of previous and next time steps. Several methods for static state estimation is proposed in the literature and a brief review is presented in (Shafiu 2005). Some of the most popular ones are as follows:

  - The Weighted Least Squares (WLS) method
    The objective in the WLS is to minimise the weighted sum of squares of differences between values of measurements of the network and calculated values of the measured parameters through a measurement function, which allows calculation of them based on the values of the estimated state parameters. The method is explained further in section 2.4.

  - The equality constrained least squares method
    The performance of the WLS is affected by incorporation of zero injection measurements and requires high values of weights for this kind of measurement. As argued by Shafiu, numerical stability of the WLS method and execution time can be improved by modelling zero injection measurements by an equality constraint and solving the minimisation problem by a Lagrangian function (Shafiu 2005).

- The orthogonal decomposition method

  In this method the measurement Jacobian matrix, $H(x)$ defined later in 2.4.2 is decomposed into an orthogonal matrix and an upper trapezoidal matrix. This allows calculations to be performed while having large values of weights for zero injection measurements (Shafiu 2005).

- The decoupled method

  In this method estimation of voltage magnitude is performed based on the reactive powers measurements and separately from estimation of voltage angles, which is performed based on real powers measurements. In this way the measurement Jacobian matrix is decoupled and two separate iterative formulations are obtained for estimation of voltage magnitudes and voltage angles. This method is based on an assumption of high ratios of reactance to resistance and also neglecting resistances of transmission lines, which leads to the independence of real and reactive powers on voltage magnitudes and voltage angles, respectively. Decoupling the Jacobian matrix enhances the speed of the solution and requires less storage (Wu 1990; Shafiu 2005).

- Dynamic state estimation:

  Dynamic state estimation considers a time dependency for the state parameters of the network and the power flows of branches accordingly. Therefore, calculation of the state parameters in each time step is performed based on the values of the parameters in the previous time step. A brief review on some of the methods for the dynamic state estimation is given in (Shafiu 2005).

2.1.2.2 Distribution level SE

The methods briefly reviewed above are applicable to transmission networks and therefore need to be tailored for DSE due to the fact that distribution networks have features, which distinguish them from transmission networks and necessitate modification of the methods before being applied to DSE. These features include (Baran and Kelley 1995; Haibin and Schulz 2004; Hayes and Prodanovic 2014):

- Radial topology;
- Unbalanced three-phase;
- High resistance to reactance ratio and shorter lines;
- Very limited number of real time measurements and thus being more under-determined in terms of real time measurements;
- High number of loads and impossibility of placing real time measurements for all the loads. Therefore, more number of pseudo measurements of power injections at loads is incorporated in order to make the system overdetermined and observable in terms of state variables and to enable the SE to perform and yield results.

According to Shafiu (Shafiu 2005) "One of the initial steps to tailor transmission state estimation techniques to distribution state estimation was to model the network branch currents in the estimator. Baran and Kelly proposed a three-phase distribution state estimator suitable to handle branch currents and power injection measurements [(Baran and Kelley 1994)]. Baran and Kelly also proposed a distribution estimator model that only used branch currents as system state variables (Baran and Kelley 1995). In [(Lu et al. 1995)] Lu, et al. also converted all the measurements to current magnitudes but used voltage and angles as system state vector rather than branch currents." Shafiu then states that "These [three] techniques are three-phase state estimation methods specially oriented for radial networks." He then discusses that "Ghosh et al. used a probabilistic approach to distribution state estimation in which the radial load flow method was adapted to account for real-time measurements [(Ghosh et al. 1997)]. The method initially used a backward/forward sweep method to calculate the load flow solutions with any available measurements as solution constraints. To calculate the state statistics, probability theory was applied to a linearised set of radial power flow equations in which the states were modelled as random variables. The linearization was made around the expected values of the system states. The expected values were directly taken as the solution given by the radial load flow method. However, the method is much limited to radial systems."[1]

2.1.2.3 Choice of SE method in this research

Dynamic state estimation methods are more suitable for tracking rapidly changing networks. In addition, application of them makes the modeling of the network and estimator more complex. Therefore, dynamic state estimation is considered inappropriate for DSE (Shafiu 2005).

The decoupled form of the WLS, which assumes high reactance to resistance ratio, is widely applied and studied on transmission networks. However, this method is not applicable to DSE due to the high resistance to reactance ratio in distribution networks (Shafiu 2005). In this research, the WLS has been implemented and applied to DSE, because (Schweppe and Wildes 1970; Brown 1981; Wenwu et al. 2013):

- Several types of measurements can be dealt with by the WLS. These measurements include voltage magnitude, real and reactive power flow, real and reactive power injection as well as virtual measurements.

- Optimal solutions with minimum variance are obtained by the WLS.

- The WLS is the first, basic and widely applied and used method for SE of different networks with different configurations. Also, different techniques have been developed in order to enhance the performance of this method.

- The WLS has several other advantages, such as being an easily implementing method, having rather small computational effort and being unbiased for ideal normal distribution measurements.

2.1.2.4 Choices of state parameters

In literature, SE is applied to DSE through two different choices of state parameters:

[1] This paragraph is taken from (Shafiu 2005) page 101.

- Node Voltage State Estimation (NVSE)

  In this approach the voltage magnitude and the voltage angle of buses are considered as the state variables and the SE algorithm aims at finding an estimate for the values of these state parameters. Once the values of these state parameters are found, the currents and power flows of branches and power injections of buses can be calculated based on the values of the state variables. The advantages of this approach are as follows:

  - It is applicable to feeders with different topologies, radial feeders as well as feeders with grid topology (Baran and Kelley 1995);

  - It is more convenient to apply the method for a large number of loads (Wenwu et al. 2013).

  On the other hand, as stated by Baran and Kelley "this method has been extended for three-phase analysis. However, coupling between the phases increases the dimension and decreases the sparsity of the gain matrix [, which is explained in section 2.4,] and hence increases both the memory requirements and computational complexity of the method as compared to SE at transmission level which uses a single-phase model" (Baran and Kelley 1995).

- Branch Current State Estimation (BCSE)

  In this approach the current phasor (real and imaginary parts) of branches is considered as the state variable of the network. Therefore, the solution of the SE would be the real and imaginary parts of current in all the branches of the network. Then, the values of voltage magnitudes and voltage angles and power injections of buses and power flows of branches are calculated using the estimated values of state parameters of the network. Advantages of this approach are:

  - As stated in (Baran et al. 2009b) "measurement functions are simplified for power and current measurements taken from an unbalanced radial distribution feeder."

- BCSE is computationally more efficient and more insensitive to line parameters than the conventional node-voltage-based SE methods (Baran and Kelley 1995; Baran et al. 2009a). It also needs less memory usage (Haibin and Schulz 2004).

However, on the other hand, the disadvantages of this approach include:

- As stated in (Baran et al. 2009b) "without suitable topology error processing for BCSE, the value of the BCSE will be seriously degraded in real world and practical applications".

- Difficulty of incorporation of voltage measurements as current and power measurements are more convenient to be dealt with.

- Dealing with unbalanced nature of distribution feeders is challenging with this method (Baran and Kelley 1995).

- The method is specifically applicable to radial distribution feeders (Baran and Kelley 1995; Houari et al. 2013).

2.1.2.5 Choice of state parameters in this research

In this research NVSE is implemented due to the following reasons:

- It is more convenient to consider voltage magnitudes and voltage angles as state parameters and deal with them;

- There is no need for topology error processing in order to estimate the state of the system using voltage magnitudes and voltage angles at buses;

- Meshed distribution networks can be dealt with.

It should be noted that in this thesis the term "state parameters" of a power network solely refers to the voltage magnitude and the voltage angle of all the buses of the network.

2.2 The maximum likelihood estimation method

The objective of state estimation is to obtain the most likely values of state parameters of the network using the measured values of some of the parameters. In order to accomplish this, the method of maximum likelihood estimation is utilised, which is widely used in statistics. In this method it is assumed that measurements, which are input to the state estimation algorithm, have a known probability distribution with unknown parameters. Then, the joint probability density function for all the measurements can be rewritten in terms of these unknown parameters. Hence, a likelihood function is formed, which attains its peak value at the point where the values of unknown parameters of individual probability distributions are very close to their true values. This leads to an optimisation problem, which maximises the likelihood function as a function of these unknown parameters. The solution of this maximisation problem will yield the maximum likelihood estimates of the state parameters of the network (Abur and Exposito 2004).

In this research it is assumed that the measurement errors have a Gaussian (Normal) distribution. Hence, the parameters for such a distribution are the mean and standard deviation. Consequently, the problem of maximum likelihood estimation is then solved for finding the values of these parameters.

The Normal probability density function for a random variable z_i having mean value ψ_i and standard deviation σ_i is defined as:

$$f(z_i) = \frac{1}{\sqrt{2\pi}\sigma_i}\exp\left(-\frac{1}{2}\left\{\frac{z_i - \psi_i}{\sigma_i}\right\}^2\right) \tag{2-1}$$

The joint probability density function, which represents the probability of measuring N_m measurements, assuming all the independent individual measurements have Gaussian distribution, will be:

$$f_{JPDF}(z) = f(z_1) \times f(z_2) \times \dots \times f(z_{N_m}) \tag{2-2}$$

where $z^T = [z_1, z_2, \dots, z_{N_m}]$ is the vector of all the N_m measurements. The function $f_{JPDF}(z)$ is the likelihood function, which is a measure of the probability of observing a set of measurements in the vector z.

The objective of maximum likelihood estimation is to maximise this joint probability density function by finding the most likely values for the mean values of measurements, i.e. the vector $\psi^T = [\psi_1, \psi_2, \dots, \psi_{N_m}]$, and standard deviations of measurements, i.e. $\sigma^T = [\sigma_1, \sigma_2, \dots, \sigma_{N_m}]$.

This problem can be simplified by considering the logarithm of the maximum likelihood function. The modified function, which is called the log-likelihood function $\mathcal{L}$, is calculated using:

$$\begin{aligned} \mathcal{L} = \log f_{JPDF}(z) &= \sum_{i=1}^{N_m} \log f(z_i) \\ &= -\frac{1}{2}\sum_{i=1}^{N_m} \left(\frac{z_i - \psi_i}{\sigma_i}\right)^2 - \frac{N_m}{2}\log 2\pi - \sum_{i=1}^{N_m} \log \sigma_i \end{aligned} \tag{2-3}$$

The maximum likelihood estimate will maximise the likelihood, or the log-likelihood, function based on a set of input measurements $z^T = [z_1, z_2, \dots, z_{N_m}]$. Therefore, the problem can be solved either by maximising log-likelihood function, $\mathcal{L}$, or equivalently by minimising the first term in (2-3), i.e.:

$$\text{minimise } \sum_{i=1}^{N_m} \left(\frac{z_i - \psi_i}{\sigma_i}\right)^2 \tag{2-4}$$

This minimisation problem is usually rewritten in terms of residual r_i of measurement i, using:

$$r_i = z_i - \psi_i = z_i - E(z_i) \tag{2-5}$$

Where $E(z_i)$ is the expected (true) value of measurement i and can be expressed through $h_i(x)$, a nonlinear function, called the measurement function, relating the calculated value of the measured parameter i to the state vector of the system, x. Additionally, the values of the weights can be defined as:

$$W_{ii} = \sigma_i^{-2} \tag{2-6}$$

where the values of standard deviation of measurements are assumed to be known. Therefore, the minimisation problem of (2-4) will be equivalent to the weighted sum of squared of residuals of measurements. In other words, the optimisation problem is to minimise the following objective function for the state vector x:

$$\text{minimise} \quad \sum_{i=1}^{N_m} W_{ii} r_i^2 \tag{2-7}$$

$$\text{subject to} \quad z_i = h_i(x) + r_i, \qquad i = 1, 2, \dots, N_m \tag{2-8}$$

The solution of the above optimisation problem is called the weighted least squares estimation of the state vector x. In other words, the problem of the maximum likelihood estimation is rewritten in a form that can be solved through weighted least squares estimation technique (Abur and Exposito 2004).

2.3 Measurement model and assumptions

Measurements are rewritten in terms of their expected values and errors, as follows:

$$z = \begin{bmatrix} z_1 \\ z_2 \\ \vdots \\ z_{N_m} \end{bmatrix}_{N_m \times 1} = \begin{bmatrix} h_1(x_1, x_2, \dots, x_{N_{sp}}) \\ h_2(x_1, x_2, \dots, x_{N_{sp}}) \\ \vdots \\ h_{N_m}(x_1, x_2, \dots, x_{N_{sp}}) \end{bmatrix}_{N_m \times 1} + \begin{bmatrix} e_1 \\ e_2 \\ \vdots \\ e_{N_m} \end{bmatrix}_{N_m \times 1} = h(x) + e \tag{2-9}$$

where $h(x)$ is the nonlinear measurement function, relating values of measurements ($z^T = [z_1, z_2, \dots, z_{N_m}]$, where N_m denotes the number of measurements) to the state vector of the system, x ($x^T = [x_1, x_2, \dots, x_{N_{sp}}]$, where N_{sp} denotes the number of state parameters). In order to simplify the solution process, the following are usually assumed for statistical properties of measurement errors:

- Unbiased errors, i.e. zero expected values:

$$E(e_i) = 0 \text{ for } i = 1, 2, \dots, N_m \tag{2-10}$$

- Zero crosscorrelation errors:

$$E[e_i e_j] = 0 \text{ for } i \neq j \tag{2-11}$$

Hence:

$$Cov(e) = E[e.e^T] = W = diag\{\sigma_1^2, \sigma_2^2, \dots, \sigma_{N_m}^2\} \tag{2-12}$$

The standard deviation of each individual measurement is calculated based on the confidence level and accuracy of measurement, using (Singh et al. 2009b):

$$\sigma = \psi \times \frac{accuracy\ (\%)}{CLI \ \times 100.0} \tag{2-13}$$

where the accuracy of measurement is input in percentage. The relation between the multiplier CLI and confidence level of measurement is presented in Table 2.1. The confidence level is also another input to the algorithm.

Table 2.1: Relation between confidence level and CLI in a Normal distribution

Confidence level	Value of CLI
68.2%	1.0
95.4%	2.0
99.7%	3.0

2.4 Weighted least squares state estimation

The WLS will minimise the following objective function:

$$OF(x) = \sum_{i=1}^{N_m} \left(z_i - h_i(x)\right)^2 \Big/ W_{ii} = [z - h(x)]^T . W^{-1} . [z - h(x)] \qquad (2\text{-}14)$$

At the optimum point, the first-order optimality conditions will be satisfied. This means:

$$g(x) = \frac{\partial OF(x)}{\partial x} = -H^T(x) . W^{-1} . [z - h(x)] = 0 \qquad (2\text{-}15)$$

where $H(x)$ is the matrix of measurement Jacobian:

$$H(x) = \left[\frac{\partial h(x)}{\partial x}\right]_{N_m \times N_{sp}} \qquad (2\text{-}16)$$

where N_m and N_{sp} denote the number of measurements and the number of state parameters, respectively. Expanding the function $g(x)$ into its Taylor series around the state vector $x^{(k)}$ yields:

$$g(x) = g\left(x^{(k)}\right) + G\left(x^{(k)}\right) . \left(x - x^{(k)}\right) + \cdots = 0 \qquad (2\text{-}17)$$

By neglecting higher order terms an iterative solution, which is based on Gauss-Newton method, is obtained to find the values of the state parameters:

$$x^{(k+1)} = x^{(k)} - \left[G\left(x^{(k)}\right)\right]^{-1} . g\left(x^{(k)}\right) \qquad (2\text{-}18)$$

where:

$$\left[g\left(x^{(k)}\right)\right]_{N_{sp} \times 1} = -\left[H^T\left(x^{(k)}\right)\right]_{N_{sp} \times N_m} . [W^{-1}]_{N_m \times N_m} . \left[z - h\left(x^{(k)}\right)\right]_{N_m \times 1} \qquad (2\text{-}19)$$

with the size of $g\left(x^{(k)}\right)$ being $N_{sp} \times 1$, and the gain matrix at iteration k, i.e. $G\left(x^{(k)}\right)$, having the size $N_{sp} \times N_{sp}$, is calculated using:

$$
\begin{aligned}
\left[G\left(x^{(k)}\right)\right]_{N_{sp}\times N_{sp}} &= \frac{\partial g\left(x^{(k)}\right)}{\partial x} \\
&= \left[H^T\left(x^{(k)}\right)\right]_{N_{sp}\times N_m} \cdot \left[W^{-1}\right]_{N_m\times N_m} \cdot \left[H\left(x^{(k)}\right)\right]_{N_m\times N_{sp}}
\end{aligned}
\tag{2-20}
$$

The change in the value of state parameters in each iteration is calculated using:

$$
\Delta x^{(k)} = x^{(k+1)} - x^{(k)} \tag{2-21}
$$

2.4.1 Measurement function[1]

The measured parameters, which are considered for power networks in this thesis, are voltage magnitude and real and reactive power flow and power injection. They can be calculated based on the state parameters of power networks, which are voltage magnitude and voltage angle assuming a polar coordinate system. By using a polar coordinate for a system with N_B buses, the state vector will have $(2N_B - 1)$ elements, N_B bus voltage magnitudes and $(N_B - 1)$ bus voltage angles, since the values of voltage angles are reported relative to a reference value, which is usually set equal to 0. Therefore, the state vector for a power system will have the following form, assuming slack bus number 1 as the reference bus for the values of voltage angle:

$$
x^T = \left[\theta_2, \theta_3, \dots, \theta_{N_B}, V_1, V_2, \dots, V_{N_B}\right] \tag{2-22}
$$

The formulation for the calculation of the values of the measured parameters based on the state variables of a power network, assuming the general two-port π-model for the network branches (Figure 2.2) is as follows:

- Real and reactive power injection at bus :

$$
P_i = V_i \sum_{j=1}^{N_B} V_j \left(G_{ij}\cos\theta_{ij} + B_{ij}\sin\theta_{ij}\right) \tag{2-23}
$$

[1] The formulations of this section are taken from (Abur and Exposito 2004).

$$Q_i = V_i \sum_{j=1}^{N_B} V_j \left(G_{ij} \sin \theta_{ij} - B_{ij} \cos \theta_{ij} \right) \tag{2-24}$$

- Real and reactive power flow from bus i to bus j:

$$P_{ij} = V_i^2 \left(g_{s_i} + g_{ij} \right) - V_i V_j \left(g_{ij} \cos \theta_{ij} + b_{ij} \sin \theta_{ij} \right) \tag{2-25}$$

$$Q_{ij} = -V_i^2 \left(b_{s_i} + b_{ij} \right) - V_i V_j \left(g_{ij} \sin \theta_{ij} - b_{ij} \cos \theta_{ij} \right) \tag{2-26}$$

where

$$\theta_{ij} = \theta_i - \theta_j \tag{2-27}$$

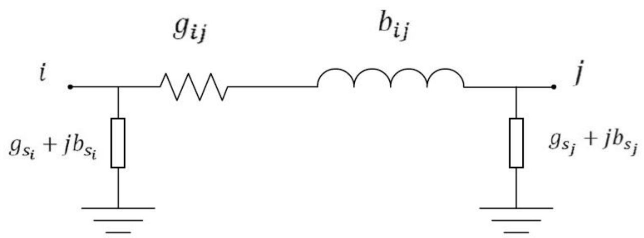

Figure 2.2: Two-port π-model of a network branch[1]

In this way the measurement function, $h(x)$, would be a vector of the following form, where the elements are calculated using the above formulations for available measurement types:

$$h(x) = \begin{bmatrix} P_{injection} \\ P_{flow} \\ Q_{injection} \\ Q_{flow} \\ V_{magnitude} \end{bmatrix} \tag{2-28}$$

[1] Figure taken from (Abur and Exposito 2004)

2.4.2 Measurement Jacobian[1]

The measurement Jacobian matrix has the following form:

$$H(x) = \begin{bmatrix} \frac{\partial P_{injection}}{\partial \theta} & \frac{\partial P_{injection}}{\partial V} \\ \frac{\partial P_{flow}}{\partial \theta} & \frac{\partial P_{flow}}{\partial V} \\ \frac{\partial Q_{injection}}{\partial \theta} & \frac{\partial Q_{injection}}{\partial V} \\ \frac{\partial Q_{flow}}{\partial \theta} & \frac{\partial Q_{flow}}{\partial V} \\ \frac{\partial V_{magnitude}}{\partial \theta} & \frac{\partial V_{magnitude}}{\partial V} \end{bmatrix} \tag{2-29}$$

Different parts of the above matrix are calculated as follows:

- Derivatives of real power injection measurements

$$\frac{\partial P_i}{\partial \theta_i} = \sum_{j=1}^{N_B} V_i V_j \left(-G_{ij} \sin \theta_{ij} + B_{ij} \cos \theta_{ij}\right) - V_i^2 B_{ii} \tag{2-30-a}$$

$$\frac{\partial P_i}{\partial \theta_j} = V_i V_j \left(G_{ij} \sin \theta_{ij} - B_{ij} \cos \theta_{ij}\right) \tag{2-30-b}$$

$$\frac{\partial P_i}{\partial V_i} = \sum_{j=1}^{N_B} V_j \left(G_{ij} \cos \theta_{ij} + B_{ij} \sin \theta_{ij}\right) + V_i G_{ii} \tag{2-30-c}$$

$$\frac{\partial P_i}{\partial V_j} = V_i \left(G_{ij} \cos \theta_{ij} + B_{ij} \sin \theta_{ij}\right) \tag{2-30-d}$$

- Derivatives of reactive power injection measurements

$$\frac{\partial Q_i}{\partial \theta_i} = \sum_{j=1}^{N_B} V_i V_j \left(G_{ij} \cos \theta_{ij} + B_{ij} \sin \theta_{ij}\right) - V_i^2 G_{ii} \tag{2-31-a}$$

[1] The formulations of this section are taken from (Abur and Exposito 2004).

$$\frac{\partial Q_i}{\partial \theta_j} = V_i V_j\left(-G_{ij}\cos\theta_{ij} - B_{ij}\sin\theta_{ij}\right) \quad \text{(2-31-b)}$$

$$\frac{\partial Q_i}{\partial V_i} = \sum_{j=1}^{N_B} V_j\left(G_{ij}\sin\theta_{ij} - B_{ij}\cos\theta_{ij}\right) - V_i B_{ii} \quad \text{(2-31-c)}$$

$$\frac{\partial Q_i}{\partial V_j} = V_i\left(G_{ij}\sin\theta_{ij} - B_{ij}\cos\theta_{ij}\right) \quad \text{(2-31-d)}$$

- Derivatives of real power flow measurements

$$\frac{\partial P_{ij}}{\partial \theta_i} = V_i V_j\left(g_{ij}\sin\theta_{ij} - b_{ij}\cos\theta_{ij}\right) \quad \text{(2-32-a)}$$

$$\frac{\partial P_{ij}}{\partial \theta_j} = -V_i V_j\left(g_{ij}\sin\theta_{ij} - b_{ij}\cos\theta_{ij}\right) \quad \text{(2-32-b)}$$

$$\frac{\partial P_{ij}}{\partial V_i} = -V_j\left(g_{ij}\cos\theta_{ij} + b_{ij}\sin\theta_{ij}\right) + 2\left(g_{ij} + g_{s_i}\right)V_i \quad \text{(2-32-c)}$$

$$\frac{\partial P_{ij}}{\partial V_j} = -V_i\left(g_{ij}\cos\theta_{ij} + b_{ij}\sin\theta_{ij}\right) \quad \text{(2-32-d)}$$

- Derivatives of reactive power flow measurements

$$\frac{\partial Q_{ij}}{\partial \theta_i} = -V_i V_j\left(g_{ij}\cos\theta_{ij} + b_{ij}\sin\theta_{ij}\right) \quad \text{(2-33-a)}$$

$$\frac{\partial Q_{ij}}{\partial \theta_j} = V_i V_j\left(g_{ij}\cos\theta_{ij} + b_{ij}\sin\theta_{ij}\right) \quad \text{(2-33-b)}$$

$$\frac{\partial Q_{ij}}{\partial V_i} = -V_j\left(g_{ij}\sin\theta_{ij} - b_{ij}\cos\theta_{ij}\right) - 2\left(b_{ij} + b_{s_i}\right)V_i \quad \text{(2-33-c)}$$

$$\frac{\partial Q_{ij}}{\partial V_j} = -V_i\left(g_{ij}\sin\theta_{ij} - b_{ij}\cos\theta_{ij}\right) \quad \text{(2-33-d)}$$

- Derivatives of voltage magnitude measurements

$$\frac{\partial V_i}{\partial \theta_i} = 0, \quad \frac{\partial V_i}{\partial \theta_j} = 0, \quad \frac{\partial V_i}{\partial V_i} = 1, \quad \frac{\partial V_i}{\partial V_j} = 0 \tag{2-34}$$

2.4.3 Algorithm of the simulation model developed in MATLAB

A simulation model was developed in MATLAB which accepts the following as inputs:

- Matpower (Zimmerman et al. 2011) specific parameters:
  Network topology and specifications
  Demands and generations

- Accuracy of measurements

- Confidence level of measurements

- Acceptable tolerance of estimation (ε)

Power flow analysis of the power network is performed using Matpower in order to obtain true (nominal) values of all the operation parameters of it. Then, values of standard deviations are calculated using (2-13). Afterwards, values of available measurements are produced using the normrnd(ψ,σ) function of MATLAB, which produces random numbers with a normal distribution. This way, the input parameters for the WLS state estimation algorithm are provided.

The inputs of the WLS state estimation algorithm are values of measurements, standard deviations, topology and specifications of the network and acceptable tolerance of estimation (ε). The weights matrix, W, is formed using (2-12) and by squaring the values of standard deviations. The solution process starts by guessing some values for state vector x, usually a flat start. Then, the values of the measurement function, $h(x^{(1)})$, measurement Jacobian, $H(x^{(1)})$, derivative function $g(x^{(1)})$ and the gain matrix $G(x^{(1)})$ at iteration number 1 is calculated using equations in sections 2.4.1 and

2.4.2 and equations (2-19) and (2-20), respectively. Afterwards, values of the state parameters are corrected using (2-18). This process is iterated until the change in the values of state parameters, which is calculated using (2-21), is less than ε. The process is depicted in Figure 2.3.

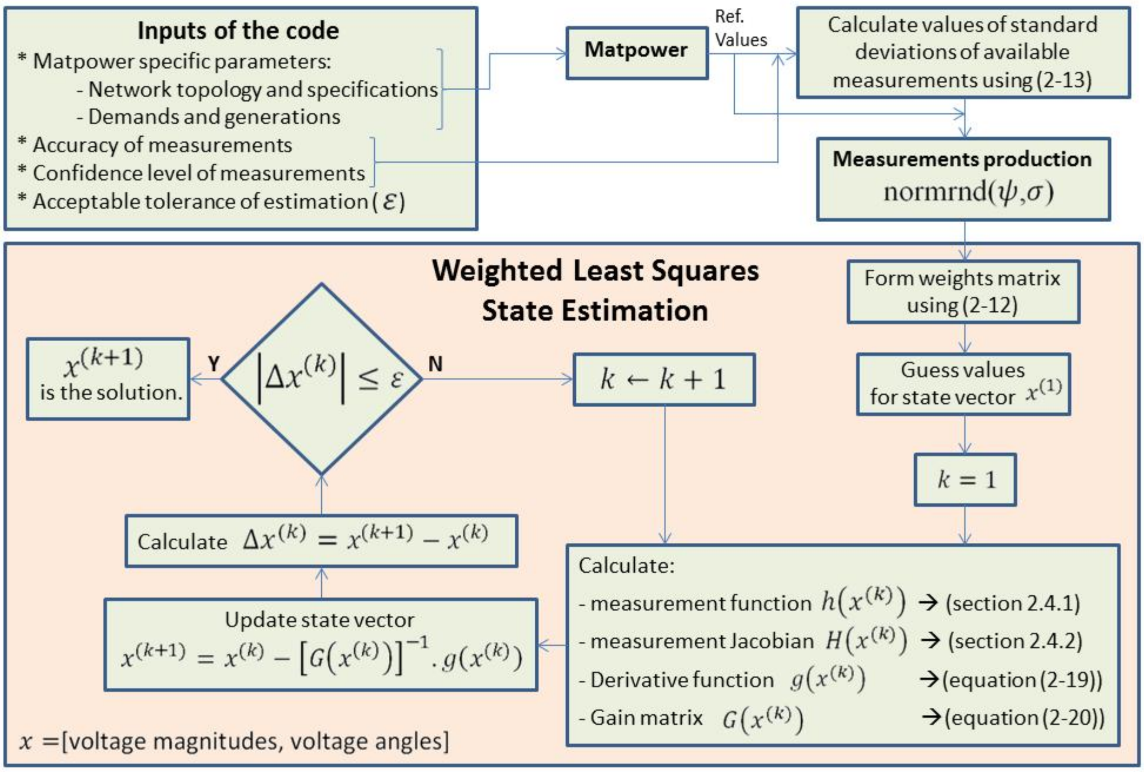

Figure 2.3: The algorithm of the state estimation simulation model based on the WLS

The WLS state estimation can be applied to any system, including power networks, gas networks, district heating networks, etc. in order to estimate the state parameters of the system based on a number of measurements. This can be done by determining state parameters of the system and then deriving formulations for measurement function and measurement Jacobian for it based on the state parameters. Then, derivative function, $g(x)$, and gain matrix, $G(x)$, can be calculated using (2-19) and (2-20), respectively. Finally, the process shown in Figure 2.3 can be applied to the system in order to estimate state parameters and operating conditions of the system accordingly.

2.5 Test results

The performance of the simulation model developed in MATLAB was evaluated using the UKGDS 95-bus test distribution network, which represents an 11 kV network. The schematic of the network is shown in Figure 2.4 (the data of the test system is presented in Appendix I). The data was taken from (Control & Power Research Group 2015) and the network was considered at the peak load condition with 100 MVA base power. The available measurements of the network along with the values of their accuracies are shown in Table 2.2. The values of standard deviations are calculated based on a 95% confidence level.

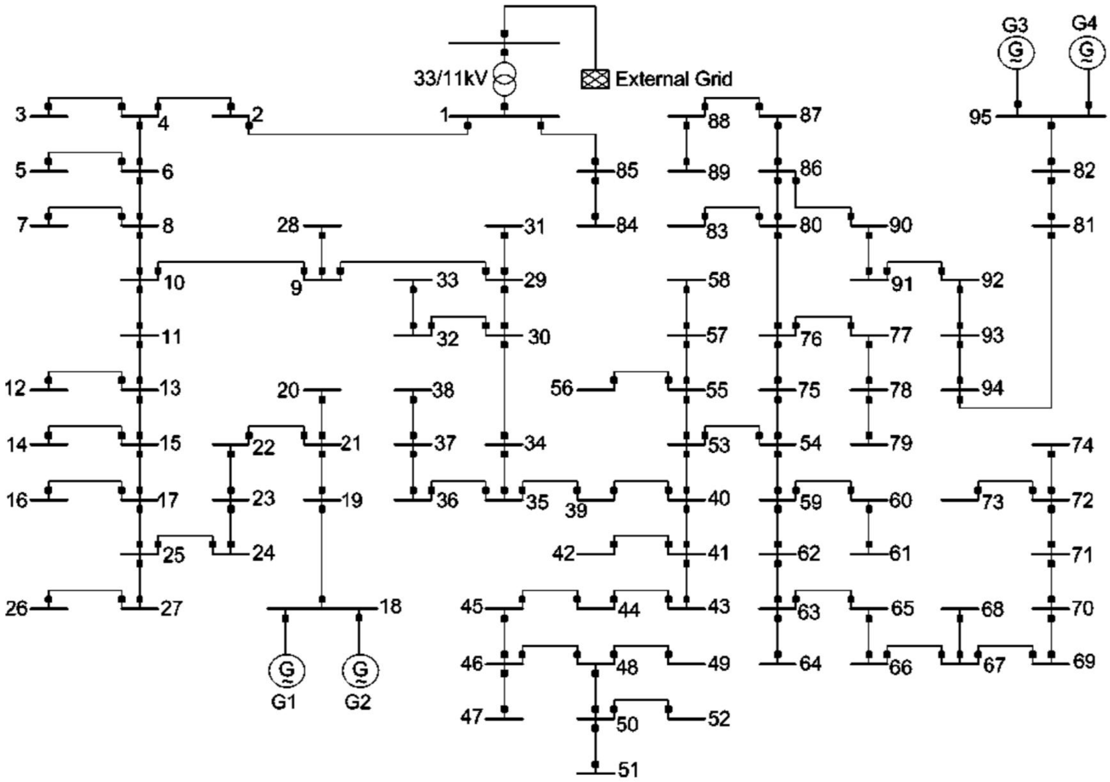

Figure 2.4: Schematic of the UKGDS 95-bus test distribution network[1]

[1] The figure is taken from (Singh et al. 2011).

Table 2.2: Accuracies of the available measurements[1]

Measured parameter	Measurement location	Measurement type	Accuracy
Voltage magnitude	Bus #1 (slack) Buses # 18 & 95 (generations)	Real time	3 %
Power flow	Branches 1-2, 1-85, 18-19 and 95-82	Real time	3 %
Power injection	All the load buses	Pseudo measurement	50 %
	All the zero injection buses	Virtual measurement*	---

*: Variance of zero injection measurements is assumed to be 1.0×10^{-8} (Singh et al. 2011).

2.5.1 SE with perfect measurements

The performance of the developed simulation model was first evaluated using perfect measurements, i.e. noise- or error-free measurements. In other words, the values of the available measurements in Table 2.2 are considered identical to the values obtained in power flow analysis. The estimated values of voltage magnitude and voltage angle at the buses are compared with true values in Figures 2.5 and 2.6, respectively. As can be seen from the figures and as was expected, all the estimated values of voltage magnitudes and voltage angles are equal to their true values, which are obtained in power flow analysis.

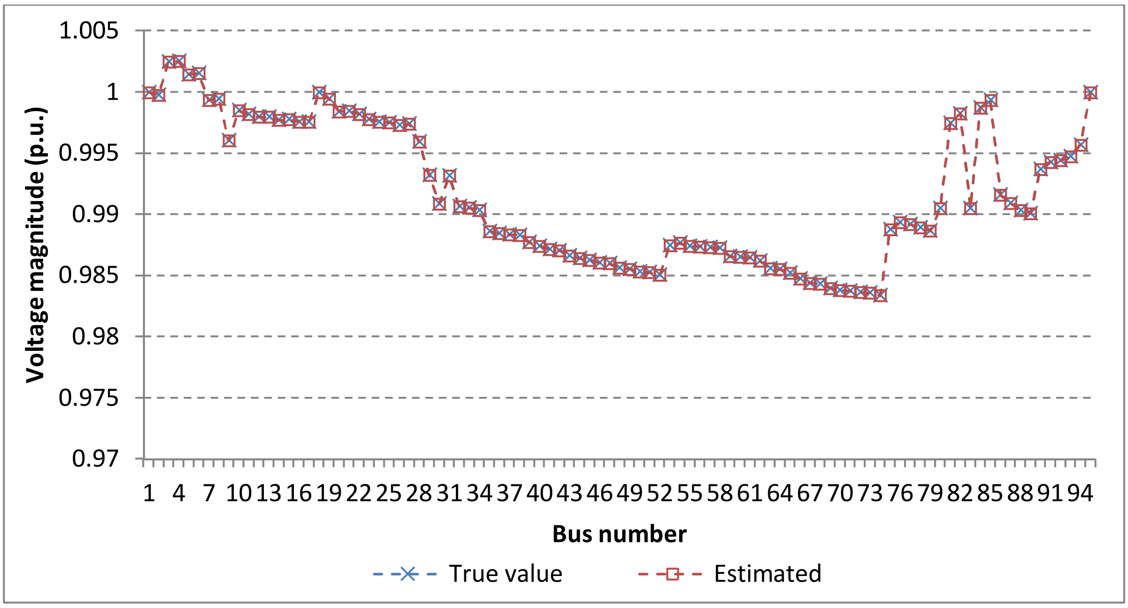

Figure 2.5: Comparison of estimated and true values of voltage magnitudes

[1] The measurement configuration and the values of the accuracies are taken from (Singh et al. 2011).

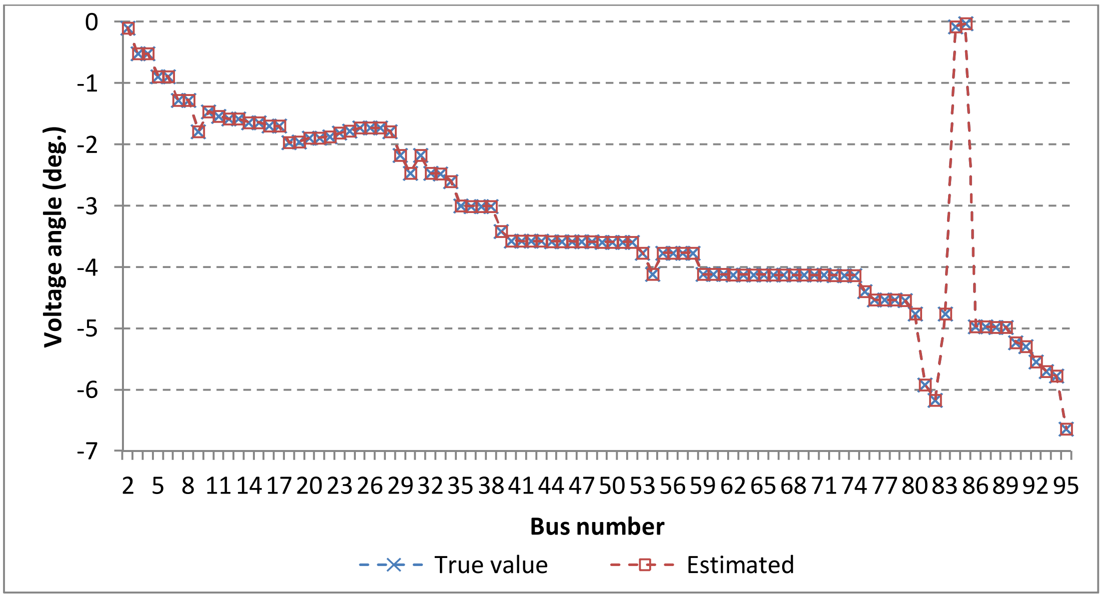

Figure 2.6: Comparison of estimated and true values of voltage angles

2.5.2 Monte Carlo simulation of state estimation of the network

In the next step 50,000 Monte Carlo simulations were performed on the network in order to observe performance of the simulation model as well as the distribution of the estimated state parameters of the network. The set of measurements for each Monte Carlo simulation was produced using the normrnd function of MATLAB. For the purpose of brevity the distribution of the values of voltage magnitudes at the buses is just shown in Figure 2.7 in boxplots. It should be noted that 25 and 75 percentile of the data are put in blue boxes and approximately 0.7% of the data are considered as the outliers, which are shown by red pluses. Also, true values are shown by red stars, which almost coincide with the 50 percentile of the data.

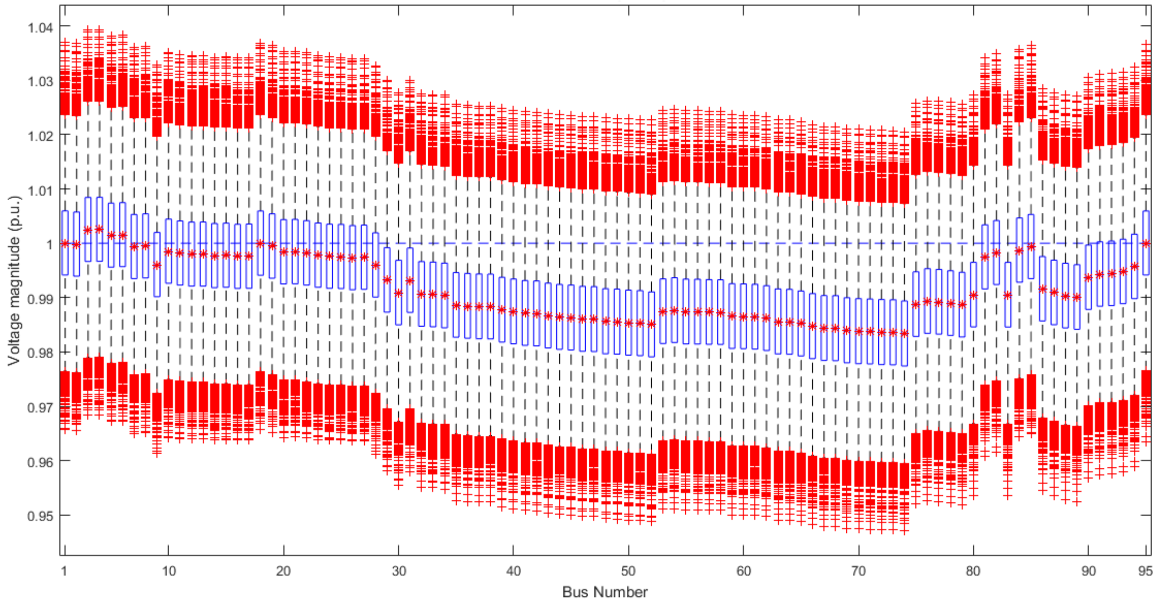

Figure 2.7: Distribution of estimated voltage magnitudes at the buses

As can be seen the average values of estimated voltage magnitudes in Figure 2.7 coincide with the true values in Figure 2.5. Additionally, the values of the estimated voltage magnitudes have a Normal distribution with an expected or mean value, which is the true value of the voltage magnitude at the buses. This behaviour is due to the fact that the measurement model is linearised in the formulations of the WLS. Therefore, the estimated state parameters follow a Normal distribution provided the WLS state estimator is fed with normally distributed measurements. This feature of the WLS-based SE is further investigated in (Singh et al. 2009a).

In the next Chapter the probability distribution function (PDF) of estimated state parameters is introduced and developed using this feature of distribution of them. The PDF is further used for finding proper locations for additional measurements to be placed within a power distribution network in order to improve the accuracy of estimation.

2.6 Summary

A simulation model was developed in MATLAB which accepts the following as inputs and estimates the state parameters of a power network, which are voltage magnitude and voltage angle at buses assuming a zero value for voltage angle at slack bus as the reference for the values of voltage angles:

- Matpower (Zimmerman et al. 2011) specific parameters:
  Network topology and specifications
  Demands and generations

- Accuracy of measurements

- Confidence level of measurements

- Acceptable tolerance of estimation (ε)

The performance of the simulation model was evaluated using the UKGDS 95-bus test distribution network in two instances:

- SE with perfect measurements
  In this instance, perfect measurements, i.e. noise- or error-free measurements, were fed to the simulation model. As was observed and was expected, the simulation model estimated the values of the state parameters identical to the values obtained in the power flow analysis.

- Monte Carlo simulation of state estimation
  In this instance, 50000 Monte Carlo simulations of state estimation were performed on the network with sets of normally distributed measurements. As was observed, the estimated state parameters have a distribution almost very similar to a Normal distribution, which is due to the fact that measurements have Normal distributions and that the measurement model is linearised.

In the next Chapter the above feature of distribution of estimated state parameters is used to develop a PDF for them to aid in finding proper locations for additional measurements to be placed within a power distribution network in order to improve the accuracy of estimation of state parameters.

3 Optimal placement of additional measurements in power distribution networks

3.1 Introduction

Since measurements are the main basis for a state estimation algorithm, in this Chapter measurement placement in power distribution networks is investigated. Firstly, a brief overview of importance of measurement placement in real time control, monitoring and management of power distribution networks is summarised, which is followed by a literature survey and the research questions. Then, the formulation of the problem of measurement placement within a power distribution network is presented. Afterwards, the algorithm of the MATLAB simulation model that was developed for this purpose is explained. Then, a case study test system is introduced and results and performance of the algorithm are evaluated. Finally, a summary and conclusions of the work are presented.

3.1.1 Importance of measurement placement in real time control and management of power distribution networks

Power distribution networks are usually equipped with fewer real time measurements compared to transmission level. Therefore, there is a lack of observability in terms of real time measurements, which leads to impossibility of operation of state estimation algorithm (Bretas and London Jr. 2001). Additionally, available real time measurements are lost at times due to telemetering communication problems of metering infrastructure (Park et al. 1988). Hence, a number of pseudo measurements of the power consumption at load buses are incorporated, which often results in large errors of estimation (Baran et al. 1996).

In order to improve observability and robustness of the state estimation algorithm, the operator of the power distribution network prefers to place various types of meters, including voltage magnitude, power flow and power injection, within the network.

However, this is costly and inconvenient (Park et al. 1988). The operator needs to spend a limited budget intelligently in order to improve metering infrastructure and meet the requirements of increasing the reliability and accuracy of state estimation (Celik and Liu 1995). In other words, they need to find an optimal set of measurements (number, type and place) to be located within the network subject to their limited budget (Baran et al. 1996).

In order to address the above challenges for real time and optimal control, monitoring and management of power distribution networks, there is a need for a measurement placement algorithm, which is capable of proposing a cost-effective investment in metering infrastructure for improving the operation and management of the network (Celik and Liu 1995; Baran et al. 1996).

3.1.2 Research questions

The research questions of this work are as follows:

- What is the best set of measurements (number, type, place, accuracy and frequency of data acquisition) to be placed within the power distribution network subject to a fixed budget of the operator for improving the metering system and the accuracy of network state estimation accordingly?

- If the budget for improving the metering infrastructure is gradually increased, how does it affect the improvement of the accuracy of estimation of the state parameters of the network?

3.1.3 Literature review

A great deal of literature has been devoted to measurement placement in power networks at both transmission and distribution levels. In this section state-of-the-art of measurement placement in power distribution networks is summarised in Table 3.1. All the methods are suitable for designing a new measurement system or improving an existing measurement system of a power distribution network.

Table 3.1: State-of-the-art of measurement placement in power distribution networks

Target		Input measurements	Input constraint	Objective function	Method	Paper
Individual measurement placement	Placement of: - Voltage magnitude measurement	These algorithms incorporate pseudo measurements ($\pm 30-50\%$ error) and/or smart meters ($\pm 10-20\%$ error) (errors are with respect to true values of loads)	Required accuracy (of estimation of state parameters)	Minimum cost	Variance moment	(Bignucolo and Caldon 2007)
					Error of estimation of voltage (magnitude and angle)	(Shafiu et al. 2005; Nusrat et al. 2012a; Abdel-Majeed et al. 2013)
	Placement of: - Power flow measurement		Required accuracy (of estimation of loads)		Error of load estimation	(Haijun et al. 2002)
	Placement of: - Voltage magnitude measurement - Power flow measurement		- Required accuracy (of estimation of state parameters) - Robust metering system		Quality index (Koglin-based)	(Muscas et al. 2006, 2007)
					Error of estimation of voltage magnitude	(Nusrat et al. 2012b)
					Probability distribution	(Pegoraro and Sulis 2012, 2013)
			Cost	Best accuracy (of estimation of state parameters)	Accuracy index (rule-based)	(Baran et al. 1996)
					Saturate number	(Wang et al. 2014)
					Probability distribution	(Singh et al. 2009; Singh et al. 2011)
	Placement of: - Voltage magnitude measurement - Power flow measurement - Current magnitude				Error of estimation of voltage (magnitude and angle)	(Haibin and Schulz 2004)
Measurement unit placement	Placement of RTU: - Power flow measurement		Required accuracy (of estimation of state parameters)	Minimum cost	Error of estimation of voltage magnitude	(Ramesh et al. 2012)
	Placement of RTU: - Voltage magnitude measurement - Active/reactive current measurement				Error variance of branch voltage phasor and error variance of power flow at PoCs	(Yu et al. 2014)
	Placement of RTU: - Voltage magnitude measurement - Power flow measurement		- Required accuracy (of estimation of loads) - Robust metering system		Error of load estimation	(Jie and Miu 2004)
	Placement of PMU: - Voltage (magnitude and angle)		- Required accuracy (of estimation of state parameters) - Robust metering system		Maximum deviation of estimation of voltage (magnitude and angle)	(Junqi et al. 2012; Pegoraro et al. 2012; Junqi et al. 2014)
			Cost	Best accuracy (of estimation of state parameters)	Variance of estimation of voltage (magnitude and angle)	(Ghasemi Damavandi et al. 2015)
	Placement of PMU: - Voltage (magnitude and angle) - Current (magnitude and angle)	These algorithms do not incorporate pseudo measurements, since they aim at observability.	Observability of the network in terms of real time measurements	Minimum cost	Observability-based	(Abdelsalam et al. 2014)
					redundancy level of measurements for a bus	(Jamil et al. 2014)

As can be seen the problem of measurement placement can be dealt with in two main approaches as follows:

- Approach 1
  The accuracy of estimation of the state parameters or the loads is the constraint of the problem and the algorithm achieves the target with the minimum cost; or

- Approach 2
  The cost of the metering infrastructure is the constraint of the problem and the measurement placement algorithm finds the best measurement set (number, type and place) in a way to optimise the accuracy of estimation of the state parameters or the loads.

In another classification, the problem of measurement placement has been investigated in the literature in the two following main categories:

- ***Individual measurement placement***
  - Placement of voltage magnitude measurements was studied by considering the error of estimation of voltage vector (Shafiu et al. 2005; Nusrat et al. 2012a; Abdel-Majeed et al. 2013) or by a new definition called “variance moment” (Bignucolo and Caldon 2007) in Approach 1.

  - Placement of power flow measurements was investigated by taking into account the error of load estimation (Haijun et al. 2002) in Approach 1.

  - Placement of both voltage magnitude and power flow measurements within the network was studied using several methods. One of them is based on a quality index of estimation (Muscas et al. 2006, 2007). This method is based on Koglin method (Koglin 1975), which introduced “interesting parameters” and the best set of measurements were found for the best accuracy of estimation of these parameters. Other methods include minimising the error of estimation of voltage magnitude (Nusrat et al. 2012b) and performing placement based on the probability distribution of estimated voltage magnitude and voltage angle (Pegoraro and Sulis 2012, 2013). All these methods follow Approach 1.

On the other hand, other methods have been developed for placement of both voltage magnitude and power flow measurements based on an accuracy index (Baran et al. 1996), the saturate number (Wang et al. 2014) and the probability distribution of estimated voltage magnitude and voltage angle (Singh et al. 2009b; Singh et al. 2011), in Approach 2.

- Placement of measurements of voltage magnitude, power flow and current magnitude was studied by minimising the error of estimation of voltage magnitudes and voltage angles (Haibin and Schulz 2004) in Approach 2.

❖ ***Measurement unit placement***

- Placement of RTU in Approach 1
    - Placement of RTU equipped with power flow meters was investigated by minimising the error of estimation of voltage magnitude (Ramesh et al. 2012).
    - Placement of RTU measuring voltage magnitude and active and reactive current was performed by minimising the error variance of branch voltage phasor and the error variance of power flow at PoCs (Yu et al. 2014).
    - Placement of RTU equipped with voltage magnitude and power flow meters was studied by minimising the error of load estimation (Jie and Miu 2004).
- Placement of PMU
    - Placement of PMUs measuring voltage phasor meters was investigated by minimising the maximum deviation of estimation of voltage magnitude and voltage angle (Junqi et al. 2012;

Pegoraro et al. 2012; Junqi et al. 2014) in Approach 1. The same topic was studied by minimising the variance of estimation of voltage magnitude and voltage angle (Ghasemi Damavandi et al. 2015) in Approach 2.

- Placement of PMUs, which measure voltage and current phasors, was studied by minimising the cost of metering infrastructure subject to achieving an observable network in terms of real time measurements by observability-based method (Abdelsalam et al. 2014) and considering the redundancy level of measurements for a bus (Jamil et al. 2014).

It should be noted that all the algorithms except the last one (the second one under "Placement of PMU" above), which is about placement of PMUs targeting an observable network in terms of real time measurements, perform the measurement placement by incorporating pseudo measurements of loads (with 30-50% error) or measurements of smart meters (with 10-20% error). However, the algorithm that was excluded (the second one under "Placement of PMU" above) deals with all the available real time measurements since it aims at achieving an observable network in terms of real time measurements.

3.2 Formulation of the problem of measurement placement

In this section the criteria for selection of measurements in power networks is explained. Then, the formulation of the problem of finding the best set of additional measurements for a power distribution network is presented. Finally, the algorithm that was developed for solving the problem is described.

3.2.1 Criteria for selection of measurements

Operators of power networks usually take into account some of the following criteria when they intend to design a metering system for their network or improve the existing one:

- ***Cost of metering infrastructure***

  The operator has either a limited budget for improving the metering system or prefers to improve the accuracy of state estimation with the minimum possible expenses (Park et al. 1988; Baran et al. 1996).

- ***Accuracy of state estimation***

  Investment on the metering infrastructure is mainly performed aiming at improving the accuracy of estimation of state parameters, loads or power flows of the network (Park et al. 1988; Junqi et al. 2013).

- ***Robustness of the state estimation algorithm***

  Robustness of the state estimation algorithm against loss of real time measurements means the algorithm is still able to perform estimation of the state parameters of the network while some of the real time measurements are lost due to telemetering communication problems. This is another important factor and is sometimes considered during selection of additional meters or designing a new metering system (Junqi et al. 2013).

- ***Observability of the network***

  Power networks are observable in terms of pseudo measurements of loads and real time measurements at slack and decentralised generation buses. However, some of the measurement placement algorithms aim at enhancing the observability of the network in terms of real time measurements (Clements et al. 1983; Monticelli and Wu 1985).

- ***Bad data detection and identification***

  One of the aspects sometimes considered for selection of meters is enabling the state estimation algorithm to detect and identify bad data received at the control and management centre of the network (Baran et al. 1996; Janssen et al. 2013).

Among all the above important factors in selection of measurements, the following has been considered in developing the measurement placement algorithm in this research:

- ***Cost***

  Cost is considered as the number of additional measurements to be placed within the network.

- ***Accuracy***

  Selection of type and place of additional measurements is performed based on the best improvement in the accuracy of estimation of the state parameters.

- ***Observability***

  Observability of the state estimation algorithm over the network is guaranteed since pseudo measurements of loads and virtual measurements are incorporated.

3.2.2 Objective functions of the optimisation problem

The objective of measurement placement is to find the type and the place of a specified number of additional measurements within the network for the best improvement of estimation of the state parameters of the network, i.e. voltage magnitudes and voltage angles. Hence, the problem of measurement placement is formulated as optimisation of an objective function subject to a fixed cost. The cost, which is the constraint, is the input to the problem in terms of the number of additional measurements. However, two optimisation approaches with different objective functions are developed and applied to the same problem in order to validate their results against each other. In the two following subsections these two optimisation approaches are explained.

3.2.2.1 Approach 1: Objective function based on the probability of estimation within a range

In the first approach the aim is to find a location in such a way that the probability that all the state parameters, i.e. voltage magnitudes and voltage angles, will fall within a "range" of their true values is maximised. The range is an input to the algorithm and is shown in Table 3.2 for this research.

Table 3.2: The desired range of falling of the estimated state parameters

State parameter	Range* (Singh et al. 2011)	Meaning
Voltage magnitude	1 %	99% to 101% of the true value
Voltage angle	5 %	95% to 105% of the true value

*: The ranges are relative to the true value of each state parameter.

Therefore, there exists a set of N_B (N_B: number of buses of the network) probability values that the estimated values will fall within a range for all the buses of the network and for every possible measurement location. The minimum value of each of the sets of probabilities of falling of the state parameters within the desired range is chosen and compared with the minimum values of the rest of the sets. The location of the measurement that gives the maximum value of all the minima is selected as the solution. This is shown through a numerical example.

Example

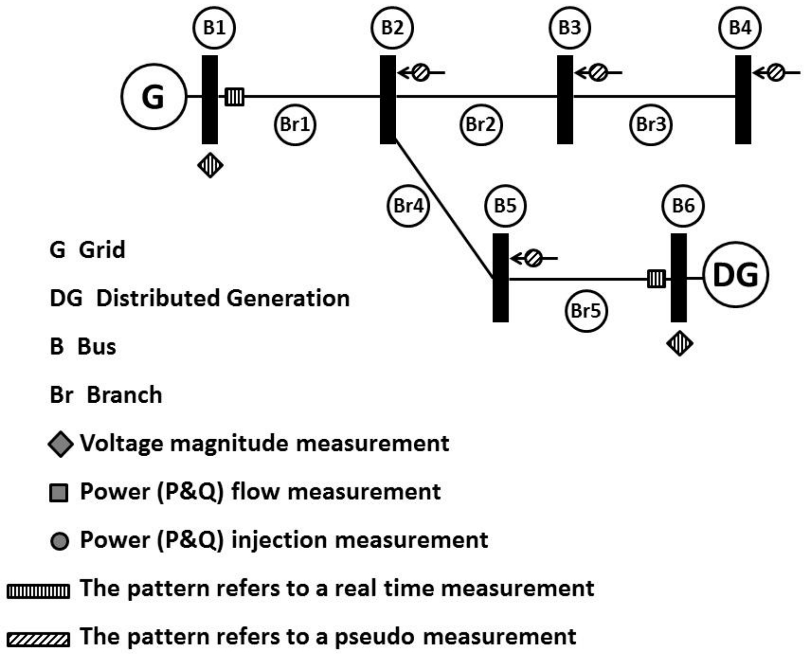

Figure 3.1: The schematic of the case study power distribution network

In this example placement of a single ***additional*** meter in a case study power distribution network, which is shown in Figure 3.1, is explained. State estimation is performed based on the measurements shown in Table 3.3, which make the network observable.

Table 3.3: List of the measurements for state estimation

Measured parameter	Measurement type	Measurement location
Voltage magnitude	Real time	Buses #1, 6
Power (real and reactive) flow	Real time	Branches #1, 5
Power (real and reactive) injection	Pseudo	Loads at buses #2, 3, 4, 5

The ***additional*** single real time meter is assumed to be either for measuring the voltage magnitude of a bus or the power flow of a branch. Based on this assumption the possible locations for placing the additional meter are shown by L1, L2, …, L7 in Figure 3.2.

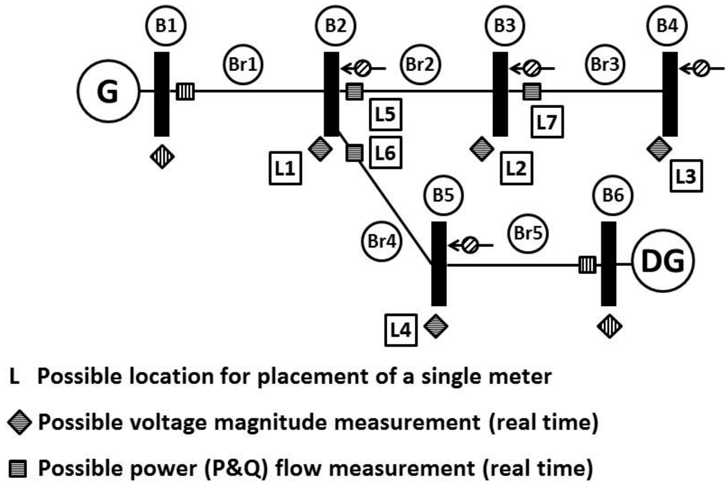

Figure 3.2: Possible locations for the additional meter

As can be seen the possible locations L1, L2, L3 and L4 refer to placement of a voltage magnitude measurement at the buses 2, 3, 4 and 5, respectively, and the possible locations L5, L6 and L7 refer to placement of a power flow measurement on the branches 2, 4 and 3, respectively. Now, the problem is to choose one of these seven possible locations such that the accuracy of state estimation is best improved. This will be done through use of a criterion in the form of an objective function and comparing the possible locations based on the criterion. Derivation of the formulation of the objective function is presented later. The focus of the example is on explanation of the methodology for finding the solution measurement placement.

A single ***additional*** meter is placed each time at each possible location and the value of the probability that the voltage magnitude and the voltage angle will fall within 1% and 5%, respectively, of their true values is calculated for all the buses of the network. For example a meter is placed at location L1 (voltage magnitude of bus 2) and the probability values that the estimated state parameters will fall within the ranges for bus 1, bus 2, bus 3, bus 4, bus 5 and bus 6 are obtained as 97%, 73%, 85%, 87%, 82% and 95%, respectively. These values are put in a column under L1 and the whole column is considered as the probability value set for measurement location 1.

Table 3.4 shows the values of the probability sets for all the possible measurement locations. The formulation used for calculation of these values is explained later and the values shown are just some example numbers to describe the methodology. Each column of the table represents each probability value set corresponding to each possible measurement location. These sets of probabilities need to be compared with each other. This is performed through definition of a fitness function.

Table 3.4: The values of the probabilities of falling of the state parameters within the desired ranges for each possible measurement location

Location / Bus#	L1	L2	L3	L4	L5	L6	L7
Bus 1	97*	99	96	97	96	98	96
Bus 2	73	89	82	76	83	75	78
Bus 3	85	76	72	82	75	78	84
Bus 4	87	74	84	89	80	70	80
Bus 5	82	87	78	71	78	84	79
Bus 6	95	96	94	96	93	95	97

*: All the values are in percentage.

Definition of the fitness function

In order to find the solution measurement location a fitness function, J, is defined as the minimum value of the probability that the voltage magnitudes and the voltage angles will fall within the ranges corresponding to each possible measurement location. Hence:

$$J = \min\{Pr_i\}_{i=1}^{N_B} \tag{3-1}$$

Comparison of the minimum probability values ensures that the rest of the probability values in each probability set corresponding to each possible measurement location are higher than the representative probability value, which is the minimum probability value.

The values of the fitness function corresponding to the possible measurement locations are compared in Table 3.5. For example in the first column, under L1, which is the first probability set corresponding to the first measurement location, the least value among 97, 73, 85, 87, 82 and 95 is 73. Hence, “73” is considered as the value of the fitness function for the first measurement location for later decision making.

Table 3.5: The fitness function (minimum probability value) for each possible location

Location	**L1**	**L2**	**L3**	**L4**	**L5**	**L6**	**L7**
Fitness function*	73**	74	72	71	75	70	78

*: Calculated from Equation (3-1)

**: All the values are in percentage.

Among all the minima, the measurement location with the maximum probability value is chosen as the solution. Comparison of the probability values in Table 3.5 shows that location 7 has the maximum probability value among all the minimum probability values. Therefore, this location, which is a measurement of power flow on branch 3, is the solution.

According to the above example, the minimum value of the probability that the estimated state parameters of the network, i.e. the voltage magnitudes and the voltage angles of the buses, will fall within ranges corresponding to each possible measurement location is compared with the rest of the minimum probability values of the rest of the possible measurement locations. The objective is to find a measurement location which has the maximum value of the probability among all the minima.

Based on the above explanation in this approach the objective function is defined as:

$$OF = Max\left\{min_j\{Pr_i\}_{i=1}^{N_B}\right\}_{j=1}^{N_p} \tag{3-2}$$

where N_p is the number of possible locations and Pr_i is:

$$Pr_i = Pr\left\{\left|\frac{V_{e,i} - V_{t,i}}{V_{t,i}}\right| \leq \varepsilon_V \; and \; \left|\frac{\theta_{e,i} - \theta_{t,i}}{\theta_{t,i}}\right| \leq \varepsilon_\theta\right\} \tag{3-3}$$

where:

Pr_i Probability value for bus i

Pr Probability of an event

$V_{e,i}$ Estimated value of voltage magnitude of bus i

$V_{t,i}$ True value of voltage magnitude of bus i

ε_V Acceptable range of estimation of voltage magnitude relative to the true value

$\theta_{e,i}$ Estimated value of voltage angle of bus i

$\theta_{t,i}$ True value of voltage angle of bus i

ε_θ Acceptable range of estimation of voltage angle relative to the true value

In order to derive the formulation for Pr_i it is assumed that the probability of the event of estimation of voltage magnitude within the range ε_V of its true value is independent of the probability of the event of estimation of voltage angle within the range ε_θ of its true value, since voltage magnitude and voltage angles themselves are assumed to be independent of each other especially in power distribution networks. Therefore, the probability of occurrence of both of these events at the same time would be the multiplication of probability of both of the events, i.e.:

$$\begin{aligned} Pr_i &= Pr\left\{\left|\frac{V_{e,i}-V_{t,i}}{V_{t,i}}\right| \le \varepsilon_V \; and \; \left|\frac{\theta_{e,i}-\theta_{t,i}}{\theta_{t,i}}\right| \le \varepsilon_\theta\right\} \\ &= Pr_i\left\{\left|\frac{V_{e,i}-V_{t,i}}{V_{t,i}}\right| \le \varepsilon_V\right\} \times Pr_i\left\{\left|\frac{\theta_{e,i}-\theta_{t,i}}{\theta_{t,i}}\right| \le \varepsilon_\theta\right\} \end{aligned} \quad (3\text{-}4)$$

The formulation for the probability of estimation of voltage magnitude of bus i in the range $(V_{t,i} - \varepsilon_V \times V_{t,i}, V_{t,i} + \varepsilon_V \times V_{t,i})$ is:

$$Pr_i\left\{\left|\frac{V_{e,i}-V_{t,i}}{V_{t,i}}\right| \le \varepsilon_V\right\} = \int_{V_{t,i}-\varepsilon_V\times V_{t,i}}^{V_{t,i}+\varepsilon_V\times V_{t,i}} PDF_{V_i} \times dV_i \quad (3\text{-}5)$$

in which the probability distribution function of estimated voltage magnitude of bus i,

PDF_{V_i}, is assumed to have a normal distribution as follows:

$$PDF_{V_i} = \frac{1}{\sqrt{2\pi \times a_{V_i}}} \exp\left\{-0.5 \times \frac{\left(V_{e,i} - V_{t,i}\right)^2}{a_{V_i}}\right\} \tag{3-6}$$

where a_{V_i} is the variance of estimation of voltage magnitude of bus i. Similarly, the formulation for probability of estimation of voltage angle of bus i in the range $(\theta_{t,i} - \varepsilon_\theta \times \theta_{t,i}, \theta_{t,i} + \varepsilon_\theta \times \theta_{t,i})$ is:

$$Pr_i\left\{\left|\frac{\theta_{e,i} - \theta_{t,i}}{\theta_{t,i}}\right| \le \varepsilon_\theta\right\} = \int_{\theta_{t,i}-\varepsilon_\theta\times\theta_{t,i}}^{\theta_{t,i}+\varepsilon_\theta\times\theta_{t,i}} PDF_{\theta_i} \times d\theta_i \tag{3-7}$$

in which the probability distribution function of estimated voltage angle of bus i, PDF_{θ_i}, is assumed to have a normal distribution as follows:

$$PDF_{\theta_i} = \frac{1}{\sqrt{2\pi \times a_{\theta_i}}} \exp\left\{-0.5 \times \frac{\left(\theta_{e,i} - \theta_{t,i}\right)^2}{a_{\theta_i}}\right\} \tag{3-8}$$

where a_{θ_i} is the variance of estimation of voltage angle of bus i.

The parameters a_{V_i} and a_{θ_i} are the diagonal elements of state error covariance matrix (A) corresponding to voltage magnitude and voltage angle of bus i, respectively. The error covariance matrix A is calculated using (Singh et al. 2011):

$$A = (H^T(x).W.H(x))^{-1} \tag{3-9}$$

where:

H Measurement Jacobian

W Weights matrix

x Vector of state parameters, i.e. voltage magnitudes and voltage angles

In derivation of the formulations for probability distribution functions of estimated voltage magnitude and voltage angle it is assumed that these PDFs have a normal distribution, since the input measurements to the estimation algorithm are also normally distributed. This is based on the conclusions of the Chapter 2. Substituting (3-6) in (3-5), and (3-8) in (3-7) and replacing (3-5) and (3-7) in (3-4) yields:

$$
\begin{aligned}
Pr_i = &\int_{V_{t,i}-\varepsilon_V \times V_{t,i}}^{V_{t,i}+\varepsilon_V \times V_{t,i}} \frac{1}{\sqrt{2\pi \times a_{V_i}}} \exp\left\{-0.5 \times \frac{\left(V_{e,i}-V_{t,i}\right)^2}{a_{V_i}}\right\}. dV_i \\
&\times \int_{\theta_{t,i}-\varepsilon_\theta \times \theta_{t,i}}^{\theta_{t,i}+\varepsilon_\theta \times \theta_{t,i}} \frac{1}{\sqrt{2\pi \times a_{\theta_i}}} \exp\left\{-0.5 \times \frac{\left(\theta_{e,i}-\theta_{t,i}\right)^2}{a_{\theta_i}}\right\}. d\theta_i
\end{aligned}
\tag{3-10}
$$

Having the formulation for Pr_i, the objective function (3-2) is calculated. Now that the formulation for calculation of the probability of estimation of state parameters within a range is explained the algorithm for finding the solution in the example network shall be described in order to better understand the way the solution is found using a sample of measurements through a Monte Carlo simulation of state estimation.

The algorithm of placement of a single additional meter in the example network

The flow chart of the algorithm of placement of a single meter in the example test network is presented in Figure 3.3.

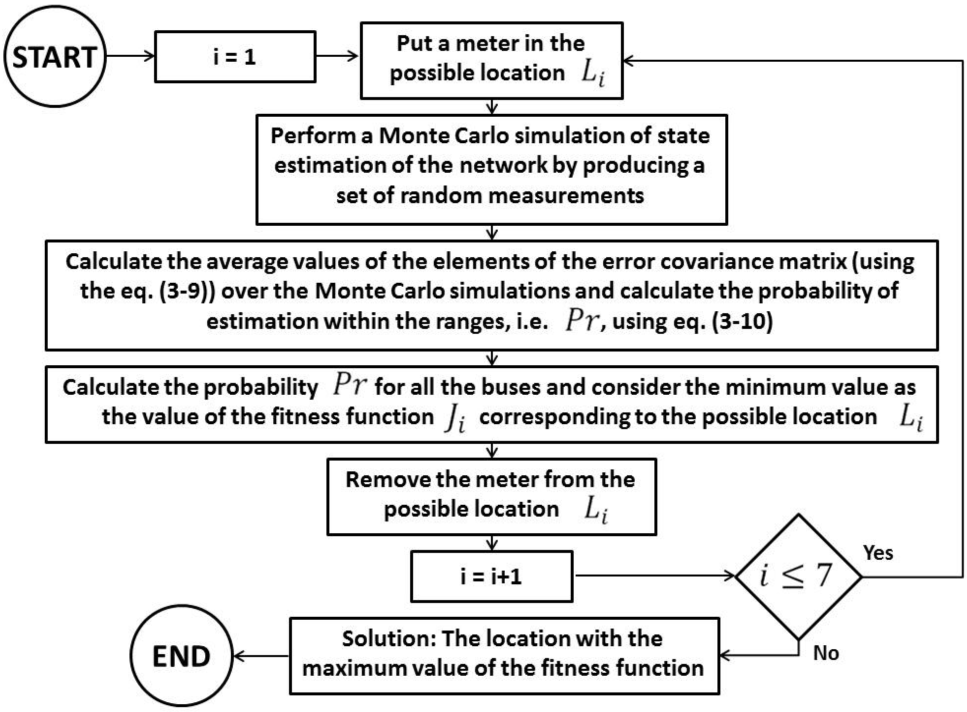

Figure 3.3: The flow chart of the algorithm of placement of a single meter in the example network

As can be seen a single meter is placed at each and every possible measurement location each time a Monte Carlo simulation is performed. By a Monte Carlo simulation, it means that a random set of measurements are produced and the values of state parameters of the network are estimated. After a Monte Carlo simulation the average values for the elements of the error covariance matrix corresponding to the buses, i.e. the average values of a_{V_i} and a_{θ_i}, are obtained and placed in Equation (3-10). Then, the probability function Pr is calculated for all the buses of the network and the least probability value, according to Equation (3-1), is considered as the fitness function, J, for that specific possible location. Finally, the possible measurement locations are ranked based on the maximum value of their fitness function and the location, which has the maximum value of fitness function, is the solution of the problem.

3.2.2.2 Approach 2: Objective function based on the accuracy index

In the second approach, selection of measurements is performed based on the least value of accuracy index of state estimation, which is the summation of the diagonal elements of the state error covariance matrix (Baran et al. 1996). In this approach the objective function is calculated as follows:

$$OF = \min \sum_{i=1}^{2N_B-1} A_{ii} \tag{3-11}$$

It should be noted that similar to the previous approach, the average values of elements of matrix A through a Monte Carlo simulation of state estimation is considered as the basis of calculations and decision making. The algorithm of measurement placement in this approach is identical to the previous approach. The only difference is the objective function. In other words, the possible measurement locations are ranked based on the minimum value of the accuracy index. The location with the minimum value, the first location in the rank, is the solution of the problem.

3.2.3 Development and implementation of the algorithm of measurement placement

The flow chart of the algorithm that was developed for measurement placement is shown in Figure 3.4. As can be seen the problem is solved through three steps by reducing the search space. For this purpose, in Step 1 the set of candidate possible locations is formed from all the possible locations. Then, the set of possible designs is formed in Step 2 using the output of Step 1. In order to reduce the search space and form the set of possible designs, i.e. performing Steps 1 and 2, the ordinal optimisation technique was applied. Finally, in Step 3, the reduced search space is investigated for the solution of the problem. The motivation behind reduction of the search space is presented in 3.2.3.1. The detailed explanation of the three Steps is presented in the later subsections.

The algorithm was implemented once for placement of additional individual measurements and once for placement of additional measurement units. The set of possible locations for placement of additional measurements in these two cases are as follows:

- Placement of additional individual measurements

  All the possible locations for placement of individual measurements include:

- the voltage magnitudes of all the buses except the slack and generations;

- the power flow of all the branches except those connected to the slack and generations.

- Placement of additional measurement units (or RTUs)

  Possible locations for placement of additional measurement units include all the buses of the network except the slack and generations assuming these buses are already equipped with RTUs. It is assumed RTUs are placed on possible buses of the network and consist of all the following real time measurements of:

  - voltage magnitude of the bus on which the TRU is placed;

  - power injection of the possible load connected to the bus;

  - power flow of all the branches connected to the bus.

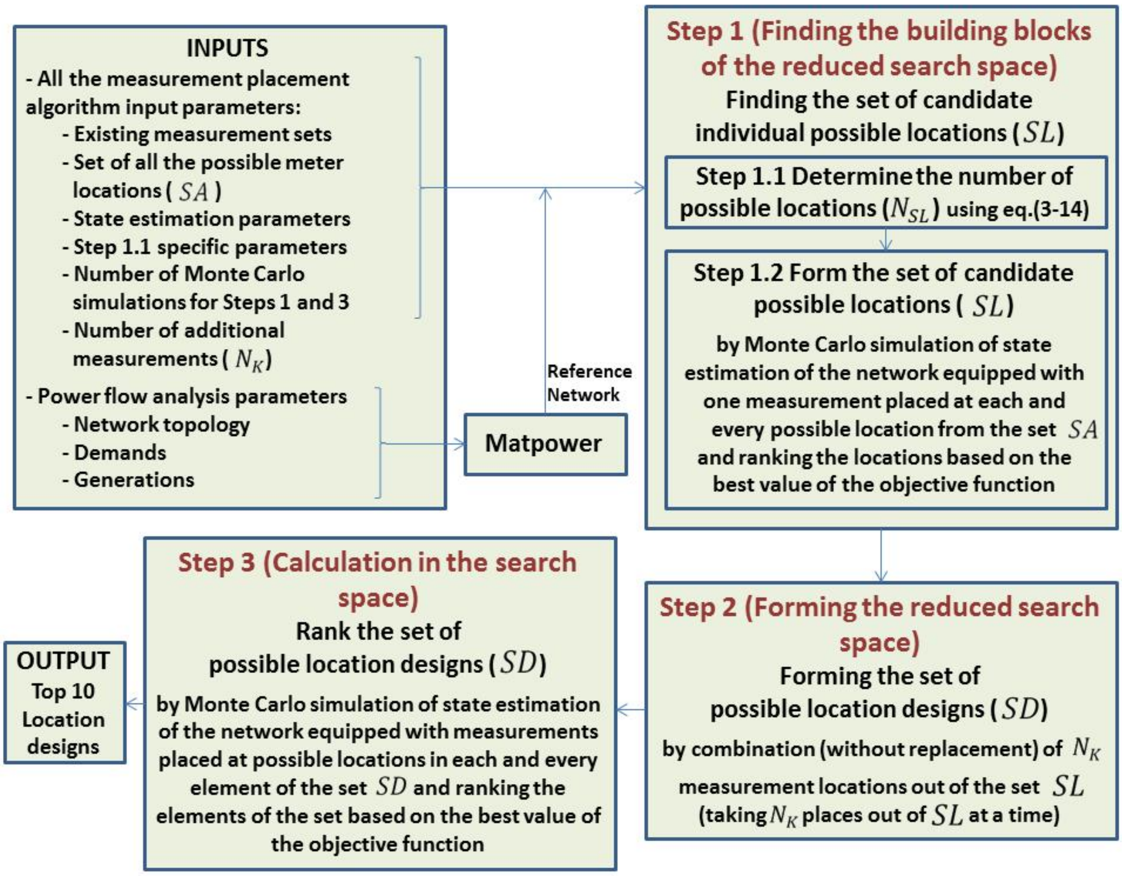

Figure 3.4: The flow chart of the developed algorithm of measurement placement

3.2.3.1 Motivation behind reducing the search space

Distribution networks normally have large numbers of possible locations for placement of measurements. Let's assume a distribution network has 100 possible locations for placement of individual measurements and the operator of the network has a limited budget to place a specific number of additional measurements on some of the possible locations within the network. The number of possible designs[1] is obtained by the combination of the number of additional measurements out of the whole number of possible locations without replacement. Assume the analysis of each and every possible design needs just 1 second to be performed. Table 3.6 shows the amount of time in order to reach the solution provided each and every element of the search space, which is the set of all the possible designs, is analysed.

[1] A "possible design" or a "possible location design" of meters in this thesis refers to one single placement of several measurements in the possible locations within a network at a time.

Table 3.6: The amount of time to reach a solution without reduction of the search space

Number of additional measurements	Number of possible designs	Time required for achieving the solution*
3	$\binom{100}{3} = \frac{100!}{3! \times (100-3)!} = 161700$	1.8 days (~ 2 days)
4	$\binom{100}{4} = \frac{100!}{4! \times (100-4)!} = 3921225$	45.3 days (~ 1.5 months)
5	$\binom{100}{5} = \frac{100!}{5! \times (100-5)!} = 75287520$	871.3 days (~ 2.5 years)

*: Assuming analysis of each possible design needs 1 second to be performed.

As can be concluded from the table, the time required for achieving a solution increases dramatically as the number of additional measurements increases. The situation even worsens in much larger networks with greater number of possible locations and/or greater number of additional measurements. Therefore, a technique is used to reduce the search space, avoid unnecessary computation effort and reach the solution in a reasonable amount of time. In this research the ordinal optimisation technique is used for this purpose, which is explained in detail in (Edward Lau and Ho 1997; Ho et al. 2007; Singh et al. 2011). In this Chapter only the way of implementation of the technique for facilitation of reaching the solution of the problem of measurement placement is described.

3.2.3.2 Step 1: Finding the set of possible locations

Let's assume the operator of the network has a limited budget just to place N_K additional measurements within the distribution network. In order to form the reduced search space, the set of possible locations[1], denoted by SL, shall be found. Once the set SL is found the set of possible designs SD is formed by combination of N_K elements out of SL without replacement.

- ***Step 1.1: Finding the number of the elements of the set SL, i.e. N_{SL}***

In order to find the set of possible locations the number of elements (or members) of this set (N_{SL}) was found first. According to the ordinal optimisation technique the following inequality needs to be satisfied for the number of elements of the set SD, i.e.

[1] A "possible location" in this thesis refers to each and every of the possible places within the network on which an individual measurement or a measurement unit can be placed.

N_{SD} (Singh et al. 2011):

$$1-(1-\alpha)^{N_{SD}} \geq CL_{PS} \tag{3-12}$$

in order to ensure that "the reduced search space contains at least one solution within the top $\alpha\%$ with a probability [or confidence] level CL_{PS}" as argued by Singh et al. (Singh et al. 2011). The set of possible designs, SD, is formed by the combination of N_K elements out of the set of possible locations , SL, without replacement, i.e.:

$$N_{SD} = \binom{N_{SL}}{N_K} = \frac{N_{SL}!}{N_K! \times (N_{SL}-N_K)!} \tag{3-13}$$

where N_{SL} is the number of elements of the set SL. Hence, replacing (3-13) in (3-12) and rearranging the inequality results in:

$$N_{SD} = \binom{N_{SL}}{N_K} = \frac{N_{SL}!}{N_K! \times (N_{SL}-N_K)!} \geq \frac{\ln(1-CL_{PS})}{\ln(1-\alpha)} \tag{3-14}$$

In other words, the number (N_{SL}) of elements of the set of possible locations (SL) is the lowest number that satisfies (3-14) once the values of the following parameters, which are inputs to the algorithm, are known:

- Number of additional measurements (N_K);
- Confidence level of having the solution in the reduced search space (CL_{PS});
- Portion of the reduced search space within which the solution exists (α).

❖ ***Step 1.2: Forming the set of candidate possible locations (SL)***

Once the number (N_{SL}) of elements of the set of possible locations (SL) is determined, the next step is to determine the elements of the set. Let SA be the set of all the possible locations for placement of additional measurements within the network. The set SL is empty at first and the elements of it will be determined gradually in a step by step process. This is performed through the following steps (Singh et al. 2011):

- Put a measurement at each and every location of the set SA, perform a Monte Carlo simulation of state estimation of the network, calculate the value of the objective function and rank the elements of the set SA based on the best value of the objective function (Both of the objective functions that were explained earlier were used as the decision criterion in the algorithm.);

- Remove the location with the best value of the objective function in the rank from SA and put it in SL.

- In this way the set SA of all the possible locations shrinks and the set SL of possible locations grows and forms. Repeat the above two steps till the number of members of SL becomes equal to N_{SL}.

In this Chapter, the problem of measurement placement is investigated in two respects:

- Placement of individual measurements

  The set (SA) of all the possible locations for placement of individual measurements includes:

  - the voltage magnitudes of all the buses except the slack and generations;

  - the power flow of all the branches except those connected to the slack and generations.

- Placement of measurement units (or RTUs)

  The set SA for placement of measurement units includes all the buses of the network except the slack and generations assuming these buses are already equipped with RTUs. It is assumed RTUs are placed on possible buses of the network and consist of all the following real time measurements of:

- voltage magnitude of the bus on which the TRU is placed;
- power injection of the possible load connected to the bus;
- power flow of all the branches connected to the bus.

In this case the cost is an input to the algorithm in terms of the number of additional measurement units to be placed within the network assuming the cost of individual measurements included in a measurement unit is neglected compared to the cost of the whole measurement unit and the communication device. This is due to the fact that the communication device and the whole measurement unit are much more expensive than the individual measurements (Baran et al. 1995). In other words, when the operator of the network decides to place an RTU at a bus, they take all the possible measurements of voltage magnitude, power flows and power injections at the bus, assuming the communicating channels of the RTU allow them to do so. Therefore, in this research it is assumed that an additional measurement unit has all the possible measurement types of voltage magnitude, power flow of all the branches connected to the bus where it is placed, and power injection of the possible load connected to the bus.

3.2.3.3 Step 2: Forming the reduced search space

Once the elements of the set of possible locations (SL) are determined, the set of possible designs (SD) can be formed by combination of N_K elements out of all the elements of the set of possible locations (SL) without replacement. Each element of the set SD is a possible design of measurements, which is analysed in Step 3.

3.2.3.4 Step 3: Ranking the possible designs

In this step, measurements are placed at all the locations in each and every subset of the set of possible designs. Then, a Monte Carlo simulation of state estimation is performed for each of the possible designs and all the possible designs are ranked based on the best value of the objective function. The top 10 designs in this research are considered as the “good enough” solutions of the problem of measurement placement (Singh et al. 2011).

3.3 Case study

Two simulation models were developed in MATLAB based on the algorithm shown in Figure 3.4 in order to study the problem of measurement placement in power distribution networks. The purpose of each simulation model is as follows:

- Simulation model 1 (individual measurement placement)

  The first simulation model was developed for placement of ***additional*** individual measurements within the network in order to ensure that the simulation model and the algorithm of measurement placement are reliable and their performance is satisfactory. The probability based objective function, i.e. Equation (3-2), was considered for selection of individual measurement sets. The validation of this simulation model was performed through comparison of the output results of it with the results presented in (Singh et al. 2011), which studied addition of individual measurements. In this simulation model possible locations for placing additional meters are voltage magnitude of all the buses of the network (except the slack and the generation buses) and power flow of all the lines except the lines connected to the slack and the generation buses, i.e. lines 1-2, 1-85, 18-19 and 59-82.

- Simulation model 2 (measurement unit placement)

  This simulation model was developed to study placement of ***additional*** measurement units within the network. The core of this simulation model is similar to Simulation model 1 after validation; however, possible locations for placement of additional measurement units differ. Also, the both objective functions explained previously, i.e. Equations (3-2) and (3-11), were "separately" implemented and considered as the decision criterion for selection of locations for addition of specific number of measurement units. In other words, the problem of measurement unit placement in each case was solved two times, each time one of the objective functions was considered. Finally, the performance of the objective functions was compared against each other.

The case study test distribution network along with the assumptions of the measurements and of the algorithm of meter placement is explained in the subsections.

3.3.1 Test network

The case study is the UKGDS 95-bus test network operating at 11 kV. The data of the network as well as the loading condition are the same as described in section 2.5. The one line diagram of the network is shown in Figure 3.5.

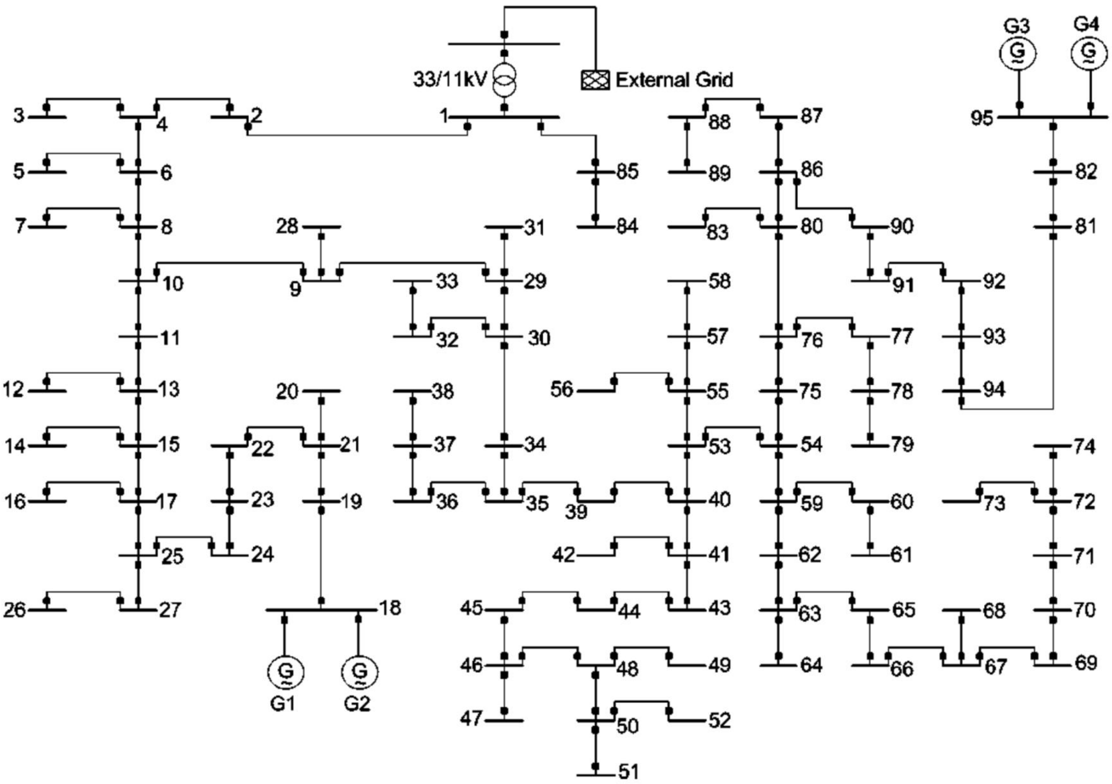

Figure 3.5: The one line diagram of the UKGDS 95-bus test distribution network[1]

3.3.2 Measurements[2]

It is assumed the network is already equipped with real time measurements of voltage magnitude at the slack bus, i.e. bus #1, and the generation buses, i.e. buses #18 and #95. Additionally, real time power flow measurements existed on the lines connected to the slack and the generation buses, i.e. lines 1-2, 1-85, 18-19 and 59-82.

[1] The Figure is taken from (Singh et al. 2011). The squares show the location of all the possible real time individual measurements in that paper.

[2] The measurement assumptions are taken from (Singh et al. 2011) for comparison purposes.

The accuracy of all the available and additional real time measurements of voltage magnitude, power flow and power injection is 3% and the accuracy of all the pseudo measurements of loads is 50%. Furthermore, the standard deviation of all the measurements was calculated using Equation (2-13) based on a 95% confidence level. The variance of zero injection measurements is assumed to be 1.0×10^{-12}. Also, all the measurements are normally distributed and are produced using the normrnd function of MATLAB.

3.3.3 Assumptions of the algorithm

The following assumptions were made for the algorithm of measurement placement:

- The WLS based SE algorithm incorporated all the pseudo and virtual measurements.

- The network is studied at the peak load conditions based on the half hourly data taken from (Control & Power Research Group 2015).

- 10 Monte Carlo simulations were used for Step 1.2 and 100 Monte Carlo simulations were performed for Step 3 (according to Figure 3.4) (Singh et al. 2011).

- Assumed values for $CL_{PS} = 0.99$, $\alpha = 0.1\%$, $\varepsilon_V = 1\%$ and $\varepsilon_\theta = 5\%$.

3.4 Results and discussion

Table 3.7 shows the description of the simulation models that were developed for investigating the problem of placement of additional measurements within a power distribution network.

Table 3.7: The description of the developed simulation models for placement of additional measurements

Simulation model	Description of the simulation model
Simulation model 1	Placement of additional individual measurements
Simulation model 2	Placement of additional measurement units

In the following subsections the results that were obtained using the simulation models are presented.

3.4.1 Optimal placement of additional individual measurements (Simulation model 1)

Three cases were defined to investigate optimal placement of 3, 4 and 5 additional individual measurements. The best individual measurements suggested by the algorithm, i.e. those which had the maximum probability of the state parameters of the network falling within the desired ranges, were considered as the solution of the problem. Table 3.8 shows the comparison of the solution of the problem in each case study with the solution of (Singh et al. 2011) (The solutions of (Singh et al. 2011) are displayed in "TABLE II" in that paper). The values of the objective function of the simulation model (Equation (3-2)) are also presented in Table 3.8 and are compared against the values of the objective function of (Singh et al. 2011).

Table 3.8: Comparison of the solutions of Simulation model 1 with (Singh et al. 2011)

N_K*	Value of the objective function		Solution	
	(Singh et al. 2011)	Simulation model 1	(Singh et al. 2011)	Simulation model 1
3	0.9149	0.8607	$V_{89}, PQ_{f\ 10-11}, PQ_{f\ 54-75}$	V_{48}, V_{51}, V_{52}
4	0.9272	0.8872	$V_{89}, PQ_{f\ 17-25}, PQ_{f\ 34-35}, PQ_{f\ 76-80}$	$V_{27}, V_{42}, V_{47}, V_{49}$
5	0.9676	0.9071	$V_2, V_3, V_{89}, PQ_{f\ 17-25}, PQ_{f\ 34-35}$	$V_{34}, V_{37}, V_{44}, V_{51}, V_{52}$

*: $\boldsymbol{N_K}$ represents the number of additional individual measurements.

As can be seen from Table 3.8 the values of the objective function for the solution increase as the number of additional individual measurements increases. This is expected since the probability of more accurately estimation of the state parameters of the network increases by placing more individual measurements within the network. However, the values of the objective functions, i.e. the probability of falling of the state parameters within the desired ranges, differ between (Singh et al. 2011) and Simulation model 1, which is due to the difference in the equation of probability distribution function. Additionally, as can be observed the solutions of (Singh et al. 2011) are a mixture of voltage magnitude and power flow measurements while the solutions of Simulation model 1 are just voltage magnitude measurements. The difference between the solutions of (Singh et al. 2011) and Simulation model 1 may also be due to the following:

- The stochastic nature of the problem and low number of Monte Carlo simulations;
- The difference in probability distribution functions;
- Large number of reasonably "good" solutions (the ordinal optimisation technique does not guarantee a global solution (Singh et al. 2011)).

Figure 3.6 compares the performance of the solution measurement sets of (Singh et al. 2011) and Simulation model 1 in terms of the values of MAPE of estimation of voltage magnitudes and voltage angles of the buses through 50000 Monte Carlo simulations of state estimation. Table 3.9 shows the measurement sets used to equip the network for each case. The accuracies of the measurements are the same as those explained in section 3.3.2. Justification of 50000 Monte Carlo simulations is presented in section 3.4.3.

Table 3.9: Measurement sets for evaluation of the performance of Simulation model 1

Measurement type	Measured parameter	(Singh et al. 2011) solution	Simulation model 1 solution
Real time	Voltage magnitude at the slack (bus #1) and generation buses (#18 and 95)	✓	✓
	Power flow of branches connected to the above buses, i.e. branches 1-2, 1-85, 18-19 and 82-95	✓	✓
	Additional solution measurement sets (corresponding to Table 3.3)	Column "(Singh et al. 2011)"	Column "Simulation model 1"
Pseudo	Power injections at load nodes	✓	✓
Virtual	Zero injections	✓	✓

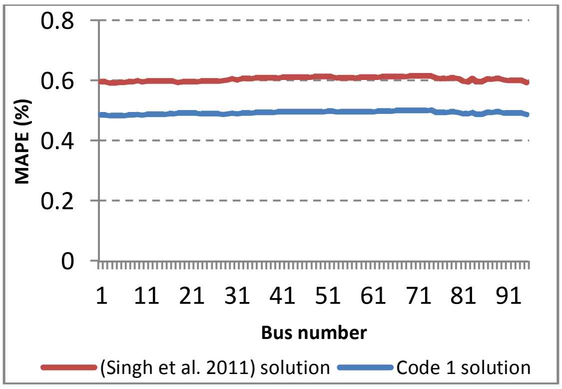

(a) MAPE of estimation of voltage magnitude (for $N_K = 3$)

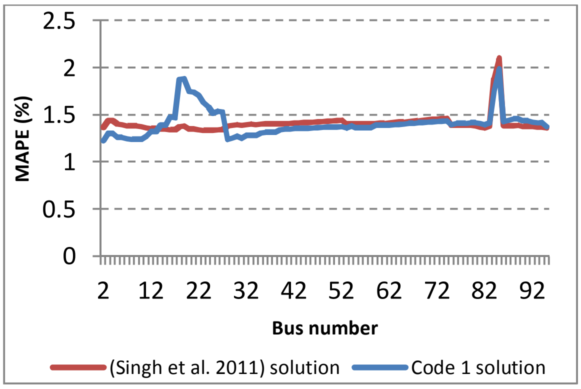

(b) MAPE of estimation of voltage angle (for $N_K = 3$)

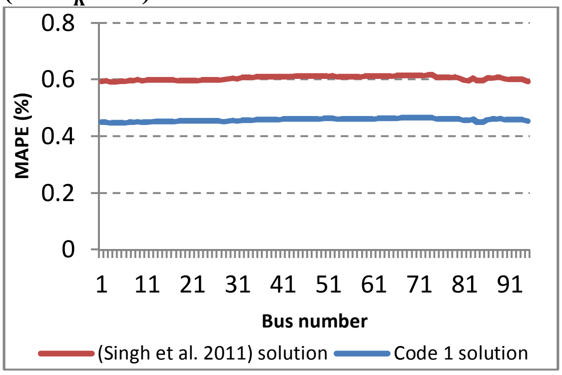

(c) MAPE of estimation of voltage magnitude (for $N_K = 4$)

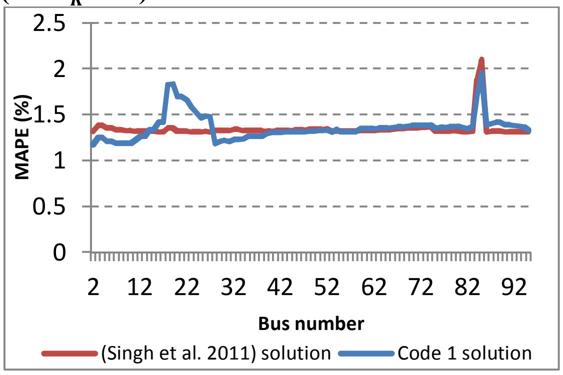

(d) MAPE of estimation of voltage angle (for $N_K = 4$)

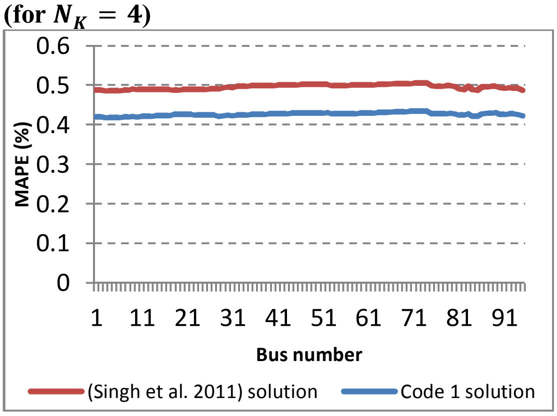

(e) MAPE of estimation of voltage magnitude (for $N_K = 5$)

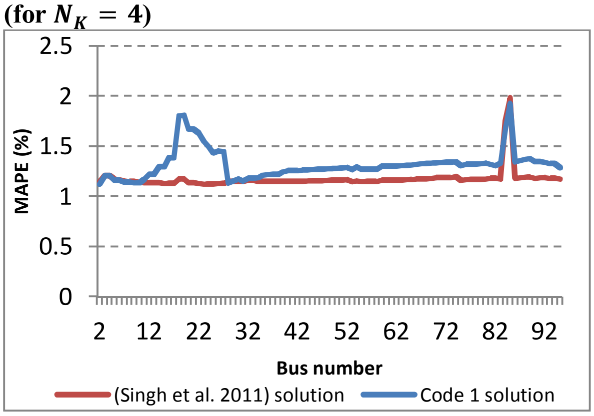

(f) MAPE of estimation of voltage angle (for $N_K = 5$)

Figure 3.6: Comparison of the values of MAPE of estimation of the state parameters for Simulation model 1

As can be seen from Figures 3.6 (a), (c) and (e) the values of MAPE of estimated voltage magnitudes for the network equipped with the solution measurements of Simulation model 1 are slightly less than the values of MAPE of estimated voltage magnitudes for the network equipped with the measurements obtained in (Singh et al. 2011).

Figures 3.6 (b), (d) and (f) show that the values of MAPE of estimated voltage angles of both the solutions of Simulation model 1 and (Singh et al. 2011) are identical in almost all the buses except for approximately 20 buses (buses #10-30), where the values of MAPE for the case of the solutions of (Singh et al. 2011) are slightly less than the MAPE values of the case of the solutions of Simulation model 1.

It can be concluded that although the solutions of Simulation model 1 do not agree with the solutions of (Singh et al. 2011), the performance of both agree in terms of the values of MAPE of estimation of the state parameters of the network through a Monte Carlo simulation.

Additionally, the values of MAPE of estimation of the state parameters for the network equipped with the solutions of Simulation model 1 are replotted in Figure 3.7. This is performed in order to observe the improvement in estimation of the state parameters by increasing the number of additional individual measurements. As can be seen from Figure 3.7, addition of only 3 individual measurements has improved estimation of voltage magnitude and voltage angle relative to the base case, where the network is not equipped with the additional measurements. However, the addition of more individual measurements demonstrates insignificant improvement in estimation of the state parameters. Also, as is observed placement of voltage magnitude measurements has slightly improved estimation of the voltage angles.

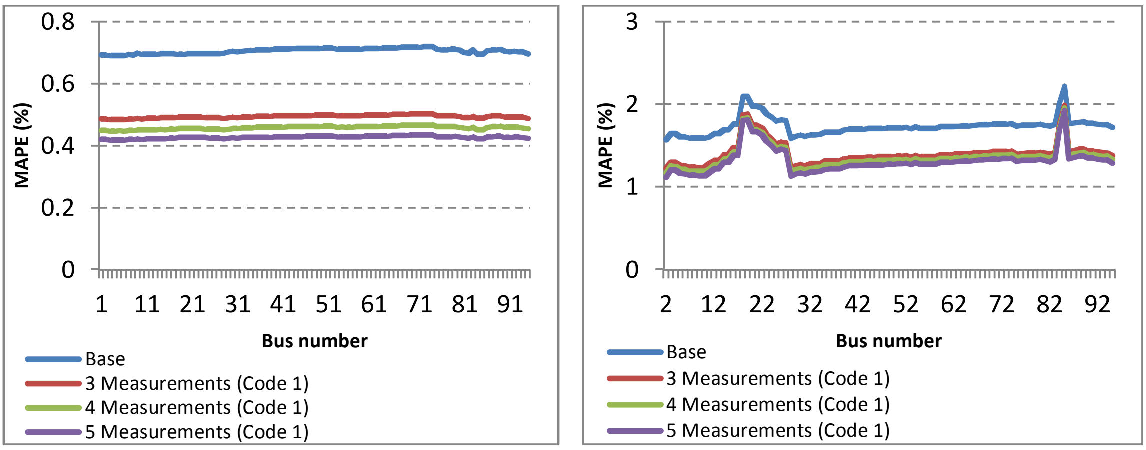

(a) Estimation of voltage magnitude **(b) Estimation of voltage angle**

Figure 3.7: Improvement in estimation of the state parameters by increasing the number of additional individual measurements

Based on the explanation it can be concluded that the performance of Simulation model 1 is satisfactory and it proposes proper places for ***additional*** individual measurements.

3.4.2 Optimal placement of additional measurement units (Simulation model 2)

Three cases of the addition of 1, 2 and 3 measurement units were studied using Simulation model 2. The simulation model has the same logic as Simulation model 1, however, the buses of the network are considered as the possible locations for placement of additional measurement units, which measure the voltage magnitude of the bus and the power flow of the branches connected to the bus. Simulation model 2 has the capability to use two different objective functions as follow:

- maximising the probability of estimation of the state parameters within the desired ranges; and

- minimising the accuracy index.

The formulation of the objective functions were explained in sections 3.2.2.1 and 3.2.2.2. Table 3.10 shows the solution of the problem in terms of the bus numbers at which the additional measurement units were suggested to be placed by the simulation model for each objective function. Table 3.10 also presents the meters within each measurement unit as well as the values of the objective functions.

Table 3.10: Solutions of Simulation model 2 for placement of additional measurement units

N_K*	Value of the objective function	Bus(es)#**	Each RTU consists of the following meters	Approach
1	0.7796	84	$V_{84}, PQ_{j\ 84}, PQ_{f\ 84-85}$	Maximising the probability of estimation within a range
2	0.8492	84 10	$V_{84}, PQ_{j\ 84}, PQ_{f\ 84-85}$ $V_{10}, PQ_{f\ 10-8}, PQ_{f\ 10-9}, PQ_{f\ 10-11}$	
3	0.8878	84 10 72	$V_{84}, PQ_{j\ 84}, PQ_{f\ 84-85}$ $V_{10}, PQ_{f\ 10-8}, PQ_{f\ 10-9}, PQ_{f\ 10-11}$ $V_{72}, PQ_{f\ 72-71}, PQ_{f\ 72-73}, PQ_{f\ 72-74}$	
1	0.0054	40	$V_{40}, PQ_{f\ 40-39}, PQ_{f\ 40-41}, PQ_{f\ 40-53}$	Minimising the accuracy index of state estimation
2	0.0043	40 74	$V_{40}, PQ_{f\ 40-39}, PQ_{f\ 40-41}, PQ_{f\ 40-53}$ $V_{74}, PQ_{j\ 74}, PQ_{f\ 74-72}$	
3	0.0035	40 74 73	$V_{40}, PQ_{f\ 40-39}, PQ_{f\ 40-41}, PQ_{f\ 40-53}$ $V_{74}, PQ_{j\ 74}, PQ_{f\ 74-72}$ $V_{73}, PQ_{j\ 73}, PQ_{f\ 73-72}$	

*: $\boldsymbol{N_K}$ represents the number of additional measurement units.

**: Measurement units are placed at these bus(es).

As it was expected in both approaches the values of the objective functions improve with addition of measurement unit in the expected direction. In the approach based on maximising the probability of estimation of the state parameters within ranges the values of the objective function increase with increase in the number of additional measurement units. This means that the probability of more accurately estimation of the state parameters within the ranges increases as the number of measurement units increases. In the second approach, which is based on minimising the accuracy index of estimation, the values of the objective function decrease by increasing the number of additional measurement units. This is due to the fact that the accuracy index, which is an indication of the error of estimation, decreases by increasing the number of additional measurement units.

Figure 3.8 shows the comparison of the performance of the solutions of Simulation model 2 between the two approaches in terms of the values of MAPE of estimation of the state parameters through 50000 Monte Carlo simulations of state estimation. In each case the additional measurement units consisting of the individual meters, which were presented in Table 3.10, are placed within the network in addition to the full measurements at the slack and the generation buses. The justification of the number of Monte Carlo simulations, i.e. 50000, is presented in section 3.4.3.

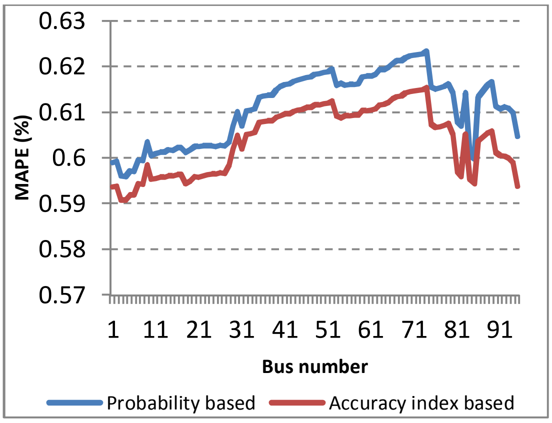

(a) MAPE of estimation of voltage magnitude (for $N_K = 1$)

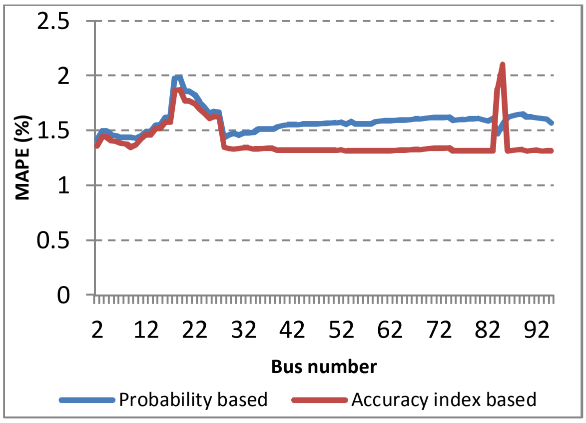

(b) MAPE of estimation of voltage angle (for $N_K = 1$)

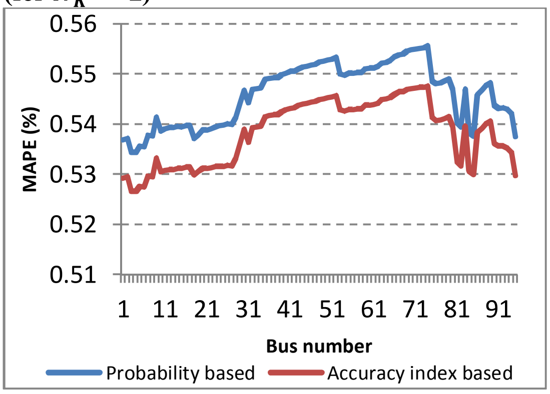

(c) MAPE of estimation of voltage magnitude (for $N_K = 2$)

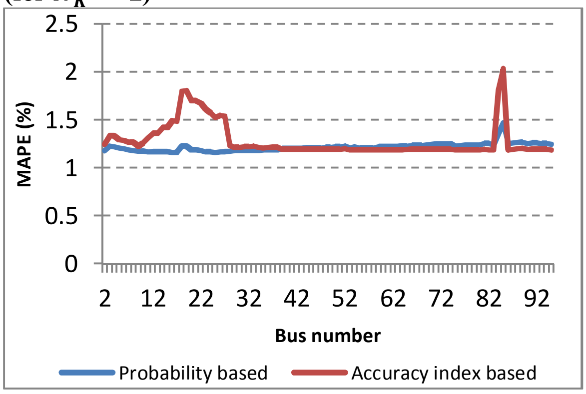

(d) MAPE of estimation of voltage angle (for $N_K = 2$)

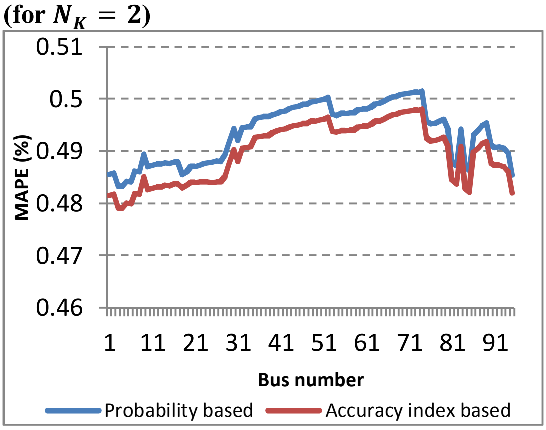

(e) MAPE of estimation of voltage magnitude (for $N_K = 3$)

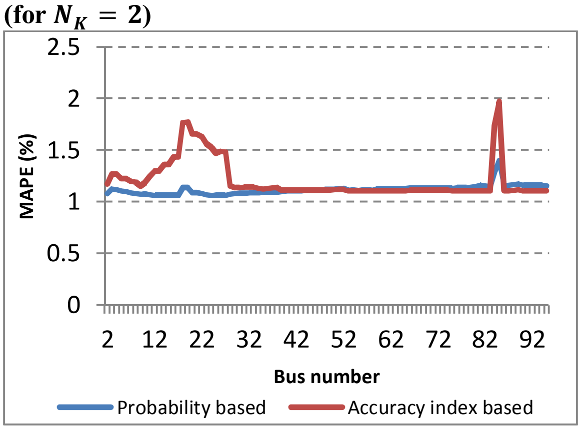

(f) MAPE of estimation of voltage angle (for $N_K = 3$)

Figure 3.8: Comparison of the values of MAPE of estimation of the state parameters for Simulation model 2

As can be seen from Figure 3.8, the values of MAPE of the estimated state parameters for both approaches are quite similar and close, although the accuracy index based approach shows MAPE values slightly less than the probability based approach especially in estimation of voltage angles of bus numbers approximately in the range of 10-30.

It can be concluded that although the solution measurement sets suggested by the two approaches do not agree, the performance of them agree in terms of the values of the MAPE of estimation of the state parameters of the network. Therefore, both approaches are supporting the results of one another and therefore both of them can be relied on and be applied for finding suitable places for additional specific number of measurement units in power distribution networks.

Figure 3.9 presents the improvement in estimation of the state parameters with increasing the number of measurement units for the accuracy index based approach. As can be seen and is expected the values of MAPE of estimation of the state parameters steadily decrease by increasing the number of additional measurement units. This implies that if a specific accuracy index is expected to be achieved, the number of measurement units needs to be increased until the target is met.

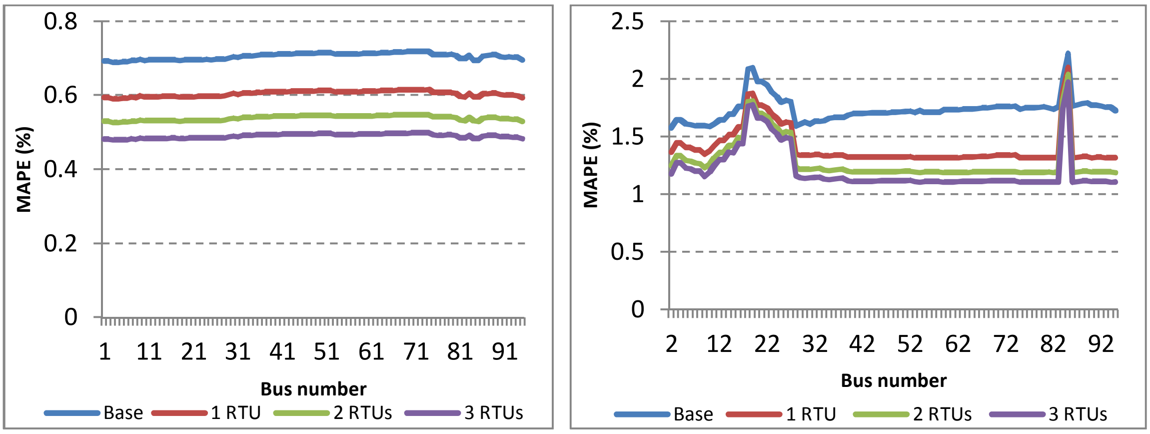

(a) Estimation of voltage magnitude **(b) Estimation of voltage angle**

Figure 3.9: Improvement in estimation of the state parameters by increasing the number of additional measurement units for the approach based on the accuracy index[1]

3.4.3 Suitability of the number of Monte Carlo simulations

In order to ensure that a suitable number of Monte Carlo simulations is performed for evaluating the performance of the selected meters, a criterion (Equation (3-15)) was defined and the change in the value of the criterion with increase in the number of Monte Carlo simulations was observed. The number of simulations started from 30000

[1] The RTU in the figure denotes measurement unit.

and was increased with the steps of 5000. The change in the value of the criterion for the both cases of individual measurement and measurement unit placement is depicted in Figure 3.10.

$$Criterion = \sum_{i=1}^{N_B} (\frac{\varepsilon_\theta}{\varepsilon_V} \times MAPE_{V_i} + MAPE_{\theta_i}) \tag{3-15}$$

The criterion was defined based on the MAPE values of the estimated state parameters. However, the MAPE values of the estimated voltage magnitudes were multiplied by the ratio $\frac{\varepsilon_\theta}{\varepsilon_V}$ in order to consider the effect of the desired ranges of falling of the estimated values of the state parameters. As described before the values of the desired ranges in this research are $\varepsilon_V = 1\%$ and $\varepsilon_\theta = 5\%$.

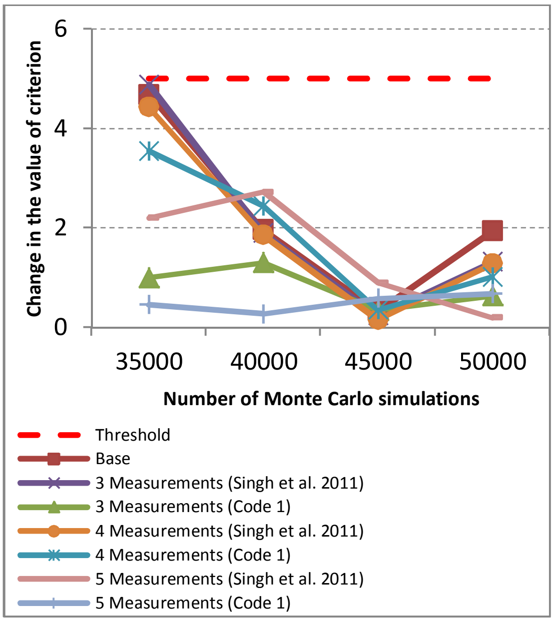

(a) Placement of additional individual measurements

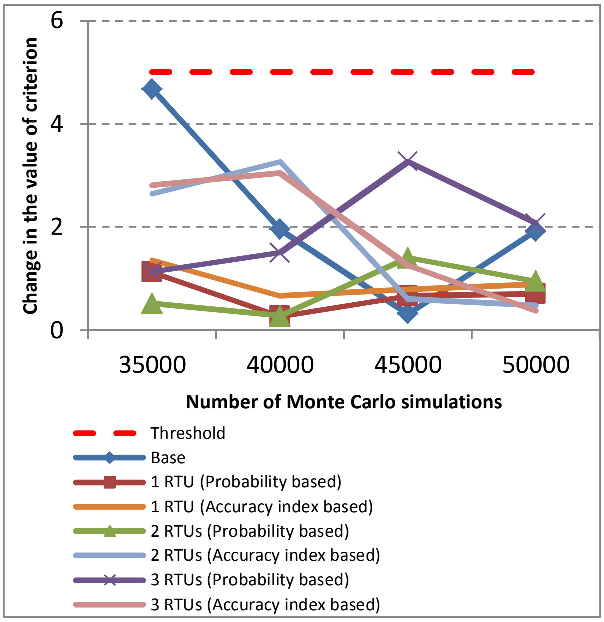

(b) Placement of additional measurement units

Figure 3.10: Change in the value of the criterion with the change in the number of Monte Carlo simulations[1]

As can be observed from Figure 3.10, the change in the value of the criterion was less than 5.0 $(= \frac{\varepsilon_\theta}{\varepsilon_V})$ after several consecutive steps of Monte Carlo simulations. Therefore, 50000 Monte Carlo simulations are large enough for assessment of performance of the solution additional measurement units to be placed within the power distribution

[1] The RTU in the figure denotes measurement unit.

network.

3.4.4 Computation effort

Figure 3.11 shows the computation time for reaching the solution measurement sets for placement of both additional individual measurements and measurement units for comparison with the time requirements presented in Table 3.6 without reduction of the search space. In Figure 3.11(b) for the case of 1 measurement unit, the amount of time is approximately a quarter an hour. This is due to the fact that the algorithm does not go through Step 1.2 (in Figure 3.4), which is performing a set of Monte Carlo simulations for determining possible locations. In other words, the number of possible locations (output of Step 1.1 in Figure 3.4) is bigger than the number of buses, meaning that all the buses must be considered as possible locations.

As can be seen from Figure 3.11 the amounts of time of reaching the solutions are much less than the values presented in Table 3.6, which shows the times for reaching a solution without reduction of the search space. Therefore, the value of application of the ordinal optimisation technique and reduction of the search space is highlighted for the problems of optimisation in really enormous search spaces.

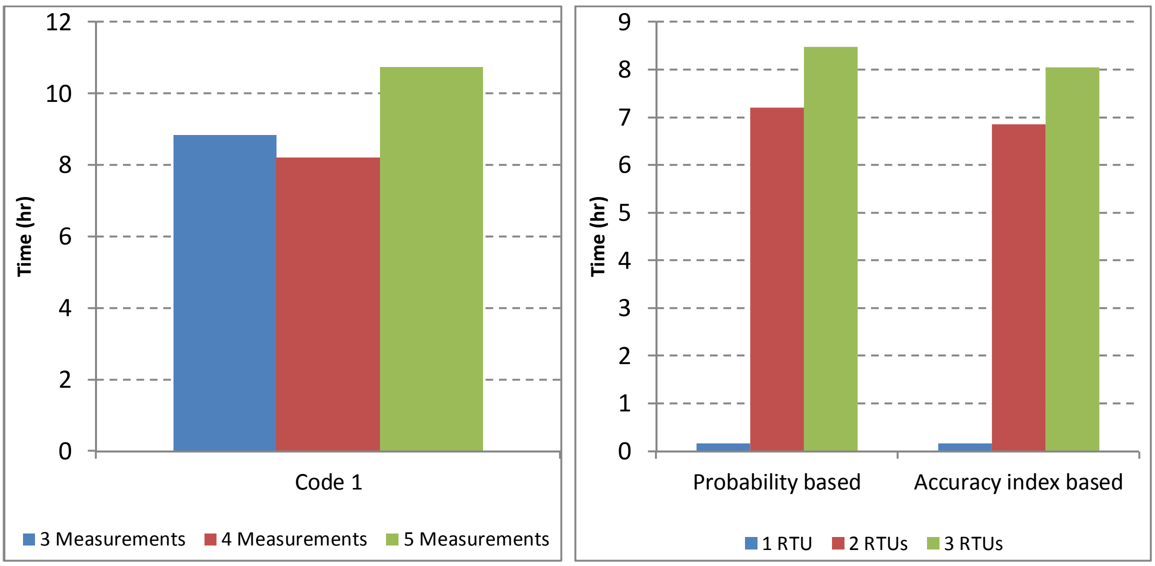

(a) Placement of additional individual measurements **(b) Placement of additional RTUs**

Figure 3.11: Time consumed for reaching the solution of measurement sets[1]

[1] The RTU in the figure denotes measurement unit.

3.5 Conclusions

In this Chapter, placement of additional real time measurements in power distribution networks in order to improve the accuracy of estimation of the state parameters of the network was investigated. An algorithm for placement of a specific number of additional measurements at possible measurement locations within the network was developed. The algorithm (Figure 3.4), which consists of three steps and makes the decision using an objective function, takes advantage of the ordinal optimisation technique in order to reach the solution in the least possible time. The cost, which is the constraint of the problem, is defined in terms of the number of additional measurements to be placed within the network and is determined by the budget of the operator of the network. The UKGDS 95 bus test distribution network at the peak load conditions was considered as the case study.

Two MATLAB simulation models were developed as follows:

- Simulation model 1 (placement of additional individual measurements)

  Simulation model 1 was developed for studying the addition of individual measurements within the network. A new formula for the probability of the estimated state parameters of a power distribution network falling within the desired range was developed and validated against the results obtained from implementing the probability formula presented in (Singh et al. 2011). Three cases of the addition of 3, 4 and 5 individual measurements were studied.
  The solution measurement sets suggested by the algorithm (Table 3.8) were different from the solution measurement sets in that paper (Table II in (Singh et al. 2011)). However, the performance of the solutions of the algorithm using the new probability formula is almost identical to the performance of the results of the paper in terms of the MAPE values of the estimated state parameters of the case study network (Figure 3.6). Therefore, the algorithm as well as the probability function were verified and can be applied for placement of more additional individual measurements within a power distribution network.

- Simulation model 2 (placement of additional measurement units)

  This Simulation model was developed for investigating the problem of placement of additional measurement units. Simulation model 2 has the same algorithm as Simulation model 1, however, the possible locations for placement of additional measurement units are the buses of the network. Also, it is assumed that every measurement unit consists of real time measurements of voltage magnitude and power flow of all the branches connected to the buses including a possible load. Three cases of addition of 1, 2 and 3 measurement units were studied.

  Simulation model 2 has two alternative objective functions, as follows:

  - Probability of the estimated state parameters of the network falling within the desired ranges (based on the new probability formula used in Simulation model 1); and

  - Accuracy index of state estimation.

  The solution sets of the measurement units that were suggested by the two objective functions differ (Table 3.10), however, the performance of the results were almost identical in terms of the values of MAPE of the estimated state parameters of the case study network (Figure 3.8). Therefore, both objective functions were supporting the solutions of one another and either of them can be utilised for finding suitable places for a specific number of additional measurement units to be located on the buses of a power distribution network.

The contribution of the Chapter is summarised as:

- An alternative formulation for probability of the estimated state parameters of a power distribution network falling within desired ranges was developed and validated against the results obtained based on the probability formulation presented in (Singh et al. 2011).

- The algorithm developed for the placement of additional individual measurements was extended for the placement of additional measurement units.

4 Simulation of operation of gas distribution networks with decentralised injection[1]

4.1 Introduction

Future gas distribution networks will have several coupling components with power distribution networks including gas to power conversion components such as gas turbines and power to gas units, which consume power and inject various gases into the gas networks. In order to perform analysis of integrated power and gas distribution networks with distributed generations and estimate the values of state parameters and energy flows in both networks, analysis of gas distribution networks is investigated first. For this purpose simulation of gas distribution networks and evaluation of impact of decentralised injection on their operation are investigated in this Chapter. Then, in the next Chapter state estimation of these networks is studied.

In this Chapter an overview of the fundamentals of operation of gas networks is presented. Then, the benefits and challenges of decentralised injection of alternative gases into gas distribution networks are reviewed, which is followed by a literature survey on the topic. Then, the formulation and the algorithm used in the simulation model developed in MATLAB for simulation of operation of gas distribution networks with decentralised injection are explained. Afterwards, a case study network is presented and the developed simulation model is validated against the commercial software Synergi Gas. Finally, the impact of decentralised injection of alternative gases on the operation of the case study gas distribution network is evaluated.

4.1.1 Fundamentals of operation of gas networks

The schematic of operation of gas networks is shown in Figure 4.1. As can be seen

[1] "Centralised injection" refers to injection (supply) of just one type of gas, normally natural gas, from one place (the main supply node) into the gas network. Whereas, "decentralised injection" refers to injection of different types of gases from one or more points within the network into the network in addition to the main supply. This definition has an analogy with distributed generation in power systems.

natural gas is provided either from gas wells after being processed or from import. Then, it is pressurised by means of gas compressors and injected into the transmission network, which operates in high pressure level (95-38 bar). In the transmission network gas compressor stations are utilised in order to compensate for the pressure losses of gas flow due to the friction inside the gas pipelines since the transmission network is spread over a nation.

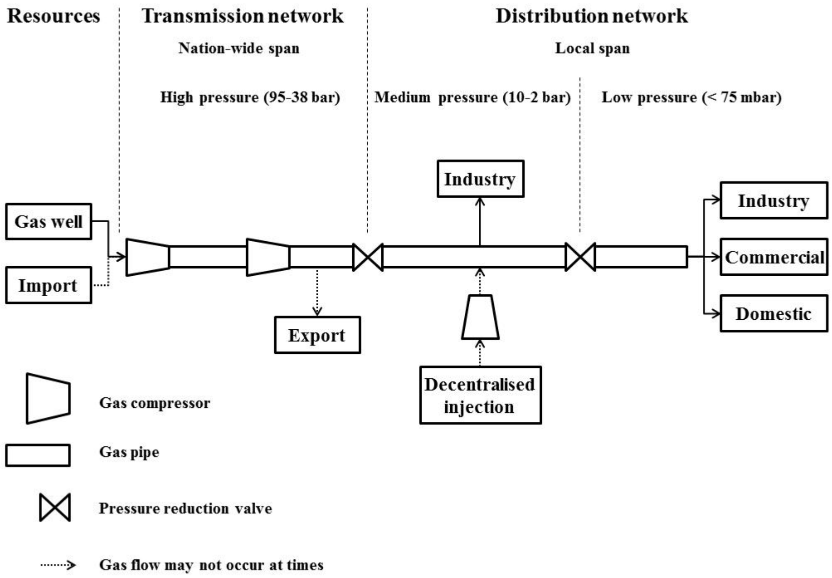

Figure 4.1: The schematic of operation of gas networks

After the transmission network, the gas passes through pressure reduction valves and the pressure is reduced to the medium pressure range (10-2 bar) for the distribution network. In the entrance of cities, the pressure is further reduced to 75 mbar and the low pressure gas is supplied to the commercial and domestic users as well as the industrial users in the suburbs.

"Natural gas" is a mixture of several gas components. The typical components of natural gas as well as their molar fraction are shown in Table 4.1. The components and the molar fractions are different in different countries based on their regulations. However, the ranges are normally close to the values shown in Table 4.1.

Table 4.1: The typical components and the molar fractions of natural gas[1]

Component	Chemical symbol	Typical analysis (mole %)	Range (mole %)
Methane	CH_4	95.0	87.0-97.0
Ethane	C_2H_6	3.2	1.5-7.0
Propane	C_3H_8	0.2	0.1-1.5
Butane	C_4H_{10}	0.03	0.01-0.3
Pentane	C_5H_{12}	0.01	trace[2]-0.04
Hexanes plus[3]	$(C_6H_{14})^+$	0.01	trace-0.06
Nitrogen	N_2	1.0	0.2-5.5
Carbon dioxide	CO_2	0.5	0.1-1.0
Oxygen	O_2	0.02	0.01-0.1
Hydrogen	H_2	trace	trace-0.02

In the conventional system of operation of the gas networks, natural gas is injected from one or several points into the transmission network. However, several other types of gases, referred to as alternative gases, are produced and decentralised injected into the medium pressure level of gas distribution networks. These gases include Biogas, Methane and Hydrogen. In the next sections the advantages and challenges of decentralised injection of alternative gases into the gas networks is studied.

4.1.2 Advantages of decentralised injection of alternative gases

Several alternative gases are injected into gas distribution networks from various sources. Power-to-gas units convert electricity into hydrogen through electrolysis process. Sometimes they inject the produced hydrogen directly into gas networks and sometimes they produce methane from the hydrogen through methanisation process and inject the generated methane. On the other hand, several other alterative gases including biogas and shale gas are injected into gas networks directly from the places they are produced, processed or imported. There are several advantages for injection of various alternative gases into gas networks as follows:

[1] (UnionGas 2016)

[2] “A trace gas is a gas that makes up an extremely small portion of a mixture of gases”. (The definition quoted from (Climate Change Guide 2016))

[3] It means the hydrocarbons that are heavier than Hexane (C_6H_{14}).

- Making use of the excess of the generated power

  Power distribution networks take advantage of incorporating renewable generation such as solar or wind, which produce electricity intermittently and may generate power more than the demand power at times. Conversion of the excess power produced from distributed generations to an alternative gas and injection of the produced gas into the gas network is one of the efficient ways of abatement of waste of generated power (Qadrdan et al. 2015).

- Reduction of the carbon footprint of gas networks

  Injection of alternative gases, which are produced from renewable energy sources rather than extraction from natural resources, reduces the carbon footprint of the network and consequently the GHG emissions (Abeysekera et al. 2014).

- Storage of excess power in the form of an alternative gas in gas networks

  Storage of generated excess power from renewable energy sources such as wind and solar in power networks needs spacious electric batteries. Whereas, it can be converted into alternative gases and be stored and transported via gas networks to the consumption places and either be used directly or converted back to electricity there (Qadrdan et al. 2015).

- Security of supply

  Possibility of injection of several alternative gases in accordance with gas network regulations enables the network not to rely on solely a few options. In this way extraction from natural limited resources decreases and also there is always some sort of energy carrier in the form of gas to supply the end user.

4.1.3 Challenges of decentralised injection

A few advantages of injection of alternative gases into gas networks were briefly reviewed. On the other hand, there are some challenges associated with decentralised injection of alternative gases into gas networks, as follows:

- Regulations

  - HSE issues

    Injection of easily flammable gases such as Hydrogen can be really dangerous to the network. Regulations have been established in order to guarantee safe and secure operation of the network while injections occur. Therefore, requirements for ensuring safety of the network as well as of the customer shall be met (HSE 1996).

  - The quality of the gas and billing

    When injections of different gases from various points within the network take place and the gases mix in the pipes, this affects the quality of the gas in terms of the calorific value and thus the final energy delivered to the end user.

    The delivered energy is evaluated and checked by Wobbe Index of the gas mixture. Currently, regulations enforce the gas distribution operators in the UK to provide the final customers with a gas mixture with Wobbe Index in the range of 47.2-51.0 MJ/m^3 (HSE 1996). The operators of gas networks bill the customers based on the calorific value or equivalently the Wobbe Index of the gas they deliver to the customers.

- Impact on the operation of the network

  Injection of various gases from different sources intermittently affects the direction of gas flow in pipes, which consequently influences quality of gas as well as the pressure profile within the network. The operators usually suffer from uncertainty of their knowledge of the state of pressures, flows and gas compositions within the network in the time of injection from several sources. This will have impact on operation, control and management of the gas distribution network accordingly and make the situation more challenging.

4.1.4 Literature review

Several commercial tools are developed in order to help the operators of gas networks with simulation and analysis of the operation of their network. These tools along with their developers are listed in Table 4.2. The tools carry out simulation of gas networks with decentralised injection of several alternative gases and calculate the state of pressures and flows as well as the quality of the gas.

Table 4.2: Some commercial tools suitable for simulation of operation of gas networks with decentralised injection

Commercial software	Developer(s)
SIMONE (Liwacom 2016)	Liwacom Informationstechnik GmbH, Germany SIMONE research group, Czech Republic
Synergi Gas (DNV.GL 2016a)	DNV GL, Norway
SPS (Stoner Pipeline Simulator) (Automind 2016)	Automind, Brazil (Links to DNV GL)
PSIganesi (PSI 2016)	PSI, Germany
SmartSim (Schley and Fiebig 2014) GasCalc (E.ON 2016)	E.ON Technologies GmbH, Germany Ruhr University Bochum, Germany
STANET (Fischer-Uhrig Engineering 2016)	Fischer-Uhrig Engineering, Germany
Pipeline Studio (EnergySolutions 2016)	Energy Solutions International, USA

Simulation and state estimation of gas networks with changing of the gas quality was performed in (Weimann et al. 1990). They have considered the heating value of the gas as the state parameter in the formulation of the problem. However, in the current research the molar fraction of all the components of the gas mixture has been considered in the vector of the state parameters of the gas network. Once, the values of the molar fraction of all the components are calculated the heating values as well as the values of all the rest of the thermal properties of the gas mixture can also be obtained.

In addition, effect of injection of several gas mixtures including Hydrogen and upgraded biogas on state parameters of a case study gas distribution network was studied (Abeysekera et al. 2014; Abeysekera et al. 2016b). It was found that injection of a gas mixture with a different composition and lower calorific value accordingly has impact on the operation of the network. This will lower the Wobbe Indices or equivalently the calorific values of the gas composition at nodes, which in turn increases the gas flow rates and consequently decreases the pressures at nodes. In their study the set of nonlinear equations was solved for the values of pressures and specific gravities at nodes. Also they did not demonstrate any validation of results. However, in this study the set of nonlinear equations will be solved for the values of nodal pressures as well as the values of molar fractions of different gas components at nodes. Also validation of the developed MATLAB simulation model is performed by comparison of the results with the results of Synergi Gas.

The developed simulation model and formulations are used as the basis for state estimation of gas distribution networks with decentralised injection, which is looked at in Chapter 5. Additionally, they are utilised for simulation and state estimation of integrated power and gas distribution networks with distributed generations, which is investigated in detail in Chapter 7.

4.2 Formulation of the problem for simulation of operation of the network

Figure 4.2 shows the algorithm that was developed for simulation of operation of gas networks with decentralised injection. The main inputs to the algorithm include:

- Energy demands;
- Specifications of sources and decentralised injection; and
- The network topology.

In order to simulate the network in steady state conditions two sets of equations were formed as follows:

- Balance of gas volumetric flow at nodes; and
- Balance of mass of components of gas at nodes.

The unknown variables are nodal pressures and molar fraction of components of gas after mixing at the nodes. The developed simulation model, which is constrained to meet the gas power demand at all the load nodes, calculates the values of unknowns through simultaneous solution of the set of above nonlinear equations. Finally, using the calculated values of unknowns the values of gas flow in branches and specific gravity and Wobbe Index of gas mixture at nodes is computed. Wobbe Index is a measure of the energy content of a gas mixture and is calculated as follows:

$$WI = \frac{GCV}{\sqrt{SG}} \tag{4-1}$$

Based on the algorithm in Figure 4.1 a MATLAB simulation model was developed, which simulates the operation of gas networks with decentralised injection. In the following subsections the formulations for formation of the nonlinear equations of balance of gas volumetric flow and mass of components of gas at nodes in addition to the solution method in MATLAB is explained.

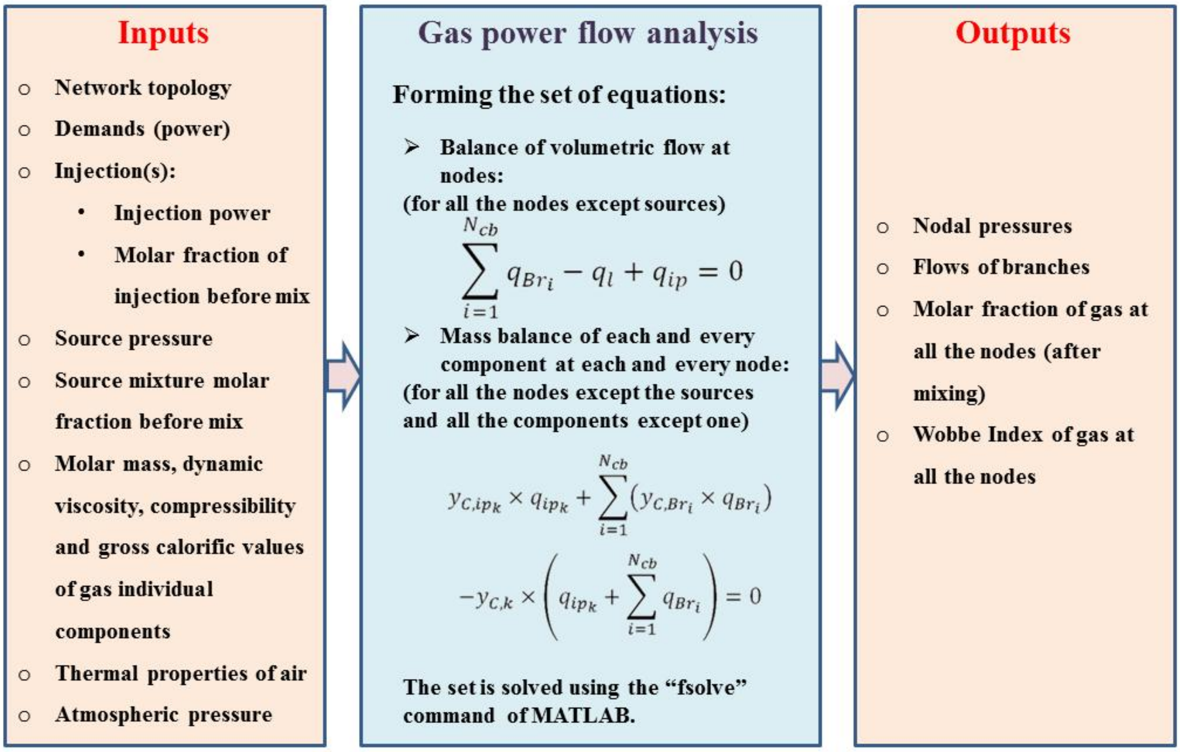

Figure 4.2: The algorithm of simulation of operation of gas networks with decentralised injection

4.2.1 Balance of gas volumetric flow at nodes

The first set of equations, which is written to ensure of the balance of volumetric flow at all the nodes of the network except the source nodes, is as follows:

$$\sum_{i=1}^{N_{cb}} q_{Br_i} - q_l + q_{ip} = 0 \tag{4-2}$$

in which the first term is algebraic sum of all the in-flow (positive sign) and out-flow (negative sign) of gas through the connected branches to the node for which the balance equation is written. In order to form the set, the following two types of flows needs to be calculated, which is explained in the following subsections:

- Flow of branches (q_{Br}); and
- Injection (q_l) or demand (q_{ip}) flows at nodes.

4.2.1.1 Calculation of the gas flow of the branches

The value of gas flow in the STP conditions in a branch connecting the node i to the node k is calculated using the general flow equation (Osiadacz 1987):

$$q = sgn(p_i - p_k) \times \frac{\pi}{8}\sqrt{\mathcal{R}_{air}}\frac{T_n}{p_n}\sqrt{\frac{|p_i^2 - p_k^2|.D^5}{f.SG_{mix}.L.T.\mathrm{Z}_{mix}}} \tag{4-3}$$

The assumptions of the above equation are as follows (Osiadacz 1987):

- Steady state flow conditions;
- Isothermal flow;
- Negligible change of kinetic energy in the pipe;
- Constant compressibility and friction factors along the pipe length;
- Validity of Darcy friction loss relationship;
- Negligible elevation change.

The values of specific gravity (SG_{mix}) and compressibility (Z_{mix}) are calculated for the gas mixture and replaced in the equation. Specific gravity of a gas mixture consisted of N_C components with molar fractions y_i ($i = 1,2, \ldots, N_C$) is calculated using (ISO 1996):

$$SG_{mix} = \frac{\mathrm{Z}_{air}.\sum_{i=1}^{N_C}(y_i.M_i)}{M_{air}.\mathrm{Z}_{mix}} \tag{4-4}$$

in which the compressibility factor of gas mixture (Z_{mix}) is calculated using (ISO 1996):

$$Z_{mix} = 1 - \left(\sum_{i=1}^{N_C} (y_i . c_i) \right)^2 \tag{4-5}$$

where the so-called summation factors (c_i) can be found on page 11 of ISO 9676:1995 (ISO 1996) under the column titled "$\sqrt{b}$" in that Standard. Replacing (4-4) in (4-3) yields:

$$q = sgn(p_i - p_k) \times \frac{\pi}{8} \sqrt{\mathcal{R}_{air}} \frac{T_n}{p_n} \sqrt{\frac{M_{air} . \left| p_i^2 - p_k^2 \right| . D^5}{Z_{air} . f . \sum_{i=1}^{N_C} (y_i . M_i) . L . T}} \tag{4-6}$$

The value of friction factor (f) is calculated based on the Reynolds number of the gas flow:

$$Re = \frac{D . v . \rho_{mix}}{\mu_{mix}} \tag{4-7}$$

The value of the velocity of the gas flow (v) is related to the volumetric flow (q) and cross sectional area (S) by:

$$v = \frac{q}{S} = \frac{q}{(\pi/4) . D^2} \tag{4-8}$$

and the value of density of the gas flow is calculated using the specific gravity of gas mixture (SG_{mix}) and density of air in the STP conditions using:

$$\rho_{mix} = SG_{mix} \times \rho_{air} \tag{4-9}$$

Also the value of dynamic viscosity of the gas mixture can be calculated using the dynamic viscosity of the components at STP conditions, i.e. μ_i $(i = 1,2, \dots, N_C)$ (Vagenes 2011):

$$\mu_{mix} = \frac{\sum_{i=1}^{N_C}\left(\mu_i . y_i . M_i^{0.5}\right)}{\sum_{i=1}^{N_C}\left(y_i . M_i^{0.5}\right)} \tag{4-10}$$

Substituting (4-8), (4-9) and (4-10) in (4-7):

$$Re = \frac{\rho_{air}}{(\pi/4)} \times \frac{q . SG_{mix}}{D} \times \frac{\sum_{i=1}^{N_C}\left(y_i . M_i^{0.5}\right)}{\sum_{i=1}^{N_C}\left(\mu_i . y_i . M_i^{0.5}\right)} \tag{4-11}$$

Once the value of Reynolds number of the gas flow is determined, the value of the friction factor is determined based on the regime of the flow as follows:

- Laminar flow ($Re < 2300$):

$$f = \frac{64}{Re} \tag{4-12}$$

- Turbulent flow ($Re > 4000$):

  This case is more frequent and the friction factor can be calculated using Colebrook's equation (Liu 2013):

$$\frac{1}{\sqrt{f}} = -2 \times log_{10}\left(\frac{\epsilon/D}{3.7} + \frac{2.51}{Re.\sqrt{f}}\right) \tag{4-13}$$

As can be seen the correlation between friction factor and gas flow, i.e. equation (4-6), is not explicit. Hence, in order to find the value of flow having the values of pressures and gas compositions and thus the specific gravity of the mixture (SG_{mix}), the following steps are performed, which are also depicted in Figure 4.3:

(i): Guess a value for flow (q)

(ii): Calculate Reynolds number using equation (4-11)

(iii): Based on the value of Reynolds number, calculate the friction factor using (4-12) or (4-13) (iv): Having the value of friction factor, calculate the new value for flow using (4-6)

(v): If the difference between the new value of the flow in (iv) and the start value of flow in (ii) is within an acceptable tolerance, stop. Otherwise, consider the new value for flow obtained in (iv) and go to step (ii).

In this way the value of flow in the branch can be calculated.

4.2.1.2 Calculation of the gas flow at the load or injection nodes

In order to calculate the value of flow at the load or injection nodes Equation (4-14) is used. It states the correlation of the flow with input gas power to the network at the decentralised injection node or with output gas power from the network at the load nodes:

$$q = \frac{d}{GCV_{mix}} \tag{4-14}$$

in which the gross calorific value of the mixture can be obtained based on the gross calorific values of components at STP conditions (GCV_i for $i = 1, \ldots, N_C$) using (ISO 1996):

$$GCV_{mix} = \frac{\sum_{i=1}^{N_C}(y_i . GCV_i)}{Z_{mix}} \tag{4-15}$$

The values of the input power and gas mixture at injection nodes are known. Therefore, the input flow at injection nodes can be calculated. At the load nodes only the value of demand power is known; however, the values of load flows still can be obtained using Equation (4-14) since the set of nonlinear equations are solved simultaneously starting from a guess value for nodal pressures and gas compositions at the nodes, which are corrected in iterations. Therefore, their values are known and input to the above formulations.

4.2.2 Balance of mass of gas components at nodes

The second subset of equations is written to ensure of the mass balance of each and every component of the gas mixture at each and every node except the pressure source nodes. In other words, the input sum of mass of each and every component from various gas streams into each and every node need to be equal to the output sum of mass of the same component leaving the node. Assuming an ideal mixing at the nodes and neglecting the change in the value of compressibility of each gas component in streams during the ideal mixing at each node, the mass balance equation for each component is converted to an equation written in terms of molar fraction of the component. The representative formulation for this subset of equations for gas component C at the node k is as follows:

$$y_{C,ip_k} \times q_{ip_k} + \sum_{i=1}^{N_{cb}} \left(y_{C,Br_i} \times q_{Br_i} \right) - y_{C,k} \times \left(q_{ip_k} + \sum_{i=1}^{N_{cb}} q_{Br_i} \right) = 0 \qquad (4\text{-}16)$$

It should be noted that injection flow at the node k, i.e. q_{ip_k}, is equal to zero if no injections take place at the node k. Also, the term of flow of branches, i.e. q_{Br_i}, is just considered for the branches that deliver a flow to the node and not for the branches that take flow away from the node.

The sum of molar fraction of all the components at each and every node is equal to one. Therefore, the above equation is written for all the components except one of them. In other words, once the set of all the nonlinear equations is solved simultaneously, molar fractions of all the components except one of them at each and every node is calculated. The value of molar fraction of the last component is obtained by subtracting the summation of known molar fractions from one.

4.2.3 Solution of the set of nonlinear equations

Classification of all the nodes of the network along with their known and unknown parameters is shown in Table 4.3. It should be noted that zero load nodes are considered in Table 4.3 in the category of loads although the value of the load, i.e. the demand gas power, is zero. The unknown parameters in Table 4.3 refer to pressures and gas compositions since the set of nonlinear equations is formed and simultaneously solved primarily for finding their values.

Table 4.3: Type of nodes of a gas network

Node type	Known parameter(s)	Unknown parameter(s)
Source(s)	Pressure Gas mixture	---
Injection(s)	Injection power Gas mixture	Node pressure
Load(s)	Demand power	Node pressure Node gas mixture

As can be seen from the table, the values of pressure and composition of gas are known and fixed for the source nodes. Therefore, the equations of balance of volumetric flow and gas components are written for all the nodes of the network except the sources.

All the inputs to the simulation model include:

- Pressure and gas composition at the source(s);
- Power and gas composition of decentralised injection(s);
- The network topology;
- Gas power demands at the load nodes;
- Atmospheric pressure;
- Thermodynamic properties of all the gas components and air in the STP condition.

Once the two subsets of equations are formed, the whole set of nonlinear equations is solved simultaneously using the “fsolve” command of MATLAB starting from a guess value for nodal pressures and molar fractions of gas compositions.

Regarding the guess values, unlike the flat start in the solution of the problems in power systems, there is not a straightforward clue for the guess values for the state parameters in a problem in gas systems, unfortunately. However, in this research the values of nodal pressures were distributed in the range of approximately 80%-100% of the source absolute pressure in a way that the nodal pressures are all different from one another. Regarding the molar fraction of the components, the guess values of them at all the nodes were very close to the molar fraction of the components at the main source.

The guess values are corrected in each iteration. Therefore, their values are known and input to the formulations explained in previous subsections. The correction of pressures and gas compositions are performed till the convergence occurs; meaning that the operation of the network is feasible and that all the parameters of the network are calculated. The flow chart of the solution of the problem is depicted in Figure 4.3.

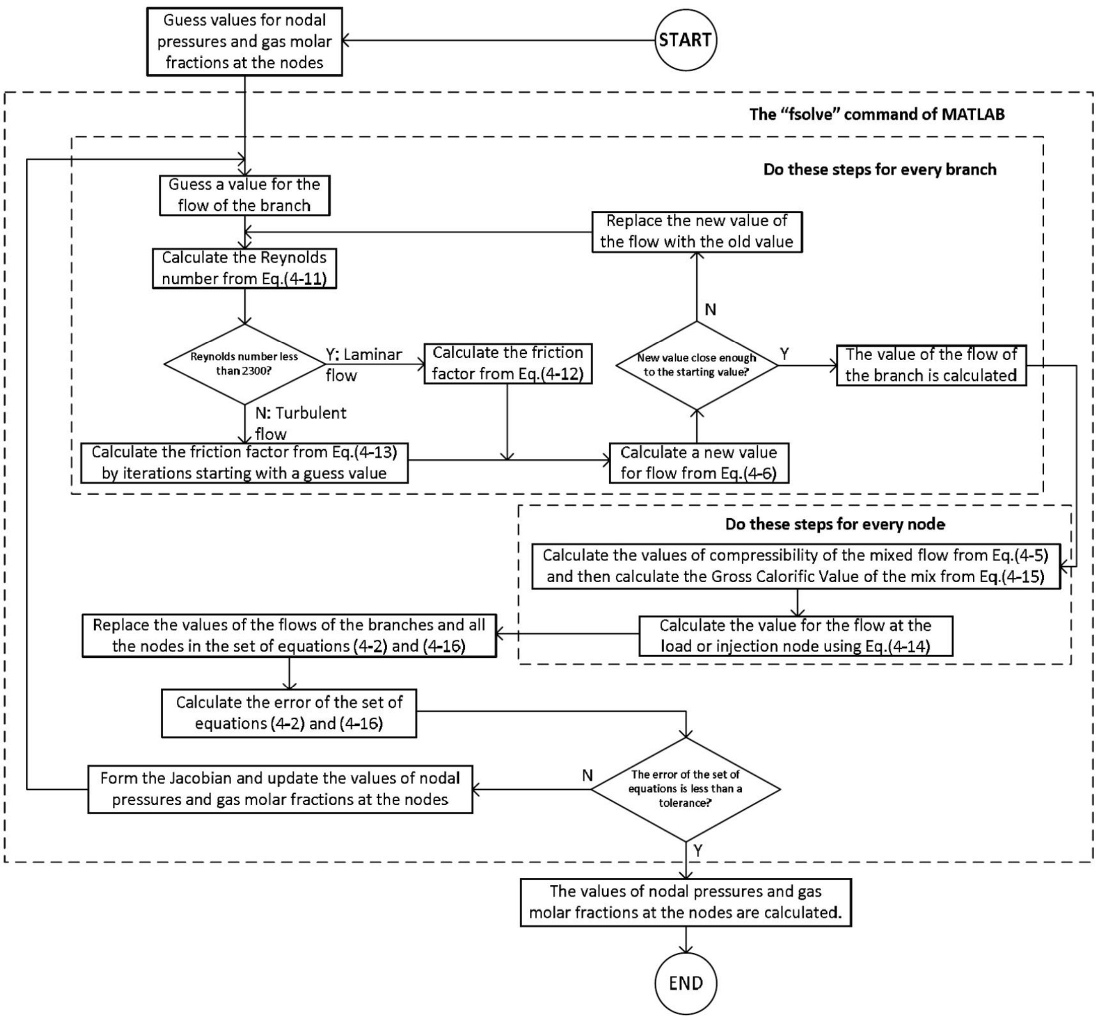

Figure 4.3: The flow chart of the solution of the problem of operation analysis of the gas networks with decentralised injection

Once the set of nonlinear equations is solved and the values of unknown parameters, i.e. pressures and gas compositions, are calculated the values of flow of the branches and the total flow at all the nodes including the source nodes as well as the specific gravities and Wobbe Indices are computed.

4.3 Case study

Figure 4.4 shows the schematic of the network that was considered[1] in order to evaluate the performance of the MATLAB simulation model, which was developed to study the impact of decentralised injection on the operation of gas distribution networks. The gauge pressure at the source node is 75 mbar. As can be seen Network B is the same as Network A except having a decentralised injection at the additional node 12. The topology and specifications of the network are presented in (Abeysekera et al. 2016b) as the network was taken from this reference.

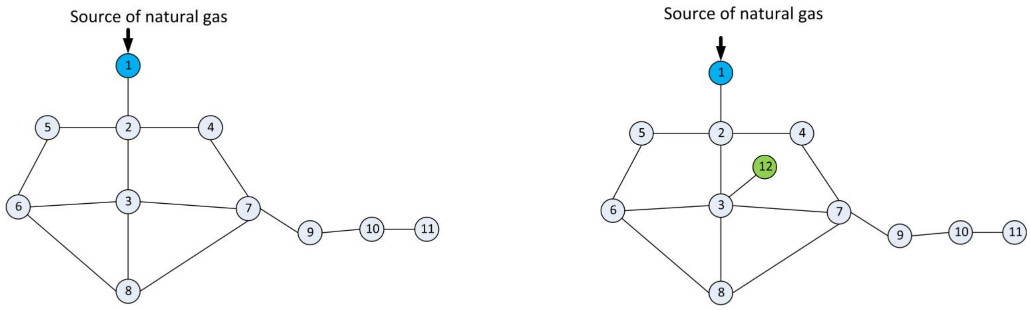

(a): Network A (reference network without decentralised injection)

(b): Network B (network A with a decentralised injection at the additional node 12)

Figure 4.4: Schematic of the gas distribution test network[2]

The case studies that were designed for validation purposes are shown in Table 4.4[3]. As can be observed three cases are considered; the reference Case 1 was established by simulation of the network having a conventional injection of natural gas at the source node. Case 2 is designed in order to investigate injection of upgraded biogas and Case 3 is designed to study injection of Hydrogen at a decentralised node within the network in order to evaluate the impact of the distributed injection of various alternative gases on the operation parameters of the network. The molar fraction of components of different

[1] The test network is taken from (Abeysekera et al. 2016b).

[2] The figure is taken from (Abeysekera et al. 2016b).

[3] The case studies are taken from (Abeysekera et al. 2016b).

gas mixtures are displayed in Table 4.5.

The performance of the developed simulation model and the results obtained were compared and validated with Synergi Gas, which is a commercial tool widely used by gas network operators to control and manage the operation of their network (DNV.GL 2016a). The powerful tool is used for on-line monitoring and control of the gas network and helps the operator of the network to manage the network efficiently and use their assets in an optimised way. The tool is capable of simulation of operation of the transmission level as well as the distribution level in addition to all the connections in the network including gas compressors and valves. Some studies were carried out with the tool for simulation of operation of several gas networks with decentralised injection.

Table 4.4: The case studies

Case study #	Description
1	Injection of natural gas at the source node in Network A
2	Injection of natural gas at the source node plus injection of 200 kW of upgraded biogas at node 12 in Network B
3	Injection of natural gas at the source node plus injection of 200 kW of Hydrogen at node 12 in Network B

Table 4.5: The molar fraction of components in gas mixtures

Gas mixture	Molar fraction of components (%)						
	CH_4	C_2H_6	C_3H_8	C_4H_{10}	CO_2	N_2	H_2
Natural gas	90.0	6.0	1.0	0.5	0.5	2	0.0
Upgraded biogas	94.0	0.0	0.0	0.0	2.5	2.5	1.0
Hydrogen	0.0	0.0	0.0	0.0	0.0	0.0	100.0

4.4 Results and discussion

In this section the results of the application of the developed MATLAB simulation model for simulation of operation of the test network in the three case studies are compared against the results obtained by Synergi Gas. Afterwards, the impact of decentralised injection on the state parameters of the network is evaluated.

4.4.1 Validation with Synergi Gas

The values of the operation parameters of the network, i.e. pressures, flows and gas compositions, calculated by the developed MATLAB simulation model are compared with the results obtained by Synergi Gas for Case 1 in Figure 4.5, for Case 2 in Figure 4.6 and for Case 3 in Figure 4.7. As can be seen the values of pressures and flows are calculated very close to the results obtained by the commercial software. The differences are small. Also, the calculated values of gas compositions are exactly the same as those obtained by Synergi Gas. In this way, the developed simulation model is validated and can be used for further analysis of the operation of gas networks.

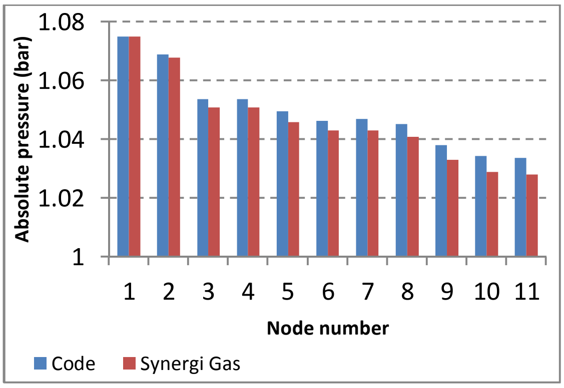

(a) Nodal pressures

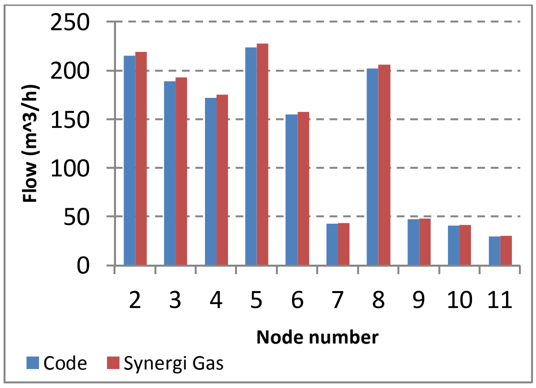

(b) Flow at load nodes

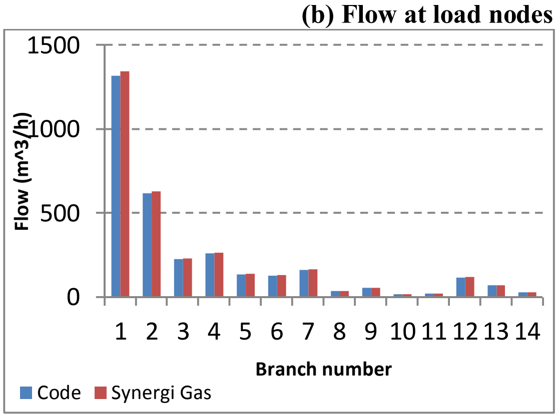

(c) Flow of branches

Figure 4.5: Validation of the simulation model with Synergi Gas for Case 1

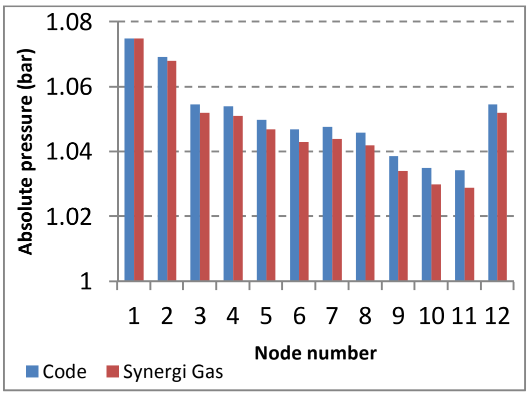

(a) Nodal pressures

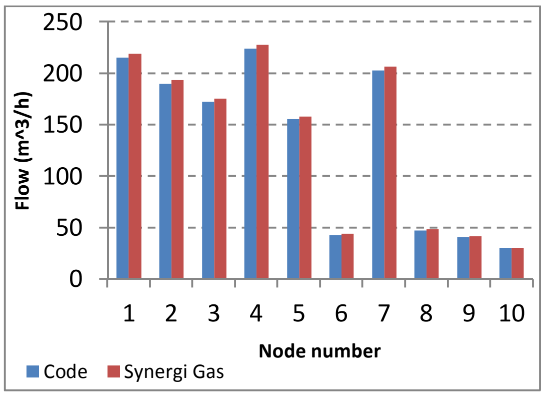

(b) Flow at load nodes

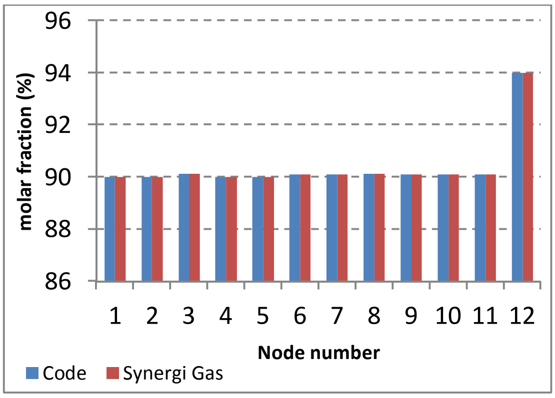

(c) Molar fraction of CH_4 at nodes after mixing

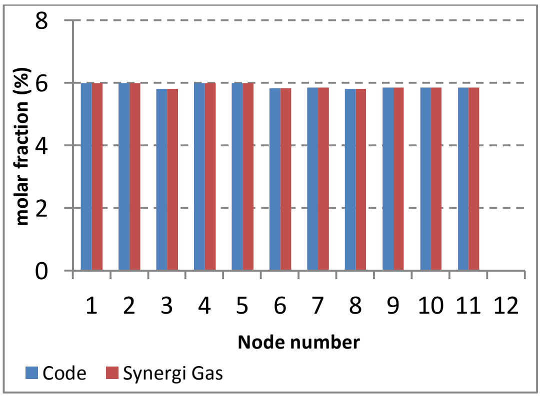

(d) Molar fraction of C_2H_6 at nodes after mixing

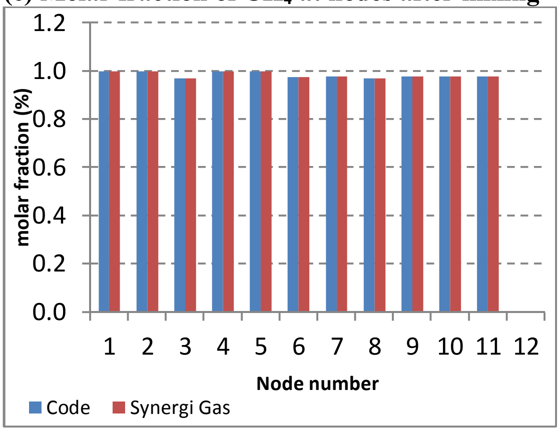

(e) Molar fraction of C_3H_8 at nodes after mixing

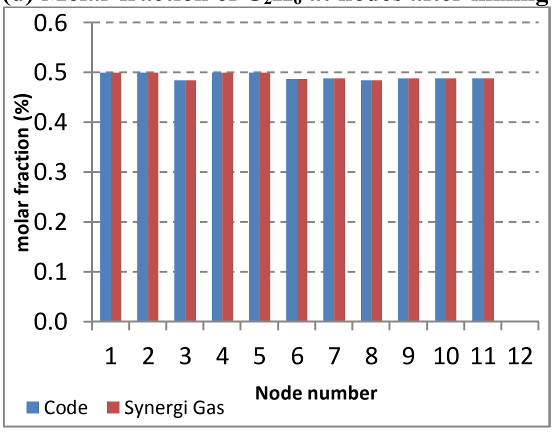

(f) Molar fraction of C_4H_{10} at nodes after mixing

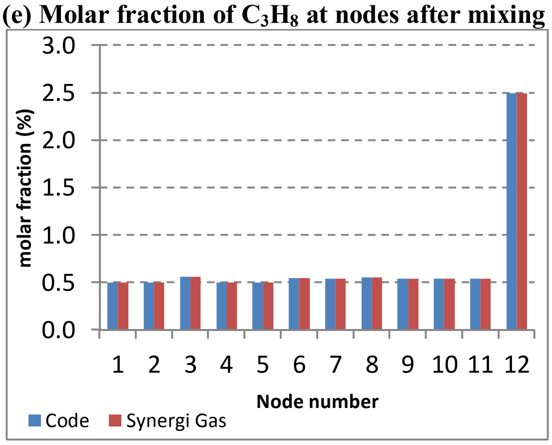

(g) Molar fraction of CO_2 at nodes after mixing

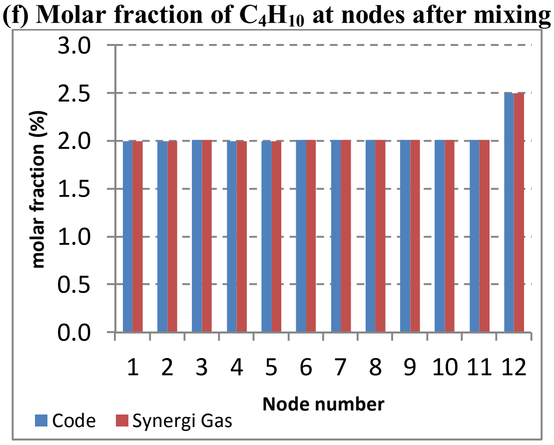

(h) Molar fraction of N_2 at nodes after mixing

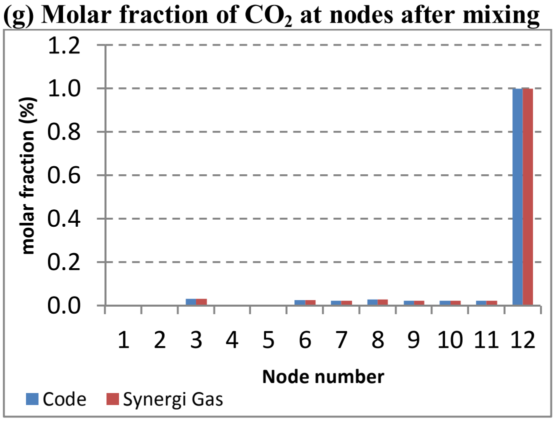

(i) Molar fraction of H_2 at nodes after mixing

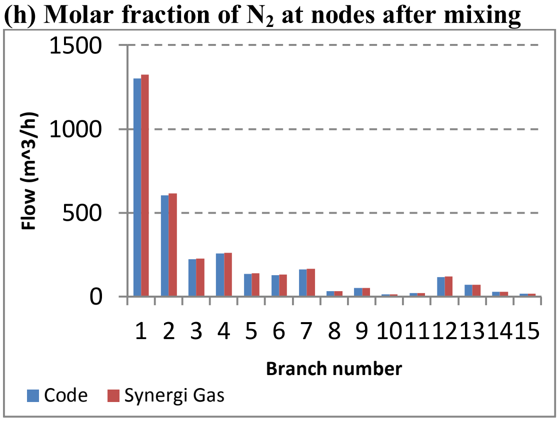

(j) Flow of branches

Figure 4.6: Validation of the simulation model with Synergi Gas for Case 2

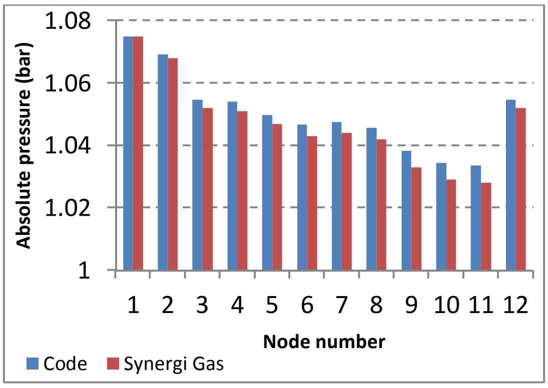

(a) Nodal pressures

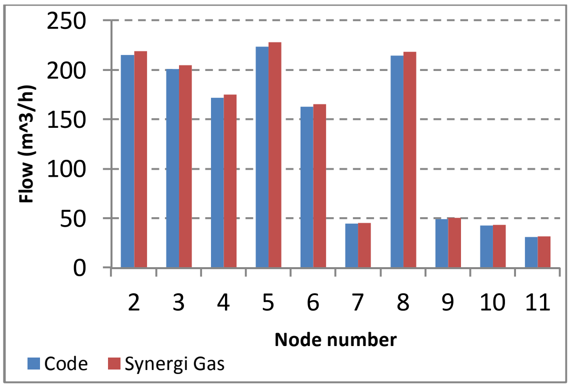

(b) Flow at load nodes

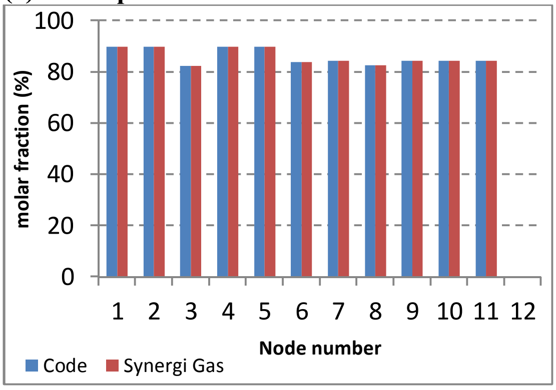

(c) Molar fraction of CH_4 at nodes after mixing

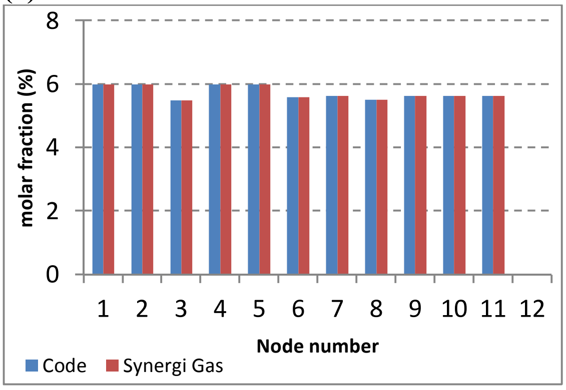

(d) Molar fraction of C_2H_6 at nodes after mixing

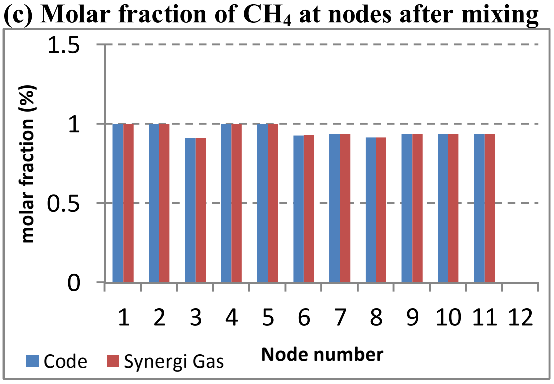

(e) Molar fraction of C_3H_8 at nodes after mixing

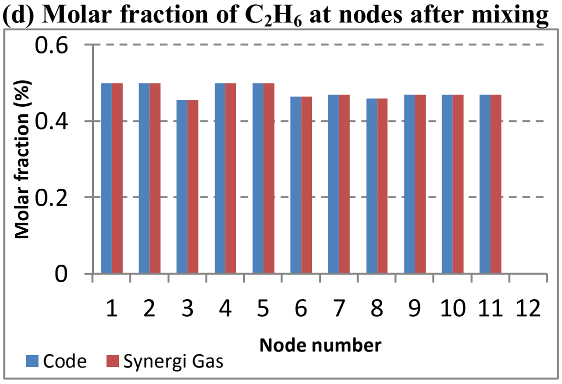

(f) Molar fraction of C_4H_{10} at nodes after mixing

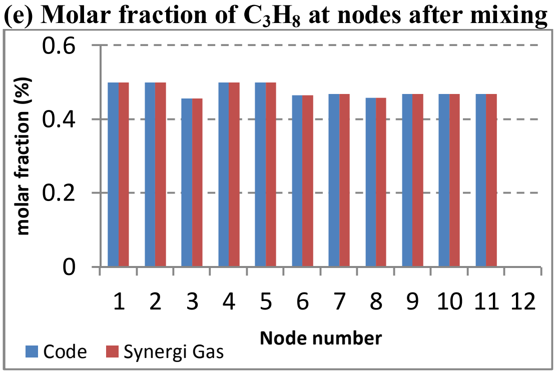

(g) Molar fraction of CO_2 at nodes after mixing

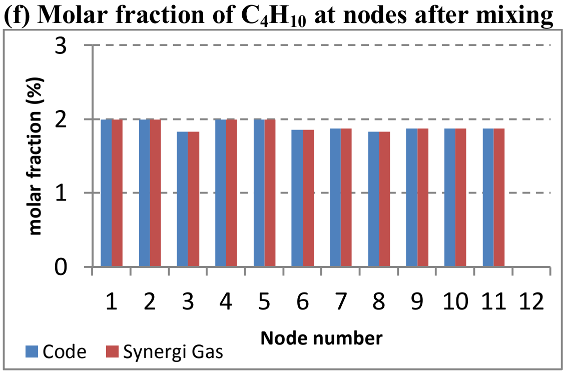

(h) Molar fraction of N_2 at nodes after mixing

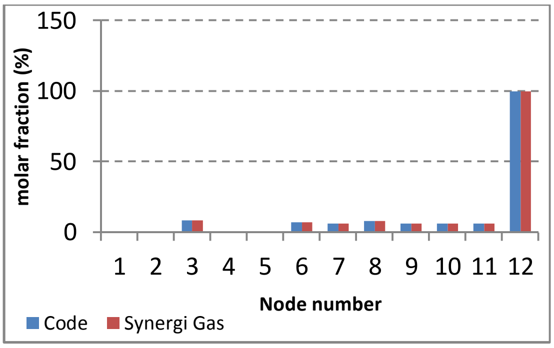

(i) Molar fraction of H_2 at nodes after mixing

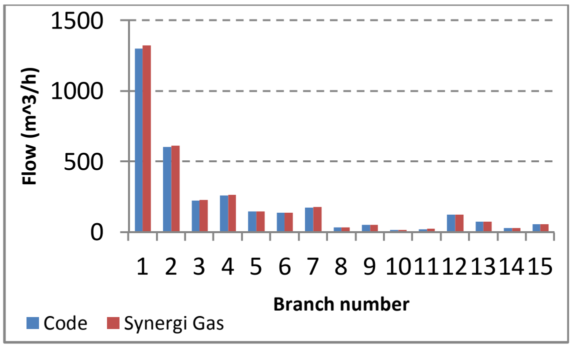

(j) Flow of branches

Figure 4.7: Validation of the simulation model with Synergi Gas for Case 3

4.4.2 Impact of decentralised injection on operation of the network

In order to evaluate the impact of decentralised injection of alternative gases on the operation of the network the energy content of mixture of natural gas and different gases that are injected within the network was considered in the first place. Figure 4.8 shows the comparison of the energy content, in terms of the Wobbe Indices, of gas mixtures after mixing at nodes for the case studies. As can be seen energy content of natural gas (Case 1) is higher than mixture of natural gas and upgraded biogas in Case 2 and the mixture in Case 2 has more energy content than the mixture of natural gas and Hydrogen in Case 3. This is reasonable since the calorific value of Hydrogen is much lower than the calorific value of upgraded biogas and the energy content of upgraded biogas is less than the calorific value of natural gas. The nodes 2, 4 and 5 receive the same gas as supplied at the source node. Thus, Wobbe Indices at these nodes are independent of the decentralised injection and thus are all identical in all the cases.

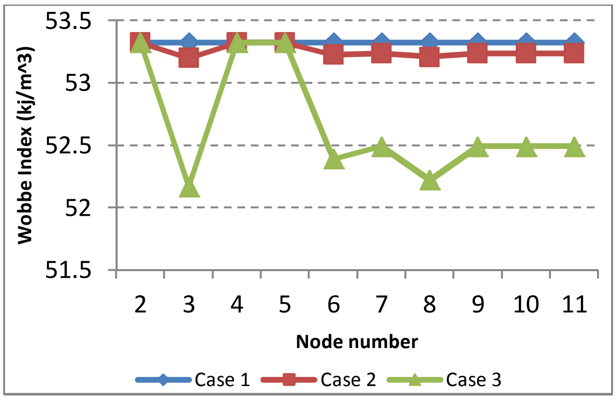

Figure 4.8: Values of Wobbe Index in case studies

The developed simulation model is constrained to meet the gas power demand at all the load nodes. Therefore, if a gas mixture with lower energy content and hence lower Wobbe Index exists at some of the nodes the simulation model increases the gas flow in order to meet the demand in amount at those nodes. Values of gas volumetric flow at the load nodes are shown in Figure 4.9. As can be seen gas flows for Case 2 almost coincide with those of Case 1 due to the fact that the difference in Wobbe Indices of Case 2 and Case 1 is really negligible; hence, insignificant impact on the gas flow at the load nodes is observed. However, in Case 3, where a mixture of Hydrogen and natural gas with Wobbe Indices lower than Case 2 exists in pipes, the values of gas flows at load nodes are slightly higher than those of Case 2, although the difference is not significant due to the small difference between Wobbe Indices of Case 3 and Case 2.

Figure 4.9: Values of gas flow at load nodes in case studies

The values of nodal pressures are shown in Figure 4.10. As can be seen the nodal pressures almost coincide although it was expected to see decrease in pressures as a result of increase in flow at nodes. This seems to be due to the insignificant difference in Wobbe Indices and hence insignificant difference in gas flows between different cases.

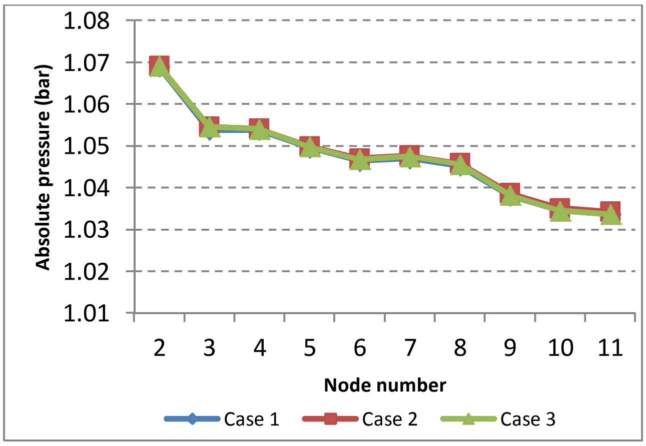

Figure 4.10: Values of nodal pressure at load nodes in case studies

4.5 Summary

In this Chapter a simulation model was developed in MATLAB, which is capable of simulation of operation of gas networks with decentralised injection. The simulation model accepts gas power demands, the network topology and specifications of sources and injections and calculates pressures, gas compositions and flows at nodes as well as flows of branches. Based on the calculated values of these parameters the values of specific gravities and energy content in terms of Wobbe Index are computed. A test gas distribution network operating in low pressure was considered and the following case studies were considered in order to validate the simulation model and afterwards to evaluate the impact of decentralised injection of alternative gases on the operation of the network:

- Case 1: injection of natural gas at the source node without any decentralised injection

- Case 2: injection of natural gas at the source node and decentralised injection of upgraded biogas

- Case 3: injection of natural gas at the source node and decentralised injection of Hydrogen

The performance of the simulation model was compared with the results obtained from the commercial software Synergi Gas for the three case studies. Based on the comparison of the results (Figures 4.5, 4.6 and 4.7) it is concluded that the simulation model is validated and it can be used for further analysis in gas networks.

In the next step, impact of decentralised injection of upgraded biogas (Case 2) and Hydrogen (Case 3) on operation of the network relative to the conventional injection of natural gas at the source node without any decentralised injection (Case 1) was evaluated. It was observed (Figure 4.8) that energy content and hence Wobbe Indices of Case 3 are less than those of Case 2 and the Wobbe Indices of Case 2 were slightly less than those of Case 1. The difference between Wobbe Indices of Cases 2 and 3 is much higher than the difference between Wobbe Indices of Cases 1 and 2.

The simulation model is designed based on the fact that it will meet the gas power demand at load nodes. Therefore, the decrease in Wobbe Indices as a result of injection of an alternative gas with lower energy content leads to increase in gas volumetric flows at the nodes that are receiving a gas mixture with less Wobbe Index relative to pure injection of natural gas, i.e. Case 1. Hence, increase in gas flows at the load nodes was observed (Figure 4.9) in general due to the decrease in Wobbe Index; however, since the difference between Wobbe Indices of Cases 1 and 2 was insignificant gas flows almost coincide. On the other hand, gas flows in Case 3 were slightly higher than Case 2 but the difference was not remarkable.

Comparison of nodal pressures (Figure 4.10) shows that their values almost coincide for all the cases due to the insignificant difference in the values of Wobbe Index and gas flow in case studies although decrease in pressures is expected as a result of decrease in Wobbe Indices, which leads to increase in gas flows at load nodes.

Based on the developed formulations, the algorithm and the simulation model capable of performing gas power flow analysis, in the next Chapter state estimation of gas distribution networks with decentralised injection will be studied. Using the simulation model developed in the next Chapter operation parameters of the network, i.e. pressures, gas compositions and flows within the network, can be estimated based on the measurements from across the network.

5 State estimation of gas distribution networks with decentralised injection using the WLS method

5.1 Introduction

In this Chapter the weighted least squares-based state estimation of gas distribution networks with decentralised injection is explained. Firstly, a brief literature review on state estimation of gas networks is presented. Then, the formulations and the algorithm of the simulation model developed in MATLAB for state estimation of gas networks are described. Afterwards, the case study gas distribution network is presented and the assumptions of the measurements of the network are summarised. Subsequently, the results of application of the state estimation simulation model to the case study network are shown. Finally, a summary of the results obtained in the Chapter for further applications in the later Chapters is presented.

5.1.1 Necessity of a tool for state estimation of gas networks

Based on the benefits and challenges of injection of alternative gases into gas networks (Chapter 4 sections 4.1.1 and 4.1.2), the operator of the network needs to have knowledge of the operation parameters of the network in terms of the values of pressures, flows and gas quality within the network in order to control and manage the network in real time and to make the right decision at the right time. Therefore, there is a need for a state estimation tool, which enables them to calculate the estimated values of the operating parameters of the network based on the values of the measurements from across the network. In this Chapter the formulations and the MATLAB simulation model that was developed for state estimation of gas networks with decentralised injection of alternative gases are explained.

5.1.2 Literature review

There are several research publications on state estimation of gas networks in different pressure levels including transmission and distribution levels in steady state as well as dynamic operation conditions of the network (Parkinson 1984; Choudhary et al. 1985; Parkinson and Wynne 1986; Choudhary 1987; Parkinson and Wynne 1992; Murray et al. 1993; Nichols and Stringer 1994; Emara-Shabaik et al. 2002; Khulief and Emara-Shabaik 2006; Reddy et al. 2006; Reddy et al. 2011a, b; Ahmadian Behrooz and Bozorgmehry Boozarjomehry 2015a, b). Some of the works have considered multi in-feeds to the gas network, however, the mixture of the gas of all the sources are assumed to be identical, which means a uniform gas flow through the entire network is considered. In (Pal 1991) the author summarises the problems of state estimation of gas networks with one single type of gas. Also, state estimation of gas networks with changing of the gas quality is carried out in (Weimann et al. 1990), where the heating value of the gas is considered as the state parameter. However, in the current work the molar fraction of all the components of the gas mixture is considered in the vector of the state parameters. This means after calculation of the values of molar fraction of all the components of the gas mixture all the thermal properties of the gas including the heating value can be computed.

Consequently, no relevant previous work or publication was found for state estimation of gas networks with decentralised injection of alternative gases either in steady state or dynamic conditions of operation. However, there are a few commercial tools that perform state estimation of gas networks with decentralised injection either in transmission or distribution level. These tools are listed in Table 5.1.

Table 5.1: Some commercial tools capable of state estimation of gas networks with decentralised injection

Commercial software	Developer(s)
SIMONE (Liwacom 2016)	Liwacom Informationstechnik GmbH, Germany SIMONE research group, Czech Republic
Synergi Pipeline Simulator (DNV.GL 2016b)	DNV GL, Norway
SPS (Stoner Pipeline Simulator) (Automind 2016)	Automind, Brazil (Links to DNV GL)
PSIganesi (PSI 2016)	PSI, Germany

There is no access to the core formulations of these commercial tools. Therefore, all the formulations presented in this Chapter for state estimation of gas distribution networks with decentralised injection of various gases are developed by the researcher based on the lessons learned from state estimation of power distribution networks in Chapters two and three.

5.2 State estimation of gas networks using the WLS method

In order to perform the state estimation of gas networks with decentralised injection of alternative gases using the weighted least squares method the same concept and formulations for state estimation of power networks using the method, which were presented in Chapter two, were developed and applied. For this purpose, the state parameters in gas networks with decentralised injection are defined as the values of pressures squared and molar fractions of all the components of the gas mixture except one of the components at all the nodes. Once the values of the state parameters of the network are known, the values of flows of the branches and flows at the nodes can be calculated. Squared values of pressures are considered since:

- Once their values are found, the values of pressures can be calculated by taking the square root of the squared pressures; and

- Formulations for the measurement Jacobian, which is the partial derivatives of the measurement functions, can be much more easily obtained with much less computation burden.

Also, the values of molar fraction of all the components except Hydrogen are considered as state parameters due to the following:

- The molar fractions of all the components will add up to one.

- If Hydrogen itself is directly injected into the network, the values of its molar fraction at nodes are very small compared to the values of molar fraction of the rest of the components. Therefore, the calculation process is not significantly affected if the values of molar fraction of Hydrogen at nodes are not considered in the vector of state parameters.

Therefore, the vector of state parameters in the state estimation of gas distribution networks with decentralised injection is:

$$x = \begin{pmatrix} PS_1 \\ PS_2 \\ \vdots \\ PS_{N_N} \\ y_{1,1} \\ y_{2,1} \\ \vdots \\ y_{N_C-1,1} \\ y_{1,2} \\ y_{2,2} \\ \vdots \\ y_{N_C-1,2} \\ \vdots \\ y_{1,N_N} \\ y_{2,N_N} \\ \vdots \\ y_{N_C-1,N_N} \end{pmatrix} \tag{5-1}$$

where $y_{i,j}$ refers to the value of molar fraction of component i at node j after mixing, N_N is the number of the nodes of the gas network and N_C denotes the number of the components of the gas mixture. In order to start the solution process calculation of the measurement function $h(x)$ and the measurement Jacobian $H(x)$ is essential, which is explained in the following subsections.

5.2.1 Measurement function in gas networks

Measurement function is a nonlinear function that enables calculation of the values of the measured parameters based on the estimated values of the state parameters. The parameters that are measured in gas distribution networks with decentralised injection are as follows:

- Flow of branches

  The value of the flow of a branch connecting node i to node k is calculated using the following equation, which is obtained by rewriting equation (4-6) and replacing p_i^2 and p_k^2 with PS_i and PS_k, respectively:

$$q = sgn(PS_i - PS_k) \times \frac{\pi}{8}\sqrt{\mathcal{R}_{air}}\frac{T_n}{p_n}\sqrt{\frac{M_{air}.|PS_i - PS_k|.D^5}{Z_{air}.f.\sum_{i=1}^{Nc}(y_i.M_i).L.T}} \tag{5-2}$$

It should be noted that the squared values of nodal pressures and the values of molar fractions at nodes after mixing are known through the iterative solution process. Therefore, the value of the flow of the branch can be computed according to the algorithm and formulations explained in the section 4.2.1.1.

- Flow at nodes

The value of the flow at a node is algebraic sum of all the in- and out-flows of all the branches connected to the node:

$$q_{node} = \sum q_{in} - \sum q_{out} \tag{5-3}$$

In this way the measurement function, $h(x)$, would be a vector of the following form, where the elements are calculated using the above formulations for available measurement types:

$$h(x) = \begin{bmatrix} PS \\ q_{branches} \\ \\ q_{nodes} \\ y \end{bmatrix} \tag{5-4}$$

5.2.2 Measurement Jacobian in gas networks

The measurement Jacobian matrix contains the partial derivatives of the measured parameters with respect to the state parameters and has the following form:

$$H(x) = \begin{bmatrix} \frac{\partial PS}{\partial PS} & \frac{\partial PS}{\partial y} \\ \frac{\partial q_{branches}}{\partial PS} & \frac{\partial q_{branches}}{\partial y} \\ \frac{\partial q_{nodes}}{\partial PS} & \frac{\partial q_{nodes}}{\partial y} \\ \frac{\partial y}{\partial PS} & \frac{\partial y}{\partial y} \end{bmatrix} \tag{5-5}$$

Different parts of the above matrix are calculated as follows:

- Derivatives of measurements of squared pressure

$$\frac{\partial PS_i}{\partial PS_i} = 1, \quad \frac{\partial PS_i}{\partial PS_j} = 0 \; (i \neq j)$$

(5-6)

$$\frac{\partial PS_i}{\partial y_{m,j}} = 0 \; (m = 1, \ldots, N_C - 1 \; and \; j = 1, \ldots, N_N)$$

where $y_{m,j}$ denotes the molar fraction of component m at node j.

- Derivatives of measurements of the flow q_{ik} of the branch connecting the nodes i and k

$$\frac{\partial q_{ik}}{\partial PS_i} = 0.5 \times \frac{q_{ik}}{(PS_i - PS_k)} \tag{5-7-a}$$

$$\frac{\partial q_{ik}}{\partial PS_k} = -0.5 \times \frac{q_{ik}}{(PS_i - PS_k)} \tag{5-7-b}$$

$$\frac{\partial q_{ik}}{\partial y_{C_j}} = \frac{-0.5 \times M_{C_j}}{\sum_{j=1}^{N_C} \left(y_{C_j} . M_{C_j} \right)} \times q_{ik} \tag{5-7-c}$$

In the development of the above formulations partial derivatives with respect to friction factor were neglected since the friction factor itself has a small value and thus its derivatives can be neglected. Also, since the value of the flow of the branch is calculated based on the molar fractions of the sending end of the branch, which can be either node i or node k, the value of the derivatives of the flow with respect to the molar fractions of the sending end are calculated using (5-7-c). In other words, all the values of derivatives of the flow of the branch with respect to the molar fractions of the receiving end are equal to zero.

- Derivatives of measurements of the flow at a node

Since the flow at a node is calculated via algebraic sum of the flow of the branches connected to the node, the partial derivatives of the flow of the node is calculated by algebraic sum of derivatives of the flow of the branches connected to the node as follows:

$$\frac{\partial q_{node}}{\partial PS_i} = \sum \frac{\partial q_{in}}{\partial PS_i} - \sum \frac{\partial q_{out}}{\partial PS_i} \tag{5-8-a}$$

$$\frac{\partial q_{node}}{\partial PS_j} = \sum \frac{\partial q_{in}}{\partial PS_j} - \sum \frac{\partial q_{out}}{\partial PS_j} \tag{5-8-b}$$

$$\frac{\partial q_{node}}{\partial y_{C_j,i}} = \sum \frac{\partial q_{in}}{\partial y_{C_j,i}} - \sum \frac{\partial q_{out}}{\partial y_{C_j,i}} \tag{5-8-c}$$

- Derivatives of the measurements of the molar fraction

The partial derivative of the molar fraction of a component at a node has a value equal to one only with respect to the molar fraction of the same component at the same node. In other words, the partial derivative of the molar fraction of a component at a node has a value of zero with respect to the squared pressure at all the nodes and also with respect to the rest of the components at the same node as well as to all the components at all the rest of the nodes, as follows:

$$\frac{\partial y_{j,i}}{\partial PS_k} = 0 \; (k = 1, \dots, N_N) \tag{5-9-a}$$

$$\frac{\partial y_{j,i}}{\partial y_{j,i}} = 1, \;\; \frac{\partial y_{j,i}}{\partial y_{k,i}} = 0 \; (k \neq j), \;\; \frac{\partial y_{j,i}}{\partial y_{m,k}} = 0 \; (k \neq i) \tag{5-9-b}$$

where $y_{j,i}$ denotes the molar fraction of component j at node i.

5.2.3 The algorithm of the simulation model developed in MATLAB

A simulation model was developed in MATLAB for performing state estimation of gas networks with decentralised injection in steady state conditions using the following inputs:

- Gas flow analysis specific parameters:
  - Network topology and specifications
  - Demands and injections
- Accuracy of measurements
- Confidence level of the measurements
- Acceptable tolerance of estimation (ε)

Gas flow analysis of the gas network is performed using the simulation model developed in MATLAB in the previous Chapter in order to obtain the true (nominal) values of all the operating parameters of the network. Then, the values of the standard deviations are calculated using (2-13). Afterwards, the values of the available measurements are produced using the normrnd(ψ,σ) function of MATLAB, which generates random numbers with a normal distribution. This way, the input parameters for the WLS state estimation algorithm are provided.

The inputs of the WLS state estimation algorithm are the values of the measurements, the standard deviations, the topology and specifications of the network and the acceptable tolerance of estimation (ε). The weights matrix, W, is formed using (2-6) and by squaring the values of the standard deviations. The solution process starts by guessing values for the state vector x.

Regarding the guess values, unlike the flat start in the solution of the problems in power systems, there is not a straightforward clue for the guess values for the state parameters in a problem in gas systems, unfortunately. However, in this research the values of nodal pressures were distributed in the range of approximately 80%-100% of the source absolute pressure in a way that the nodal pressures are all different from one another. Regarding the molar fraction of the components, the guess values of them at all the nodes were very close to the molar fraction of the components at the main source.

Once the values of the state parameters are guessed, the measurement function, $h\left(x^{(1)}\right)$, at iteration number 1 is calculated using the equations in section 5.2.1. The measurement Jacobian, $H\left(x^{(1)}\right)$, at iteration number 1 is calculated using the equations in section 5.2.2. The derivative function $g\left(x^{(1)}\right)$ at iteration number 1 is calculated using the equation (2-19) and finally the gain matrix $G\left(x^{(1)}\right)$ at iteration number 1 is calculated using the (2-20). Afterwards, the values of the state parameters are updated using (2-18). This process is iterated until the change in the values of the state parameters, which is calculated using (2-21), is less than ε. The process is depicted in Figure 5.1.

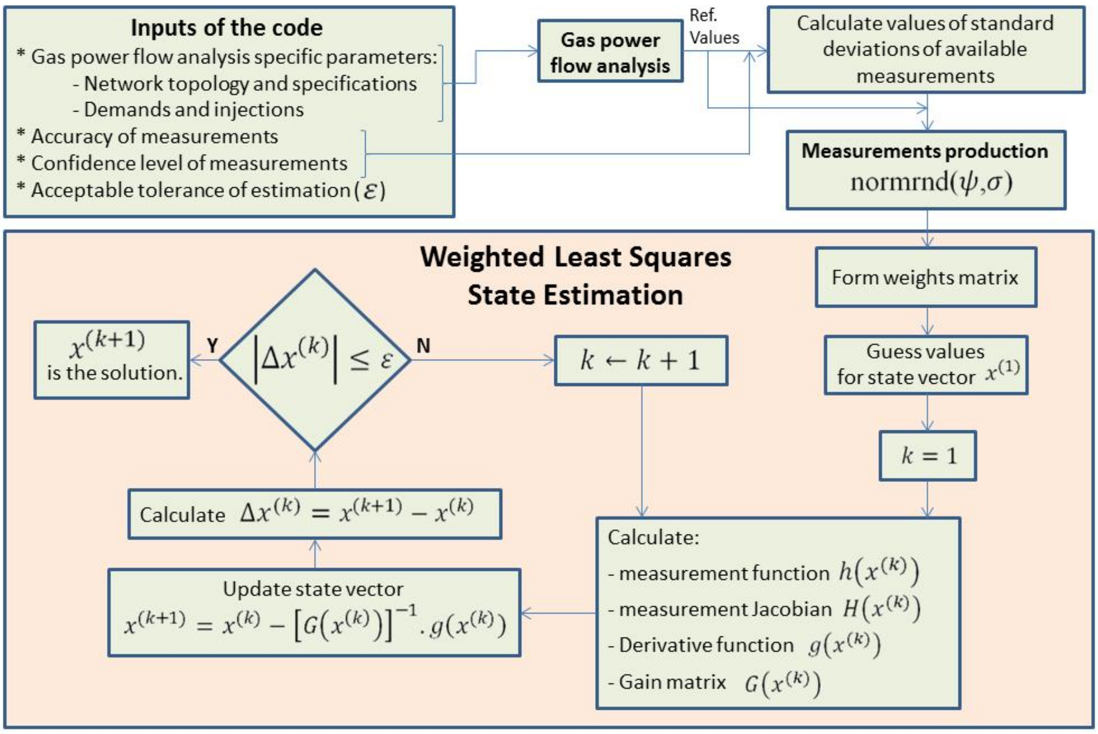

Figure 5.1: The flow chart of the algorithm of the WLS-based state estimation in gas networks

5.3 Test results

The schematic of the case study gas distribution network operating at medium pressure is shown in Figure 5.2. The pressure at the source node is assumed to be 7.0 bar gauge and the ambient pressure is assumed to be 1.0 bar. Injected power at node 6 is 40 MW. The topology of the network, node data and the composition of the injected gas at the source and injection nodes are presented in Appendix II.

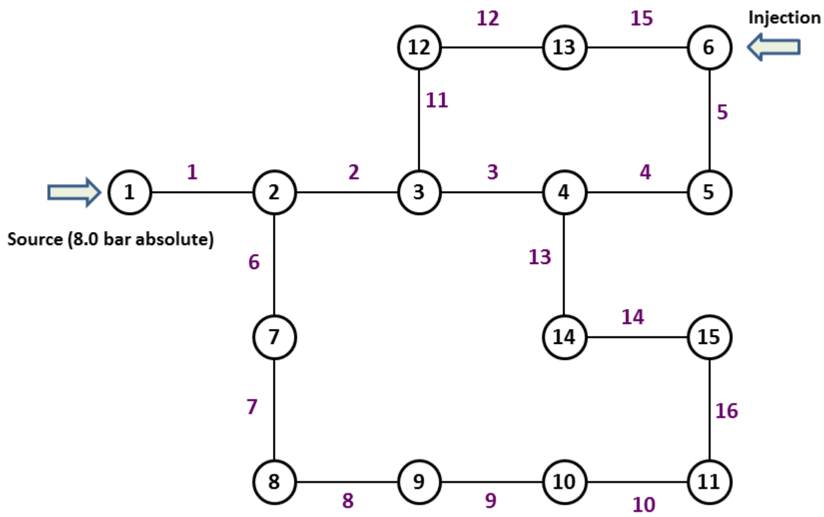

Figure 5.2: The schematic of the case study gas distribution network

The available measurements of the network along with the values of their accuracies are shown in Table 5.2. The values of accuracies of real time measurements are chosen close to the values found in BS and AGA standards. However, the focus of the work is more on developing the algorithm and studying the SE of gas networks. The values of standard deviations are calculated based on a 95% confidence level (for more explanation see section 2.3 in Chapter 2). Also, virtual injection measurements at nodes without loads are considered with variance of $\sigma^2 = 1.0 \times 10^{-8}$.

Table 5.2: Available measurements of the network for SE

Measured parameter	Measurement location	Measurement type	Accuracy
Pressure	Source node #1 Injection node #6	Real time	1 %
Branch flow	Branch 1-2	Real time	1 %
Node flow	Source node #1 Injection node #6	Real time	1 %
	All the load nodes	Pseudo	50 %

Molar fraction	Source node #1 Injection node #6	Real time	1 %
	All the nodes except nodes #1 and 6	Pseudo	10 %

5.3.1 SE with perfect measurements

The performance of the developed simulation model was first evaluated using perfect measurements, i.e. noise- or error-free measurements. In other words, the algorithm of SE was fed with the true values of the available measurements presented in Table 5.2, which were obtained from the gas power flow analysis (see section 4.2). The results of estimation of the state parameters, i.e. the values of pressures and molar fractions of all the components at all the nodes, are compared with the values calculated by the gas flow analysis in Figure 5.3. As can be seen and as was expected all the results of state estimation with perfect measurements coincide and follow the results obtained in the gas power flow analysis.

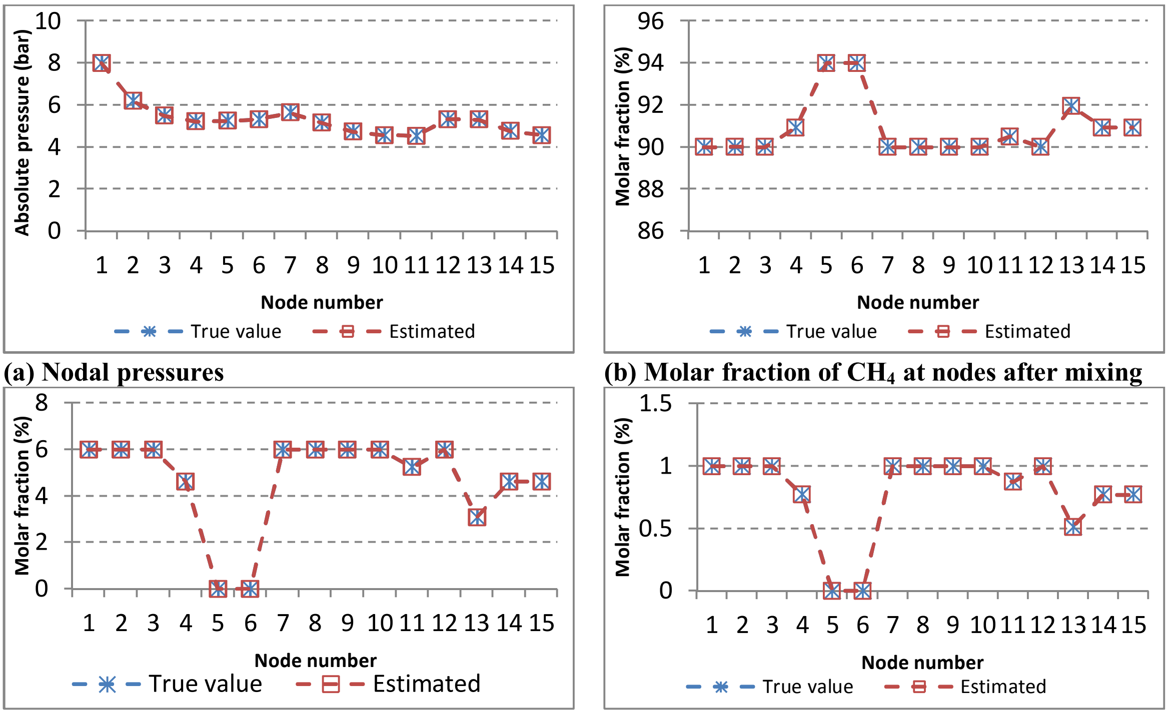

(a) Nodal pressures

(b) Molar fraction of CH_4 at nodes after mixing

(c) Molar fraction of C_2H_6 at nodes after mixing

(d) Molar fraction of C_3H_8 at nodes after mixing

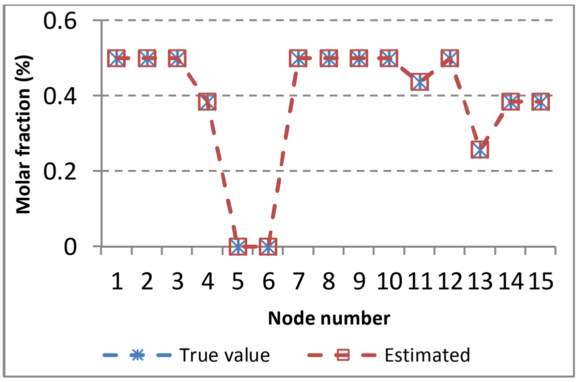

(e) Molar fraction of C_4H_{10} at nodes after mixing

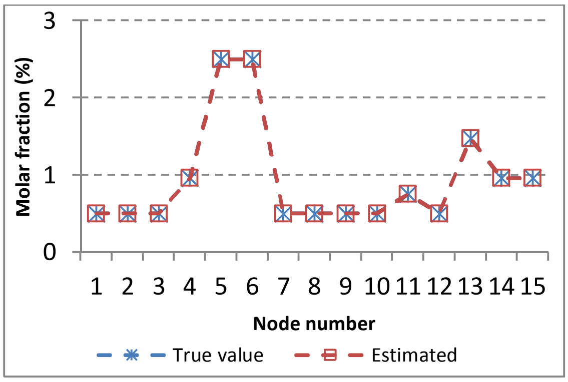

(f) Molar fraction of CO_2 at nodes after mixing

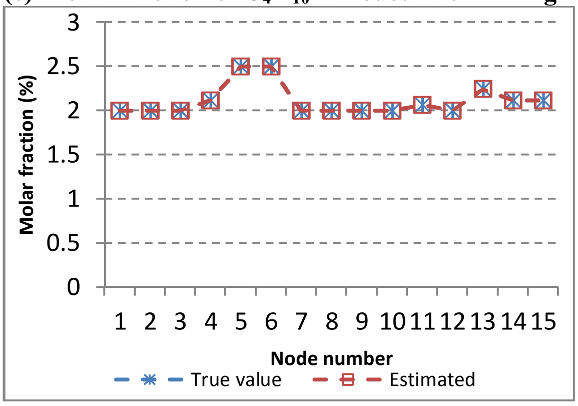

(g) Molar fraction of N_2 at nodes after mixing

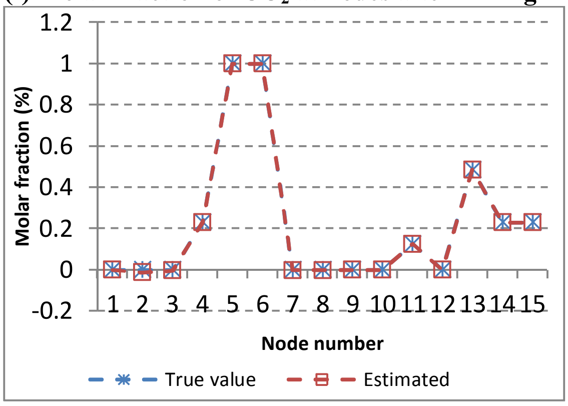

(h) Molar fraction of H_2 at nodes after mixing

Figure 5.3: Comparison of the estimated and true values of the state parameters of the network[1]

5.3.2 Monte Carlo simulation of state estimation of the network

In the next step 20,000 Monte Carlo simulations were performed on the network in order to observe performance of the simulation model as well as the distribution of the estimated state parameters of the network. The available measurements of the network as well as the assumed values of their accuracies were shown in Table 5.2. The set of measurement values for each Monte Carlo simulation was produced using the normrnd function of MATLAB. This function produces random numbers that follow Normal distribution. The standard deviation of the distribution was calculated using Equation (2-13) with the "True values" computed based on the results of gas power flow analysis (section 4.2).

The distribution of the values of all the state parameters of the network is shown in

[1] The "True value" of the parameters refers to the values calculated in the gas power flow analysis as explained in Chapter 4, section 4.2. Also, the "Estimated" value of the parameters refers to the results of the state estimation algorithm, which is developed in section 5.2 in this Chapter.

Figure 5.4 in boxplots. In all the plots of Figure 5.4, 25 and 75 percentile of the data are put in the boxes and approximately 0.7% of the data are considered as the outliers, which are shown by pluses. Also, true values are shown by stars in the plots, which almost coincide with the 50 percentile of the data.

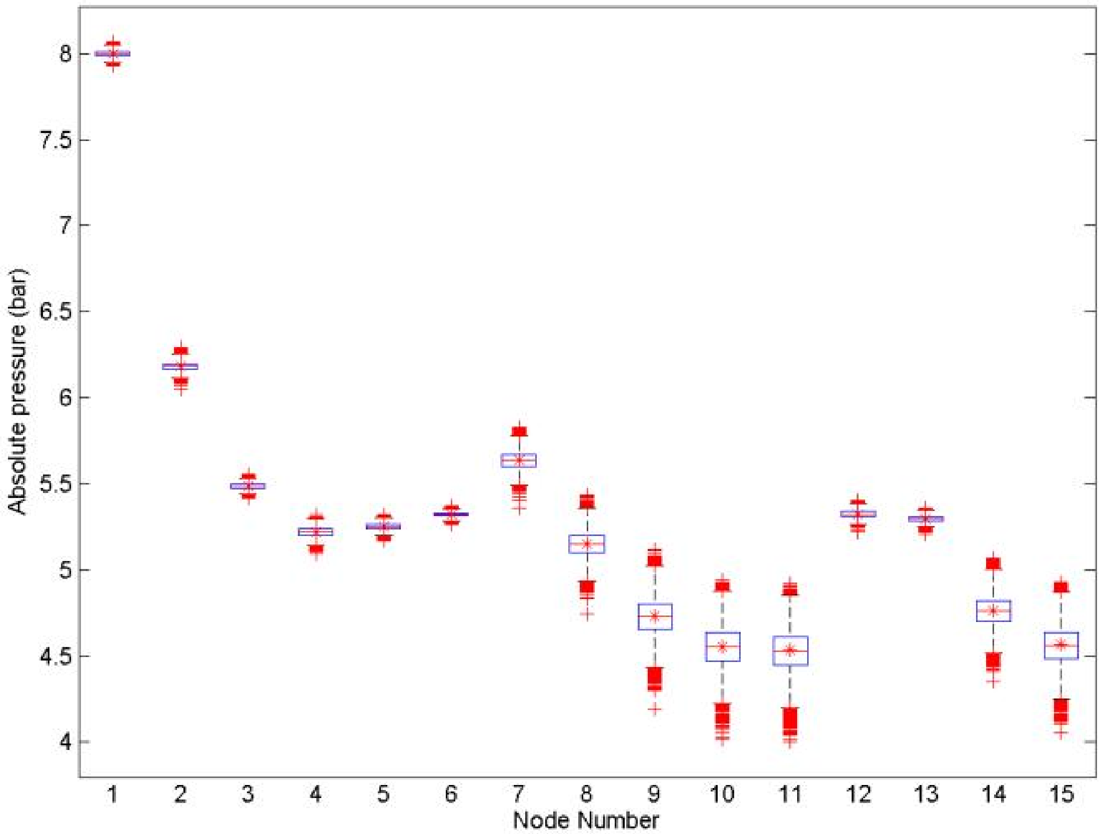

(a) Nodal pressures

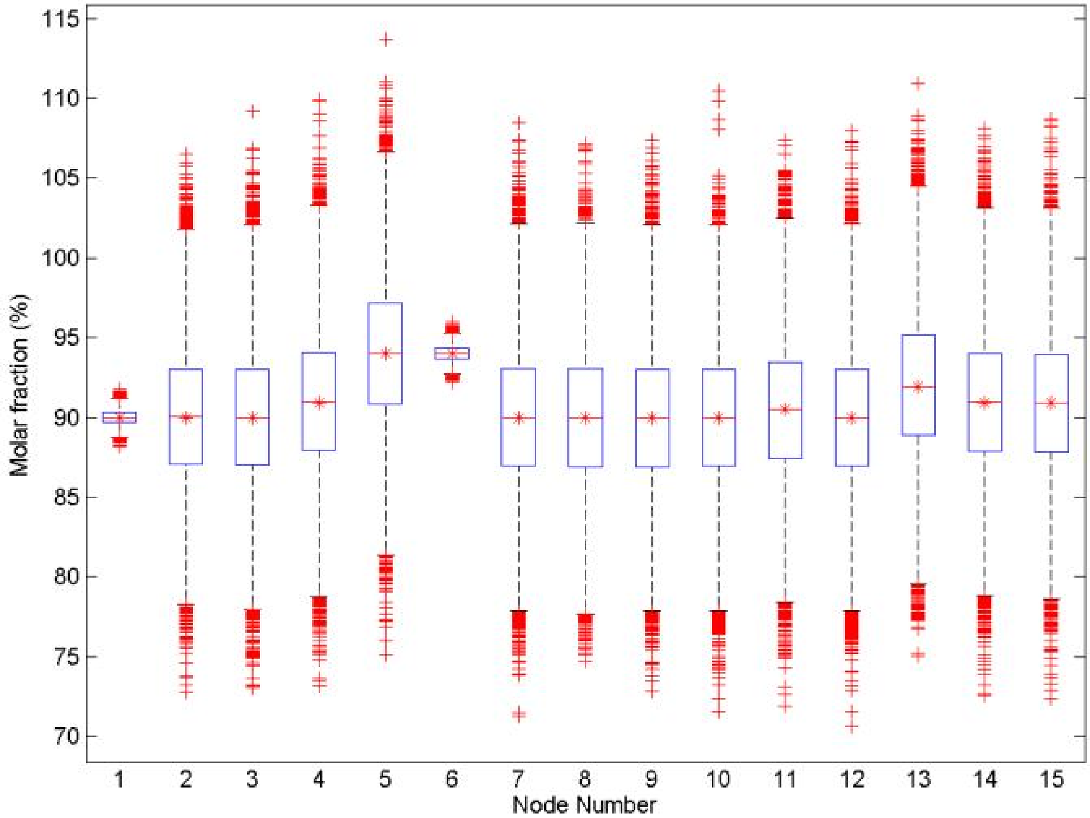

(b) Molar fraction of CH_4 at nodes after mixing

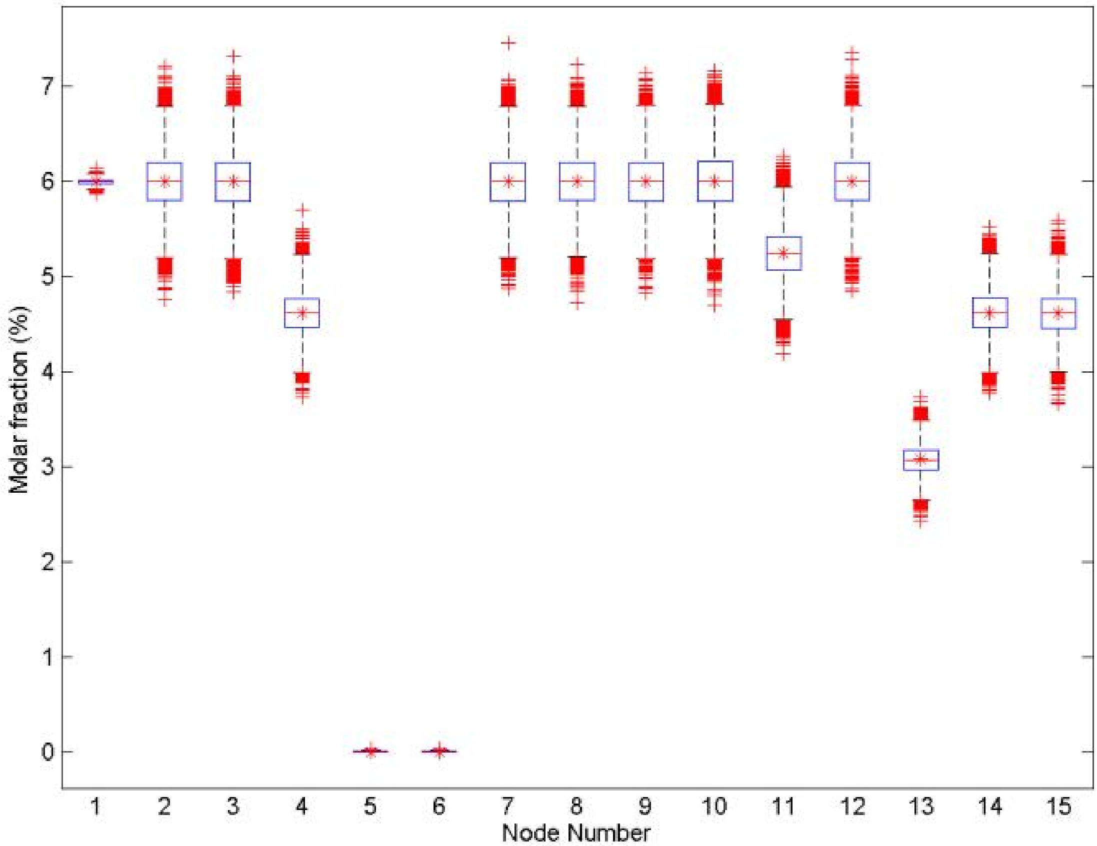

(c) Molar fraction of C_2H_6 at nodes after mixing

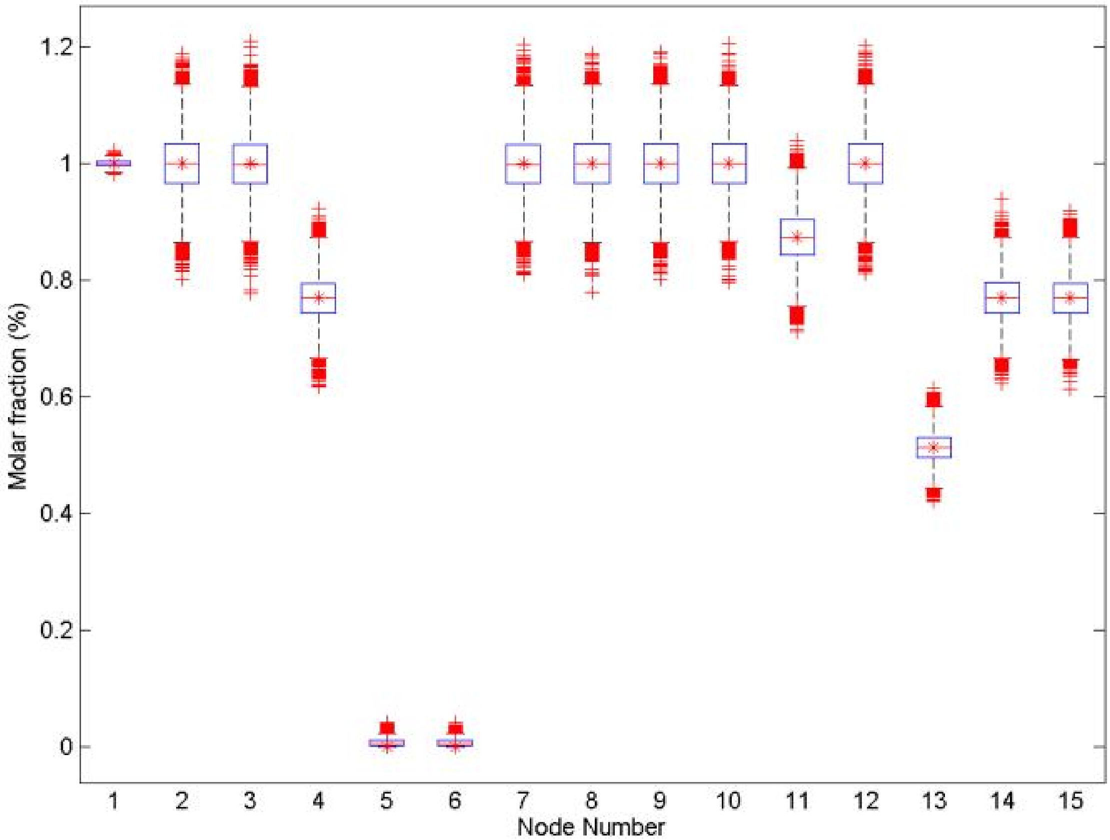

(d) Molar fraction of C_3H_8 at nodes after mixing

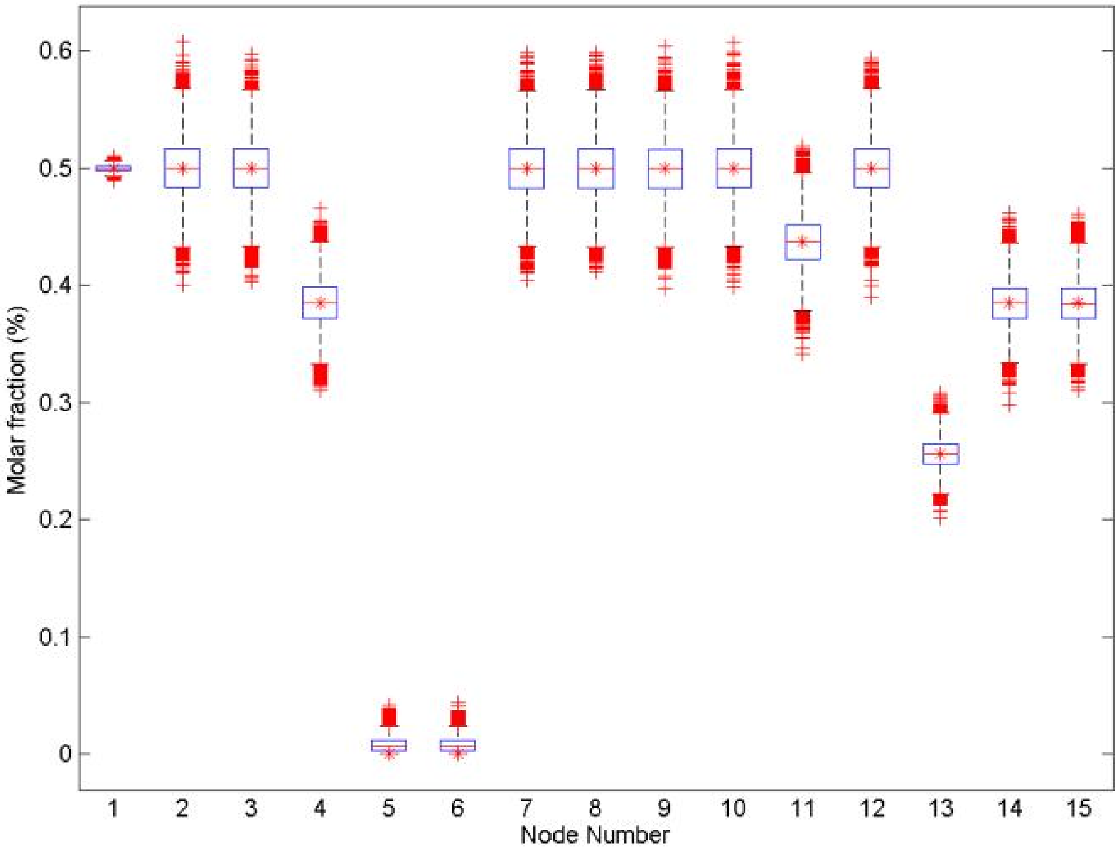

(e) Molar fraction of C_4H_{10} at nodes after mixing

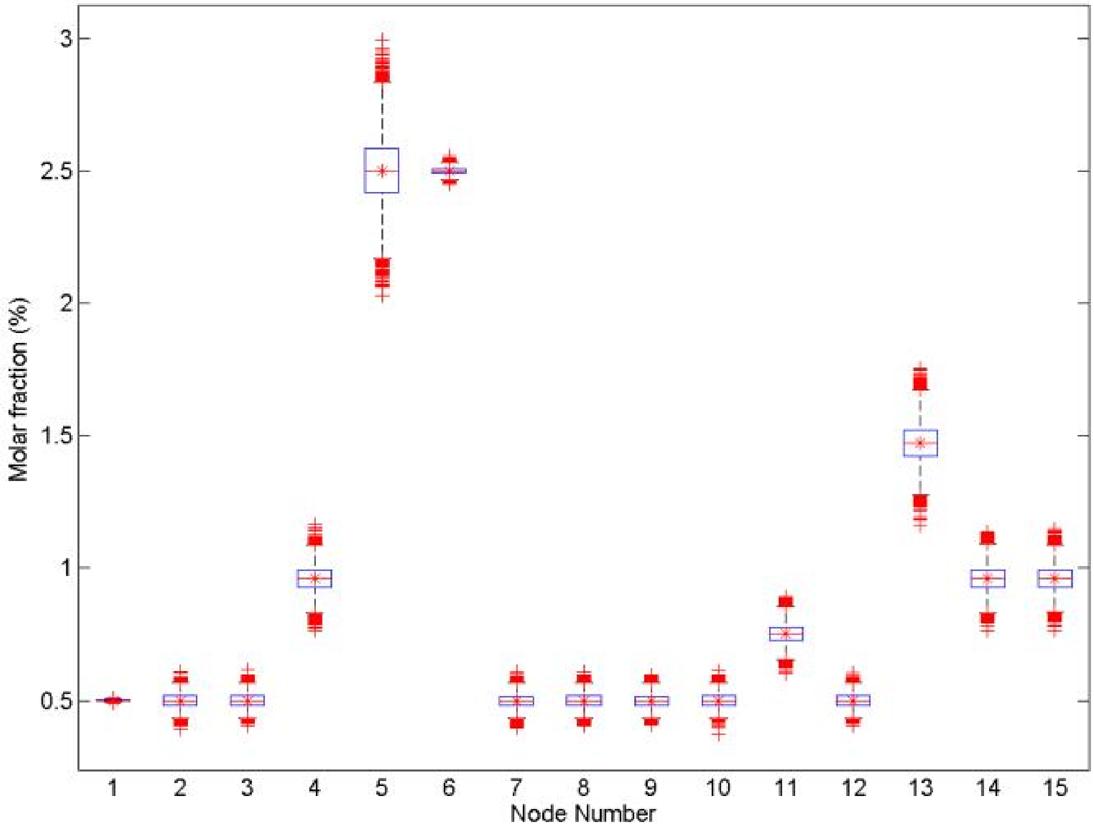

(f) Molar fraction of CO_2 at nodes after mixing

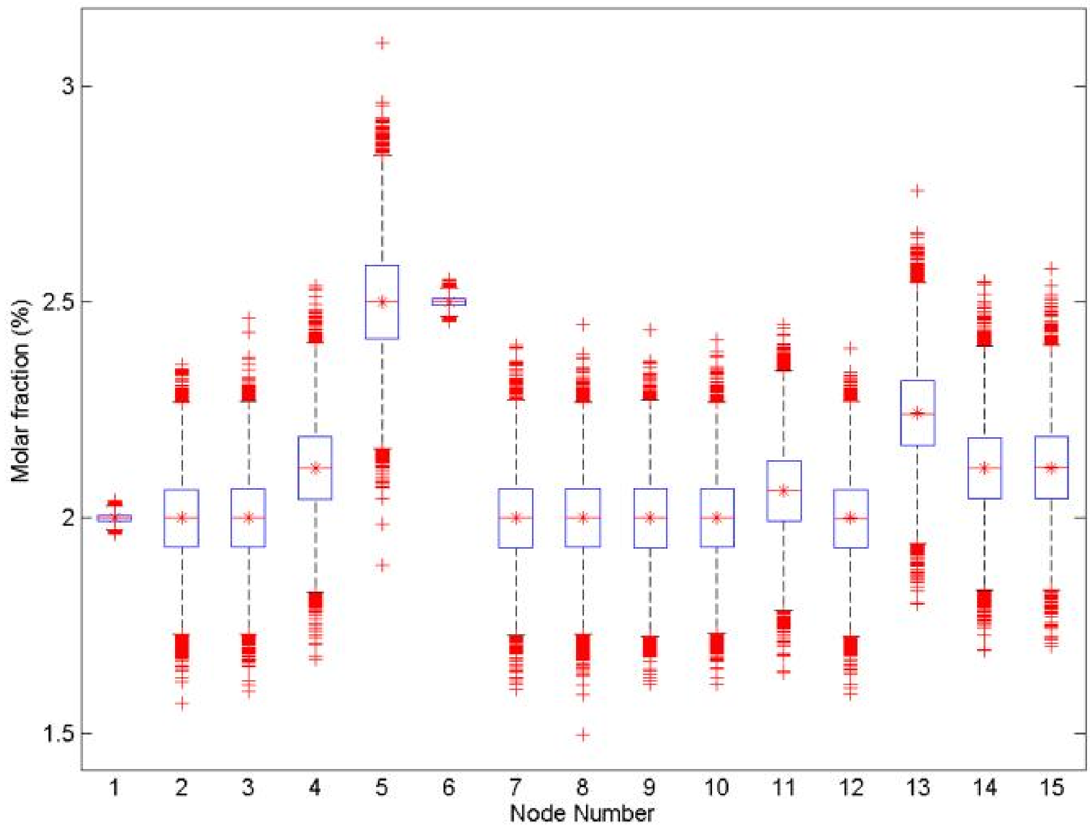

(g) Molar fraction of N_2 at nodes after mixing

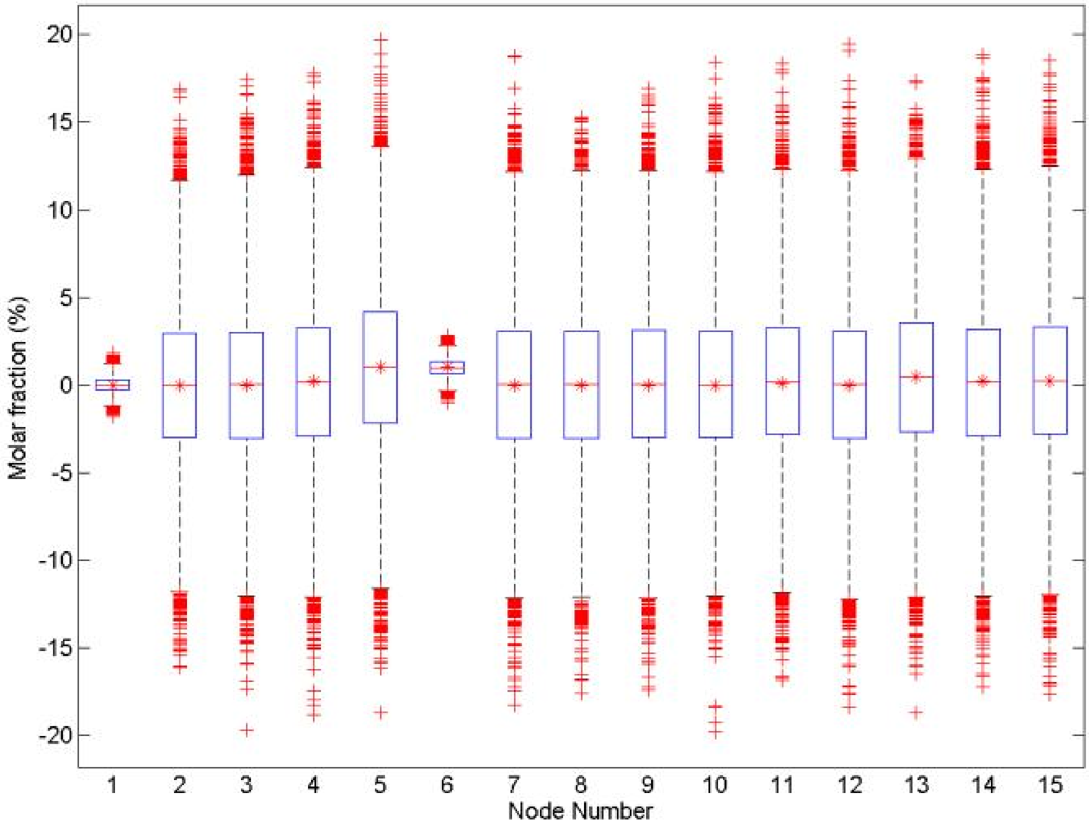

(h) Molar fraction of H_2 at nodes after mixing

Figure 5.4: Distribution of estimated values of the state parameters of the network

As can be seen the average values of the distributions of estimated values in Figure 5.4 coincide with the true values obtained from gas power flow analysis, which was presented in Figure 5.3. In fact, the estimated values of all the state parameters follow a Normal distribution with a mean value equal to the true values computed in gas power flow analysis (section 4.2). This behaviour was expected due to the assumptions made in the WLS-based state estimation discussed in 2.5.2.

5.4 Summary

A simulation model was developed in MATLAB in this Chapter in order to estimate the state parameters of gas networks with decentralised injection using the measurements from across the network subject to observability of the network. The state parameters are values of squared pressures and molar fractions of all the gas components except Hydrogen at all the nodes. The inputs of the simulation model are as follows:

- Gas flow analysis parameters:

    - Network topology and specifications

    - Demands and injections

- Accuracy of measurements

- Confidence level of the measurements

- Acceptable tolerance of estimation

The performance of the simulation model was evaluated using an example gas distribution network operating in medium pressure level in two instances:

- SE with perfect measurements

    The simulation model was first fed with perfect measurements, i.e. accurate measurements with values equal to the values obtained in gas flow analysis. Based on the results and as was expected the simulation model estimated the values of the state parameters of the network identical to their true (nominal) values.

- Monte Carlo simulation of state estimation

    In this case, 20000 Monte Carlo simulations of state estimation were performed on the test network with normally distributed measurements. As was observed and was expected, the estimated state parameters have a distribution very similar to a Normal distribution. This is due to the fact that measurements have Normal distributions and that the measurement model is linearised.

In the next Chapter the developed state estimation tool is used in order to investigate the problem of placement of additional measurements in a gas distribution network in order to enhance the accuracy of estimation of the state parameters of the network.

6 Optimal placement of additional measurements in gas distribution networks with decentralised injection

6.1 Introduction

Placement of additional measurements for improvement of estimation of the state parameters of gas distribution networks with decentralised injection is investigated. Firstly, the reason that the operator of a gas distribution network with decentralised injection needs a tool that helps them for placement of additional meters within the network is briefly reviewed. Then, the method of formulation of the problem for placement of additional measurements subject to the limited budget of the operator of the network as well as the developed algorithm for measurement placement are explained. Afterwards, the case study test network along with the assumptions of the algorithm of the simulation model developed in MATLAB is described. Finally, the impact of different types of measurements on the state estimation of the network as well as the results and discussion of the performance of the algorithm of additional measurement placement are presented.

6.1.1 Necessity of a tool capable of placement of additional measurements in gas distributions networks with decentralised injection

Gas networks can be used for the transport and storage of alternative gases, which might be produced due to excessive amounts of renewable power, and also for reducing the carbon footprint of the network as a whole. Therefore, reverse flows occur at times in pipelines due to decentralised injection, which affect the performance of the network and influence gas quality. Hence, the operator of the gas network needs to have an estimate of the state of pressures, flows and gas compositions within the network particularly when injections take place, so that network regulations in term of safety issues and Wobbe index are not violated. Moreover, having knowledge of the quality and calorific value of the gas mixture in different points within the network helps the operator with accurate billing.

Consequently, there is a necessity of a tool that helps the operator with a cost-effective investment in metering infrastructure, so that improvement in operation and real time control and management of the network is achieved. The tool will have to operate based on the fusion of all the information within the network, including pressures, flows, gas compositions and pseudo measurements of loads through a state estimation algorithm.

6.1.2 Research questions

The research questions that are addressed in this Chapter are as follows:

- What is the impact of various meters, i.e. real time measurements of pressure, flow and gas composition, on estimation of the state of pressures, flows and molar fraction of gas compositions in a gas distribution network with decentralised injection?

- What is the best set of measurements, in terms of number, type, place, accuracy and frequency of data acquisition, to be placed within a gas distribution network with decentralised injection subject to a limited budget of the operator for improving the metering infrastructure and accuracy of the network state estimation accordingly?

- What is the accuracy of estimation of the state parameters of the network, i.e. pressures, flows and gas compositions for the best set of measurements (umber, type and place) determined from previous step? How the accuracy of estimation is influenced by the accuracy of pseudo measurements of load and gas composition?

6.1.3 Literature Review

The efficient measurement placement in gas distribution networks has been studied in several articles. In (Davenport and Bramellar 1972) and (Parkinson and Wynne 1992) optimum placement of a minimum number of measurements for the purpose of control of the minimum pressure profile within multi-feed gas distribution networks was studied. These authors considered dynamic operation conditions of the network; however, they haven't considered injection of different types of gases within the network. In (Musulin et al. 2005) a measurement placement algorithm has been developed, which maximises the accuracy of estimation based on the limited cost of the meters using a genetic algorithm. The state estimation algorithm is based on a Kalman filter for the dynamic operation conditions of the network. Their research again considered a single type of gas flowing within the network.

6.2 Formulation of the problem of measurement placement

In order to find the best set of measurements (number, type and place) with a predetermined accuracy, an objective function has been defined and an algorithm has been developed. The algorithm ranks the possible solutions of the search space in terms of the value of the objective function and selects the best possible solution as the solution of the problem. The objective function includes an accuracy index. Therefore, the definition of some accuracy indices of the state estimation is explained first and then the objective function is described.

6.2.1 Definition of different accuracy indices of the state estimation

6.2.1.1 Accuracy index of the whole state estimation

Similar to the state estimation of power networks, the state error covariance matrix in gas network state estimation is defined as follows:

$$A_{SE} = (H^T . W . H)^{-1} \tag{6-1}$$

where H denotes the measurement Jacobian and W is the diagonal weights matrix, which contains the inverse of the variances σ^2 of the measurements.

The sum of the diagonal elements of the state error covariance matrix A_{SE} is defined as the accuracy index of the whole state estimation as follows:

$$AI_{SE} = \sum_{i=1}^{N_{sp}} (A_{SE})_{ii} \tag{6-2}$$

where N_{sp} shows the number of the state parameters of the network.

6.2.1.2 Accuracy index of pressure

The first N_N elements of the N_{sp} diagonal elements of the state error covariance matrix A_{SE} correspond to the accuracy with which the squared pressures at all the N_N nodes are estimated. Therefore, the accuracy index of pressure is defined as the sum of these N_N elements of the state error covariance matrix as follows:

$$AI_p = \sum_{i=1}^{N_N} (A_{SE})_{ii} \tag{6-3}$$

6.2.1.3 Accuracy index of molar fraction

Apart from the first N_N elements of the N_{sp} diagonal elements of the state error covariance matrix A_{SE} that correspond to the accuracy of estimation of the squared pressures the rest of the elements of the diagonal elements of the state error covariance matrix correspond to the accuracy with which the molar fractions are estimated. Hence, the accuracy index of molar fraction is defined as the sum of these elements of the state error covariance matrix A_{SE} as follows:

$$AI_c = \sum_{i=1}^{N_c} (A_{SE})_{ii} \tag{6-4}$$

where N_c denotes the number of the state parameters of the network corresponding to the molar fraction of the components of the gas except one of them at all the nodes of the gas network.

6.2.2 Objective function

The operator of a gas distribution network with decentralised injection is more interested in gas quality and molar fraction of various gas compositions than the state of pressures and flows within the network especially at times that decentralised injection occur. Therefore, they need to equip the network with sets of measurements which better help them to have more accurate estimates of molar fractions of different gas components within the network. Hence, the accuracy index of molar fraction is considered as the decision criterion. Consequently, the objective function is defined as:

$$\text{minimise} \quad OF = \frac{\sum_{k=1}^{N_{MC}} AI_{c,k}}{N_{MC}}$$

$$\text{subject to} \quad \sum_{i=1}^{N_{MP}} PC_i \leq OB \tag{6-5}$$

where:

OF	The defined objective function
N_{MC}	Number of Monte Carlo simulations
$AI_{c,k}$	Accuracy index of molar fraction for the k 'th Monte Carlo simulation
N_{MP}	Number of measurement packages
PC_i	Cost of package i
OB	Operator budget

and the cost of package i, PC_i is calculated using:

$$PC_i = DC_{RTU_i} + DC_{PM_i} + DS_{GC_i} \times DC_{GC_i} + DS_{FM_i} \times \sum_{j=1}^{N_{FM_i}} DC_{FM_{j},i} \tag{6-6}$$

where:

DC_{RTU_i}	Cost of the RTU of the package i
DC_{PM_i}	Cost of the pressure meter of package i
DS_{GC_i}	Status of the gas chromatograph in package i (1 if the package has a gas chromatograph, 0 if not)
DC_{GC_i}	Cost of the gas chromatograph of package i
DS_{FM_i}	Status of the flow meter in package i (1 if the package has at least a flow meter, 0 if not)
N_{FM_i}	Number of the flow meters of package i
$DC_{FM_{j},i}$	Cost of the j'th flow meter of package i

In the formulation of the objective function all the gas components except one of them, Hydrogen, is considered. This is due to the fact that the molar fraction of the components of natural gas will add up to 1.0. Hence, molar fraction of one of the components is dependent on the rest of the components.

In the next section the developed algorithm for finding the best solution, which investigates the minimum value of the objective function, is presented.

6.2.3 The algorithm of additional measurement placement

An algorithm for placement of additional measurements in a gas distribution network with decentralised injection was developed. The algorithm accepts the following parameters as input:

- Operator relative budget (the budget divided by the cost of a flow meter)
- Relative cost of metering devices (the cost of each metering device divided by the cost of a flow meter)
- Minimum budget usage percentage (this defines the minimum percentage of the budget that the operator prefers to use)
- Gas power flow specific parameters:
  - Network topology
  - Demands and injections
  - Ambient pressure
  - Properties of air and gas components at STP conditions
- State estimation parameters:
  - Maximum number of iterations
  - Acceptable tolerance of the state estimation algorithm
- Measurements specifications:
  - Accuracy of different meters
  - Confidence level
  - Variance of zero injections
- Number of Monte Carlo simulations

The flow chart of the simulation model developed based on the algorithm is shown in Figure 6.1. The simulation model produces a list of the top ten measurement sets (number, type and place) along with the values of accuracy index of molar fraction and accuracy index of pressure for each set. Production of a list is due to the fact that it is impossible to obtain a global solution for a problem of measurement placement. Therefore, the operator is offered a list of measurement sets along with the performance of each set in terms of the values of accuracy indices of pressure and molar fraction. This way they can choose a measurement set to be placed within the network probably taking into account other practical constraints and difficulties.

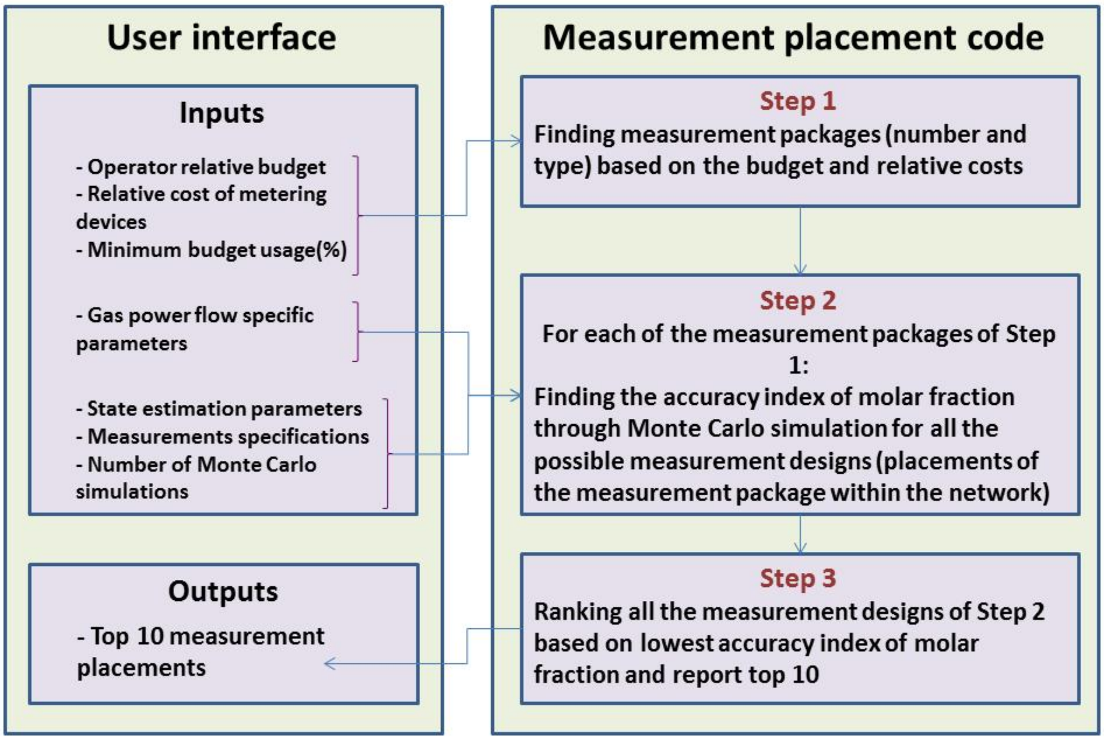

Figure 6.1: Flowchart of the simulation model developed for measurement placement

As can be seen from Figure 6.1, the algorithm performs three steps sequentially:

- Step 1: Finding the number and type of measurements

In this step the measurement packages[1] (number and type) are determined. In this step different measurement packages (number and

[1] **Measurement package** refers to the combination of different measurement numbers and types. For example a measurement package may include 1 RTU, 1 pressure meter and 2 flow meters.

type) are selected based on the fact that the cost of each package should be between the minimum budget usage and the whole budget of the operator. However, once the measurement packages are determined in this step, the ranking of the possible solutions is performed based on the performance of each of them and independent of the cost. For example if the algorithm finds that the performance of possible solution A with cost of 1 MU is better than the performance of the possible solution B with cost of 1.2 MU, then the possible solution A will be considered as the solution of the problem although the cost of it is less than the cost of possible solution B.

- Step 2: Calculating the accuracy index of molar fraction for all the possible measurement designs[1] (umber, type and place)

  In this step, each of the sets of measurement packages determined in Step 1, is placed in the network and the value of accuracy index of molar fraction for each set is calculated through a Monte Carlo simulation. The output of this step is a list of measurement designs (number, type and place) along with their values of accuracy index of molar fraction.

- Step 3: Ranking the measurement designs (umber, type and place)

  In this step, all the measurement designs (umber, type and place) are ranked and organised based on the lowest value of accuracy index of molar fraction and the top ten measurement designs along with their values of accuracy indices of molar fraction and pressure is sent to the output of the simulation model.

The method of performing Steps 1 and 2 is explained in the following sections. Step 3 is only a simple ranking process.

[1] **Measurement design** refers to the specific location that a specific measurement package is placed. In other words a measurement design is defined once the number, type and place of the meters are all determined.

6.2.3.1 Step 1: Finding the number and the type of measurements

The final aim of the algorithm of measurement placement is to place additional measurement units, which is called measurement packages in this Chapter, at some of the nodes of the network. Therefore, firstly these measurement packages are defined and then the algorithm developed in Step 1 determines some sets of packages as output.

In order to keep the problem simple and to be able to develop a preliminary algorithm, four packages of measurements were considered as shown in Figure 6.2. In fact, it was possible to consider more packages of measurements, however, for the purpose of simplicity these four packages were considered.

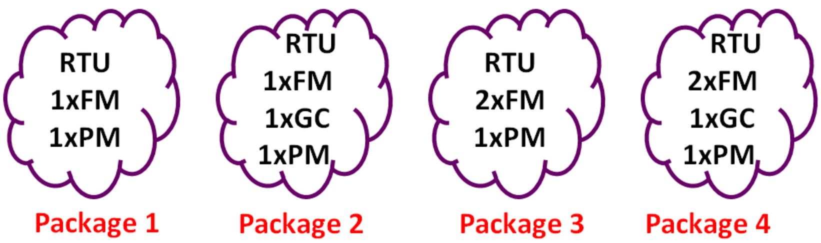

Figure 6.2: Packages of measurements[1]

The sets of number and type of measurements in Step 1 are determined based on the relative cost of metering devices, i.e. the cost of a device relative to a base cost. In order to have an estimate of the cost of different metering devices, i.e. pressure meter, flow meter, gas chromatograph and communication unit (RTU), an approximate value for the cost of these devices manufactured by SIEMENS were found, which is shown in Table 6.1.

Table 6.1: Approximate cost of metering devices used in gas networks

Device	Cost (£)
Pressure meter	< 500.0
Flow meter	3000.0 - 8000.0
Gas chromatograph	12000.0 - 18000.0
Remote Terminal Unit (RTU)	7000.0 - 13000.0

As can be seen flow meters are much more expensive than pressure meters. Therefore, the cost of a flow meter was considered as the base cost. In other words, the cost of a flow meter was assumed to be 1 Money Unit (1 MU). Also the cost of a pressure meter was assumed to be negligible relative to the base cost. Hence, it is assumed that all the

[1] RTU: Remote Terminal Unit; FM: Flow Meter; PM: Pressure Meter; GC: Gas Chromatograph

measurement packages are equipped with pressure meters. Furthermore, the relative cost of a gas chromatograph and an RTU in Money Units was obtained by dividing their cost by the base cost, i.e. the cost of a flow meter. Additionally, the relative operator budget in Money Units was calculated by dividing the operator budget by the base cost. All the relative costs of gas chromatograph and RTU and relative budget of the operator, after being calculated, were given as inputs to the measurement placement algorithm.

The algorithm developed in Step 1, which determines the measurement packages for Step 2, is described through an example. The assumption for the numbers and values in the example is just for explanation purposes and they all differ from the values assumed in the case study of the Chapter. Assume the operator relative budget is 5 MU and the minimum budget usage is 80%, i.e. the operator would like to use at least 80% of 5 MU. Hence, the algorithm in this Step should determine the measurement packages that have the cost in the range of 4 MU to 5 MU. The values assumed as the cost of different measurement packages are shown in Table 6.2.

Table 6.2: The values assumed for the cost of the measurement packages of the example

Measurement package	Cost
Measurement package 1	2 MU
Measurement package 2	3 MU
Measurement package 3	4 MU
Measurement package 4	5 MU

The following steps are taken in order to find the measurement packages:

- Step 1-1: Determine the package with the least cost
  Measurement package 1 has the least cost among the measurement packages.

- Step 1-2: Calculate the number N, which is the integer part of the division of the operator budget by the cost of the measurement package determined in Step 1-1.

$$N = \left\lfloor \frac{operator\ budget}{cost\ of\ the\ measurement\ package\ in\ Step\ 1-1} \right\rfloor = \left\lfloor \frac{5\ MU}{2\ MU} \right\rfloor = 2 \qquad (6\text{-}7)$$

- Step 1-3: Put $i = 1$

- Step 1-4: Select i (=1) of the measurement packages at a time and put them in a list

Number i	The list of measurement packages
1	Measurement package 1
1	Measurement package 2
1	Measurement package 3
1	Measurement package 4

- Step 1-5: Add 1 to i ($i = 2$)

- Step 1-6: Select a combination with replacement of i (=2) of the measurement packages at a time and add them to the list

Number i	The list of measurement packages
1	Measurement package 1
1	Measurement package 2
1	Measurement package 3
1	Measurement package 4
2	Measurement packages 1 and 1
2	Measurement packages 1 and 2*
2	Measurement packages 1 and 3
2	Measurement packages 1 and 4
2	Measurement packages 2 and 2
2	Measurement packages 2 and 3
2	Measurement packages 2 and 4
2	Measurement packages 3 and 3

2	Measurement packages 3 and 4
2	Measurement packages 4 and 4

*: "Measurement packages 2 and 1" is the same as "Measurement packages 1 and 2". Therefore, the similar combinations are not repeated in the list.

Add 1 to i and perform Step 1-6 up to $i = N$. In this example the maximum number for i ($i = N = 2$) is reached.

- Step 1-7: For each of the elements of the list calculate the cost of the sets of the measurement packages using the cost values in Table 6.2.

Number i	**The list of measurement packages**	**Cost of each set of measurement package**
1	Measurement package 1	2 MU
1	Measurement package 2	3 MU
1	Measurement package 3	4 MU
1	Measurement package 4	5 MU
2	Measurement packages 1 and 1	4 MU
2	Measurement packages 1 and 2	5 MU
2	Measurement packages 1 and 3	6 MU
2	Measurement packages 1 and 4	7 MU
2	Measurement packages 2 and 2	6 MU
2	Measurement packages 2 and 3	7 MU
2	Measurement packages 2 and 4	8 MU
2	Measurement packages 3 and 3	8 MU
2	Measurement packages 3 and 4	9 MU
2	Measurement packages 4 and 4	10 MU

- Step 1-8: Select the sets of the measurement packages that are in the desired range

Since the target was to use 4 MU to 5 MU the sets of the measurement packages, which have the cost in the desired range, are selected from the list.

Measurement package 3	4 MU
Measurement package 4	5 MU
Measurement packages 1 and 1	4 MU
Measurement packages 1 and 2	5 MU

This list is the output of Step 1.

In order to summarise, the algorithm of Step 1 is shown in Figure 6.3.

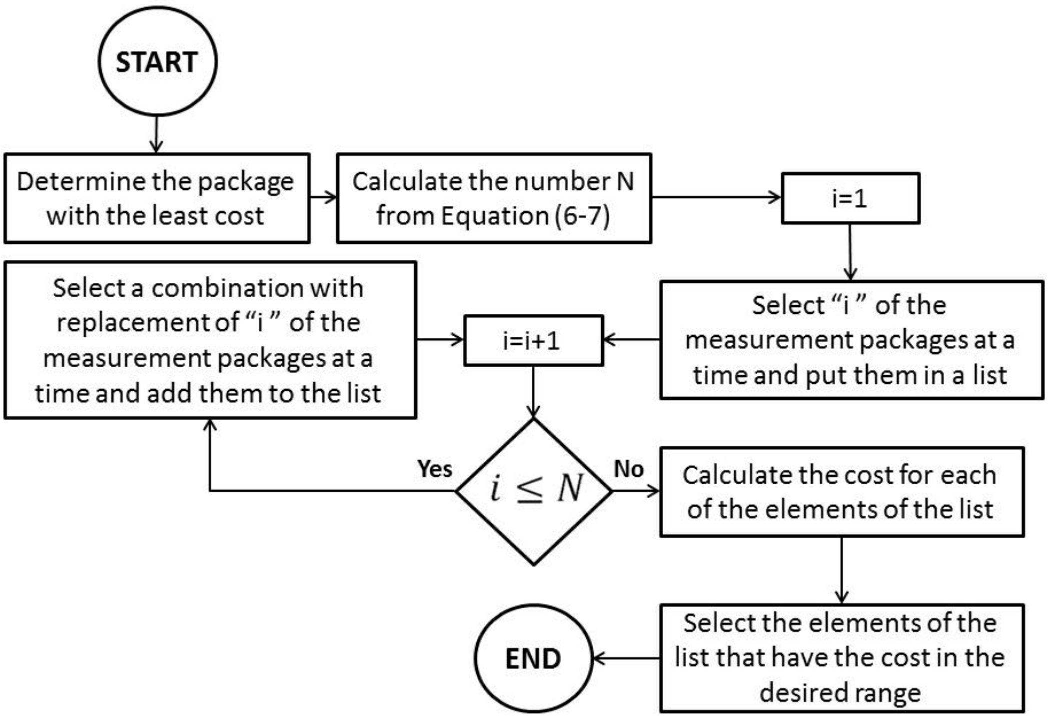

Figure 6.3: The algorithm of Step 1

The output of Step 1 is sets of packages, in which the number and type of metering devices is determined, however, the places of these measurement packages is not yet determined, which is performed in Step 2.

6.2.3.2 Step 2: Calculating the value of accuracy index of molar fraction for all the possible measurement designs

For each and every set of measurement packages (number and type) determined in Step 1, a search space, called the set of possible designs, is formed by combination of placement of packages in the possible locations within the network. Each placement of packages in possible locations within the network is called a possible design. Then, a

Monte Carlo simulation of state estimation, which was described in Chapter 5, is performed on each possible design in the search space in order to obtain an average value for accuracy index of the molar fraction for it. Afterwards, all possible designs corresponding to each set of measurement packages of Step 1 are ranked based on lowest value of accuracy index of molar fraction.

The top ten possible designs of all the output sets (number, type and place) of Step 2 are compared against each other and are ranked based on lowest value of accuracy index of molar fraction. Finally, the top ten possible designs with lowest value of accuracy index of molar fraction are considered as the problem solutions and are sent to the output along with the values of accuracy index of molar fraction and accuracy index of pressure.

As explained before, the problem of additional measurement placement is to place additional measurement packages at some of the nodes. The set of possible nodes is assumed to be all the nodes except the following nodes:

- Source (pressure source) and injection nodes, since it is assumed that real time measurements of pressure, node flow (injection) and gas chromatograph are already placed at these nodes and the problem is to enforce the measurement infrastructure of the network with additional measurements.

- Nodes which are the only nodes connected to either source or injection nodes. In other words, if each of the source or injection nodes is connected to more than one node, those nodes are considered in the set of possible nodes. For example the nodes 3, 4 and 5 in Figure 6.4(b) are considered in the set of possible nodes. However, if any of the source or injection nodes is only connected to one node, that node is removed from the set of possible nodes due to having real time measurements at one of the neighbouring nodes, i.e. that source or the injection node. For example node 2 in Figure 6.4(a) is not considered in the set of possible nodes.

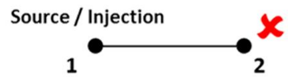

(a) Node 2 is not considered in the set of possible nodes.

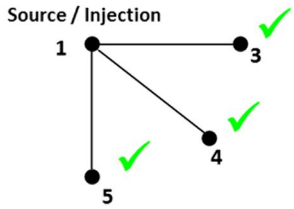

(b) Nodes 3, 4 and 5 are considered in the set of possible nodes.

Figure 6.4: The nodes that are/are not considered in the set of possible nodes

For placement of measurement packages at nodes the following has been considered:

- Pressure meter:

Pressure meter is placed on the node to measure nodal pressure.

- Gas chromatograph:

Gas chromatograph is placed on the node to measure gas composition of the node after mixing assuming ideal mixing occurs at the node.

- Flow meter:

For placement of flow meters on branches connected to a node, the following rules have been considered in order to keep the problem simple, avoid expansion of search space and computation effort and finally to be able to solve the problem:

- Real time flow meters at each node are placed on branches connecting the node to other nodes. In other words, the flow meter is not placed for real time measurement of load at the load nodes since it is assumed the measurements of the loads are already incorporated through pseudo measurements of the loads.

- Flow meters are placed on branches in order of lowest branch number, for the branches connected to the node.

6.3 Case study

6.3.1 The network

In order to study the impact of different types of measurements on the SE of gas networks as well as to investigate the problem of placement of additional measurements within a gas distribution network the case study of Chapter 5 operating at medium pressure level was considered (Figure 6.5). The single decentralised injection occurs at node 6 with the injection power of 40 MW. The pressure at the source node is assumed to be 7.0 bar gauge and the ambient pressure is assumed to be 1.0 bar gauge. All the data of the network is presented in Appendix II.

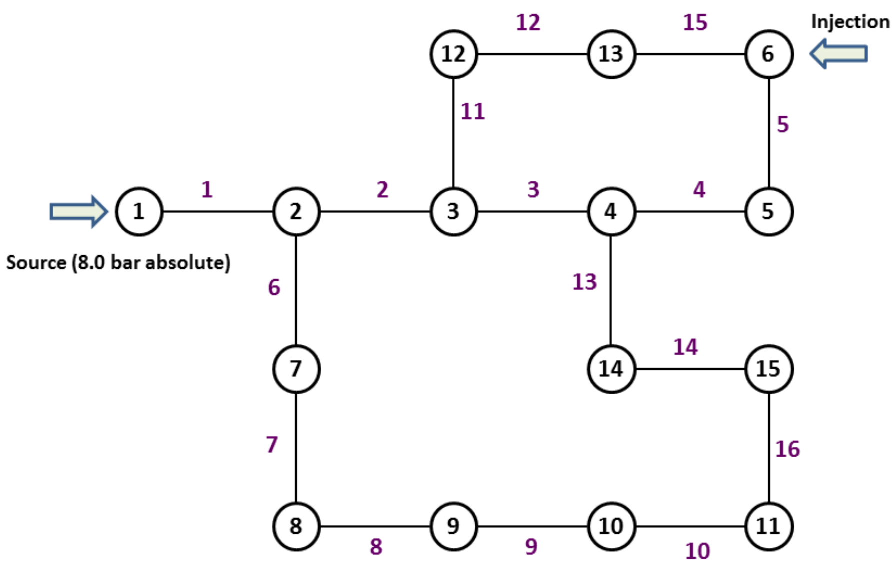

Figure 6.5: The schematic of the case study gas distribution network

6.3.2 Measurements

The available measurements of the network along with the values of their accuracies are shown in Table 6.3. The standard deviation of the measurements is calculated based on a 95% confidence level and the accuracy of the measurements using Equation (2-13). Also, variance of virtual measurements, i.e. measurements of load at zero load nodes, is assumed to be 1.0×10^{-8}. Additionally, for every Monte Carlo simulation of the network new values of all the pseudo measurements and real time measurements were produced using the $normrnd(\psi, \sigma)$ function of MATLAB, which generates normally distributed values.

Table 6.3: Available measurements of the test network

Measured parameter	Measurement location	Measurement type	Accuracy
Pressure	Source node #1 Injection node #6	Real time	1 %
Branch flow	Branch 1-2	Real time	1 %
Node flow	Source node #1 Injection node #6	Real time	1 %
	All the load nodes	Pseudo	50 %
Molar fraction	Source node #1 Injection node #6	Real time	1 %
	All the nodes except nodes #1 and 6	Pseudo	10 %

6.3.3 The assumptions of the case study

It is assumed that the source and injection nodes are already equipped with real time measurements of pressure, node flow and gas composition. In other words, the cost of metering devices at these nodes is not considered. Therefore, the measurement placement algorithm tries to place additional measurement sets (number, type and place) within the network subject to the limited budget of the operator for improvement of the metering infrastructure. The assumed values for relative cost of metering devices are shown in Table 6.4, assuming all RTUs are equipped with real time pressure meters. Also, the number of Monte Carlo simulations for evaluating each possible measurement design is selected to be 15. A discussion on selection of this number will be given in section 6.4.2.2. Additionally, in this work it is assumed that the operator should use at least 70% of their budget for improvement of the measurement infrastructure, i.e. the minimum budget usage is assumed to be 70%. Also, it is assumed that brand and model and hence the cost of different devices in different packages are all identical.

Table 6.4: Relative cost of metering devices

Device	Cost (MU)
RTU	2.0
Flow meter	1.0
Gas chromatograph	2.5

6.4 Results and discussion

6.4.1 Evaluating the impact of different measurements on state estimation

In order to investigate the impact of different types of measurements on the state estimation of the network, 5 cases have been designed. The set of measurements in each case is shown in Table 6.5.

Table 6.5: Cases considered for investigating impact of measurements on the state estimation

Case number	Case description	Included measurements*		
		Measurement type	**Real time**	**Pseudo**
Case 1	Typical system	Pressure	source and injection	---
		Molar fraction		all the nodes except source and injection nodes
		Load	---	
Case 2	All real time pressure meters	Pressure	all the nodes	---
		Molar fraction	source and injection	all the nodes except source and injection nodes
		Load	---	
Case 3	All real time molar fraction meters	Pressure	source and injection	---
		Molar fraction	all the nodes	---
		Load	---	all the nodes except source and injection nodes
Case 4	All real time load flow meters	Pressure	source and injection	---
		Molar fraction		all the nodes except source and injection nodes
		Load	all the nodes	---
Case 5	Full real time meters of pressures, molar fractions and load flow	Pressure	all the nodes	---
		Molar fraction		---
		Load		---

*: in all the cases virtual measurements of zero flow at nodes without load were considered.

6.4.1.1 Suitable number of Monte Carlo simulations for state estimation of the network

In order to obtain a suitable number of Monte Carlo simulations for state estimation of the test network, a criterion has been defined, which is the average value of accuracy index of the state estimation. Then the number of Monte Carlo simulations of the network started from 15000 and increased in steps of 1000 and the change in the value of the criterion was monitored after they converged and stabilised (Figure 6.6). As can be seen the change in the value of the criterion is observed to be less than 0.01 for 5 consecutive steps up to 20000 Monte Carlo simulations. Therefore, the results obtained by 20000 Monte Carlo simulations of state estimation of the network were considered as reliable.

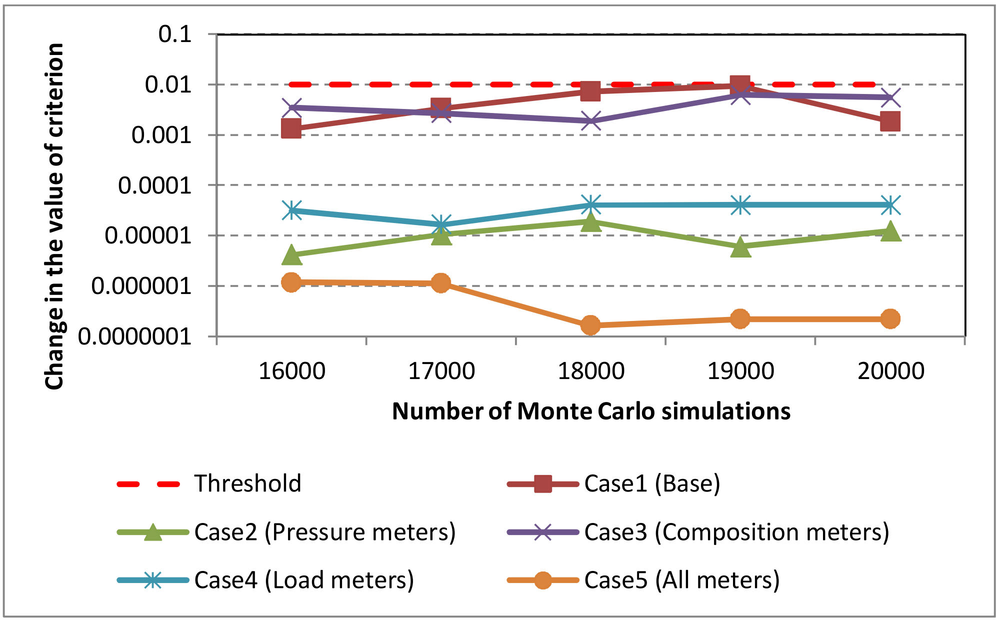

Figure 6.6: Change in the value of the criterion with the change in the number of Monte Carlo simulations

6.4.1.2 Results and discussion of impact of measurements on state estimation of the network

- *Impact on estimation of the pressures*

The values of MAPE of estimation of the nodal pressures for all the cases are shown in Figure 6.7(a). The values of accuracy index of pressure for all the cases are presented in Figure 6.7(b).

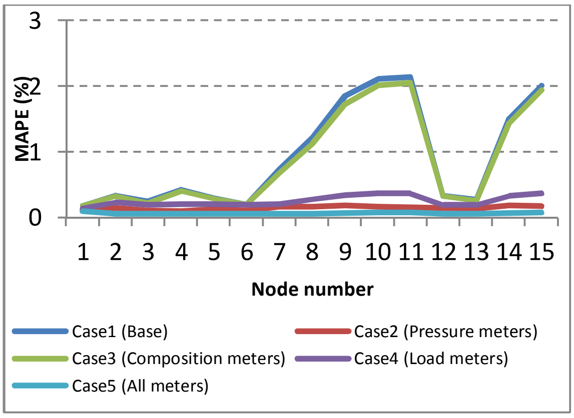

(a) MAPE values of estimated nodal pressures

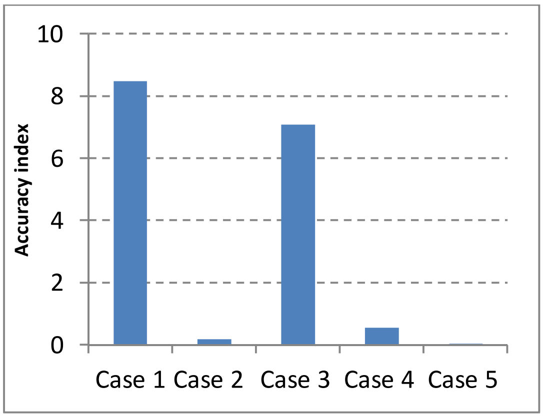

(b) Accuracy index of pressure

Figure 6.7: The impact of measurements on the estimated nodal pressures

As can be seen from Figures 6.7(a) and 6.7(b) equipping the network with all the real time measurement types, i.e. Case 5, leads to the least values of MAPE of estimation of pressures and accuracy index of pressure. In the next step placing real time pressure meters, i.e. Case 2, has slightly higher values of MAPE and accuracy index of pressure relative to Case 5 and less values than Case 4, where the network is equipped with real time measurements of loads. As can be seen highest values of MAPE and accuracy index of pressure are observed for the typical system, i.e. Case 1, where the values of MAPE and accuracy index of pressure are slightly higher than the values in Case 3, in which real time measurements of molar fractions were placed in the network. Hence, placing measurements of molar fraction has impact on estimation of nodal pressures. However, the impact is really insignificant. Also, the impact of real time measurements of pressure on accuracy of estimation of pressures is higher than the impact of load measurements.

To conclude, placement of all the various real time measurement types is the best way to estimate the nodal pressures accurately, however, this solution is highly costly. The practical and less expensive way is to place real time measurements of pressure in the network. Placement of real time measurements of load also helps, however it is not as effective as the real time measurements of pressure. Finally, equipping the network with expensive gas chromatographs does not help to better estimate the values of nodal pressures.

- *Impact on estimation of the flows*

The values of MAPE of estimation of the loads in all the cases are shown in Figure 6.8(a). The values of MAPE of estimation of the flows of the branches in all the cases are presented in Figure 6.8(b).

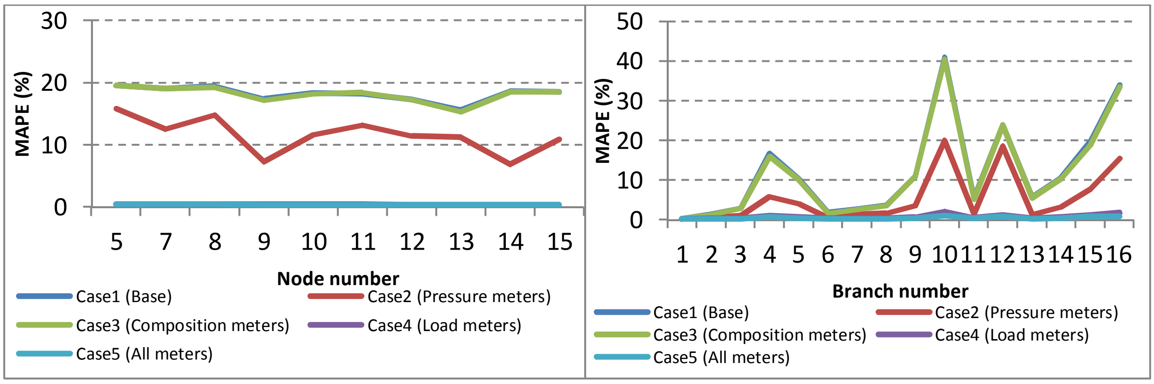

(a) MAPE values of estimated loads **(b) MAPE values of estimated flows of branches**

Figure 6.8: The impact of measurements on the estimated flows

According to Figure 6.8 in Case 4 (load measurements) and Case 5 (all full measurements) the values of MAPE of estimation of flows, either load flows or flows of branches, are almost the same and minimum. However, putting just measurements of pressure, i.e. Case 2, results in an increase in the values of MAPE of estimation of all the flows. In fact, impact of measurement of load on estimation of pressures is much more than the impact of measurements of pressure on estimation of the flows. Finally, the values of MAPE of estimation of flows for Case 1 (typical system) and Case 2 (measurements of molar fraction) are almost the same and highest. This means the measurements of molar fraction had no impact on estimation of flows. Also, the impact of measurements of pressure on estimation of flows was observed to be much less than the impact of measurements of load.

To conclude, in order to obtain the most accurate estimated values for the flows all the measurement types need to be placed in the network, which is very costly. However, the practical solution is to locate real time measurements of load flow in the network, which is much more effective than placing real time measurements of pressure that is less expensive than placement of measurements of load flow. Placement of measurements of molar fraction seems to be unhelpful in estimation of the flows.

- *Impact on estimation of the molar fractions*

The values of accuracy index of molar fraction for all the cases are shown in Figure 6.9(a). The values of MAPE of estimation of the molar fraction of all the components for all the cases are presented in Figures 6.9(b) to 6.9(h). High values of MAPE of estimation of Hydrogen (H_2) at some of the nodes is due to the fact that the true value of molar fraction of Hydrogen at those nodes is zero (Figure 6.9(h)).

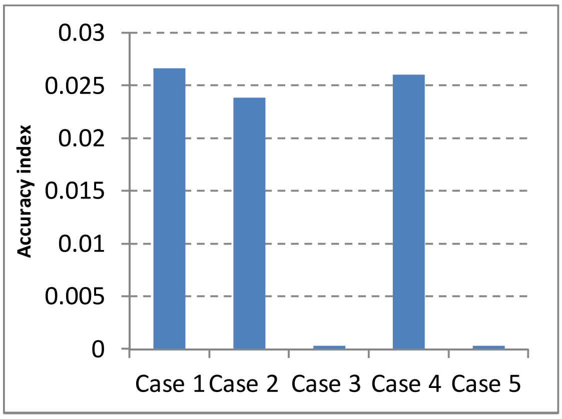

(a) Accuracy index of molar fraction

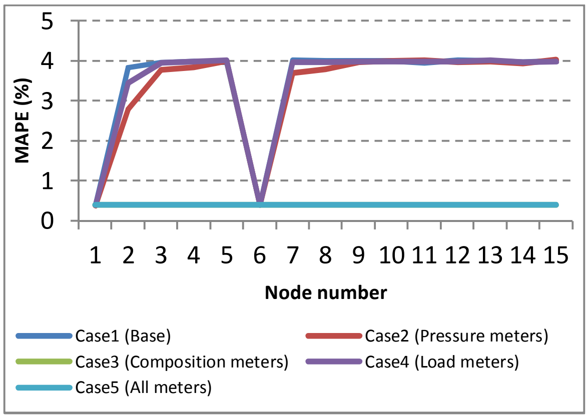

(b) MAPE values of estimated molar fraction of CH_4

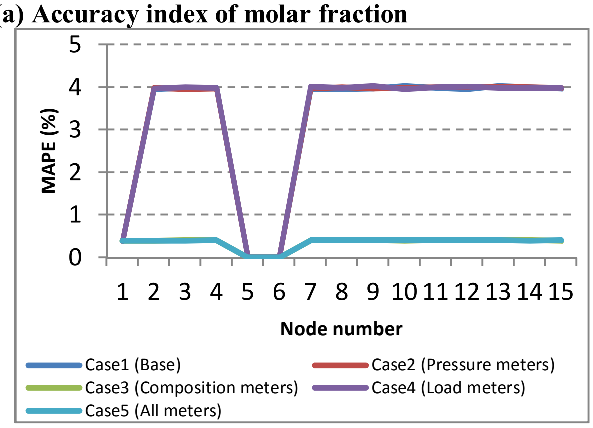

(c) MAPE values of estimated molar fraction of C_2H_6

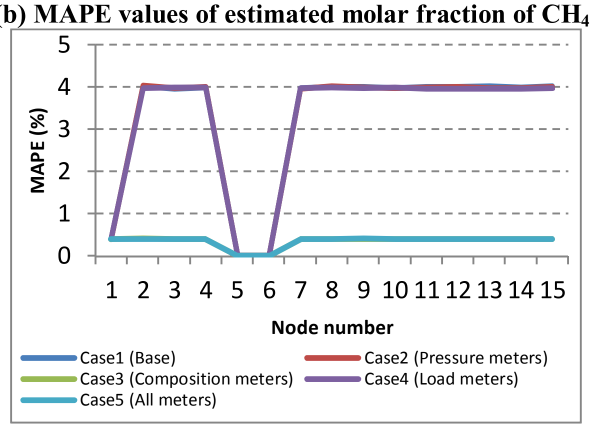

(d) MAPE values of estimated molar fraction of C_3H_8

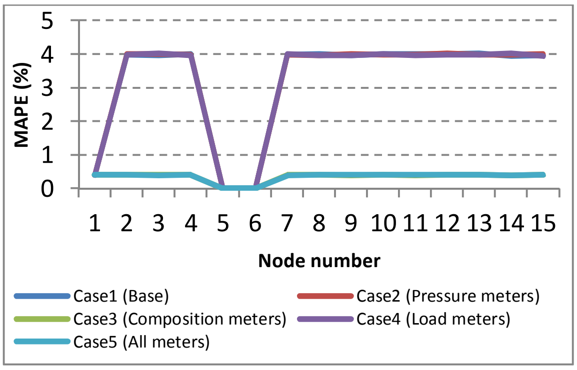

(e) MAPE values of estimated molar fraction of C_4H_{10}

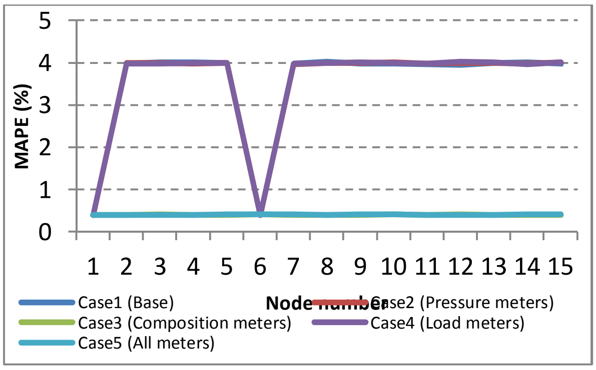

(f) MAPE values of estimated molar fraction of CO_2

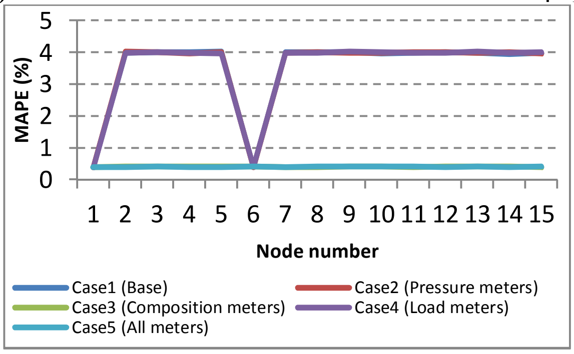

(g) MAPE values of estimated molar fraction of N_2

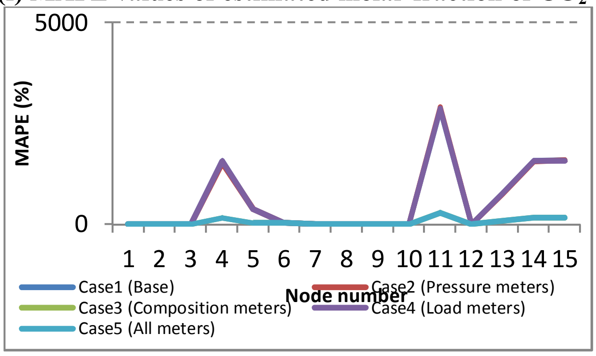

(h) MAPE values of estimated molar fraction of H_2

Figure 6.9: The impact of measurements on the estimated molar fractions

As can be seen from Figure 6.9(a), the value of accuracy index of molar fraction is minimum for Case 5, i.e. network equipped with all the real time measurements, and then slightly more in Case 3, the network equipped with measurements of molar fraction. The difference between Cases 3 and 5 is insignificant. The value of accuracy index of molar fraction is highest for the basic network, Case 1, and then the value in Case 4, network equipped with real time measurements of load flow, is slightly less than Case 1. Then the value of accuracy index of molar fraction in Case 2, real time measurements of pressure, is slightly less than Case 4.

As can be seen from Figures 6.9(b) to 6.9(h) the values of MAPE of estimation of molar fraction of gas components are almost equally minimum for Case 3 (measurements of molar fraction) and Case 5 (all full measurements) that they coincided. The values of MAPE of estimation of molar fraction is almost equal and highest for Cases 1 (typical system), 2 (measurements of pressure) and 4 (measurements of load flow). The values for Cases 1, 2 and 4 are also the same that they coincided in all the MAPE graphs except 6.9(b). However, for the case of molar fraction of CH_4, where the true values of molar fraction at nodes are high, i.e. more than 90.0%, the MAPE value is highest for Case 1 (Base system) and then the values for Case 4 is less than Case 1 and finally values for Case 2 are obviously less than Case 4, at some of the nodes. This seems to be due to the fact that pressure and flow measurements have slight impacts on estimation of molar fractions, although the effect is insignificant. Also, the impact of load measurements is less than the impact of pressure measurements in reducing the values of MAPE. Additionally, it can be deduced that for the gas compositions, which have small true values of molar fraction, i.e. less than 10%, the pressure and flow measurements have shown almost no impact on MAPE values of estimation of molar fraction.

To conclude, the practical solution for accurate estimation of the molar fractions is to place expensive gas chromatographs in the network, which is still costly but still cheaper than placement of all the measurement types in the network. Placement of measurements of pressure and load flow shows no sensible impact on estimation of the molar fractions.

6.4.2 Optimal placement of additional measurements

The problem of measurement placement was investigated subject to three cases of a limited budget of the operator, which are presented in Table 6.6.

Table 6.6: The cases of the limited budget of the network operator

Case #	Budget (MU)
Case 1	5.5
Case 2	8.5
Case 3	11.5

The best measurement design (number, type and place) is considered as the first design in the top ten output measurement designs. Then the improvement of estimation of pressures, flows and molar fractions for the network equipped with the best measurement design, with increase in the budget of the operator corresponding to the cases was studied. Finally, a sensitivity analysis to the accuracy of the pseudo measurements of load and molar fraction was performed.

6.4.2.1 Best measurement designs

The best solution, in terms of the value of accuracy index of molar fraction, corresponding to each of the output sets of Step 1 of the algorithm of additional measurement placement along with the values of accuracy index of pressure and molar fraction is shown in Table 6.7. The best measurement design in each case of budget is highlighted.

Table 6.7: The best solution corresponding to each measurement set of the outputs of Step 1 of the algorithm*

Budget Case	Output sets of Step1**				N_{IM}	Best solution for each set						AI_p	$AI_y \times 10^3$	Cost (MU)
	$MP\ 1$	$MP\ 2$	$MP\ 3$	$MP\ 4$		$MP\#$	$GN\#$	$MP\#$	$GN\#$	$MP\#$	$GN\#$			
5.5 MU	0	1	0	0	3	2	3	---	---	---	---	2.72	20.66	5.5
	0	***0***	***1***	***0***	***3***	***3***	***3***	***---***	***---***	***---***	***---***	***2.21***	***20.52***	***4.0***
8.5 MU	1	1	0	0	5	1	7	2	8	---	---	1.60	19.82	8.5
	0	***0***	***2***	***0***	***6***	***3***	***3***	***3***	***14***	***---***	***---***	***0.83***	***19.52***	***8.0***
	1	0	1	0	5	1	14	3	3	---	---	1.60	19.56	7.0
	0	0	0	1	4	4	3	---	---	---	---	2.30	20.51	6.5
	2	0	0	0	4	1	7	1	8	---	---	1.61	19.83	6.0
11.5 MU	2	1	0	0	5	1	7	1	8	2	9	1.17	18.75	11.5
	0	2	0	0	6	2	7	2	8	---	---	1.60	19.83	11.0
	1	***0***	***2***	***0***	***8***	***1***	***10***	***3***	***3***	***3***	***8***	***0.48***	***18.47***	***11.0***
	0	0	1	1	7	3	3	4	14	---	---	0.81	19.51	10.5
	2	0	1	0	7	1	8	1	9	3	3	0.96	18.65	10.0
	1	0	0	1	6	1	14	4	3	---	---	1.55	19.56	9.5
	0	1	1	0	6	2	14	3	3	---	---	1.57	19.56	9.5
	3	0	0	0	6	1	7	1	8	1	9	1.25	18.76	9.0
	1	1	0	0	5	1	3	2	14	---	---	1.58	19.83	8.5

*: MP: Measurement Package; N_{IM}: Total number of individual meters that are included in the measurement set; MP# and GN#: The number of the measurement package (MP#) that is suggested to be placed at the specific node (GN#) of the gas network; AI_p: Average value of accuracy index of pressure of the best measurement design; AI_y: Average value of accuracy index of molar fraction of the best measurement design.

**: The numbers in these 4 columns are number of each of the measurement packages that is included in each measurement set. For example, the number "2" under MP3 means that the measurement set includes 2 measurement packages number 3.

In order to understand Table 6.7 the third row for the budget case of 11.5 MU, which is also highlighted as the best measurement design solution of this case, is explained. This measurement design has 1 Measurement Package 1 (MP1), 0 Measurement Package 2 (MP2), 2 Measurement Package 3 (MP3) and 0 Measurement Package 4 (MP4). The total number of individual measurements in this measurement design is 8, since MP1 has 1 flow meter and 1 pressure meter and MP 3 has 2 flow meters and 1 pressure meter. Hence, the measurement set of 1 measurement package 1 and 2 measurement package 3 has 8 individual meters. The next part of the table, under the title of "Best solution for each set" states that the MP1 must be placed at the Gas network node number 10 (GN#10) and one MP3 at GN#3 and one MP3 at GN#8 must be placed. The average value of accuracy index of pressure of this measurement design is 0.48 and the average value of accuracy index of molar fraction of this measurement design is 0.001847. Finally, the cost of this measurement design is 11.0 MU.

By comparing the values of accuracy index of molar fraction for the best solution of each output set of Step 1, the algorithm has selected sets of measurement packages with the most number of metering devices assuming a gas chromatograph measuring several components as a single device. Also, it is observed that in none of the budget cases the best measurement design includes either of the measurement packages 2 or 4, which includes a gas chromatograph. This seems to be due to the two following facts, which is further discussed in Table 6.8:

- The values of molar fraction of the components at nodes are very small, i.e. except CH_4, which has true values of more than 90%, the rest of the components have true values less than 10%. Therefore, placing a gas chromatograph at a node has really insignificant impact on improvement of the accuracy index of molar fraction.

- As discussed in section 6.4.1.3 the pressure and flow measurements have an impact on estimation of molar fraction, although their impact is not very significant.

Table 6.8 shows the amount of improvement of accuracy index of pressure and accuracy index of molar fraction for each measurement design solution. For this purpose, the values of accuracy indices of pressure and molar fraction for each measurement design solution is compared with the corresponding values of the base network, i.e. the network that is not equipped with the additional measurements. The values are demonstrated in terms of percentage improvement in the accuracy index of pressure or molar fraction.

Table 6.8: Improvement of the accuracy indices of pressure and molar fraction relative to the base network for the best measurement designs

Case	$AI_y \times 10^3$	Improvement (%)	AI_p	Improvement (%)
Base network	21.40	--	4.78	--
5.5 MU*	20.52	4.1**	2.21	53.7
8.5 MU*	19.52	8.7	0.83	82.6
11.5 MU*	18.47	13.6	0.48	89.9

*: These correspond to the best measurement design of each budget case

**: This value is calculated as follows: $(21.40 - 20.52)/21.40 \times 100$.

As can be seen from Table 6.8 although the values of accuracy index of molar fraction are generally small, placement of additional measurements of pressure and flow within the network improves their values gradually. This is due to the two facts that were discussed earlier above Table 6.8. Therefore, the improvement in the values of accuracy index of molar fraction is not very significant. Hence, slight improvement in estimation of the values of molar fraction of gas components should be expected. Also, Table 6.8 shows that the improvement in the accuracy index of pressure is high. This was expected since the impact of pressure and flow meters on improvement of accuracy index of pressure is higher than the impact of them on improvement of accuracy index of molar fraction. This was already shown and discussed in section 6.4.1.2.

6.4.2.2 Discussion on suitability of the number of Monte Carlo simulations selected in Step 2 of the measurement placement algorithm

In order to investigate the suitability of the number of Monte Carlo simulations in Step 2, i.e. 15 Monte Carlo simulations, for evaluating the performance of each possible measurement design (number, type and place) in the search space, the problem was solved with 16, 18 and 20 Monte Carlo simulations for each budget case. This was done to make sure that the Monte Carlo simulation is stabilised and has converged to the solution. Top ten solutions in terms of the measurement packages to be placed at the nodes are compared against the results obtained by 15 Monte Carlo simulations in Table 6.9.

Table 6.9: Top ten designs obtained through different number of Monte Carlo simulations

Budget case	Design rank	15 Monte Carlo*		16 Monte Carlo		18 Monte Carlo		20 Monte Carlo	
		$MP\#$	$GN\#$	$MP\#$	$GN\#$	$MP\#$	$GN\#$	$MP\#$	$GN\#$
5.5 MU	1	3	3	3	3	3	3	3	3
	2	3	14	3	14	3	14	3	14
	3	2	3	2	14	2	14	2	14
	4	2	14	2	3	2	3	2	3
	5	3	8	3	8	3	8	3	8
	6	2	8	2	8	3	4	2	8
	7	3	7	3	7	2	8	3	4
	8	3	4	3	4	3	7	3	7
	9	2	7	3	9	2	7	2	7
	10	3	9	2	7	3	9	3	9
8.5 MU	1	3 3	3 14	3 3	3 14	3 3	3 14	3 3	3 14
	2	1 3	14 3	1 3	14 3	1 3	14 3	3 3	7 9
	3	3 3	7 9	3 3	7 9	3 3	7 9	1 3	14 3
	4	1 3	9 7	1 3	9 7	1 3	9 7	1 3	9 7
	5	3 3	3 8	3 3	3 8	3 3	3 8	3 3	3 8
	6	1 3	8 3	1 3	8 3	1 3	8 3	1 3	8 3
	7	3 3	4 12	3 3	4 12	3 3	4 12	3 3	4 12
	8	3 3	3 9	3 3	3 9	3 3	3 9	3 3	3 9
	9	1 3	9 3	1 3	9 3	1 3	3 14	1 3	9 3
	10	1 3	3 14	1 3	3 14	3 3	8 10	1 3	3 14
11.5 MU	1	1 3 3	10 3 8	1 3 3	10 3 8	1 3 3	10 3 8	1 3 3	10 3 8
	2	1 3 3	8 3 9	1 3 3	8 3 9	1 3 3	8 3 9	1 3 3	8 3 9
	3	1 3 3	8 3 14	1 3 3	7 8 10	1 3 3	8 3 14	1 3 3	8 3 14
	4	1	7	1	9	1	8	1	7

Budget case	Design rank	15 Monte Carlo*		16 Monte Carlo		18 Monte Carlo		20 Monte Carlo	
		$MP\#$	$GN\#$	$MP\#$	$GN\#$	$MP\#$	$GN\#$	$MP\#$	$GN\#$
		3 3	8 10	3 3	3 8	1 3	9 3	3 3	8 10
	5	1 1 3	8 9 3	1 3 3	8 3 14	1 3 3	7 8 10	1 1 3	8 9 3
	6	1 3 3	9 3 8	1 1 3	8 9 3	1 3 3	9 3 8	1 3 3	9 3 8
	7	1 1 3	7 10 8	1 3 3	10 7 8	1 1 3	7 10 8	1 1 3	7 10 8
	8	1 3 3	10 7 8	1 1 3	7 10 8	1 3 3	10 7 8	1 3 3	10 7 8
	9	1 1 3	8 14 3	1 1 3	8 14 3	1 3 3	14 3 8	1 3 3	14 3 8
	10	1 3 3	14 3 8	1 3 3	14 3 8	1 1 3	8 14 3	1 1 3	8 14 3

*: MP# and GN# denote the measurement package number (MP#) that is suggested to be placed at the specific node (GN#) of the gas network.

The column "Design rank" in Table 6.9 states the first 10 top measurement designs of the output of the measurement placement algorithm for each budget case. For example the row corresponding to Design rank 5 in each budget case shows the fifth ranked measurement design that is suggested by the algorithm for each selected value of the number of Monte Carlo simulations in Step 2. In order to understand Table 6.9 the last row of the table is explained. For the budget case of 11.5 MU, the 10th measurement design that is suggested by the algorithm is as follows for each selected number of Monte Carlo simulations of the Step 2 of the measurement placement algorithm:

- For 15 and 16 Monte Carlo simulations place one Measurement Package number 1 (MP# 1) at node number 14 (GN# 14) of the network, one measurement package number 3 (MP# 3) at node 3 (GN# 3) and one measurement package number 3 (MP# 3) at node 8 (GN# 8).

- For 18 and 20 Monte Carlo simulations place one measurement package number 1 (MP# 1) at node number 8 (GN# 8) of the network, one measurement package number 1 (MP# 1) at node 14 (GN# 14) and one measurement package number 3 (MP# 3) at node 3 (GN# 3).

As can be seen from Table 6.9, the top (best) measurement design was unchanged with increase in the number of Monte Carlo simulations in each budget case. Additionally, the list of top ten solutions is almost the same and the replacements in measurement designs are insignificant. Therefore, it can be concluded that 15 Monte Carlo simulations can be considered sufficient in order to obtain reliable solutions.

6.4.3 Monte Carlo simulation of state estimation of the best measurement designs of output of Step 3 of the algorithm

20,000 Monte Carlo simulations of state estimation of the best measurement design of each budget case were carried out. The values of MAPE of estimation of the state parameters and the operation parameters of the network are plotted and discussed.

6.4.3.1 Estimation of the nodal pressures

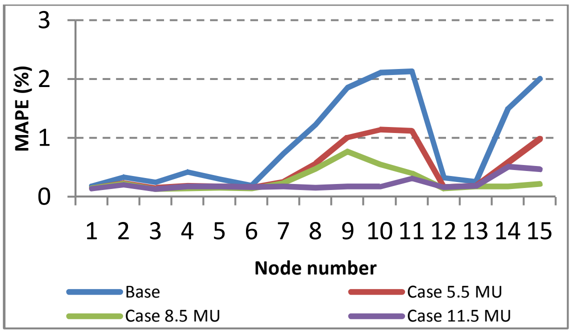

Figure 6.10: MAPE of estimation of the nodal pressures for the best measurement designs

The values of MAPE of estimation of the nodal pressures are presented in Figure 6.10. As can be seen from Figure 6.10 increasing the number of pressure meters improves the estimation of nodal pressures in general. For the nodes that are located on the shortest routes connecting the source and the injection nodes, i.e. the routes denoted by the nodes 1-2-3-4-5-6 and 1-2-3-12-13-6, the MAPE of estimation of the pressures are almost the same and low. This may be due to the fact that the source and injection nodes are already equipped with the real time measurements of pressure and flow. Hence, estimation of the nodal pressures on the shortest routes connecting these two nodes is very accurate. Apart from these nodes placement of additional measurements decreases the MAPE values of estimation of the nodal pressures at the rest of the nodes.

6.4.3.2 Estimation of the loads

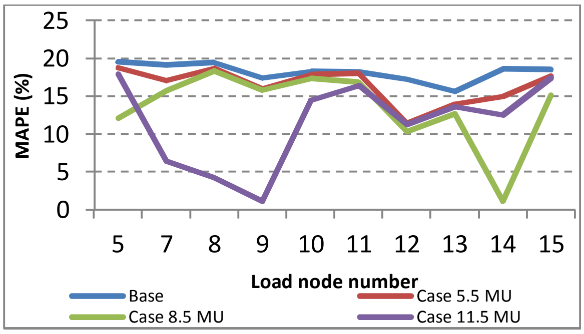

Figure 6.11: MAPE of estimation of the loads for the best measurement designs

The values of MAPE of estimation of the loads are shown in Figure 6.11. As can be seen from Figure 6.11 placing additional measurements within the network decreases the MAPE values of estimation of the loads in general. In the budget case of 8.5 MU two measurement packages 3 are placed at nodes 3 and 14. These measurement packages include 2 flow meters. Placement of this package on node 14 means that the branches connecting this node to the two neighbouring nodes, i.e. branches 13 (between nodes 4 and 14) and 14 (between nodes 14 and 15), are equipped with flow meters. This results in the estimation of the load at node 14 with a much lower error. This is the reason estimation of the load at the load node 14 has less errors relative to the rest of the nodes.

Also, for the budget case of 11.5 MU one measurement package 1 at node 10, one measurement package 3 at node 3 and one measurement package 3 at node 8 are suggested to be placed. This means that branches 9 (between nodes 9 and 10), 2 (between nodes 2 and 3), 3 (between nodes 3 and 4), 7 (between nodes 7 and 8) and 8 (between nodes 8 and 9) are equipped with flow meters. Therefore, estimation of the load at the nodes 7, 8 and 9 is performed with an error lower than the load at the rest of the load nodes. Apart from all these exceptions improvement in the MAPE value of estimation of the loads with increasing the number of measurements within the network is observed.

6.4.3.3 Estimation of the flow of the branches

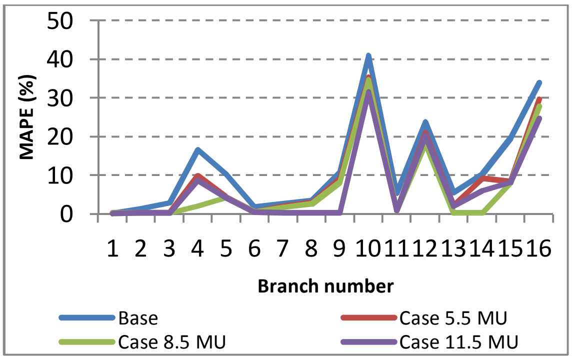

Figure 6.12: MAPE of estimation of the flow of the branches for the best measurement designs

The values of MAPE of estimation of the flow of the branches are presented in Figure 6.12. As can be seen from Figure 6.12 placement of additional measurements within the network improved estimation of the flows of the branches in general although the amount of improvement is small compared among the cases. For the budget case of 8.5 MU, in which the branches 2, 3, 13 and 14, are equipped with flow meters and also because node 4 is just a connection node and not a load node, estimation of the flow of the branches 2, 3, 4, 13 and 14 in this case has a very low error compared to the rest of the cases. Also, for the budget case of 11.5 MU the branches 2, 3, 7, 8 and 9 are equipped with flow meters. Hence, estimation of the value of the flow of these branches is more accurate relative to the rest of the cases.

In all the cases node 3 is equipped with measurement package 3, i.e. the flows of branches 2 and 3 are measured. Since the source node is also equipped with a flow meter on branch 1 and node 2 is just a connecting node rather than a load node, the flow of branch 6 has a very low error in all the cases. Additionally, due to the same reason, i.e. package 3 at node 3, and node 3 being a connecting node the flow of branch 11 is estimated accurately in all the cases.

Apart from these exceptions in some of the branches improvement in estimation of the flow of the branches is observed with increase in the number of additional measurements within the network.

6.4.3.4 Estimation of the molar fraction of gas components at the nodes

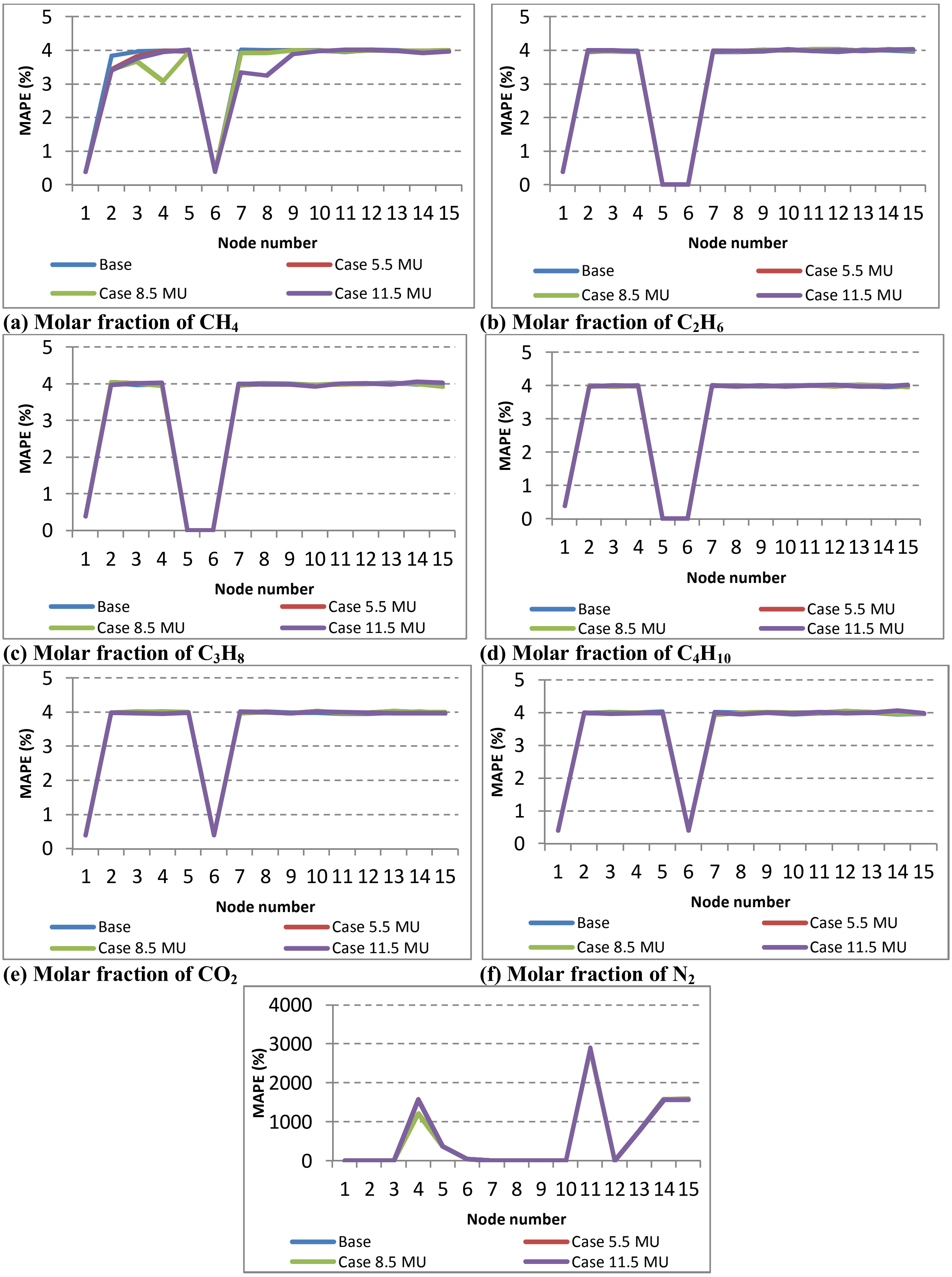

(a) Molar fraction of CH_4
(b) Molar fraction of C_2H_6
(c) Molar fraction of C_3H_8
(d) Molar fraction of C_4H_{10}
(e) Molar fraction of CO_2
(f) Molar fraction of N_2
(g) Molar fraction of H_2

Figure 6.13: MAPE of estimation of the molar fraction of gas components at the nodes for the best measurement designs

The values of MAPE of estimation of the molar fraction of gas components at the nodes are shown in Figure 6.13. As can be seen from Figure 6.13 placing more meters has not improved estimation of molar fractions at nodes, except in the case of CH_4, where the true values are more than 90% and increasing the number of meters resulted in partially improvement of estimation of CH_4 at some of the nodes.

6.4.4 Sensitivity analysis

A sensitivity analysis was performed in order to study the impact of accuracy of the pseudo measurements (of loads and gas mixtures, separately) on the error of estimation of the state parameters of the network for each budget case of 5.5, 8.5 and 11.5 MU. In all the cases, 20000 Monte Carlo simulations were carried out.

6.4.4.1 Sensitivity to the pseudo measurements of loads

The error of pseudo measurements of loads at load nodes was reduced gradually from 50% to 30% and then 10%, while the accuracy of pseudo measurements of gas mixture at all the nodes except the source and injection nodes was held constant at 10% in all the cases.

- *Estimation of the nodal pressures*

  The values of MAPE of estimation of the nodal pressures for the budget cases are shown in Figure 6.14.

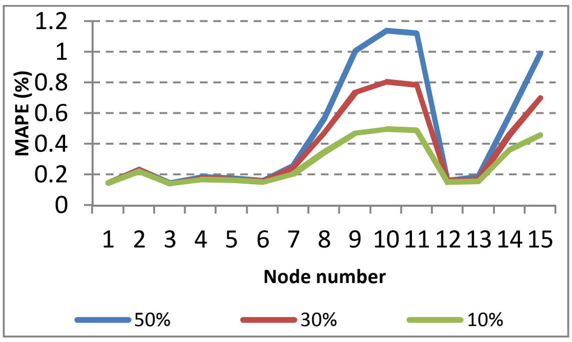

(a) Case 5.5 MU

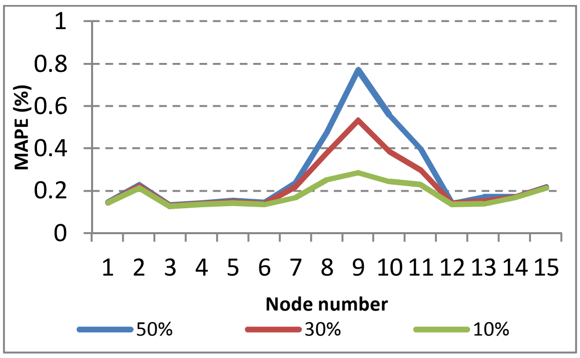

(b) Case 8.5 MU

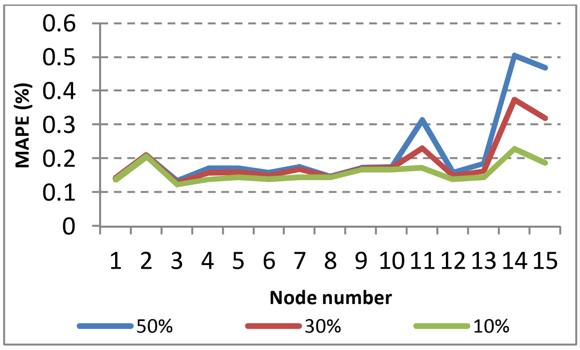

(c) Case 11.5 MU

Figure 6.14: The values of MAPE of estimation of the nodal pressures for the budget cases (sensitivity to the error of the loads)[1]

As can be seen from Figure 6.14(a) every 20% reduction in the error of pseudo measurements of the loads leads to an average 0.098% reduction in the error of estimation of the nodal pressures in the budget case of 5.5 MU. Figure 6.14(b) shows that every 20% reduction in the error of pseudo measurements of the loads leads to an average 0.045% reduction in the error of estimation of the nodal pressures in the budget case of 8.5 MU. According to Figure 6.14(c) every 20% reduction in the error of pseudo measurements of the loads leads to an average 0.030% reduction in the error of estimation of the nodal pressures in the budget case of 11.5 MU.

- *Estimation of the loads*

The values of MAPE of estimation of the loads for the budget cases are presented in Figure 6.15.

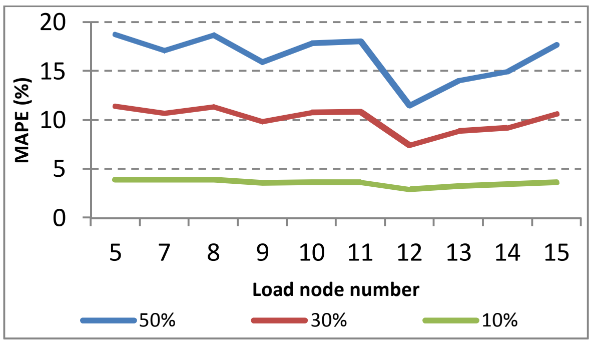

(a) Case 5.5 MU

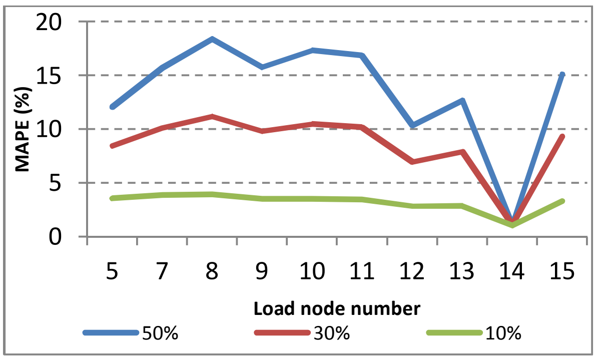

(b) Case 8.5 MU

[1] Different load errors are shown in different colours in the legend of the graph.

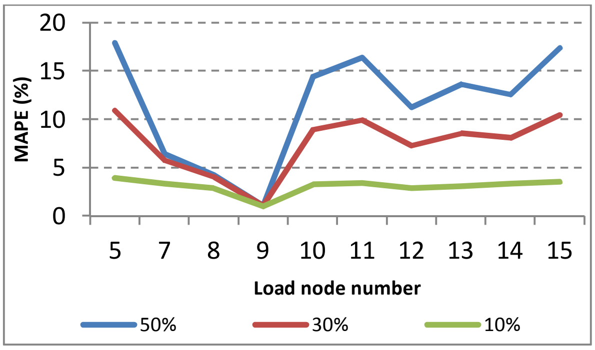

(c) Case 11.5 MU

Figure 6.15: The values of MAPE of estimation of the loads for the budget cases (sensitivity to the error of the loads)[1]

Figure 6.15(a) indicates that every 20% reduction in the error of pseudo measurements of the loads results in an average 6.446% reduction in the error of estimation of the values of the loads in the budget case of 5.5 MU. As can be seen from Figure 6.15(b) every 20% reduction in the error of pseudo measurements of the loads results in an average 5.186% reduction in the error of estimation of the values of the loads in the budget case of 8.5 MU. Figure 6.15(c) shows that every 20% reduction in the error of pseudo measurements of the loads results in an average 4.253% reduction in the error of estimation of the values of the loads in the budget case of 11.5 MU.

- *Estimation of the flows of the branches*

The values of MAPE of estimation of the flows of the branches for the budget cases are shown in Figure 6.16.

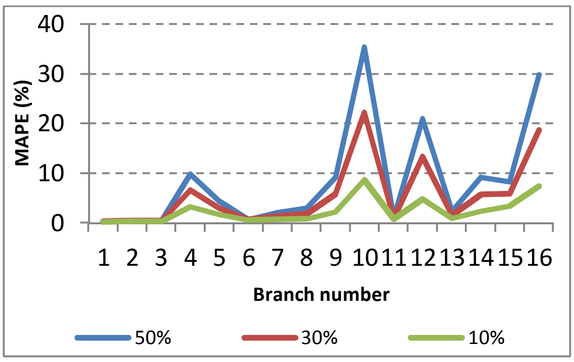

(a) Case 5.5 MU

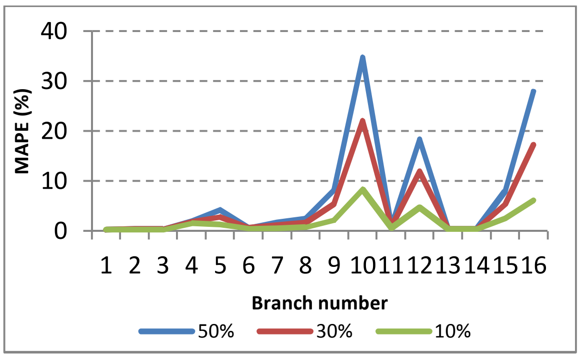

(b) Case 8.5 MU

[1] Different load errors are shown in different colours in the legend of the graph.

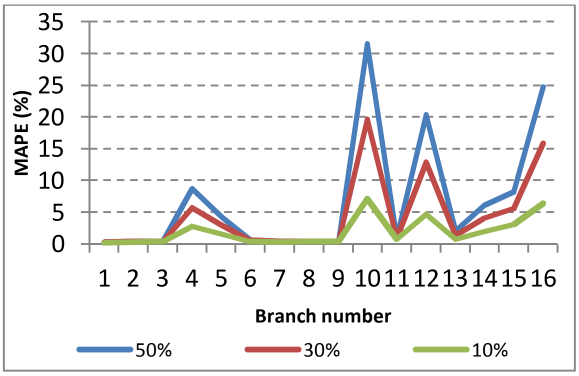

(c) Case 11.5 MU

Figure 6.16: The values of MAPE of estimation of the flows of the branches for the budget cases (sensitivity to the error of the loads)[1]

Figure 6.16(a) shows that every 20% reduction in the error of pseudo measurements of the loads leads to an average 3.094% reduction in the error of estimation of the values of the flows of the branches in the budget case of 5.5 MU. According to Figure 6.16(b) every 20% reduction in the error of pseudo measurements of the loads leads to an average 2.525% reduction in the error of estimation of the values of the flows of the branches in the budget case of 8.5 MU. As can be seen from Figure 6.16(c) every 20% reduction in the error of pseudo measurements of the loads leads to an average 2.448% reduction in the error of estimation of the values of the flows of the branches in the budget case of 11.5 MU.

- *Estimation of the molar fractions*

The values of MAPE of estimation of the molar fraction of the components of the gas mixture for the budget case of 5.5 MU are shown in Figure 6.17. The values of MAPE of estimation of the molar fraction of the components of the gas mixture for the budget case of 8.5 MU are presented in Figure 6.18. The values of MAPE of estimation of the molar fraction of the components of the gas mixture for the budget case of 11.5 MU are depicted in Figure 6.19.

[1] Different load errors are shown in different colours in the legend of the graph.

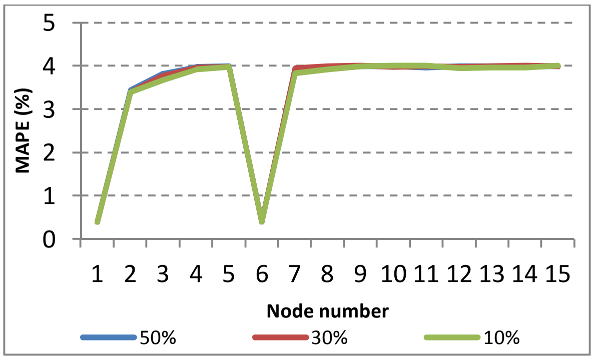

(a) Molar fraction of CH_4

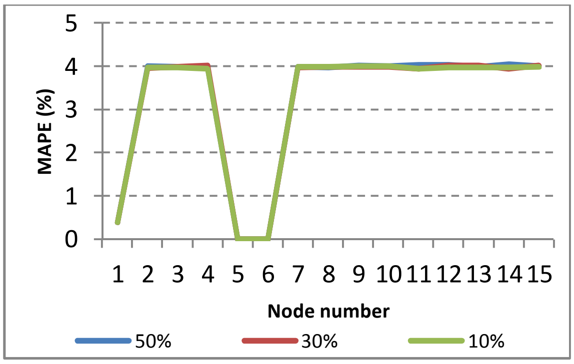

(b) Molar fraction of C_2H_6

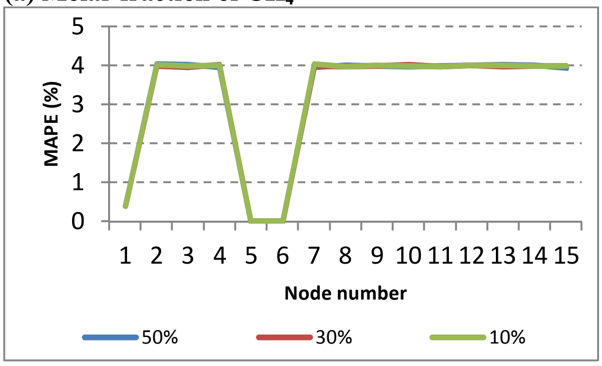

(c) Molar fraction of C_3H_8

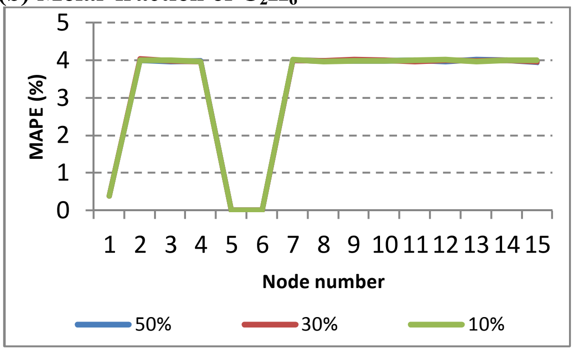

(d) Molar fraction of C_4H_{10}

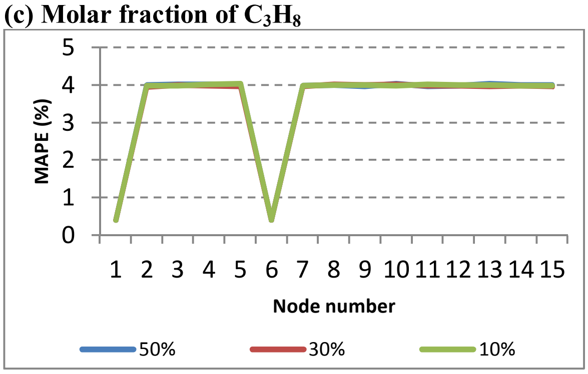

(e) Molar fraction of CO_2

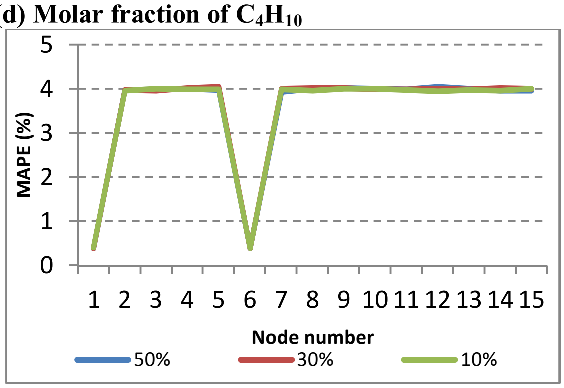

(f) Molar fraction of N_2

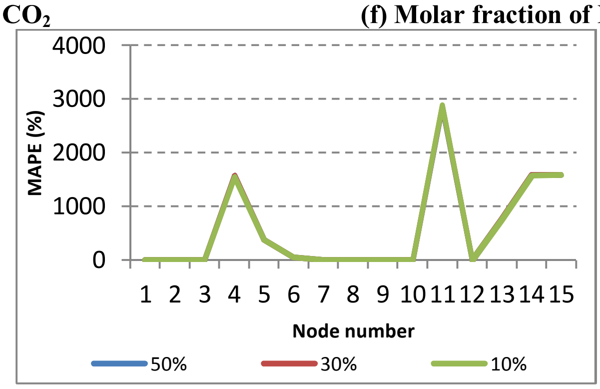

(g) Molar fraction of H_2

Figure 6.17: The values of MAPE of estimation of the molar fraction of the gas mixture components for the budget case of 5.5 MU (sensitivity to the error of the loads)[1]

[1] Different load errors are shown in different colours in the legend of the graph.

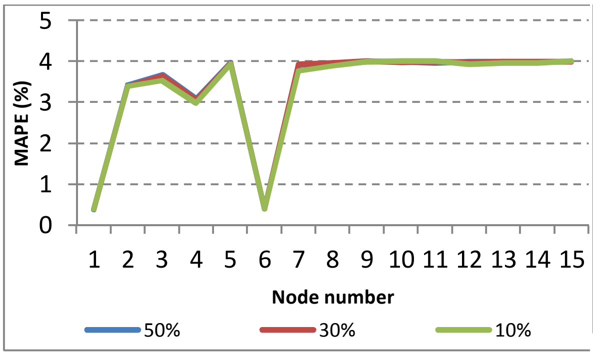

(a) Molar fraction of CH_4

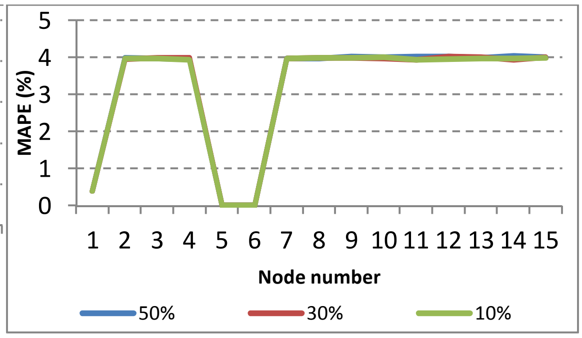

(b) Molar fraction of C_2H_6

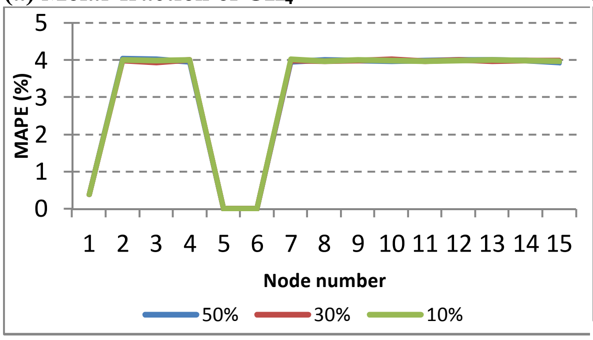

(c) Molar fraction of C_3H_8

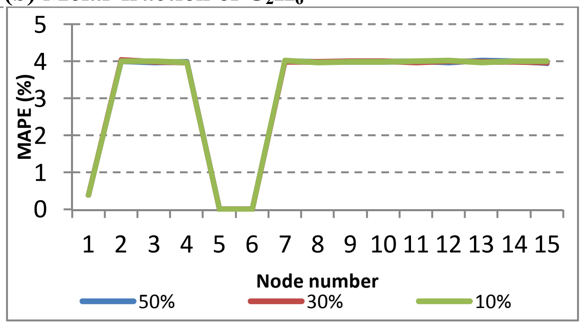

(d) Molar fraction of C_4H_{10}

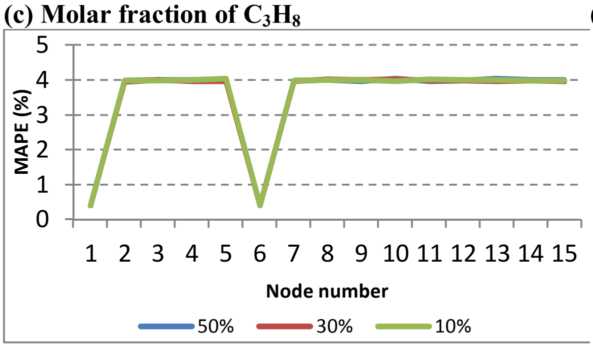

(e) Molar fraction of CO_2

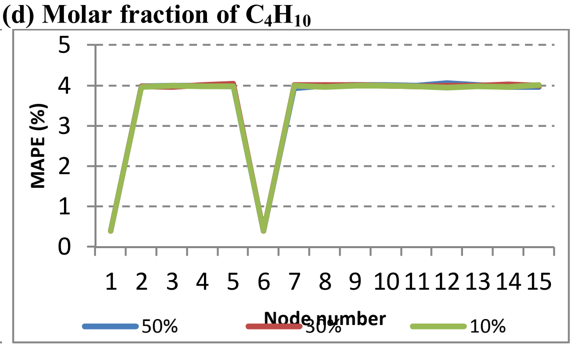

(f) Molar fraction of N_2

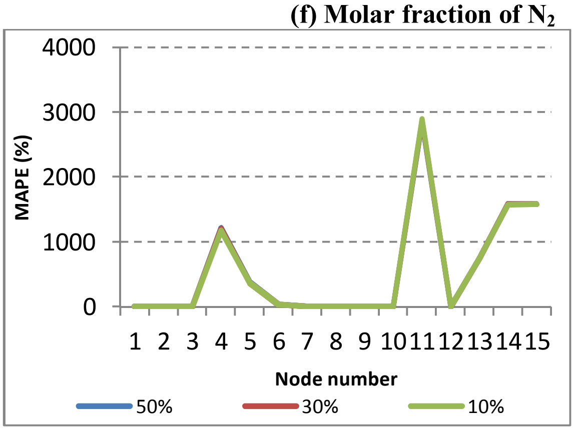

(g) Molar fraction of H_2

Figure 6.18: The values of MAPE of estimation of the molar fraction of the gas mixture components for the budget case of 8.5 MU (sensitivity to the error of the loads)[1]

[1] Different load errors are shown in different colours in the legend of the graph.

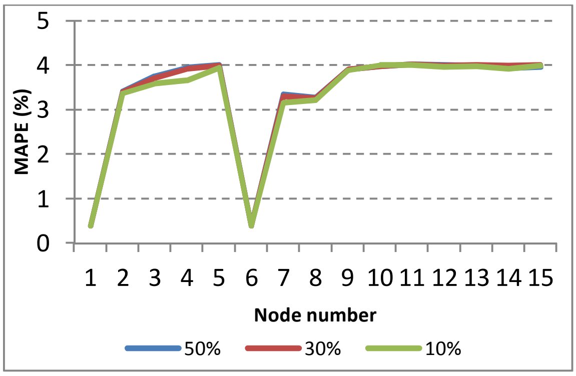

(a) Molar fraction of CH_4

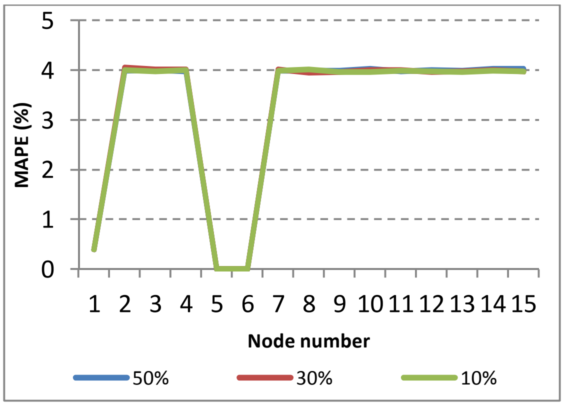

(b) Molar fraction of C_2H_6

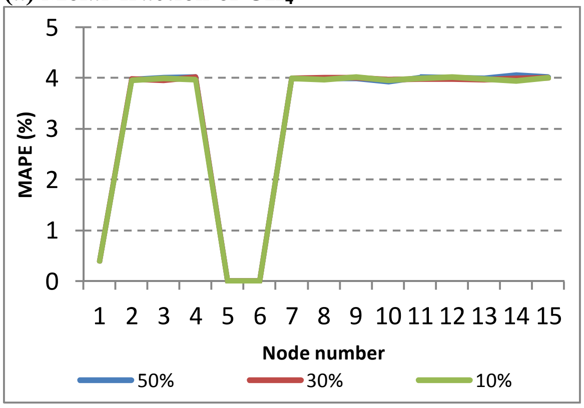

(c) Molar fraction of C_3H_8

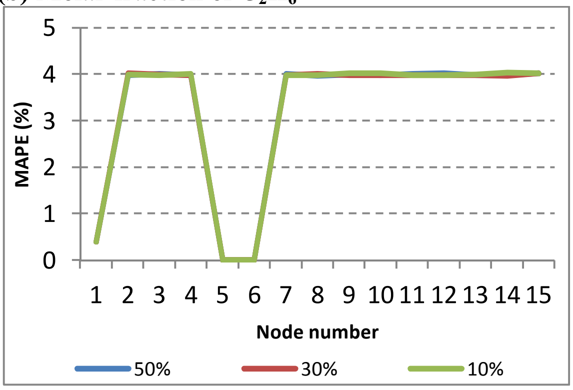

(d) Molar fraction of C_4H_{10}

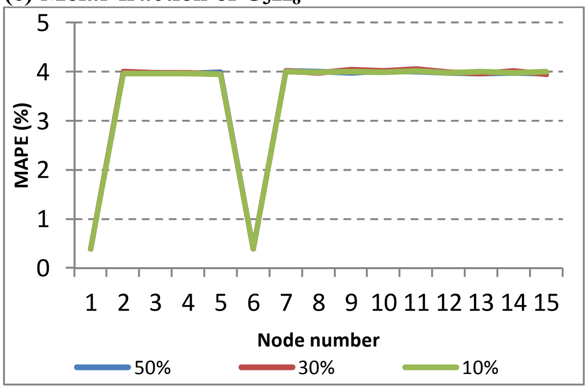

(e) Molar fraction of CO_2

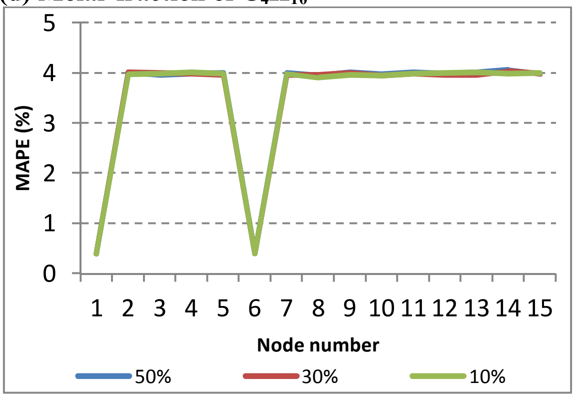

(f) Molar fraction of N_2

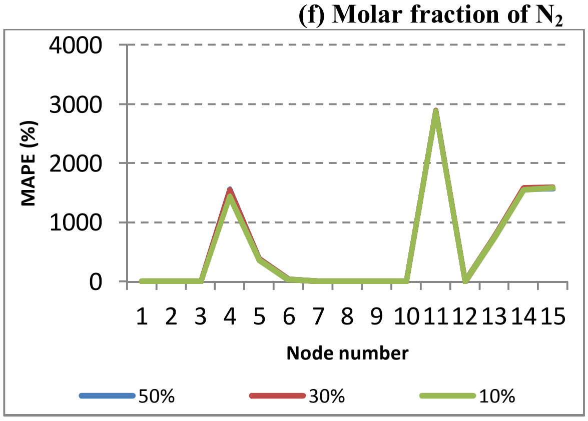

(g) Molar fraction of H_2

Figure 6.19: The values of MAPE of estimation of the molar fraction of the gas mixture

components for the budget case of 11.5 MU (sensitivity to the error of the loads)[1]

Figures 6.17, 6.18 and 6.19 show that decrease in the error of pseudo measurements of the loads had almost no effect on estimation of the gas components except CH_4, which has true values of molar fraction of more than 90%. The improvement in estimation of molar fraction of CH_4 seems to be really insignificant. This was also expected from the analysis of the impact of the measurements of pressure and flow on estimation of the molar fractions, which was observed to be very small.

6.4.4.2 Sensitivity to the pseudo measurements of molar fraction at the nodes

The accuracy of the pseudo measurements of molar fraction of gas components at all the nodes except the source and injection nodes was reduced gradually from 10.0% to 7.5% and 5.0%, while the accuracy of the pseudo measurements of loads at the load nodes was held constant at 50.0% in all the cases.

- *Estimation of the nodal pressures*

The values of MAPE of estimation of the nodal pressures for the budget cases are shown in Figure 6.20.

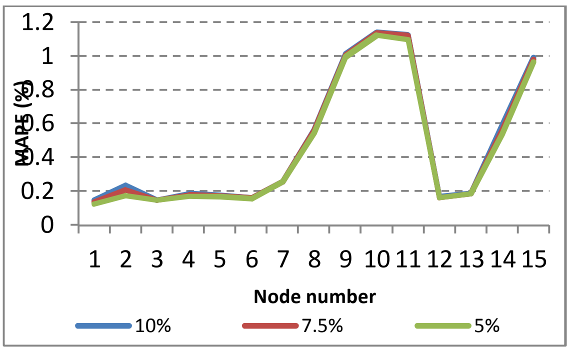

(a) Case 5.5 MU

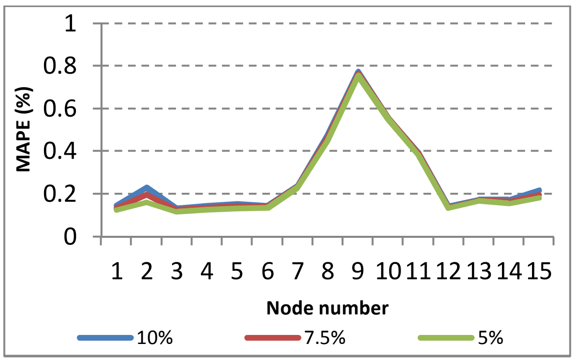

(b) Case 8.5 MU

[1] Different load errors are shown in different colours in the legend of the graph.

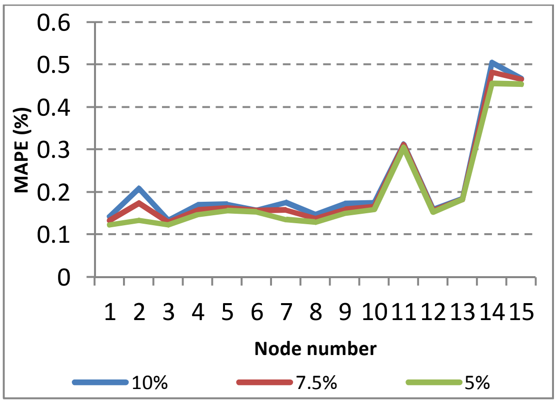

(c) Case 11.5 MU

Figure 6.20: The values of MAPE of estimation of the nodal pressures for the budget cases (sensitivity to the error of the molar fractions)[1]

As can be seen from Figure 6.20 every 2.5% reduction in the error of the pseudo measurements of molar fraction leads to an insignificant (average 0.010%) reduction in the error of estimation of the nodal pressures in all the budget cases. According to the results of the analysis of impact of different measurements on the state estimation the insignificant improvements of the estimation of nodal pressures was already anticipated.

- *Estimation of the loads*

The values of MAPE of estimation of the loads for the budget cases are presented in Figure 6.21.

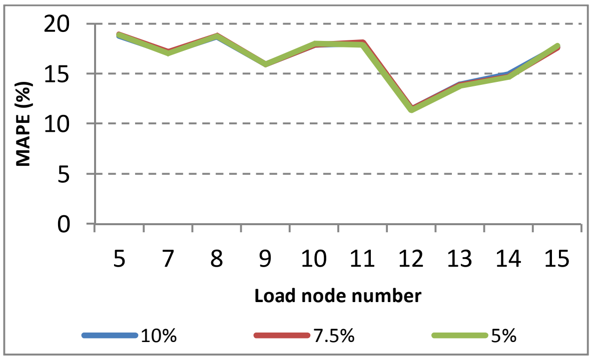

(a) Case 5.5 MU

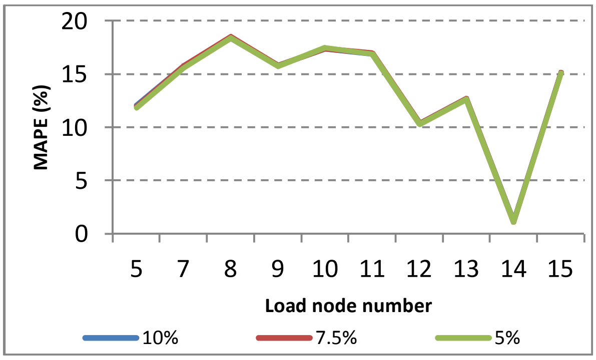

(b) Case 8.5 MU

[1] Different molar fraction errors are shown in different colours in the legend of the graph.

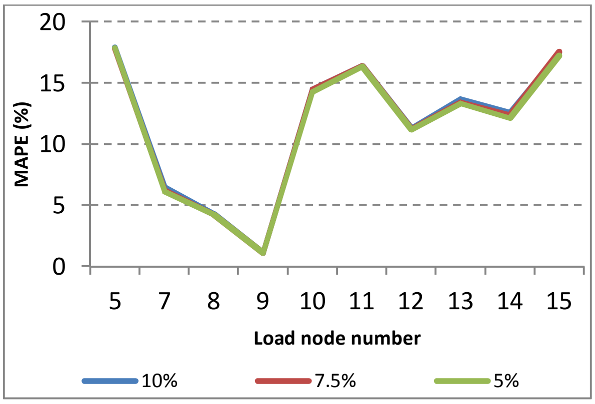

(c) Case 11.5 MU

Figure 6.21: The values of MAPE of estimation of the loads for the budget cases (sensitivity to the error of the molar fractions)[1]

As can be seen from Figure 6.21(a) every 2.5% improvement of the accuracy of the pseudo measurements of molar fraction results in an average 0.017% reduction in the error of estimation of the values of the loads in the budget case of 5.5 MU. Figure 6.21(b) shows that every 2.5% improvement of the accuracy of the pseudo measurements of molar fraction results in an average 0.023% reduction in the error of estimation of the values of the loads in the budget case of 8.5 MU. According to Figure 6.21(c) every 2.5% improvement of the accuracy of the pseudo measurements of molar fraction results in an average 0.093% reduction in the error of estimation of the values of the loads in the budget case of 11.5 MU. The small change in the accuracy of estimation of the loads was already expected based on the analysis of impact of different measurement types on the state estimation.

- *Estimation of the flows of the branches*

The values of MAPE of estimation of the flows of the branches for the budget cases are shown in Figure 6.22.

[1] Different molar fraction errors are shown in different colours in the legend of the graph.

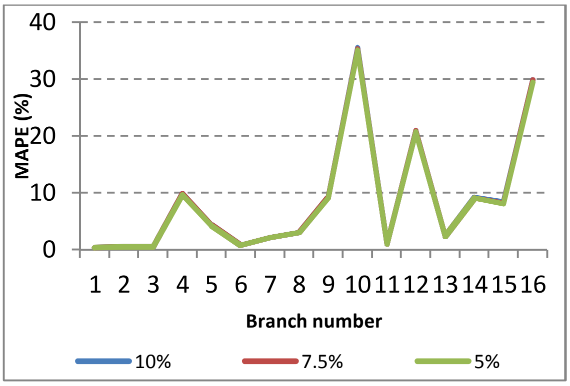

(a) Case 5.5 MU

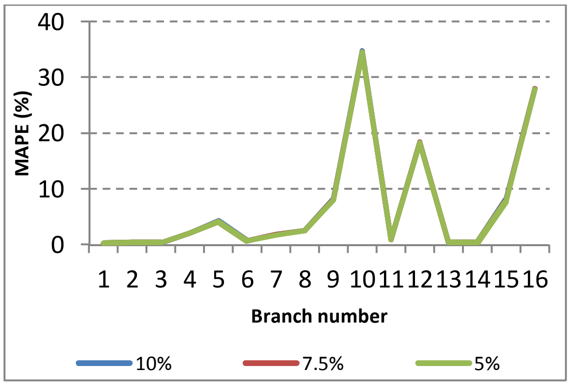

(b) Case 8.5 MU

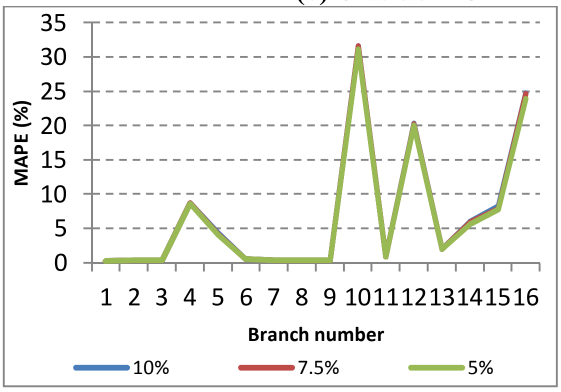

(c) Case 11.5 MU

Figure 6.22: The values of MAPE of estimation of the flows of the branches for the budget cases (sensitivity to the error of the molar fractions)[1]

Figure 6.22(a) indicates that every 2.5% reduction in the error of the pseudo measurements of molar fraction leads to an average 0.063% reduction in the error of estimation of the values of the flows of the branches in the budget case of 5.5 MU. Figure 6.22(b) indicates that every 2.5% reduction in the error of the pseudo measurements of molar fraction leads to an average 0.032% reduction in the error of estimation of the values of the flows of the branches in the budget case of 8.5 MU. According to Figure 6.22(c) every 2.5% reduction in the error of the pseudo measurements of molar fraction leads to an average 0.090% reduction in the error of estimation of the values of the flows of the branches in the budget case of 11.5 MU. The insignificant impacts were also anticipated from the analysis of impact of different measurement types on the accuracy index of state estimation.

[1] Different molar fraction errors are shown in different colours in the legend of the graph.

- *Estimation of the molar fractions*

The values of MAPE of estimation of the molar fraction of the components of the gas mixture for the budget case of 5.5 MU are shown in Figure 6.23. The values of MAPE of estimation of the molar fraction of the components of the gas mixture for the budget case of 8.5 MU are presented in Figure 6.24. The values of MAPE of estimation of the molar fraction of the components of the gas mixture for the budget case of 11.5 MU are depicted in Figure 6.25.

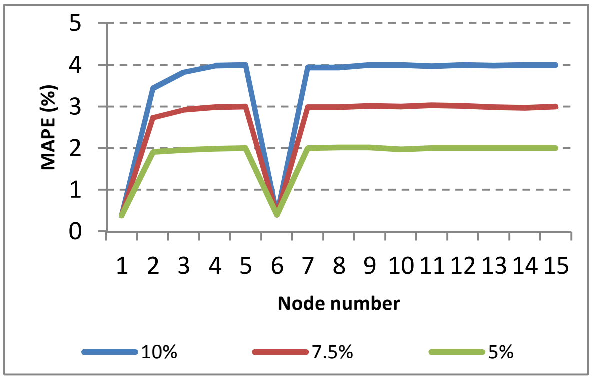

(a) Molar fraction of CH_4

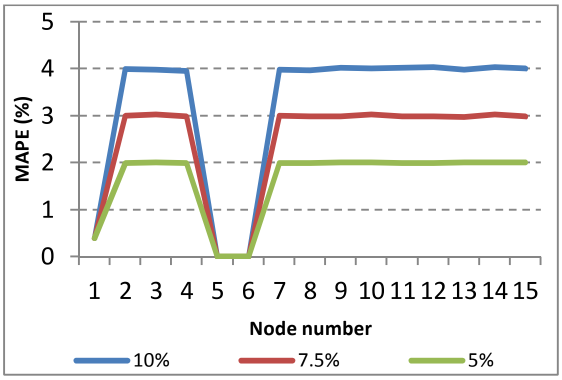

(b) Molar fraction of C_2H_6

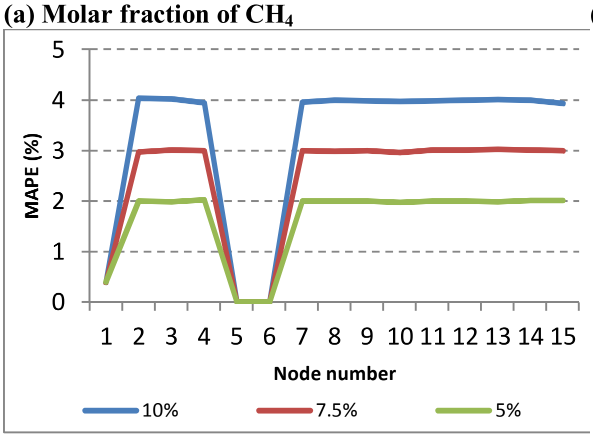

(c) Molar fraction of C_3H_8

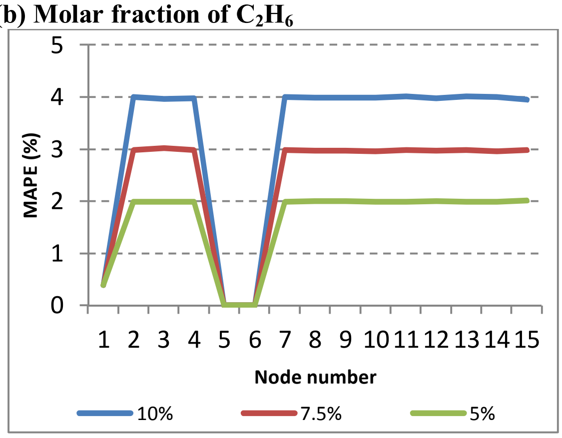

(d) Molar fraction of C_4H_{10}

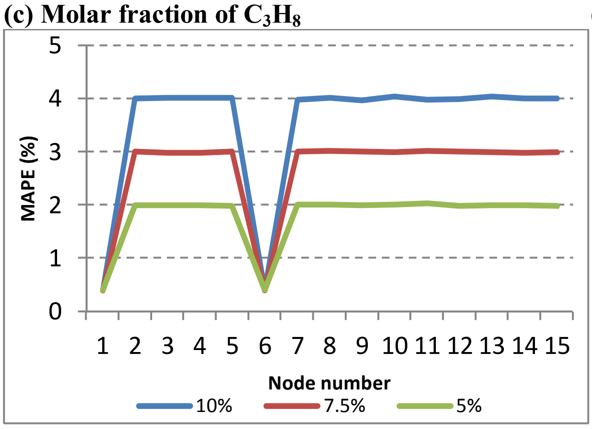

(e) Molar fraction of CO_2

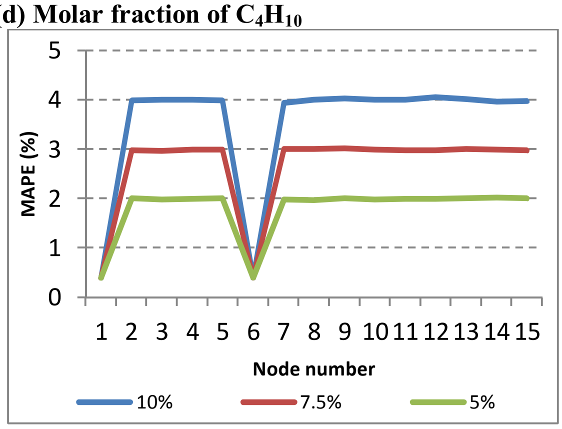

(f) Molar fraction of N_2

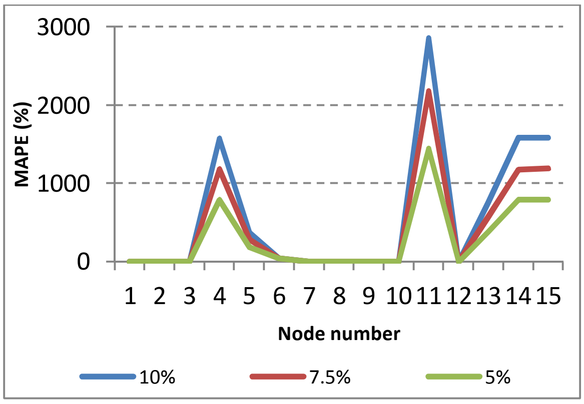

(g) Molar fraction of H_2

Figure 6.23: The values of MAPE of estimation of the molar fraction of the gas mixture components for the budget case of 5.5 MU (sensitivity to the error of the molar fractions)[1]

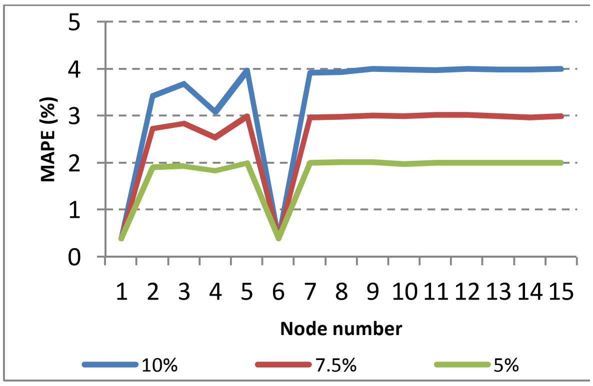

(a) Molar fraction of CH_4

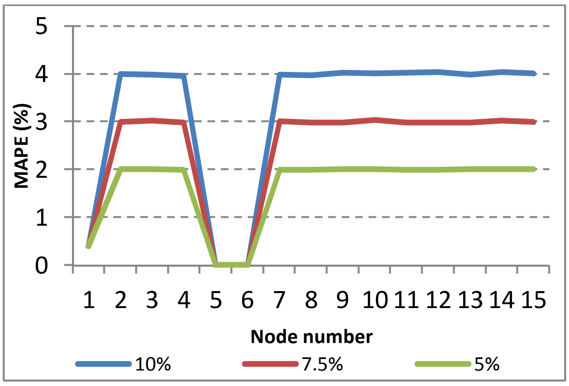

(b) Molar fraction of C_2H_6

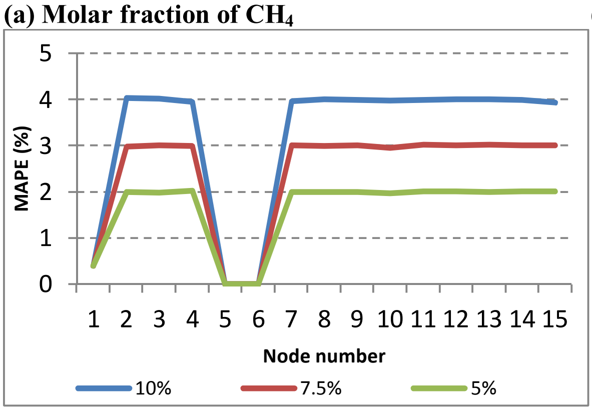

(c) Molar fraction of C_3H_8

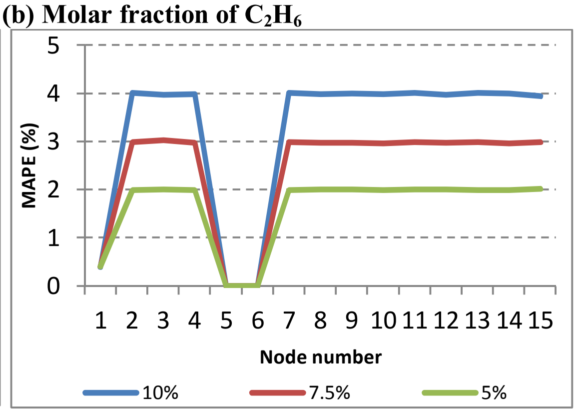

(d) Molar fraction of C_4H_{10}

[1] Different molar fraction errors are shown in different colours in the legend of the graph.

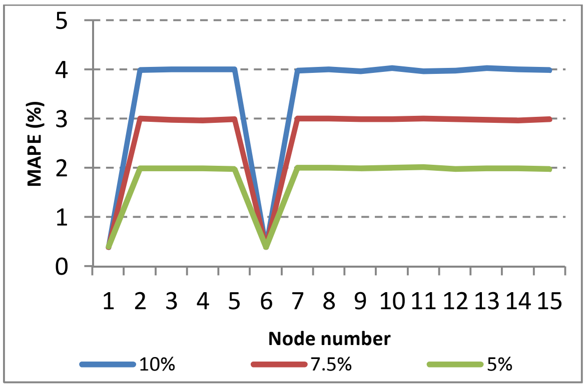

(e) Molar fraction of CO_2

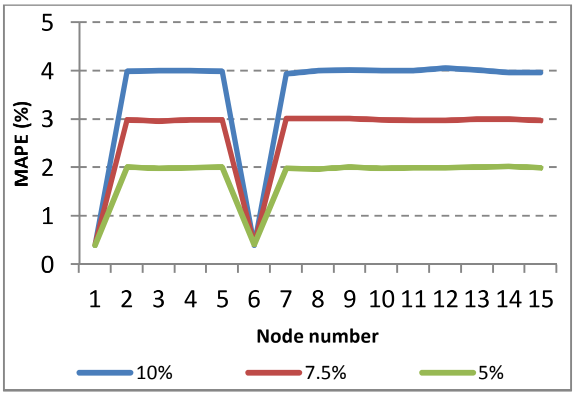

(f) Molar fraction of N_2

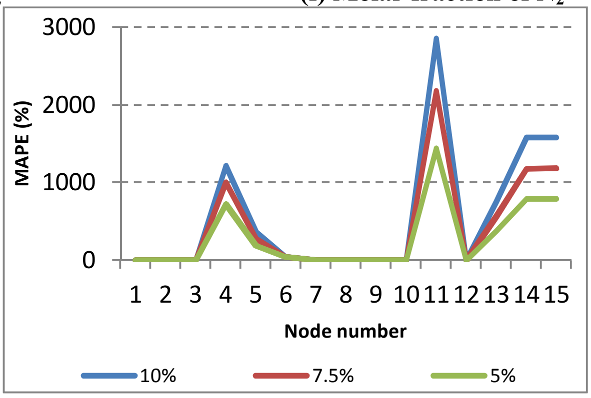

(g) Molar fraction of H_2

Figure 6.24: The values of MAPE of estimation of the molar fraction of the gas mixture components for the budget case of 8.5 MU (sensitivity to the error of the molar fractions)[1]

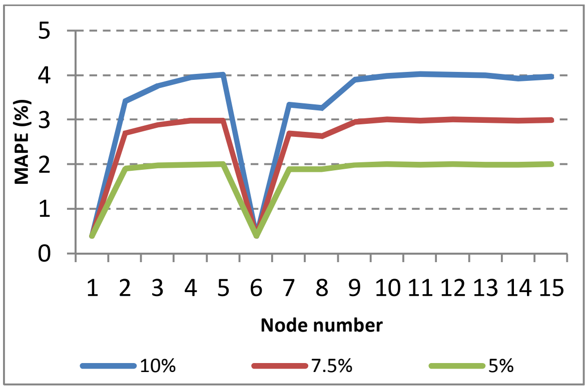

(a) Molar fraction of CH_4

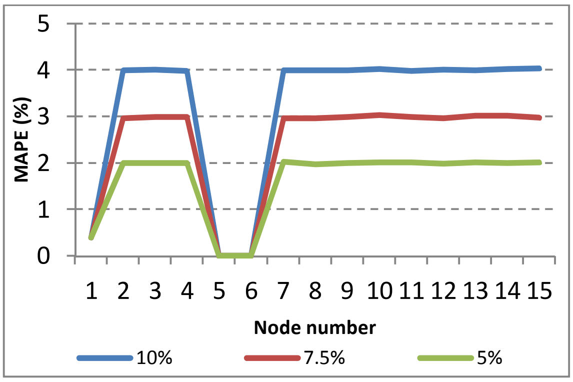

(b) Molar fraction of C_2H_6

[1] Different molar fraction errors are shown in different colours in the legend of the graph.

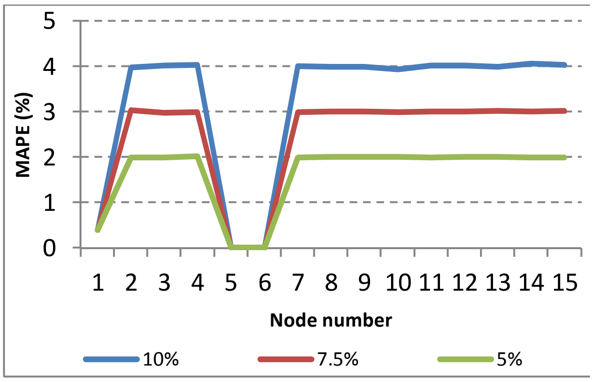

(c) Molar fraction of C_3H_8

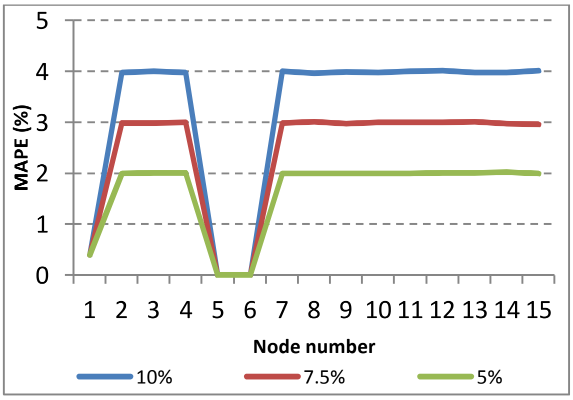

(d) Molar fraction of C_4H_{10}

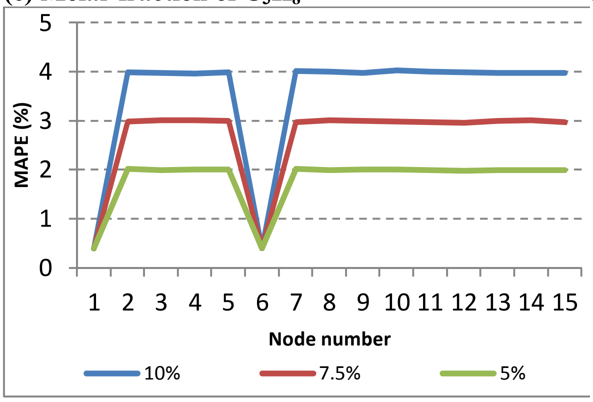

(e) Molar fraction of CO_2

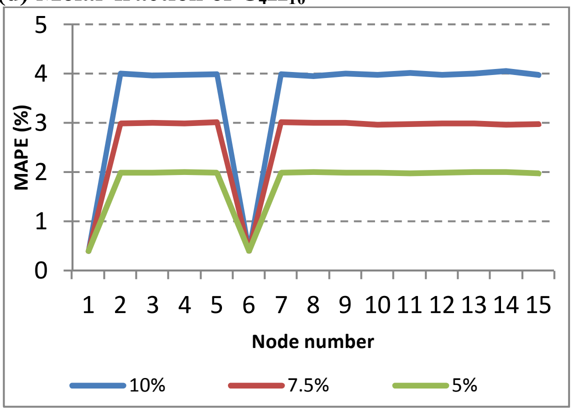

(f) Molar fraction of N_2

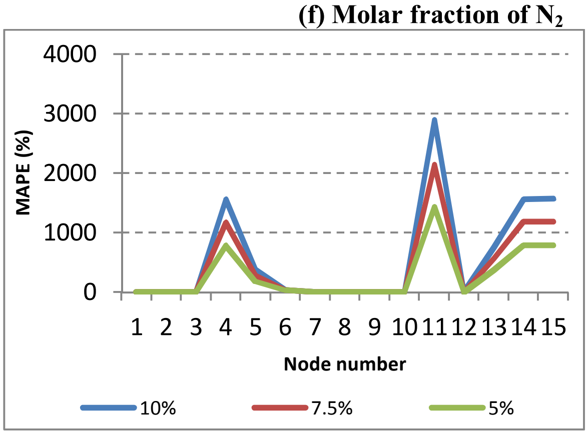

(g) Molar fraction of H_2

Figure 6.25: The values of MAPE of estimation of the molar fraction of the gas mixture components for the budget case of 11.5 MU (sensitivity to the error of the molar fractions)[1]

Figures 6.23, 6.24 and 6.25 indicate that every 2.5% reduction in the error of pseudo measurements of molar fraction results in an approximately 1% reduction in the error of estimation of molar fraction of all the gas components except Hydrogen in all the budget cases. Figure 6.23(g) shows that every 2.5% reduction in the error of pseudo measurements of molar fraction results in 310.52% reduction in the error of estimation of molar fraction of Hydrogen in the budget case of 5.5 MU. According to Figure 6.24(g) every 2.5% reduction in

[1] Different molar fraction errors are shown in different colours in the legend of the graph.

the error of pseudo measurements of molar fraction results in 289.05% reduction in the error of estimation of molar fraction of Hydrogen in the budget case of 8.5 MU. Figure 6.25(g) indicates that every 2.5% reduction in the error of pseudo measurements of molar fraction results in 310.65% reduction in the error of estimation of molar fraction of Hydrogen in the budget case of 11.5 MU.

6.5 Remarks

The application and performance of the algorithm of measurement placement was demonstrated for a meshed network comprising of one source node and one injection node. However, in reality gas distribution networks have several sources of pressures and injections, which are intermittent, i.e. the injection nodes may operate in a period of the year and may not be in service at other times. The developed algorithm can be applied to real gas distribution networks at their peak load considering all possible injections with an average value for injection power in order to solve the problem in a more realistic way.

The focus of this work was on developing an algorithm for placement of metering devices subject to a limited budget, while considering relative costs of the metering devices. In other words, the relative costs used in the problem are just some assumed values, which were chosen not far from the reality. Therefore, in realistic cases, more real solutions can be obtained provided more real relative costs of devices are known.

In this work a preliminary measurement placement algorithm was developed based on just four packages of measurements. However, for more realistic solutions more packages of measurements can be considered and the algorithm can be adjusted for those packages accordingly.

6.6 Conclusions

The impact of different measurements on state estimation of gas distribution networks with decentralised injection was investigated. It was observed that equipping the network with all the possible measurements of pressure, load and molar fraction leads to the least value of accuracy index of pressure and molar fraction. However, this choice is costly and almost impossible for the operator of the network. However, placing pressure meters in the network increases the accuracy of estimation of the pressures and gas flows without any effects on improving the estimation of molar fractions. Also, placing the flow meters of branches and loads improves estimation of the gas flows in the branches and at the loads as well as estimation of the pressures without any impact on estimation of molar fractions. Additionally, placement of expensive gas chromatograph in the network just improves estimation of molar fractions without any significant impact on estimation of pressures and gas flows in the branches and at the loads.

Placement of additional measurements in gas distribution networks with decentralised injection subject to a limited budget was also investigated. This was fulfilled due to the fact that the budget of the operator of the network is limited and they want to make the most of it in terms of improving their metering infrastructure. An algorithm for placement of a number of additional measurement units, each including all possible measurements of pressure, flow and gas chromatograph, to be placed at nodes of a gas network was developed and implemented. The algorithm suggests a list of best measurement designs (number, type and place) with accuracy of real time individual meters being input and predetermined. The algorithm ranks the measurements designs based on the best accuracy index of molar fraction through a Monte Carlo simulation. The performance of the algorithm was investigated using a case study gas distribution network with one decentralised injection.

The problem of measurement placement was investigated for three budget cases of 5.5, 8.5 and 11.5 Money Units. Also four different measurement packages (Figure 6.2) were considered. It was observed that the algorithm suggests placing the most number of possible meters for each budget case. This is due to the fact that all the molar fractions of gas components except one, i.e. CH_4, have small values of less than 10% and thus putting a gas chromatograph at a node has less influence on improving the accuracy of estimation of molar fractions. Additionally, impact of pressure and flow meters on improvement of estimation of molar fraction, although being small, led to selection of most number of meters by the algorithm.

The performance of the best measurement design of all the budget cases was compared against each other to study improvement in estimation of the pressures, flows and molar fractions with increase in the budget. It was observed that increasing the number of pressure meters improves estimation of the nodal pressures. Also increasing the number of pressure and flow meters improved estimation of flows of branches. Estimation of loads was improved by increasing the budget, however, without any trends. Additionally, it was observed that placing more meters did not improve estimation of molar fractions at nodes, except in the case of CH_4, where the true values are more than 90% and increasing the number of meters resulted in improvement of estimation of CH_4 at some of the nodes (See section 6.4.3 for the detailed description).

Sensitivity analysis of the best measurement designs against improvement in the accuracy of the pseudo measurements of loads and molar fractions was also performed separately. It was observed that every 20% improvement in the accuracy of pseudo measurements of loads results in less than 0.1% reduction in the error of estimation of the nodal pressures, in approximately 5% reduction in the error of estimation of the values of the loads and in around 2.5% reduction in the error of estimation of the values of flow of the branches for all the budget cases. Also, it was observed that decrease in the error of pseudo measurements of loads had almost no effect on estimation of gas components except CH_4. It was observed that estimation of CH_4 was slightly improved at some of the nodes (See section 6.4.4.1 for the detailed description).

Sensitivity analysis of pseudo measurements of molar fraction shows that every 2.5% reduction in the error of pseudo measurements of molar fraction leads to an insignificant (an average 0.010%) reduction in the error of estimation of the nodal pressures, in less than 0.1% reduction in the error of estimation of the values of the loads and in less than 0.1% reduction in the error of estimation of the values of flow of the branches in all the budget cases. Additionally, every 2.5% reduction in the error of pseudo measurements of molar fraction results in an approximately 1% reduction in the error of estimation of molar fraction of all the gas components except Hydrogen in all the budget cases. Also, an average 300% reduction in the error of estimation of molar fraction of Hydrogen in all the budget cases was observed (See section 6.4.4.2 for the detailed description).

7 Simulation and state estimation of integrated power and gas distribution networks with decentralised injection

7.1 Introduction

Future energy networks are likely to be highly integrated with several energy conversion utilities operating between them, which make the control and management of the whole system more complicated. Therefore, analysis of operation and management of the whole system needs to be performed in an integrated approach. In order to perform an effective control and management of the whole system, an accurate and reliable estimation of the state parameters and the energy flows within the integrated network is essential. The state parameters of the integrated network are estimated using the measurements from across the network.

Simulation and state estimation of integrated power and gas distribution networks with decentralised injection and generation in both networks is investigated. For this purpose, a brief literature review on simulation and state estimation of integrated power and gas distribution networks is described firstly. Then, the WLS-based algorithm of the simulation model developed in MATLAB for integrated state estimation of the integrated network is explained. The algorithm is developed based on the lessons learnt from the WLS-based algorithms for state estimation of power and gas distribution networks in previous Chapters. Afterwards, a test integrated power and gas distribution network along with the designed case studies and assumptions on the measurements is presented and validated. Finally, the impact of deployment of smart meters in one of the networks on state estimation of the other coupled network is investigated.

7.1.1 Literature review

7.1.1.1 Simulation of operation of integrated power and gas networks

There are several publications in the literature on simulation of operation of integrated power and gas networks including (Unsihuay et al. 2007; Qadrdan et al. 2009; Qadrdan 2012; Chaudry et al. 2013; Chaudry et al. 2014; Erdener et al. 2014; Qadrdan et al. 2015). All these works consider a single gas mixture flow in the gas network. However, in the current work injection of different gases in the gas network is considered.

7.1.1.2 State estimation of integrated power and gas networks

In order to find formulations for the WLS state estimation of integrated power and gas distribution networks all the accessible databases were investigated and no previous works or publications were found on the subject. Therefore, all the formulations and algorithms presented for simulation and state estimation of integrated power and gas distribution networks in the steady state conditions are developed by the researcher based on the lessons learnt from the state estimation of power and gas distribution networks in Chapters two and five.

7.1.2 Research questions

The following research questions are addressed in this Chapter:

- Does integrated state estimation of interconnected power and gas distribution networks lead to more accurate results compared to performing the state estimation in the individual networks separately?

- Does deployment of smart meters in one of the networks lead to more accurate estimation of state parameters and energy flows in the other network due to presence and consideration of coupling components?

7.2 Simulation of operation of integrated power and gas distribution networks

In order to perform state estimation of an energy system the true values of all the state parameters and the energy flows within the system need to be known. This is needed since the values of measurements can be simulated by adding noise to the true values using a random number generator. The algorithm for simulation of operation of an integrated power and gas distribution network is presented in Figure 7.1. The integrated network is analysed in steady state conditions in this research. It is assumed that the power network is connected to the grid and is equipped with gas turbine(s) as the coupling component(s) for connection to the gas network. Also, the gas network has power to gas units as decentralised injection, which consume the power from renewable sources in the coupled power network and produce Hydrogen. Hydrogen can either be directly injected into the gas network or be further processed and the final product be injected in the gas network.

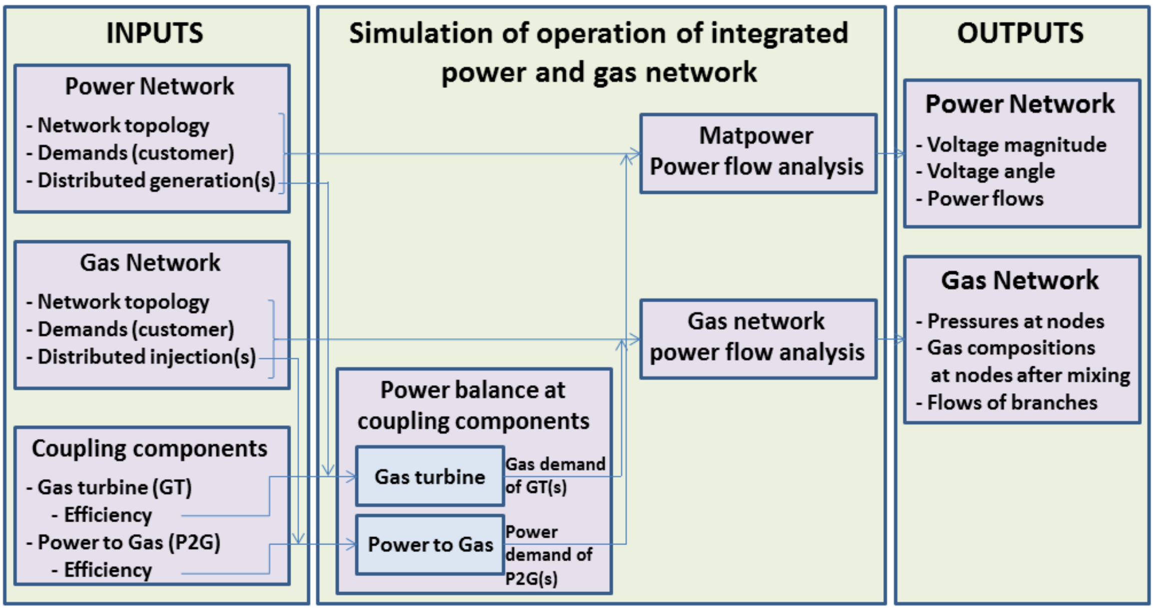

Figure 7.1: The algorithm for simulation of operation of an integrated power and gas distribution network

As can be seen simulation of operation of the integrated system is performed separately once the demands of the gas turbines on the gas network and the demands of the power to gas units on the power network is calculated. This is possible since it is assumed the amount of generation of power by the gas turbines and the amount of power injection of alternative gas by the power to gas units are known and inputs to the algorithm.

Operation of the power and gas networks is simulated independently of one another due to the following:

- The operation point of a system is such a specific point that all the energy flows in all over the system match. It is shown that achieving this point is independent of mathematical formulations and of whether to implement sequential or integrated analysis (Liu 2013).

- True values of operation parameters are just used for producing measurements. Therefore, it is not really important the way the nominal values of them are obtained.

Consequently, in order to avoid computation burden, operation simulation of the integrated power and gas distribution network is performed separately.

The following equations are used as the power balance of the coupling components:

- Gas turbine:

$$d_{GT} = \frac{P_{GT} \times MVA_{Base}}{\eta_{GT}} \tag{7-1}$$

where:

d_{GT} load of the gas turbine (GT) in the gas network (in units of power)

P_{GT} real power injected in the power network by the GT

η_{GT} efficiency of energy conversion of the GT

It is assumed the gas turbine generates real power and has no contributions to the generation of reactive power.

- Power to gas units

$$P_{P2G} = \frac{d_{P2G}}{MVA_{Base} \times \eta_{P2G}} \tag{7-2}$$

where:

P_{P2G} real power demand of the power to gas unit in the power network

d_{P2G} injection power of the unit in the gas network

η_{P2G} efficiency of the energy conversion of the unit

It is assumed the power to gas units consume real power rather than reactive power.

In the above formulations it is assumed that the efficiency of energy conversion units, i.e. η_{GT} and η_{P2G}, at the true operation conditions is fixed and input to the algorithm.

Once the amount of all the demands of all the loads in the gas network including the gas turbines is determined the gas power flow analysis (developed in Chapter 4) is used to obtain the nominal values of the state parameters and gas flows within the network. Similarly, once the amount of all the loads in the power network including the power to gas units is known the power flow analysis (Matpower) is applied in order to achieve the nominal values of the state parameter as well as the power flows and power injections within the power network.

7.3 State estimation of integrated power and gas distribution networks

The maximum likelihood estimation method was applied to the integrated power and gas networks similar to the case of state estimation of power and gas networks separately. Also, state estimation of the integrated network was implemented using the WLS state estimation technique explained in Chapter 2. Unlike the simulation of the integrated networks, which was performed separately, the state estimation of the integrated networks was implemented in an integrated way. In other words, the following were considered as the state parameters for the integrated system:

- Voltage magnitudes of all the buses of the power network
- Voltage angles of all the buses of the power network (except the reference bus)
- Squared pressures of all the nodes of the gas network

- Molar fractions of all the gas components except one of them at all the nodes (the reason for exception of one of the components was explained in section 5.2)

Hence, the vector of the state parameters of the integrated network has the following form:

$$x^T = [\theta_2, \theta_3, \dots, \theta_{N_B}, V_1, V_2, \dots, V_{N_B}, \\ PS_1, PS_2, \dots, PS_{N_N}, y_{1,1}, y_{2,1}, \dots y_{N_C-1,1}, \dots, y_{1,N_N}, y_{2,N_N}, \dots y_{N_C-1,N_N}] \tag{7-3}$$

where:

x^T	Transpose of the state vector of the integrated networks
N_B	number of buses of the power network
N_N	number of nodes of the gas network
N_C	number of components of the gas mixture
PS	squared pressures
$y_{i,j}$	value of molar fraction of component i at node j after mixing

Once the values of the state parameters of the integrated networks are estimated the operation condition and the energy flows of the integrated power and gas network are determined.

In order to start, the measurement function $h(x)$ and the measurement Jacobian $H(x)$ need to be calculated and formed, which is explained in the following subsections. It should be noted that the calculation of the measurement function and the measurement Jacobian for the power network, which then affects the calculation of the measurement function and the measurement Jacobian of the coupling components, was carried out using the normal system rather than in the per unit system.

7.3.1 Measurement function

The measurement function for state estimation of an integrated power and gas network has the following form:

$$h(x) = \begin{bmatrix} power\ network \begin{cases} P_{injection} \\ P_{flow} \\ Q_{injection} \\ Q_{flow} \\ V_{magnitude} \end{cases} \\ gas\ network \begin{cases} PS \\ q_{branches} \\ q_{nodes} \\ y \end{cases} \\ coupling\ components \begin{cases} PB_{GT} \\ PB_{P2G} \end{cases} \end{bmatrix} \tag{7-4}$$

where:

PB_{GT} Power balance equation at the gas turbine(s)

PB_{P2G} Power balance equation at the power to gas unit(s)

The calculation of the elements of the above function was performed as follows:

- The power network:

  The elements corresponding to the power network were calculated using the functions presented in section 2.4.1.

- The gas network:

  The elements corresponding to the gas network were calculated using the equations in section 5.2.1.

- The coupling components:

The measurements at the coupling components, i.e. the voltage magnitude and power injection at the point of connection to the power network and pressure, gas flow and molar fractions at the point of connection to the gas network, can be applied separately for state estimation of either of the networks. However, presence of a coupling component means that the amount of energy absorbed by it from one of the networks is transferred to the other network. In other words, the coupling components are dealt with in a very similar way to the points of zero loads in either of the networks where there is a virtual measurement and all the energy entering the node from different streams leaves the node.

Consequently, an equation for the balance of energy is written for each coupling component to ensure that there is no leakage of energy at the coupling components except for the amount determined by the efficiency of the energy conversion process. The equation for balance of energy is equivalent to the equation of balance of power since the system is considered in steady state conditions and the amount of power times the amount of time transforms the equation into an equation for balance of energy.

- Gas turbine:

  It is assumed the gas turbines consume gas and inject real power in the power network, i.e. they have no contribution to the production of reactive power. The equation of balance of power flow in gas turbines is:

$$PB_{GT} = p_{inj} - \eta_{GT} \times GCV_{mix} \times q_l \tag{7-5}$$

  where p_{inj} is calculated in MW using the normal system rather than per unit.

- Power to gas (P2G) units:

  It is assumed that P2G units consume real power and produce alternative gas. The equation of power balance for them is as follows:

$$PB_{P2G} = GCV_{mix} \times q_{ip} - \eta_{P2G} \times p_{inj} \tag{7-6}$$

7.3.2 Measurement Jacobian

Partial derivatives of all the measurement functions of the integrated power and gas network with respect to all the state parameters of the integrated network are placed in the measurement Jacobian matrix. Therefore, the matrix has the following form:

$$H(x) = \begin{bmatrix} \dfrac{\partial NM_{PN}}{\partial SP_{PN}} & \dfrac{\partial NM_{PN}}{\partial SP_{GN}} \\ \dfrac{\partial NM_{GN}}{\partial SP_{PN}} & \dfrac{\partial NM_{GN}}{\partial SP_{GN}} \\ \dfrac{\partial PB_{CC}}{\partial SP_{PN}} & \dfrac{\partial PB_{CC}}{\partial SP_{GN}} \end{bmatrix} \tag{7-7}$$

where:

NM_{PN} Measurements of the power network

NM_{GN} Measurements of the gas network

SP_{PN} State parameters of the power network

SP_{GN} State parameters of the gas network

Different sections of the above matrix are calculated as follows:

- Partial derivatives of the measurements of the power network (NM_{PN})

  The formulations for calculation of the partial derivatives of the measurements of the power network with respect to the state parameters of the power network, i.e. $\frac{\partial NM_{PN}}{\partial SP_{PN}}$, are already presented in state estimation of power networks (section 2.4.2). Since the measured parameters of the power network are calculated independent of the values of the state parameters of the gas network, all the partial derivatives of them with respect to the state parameters of the gas network are equal to zero, i.e. $\frac{\partial NM_{PN}}{\partial SP_{GN}} = 0$.

- Partial derivatives of the measurements of the gas network (NM_{GN})

The formulations for calculation of the partial derivatives of the measurements of the gas network with respect to the state parameters of the gas network, i.e. $\frac{\partial NM_{GN}}{\partial SP_{GN}}$, are already presented in state estimation of gas networks with decentralised injection (section 5.2.2). Since the measured parameters of the gas network are calculated independent of the values of the state parameters of the power network, all the partial derivatives of them with respect to the state parameters of the power network are equal to zero, i.e. $\frac{\partial NM_{GN}}{\partial SP_{PN}} = 0$.

- Partial derivatives of the power balance in coupling components (PB_{CC})

  - Gas turbine:

    The partial derivatives of the power balance equation of the gas turbines with respect to the voltage magnitudes and voltage angles are equal to the partial derivatives of the first term of the equation (7-5), i.e. the electric power injection term, with respect to those state parameters. This is due to the fact that the second term, i.e. the gas network term, is calculated using the state parameters of the gas network and is independent of the voltage magnitudes and voltage angles. Similarly the partial derivatives of the power balance equation with respect to the squared pressures and molar fractions are equal to the partial derivatives of the second term of the equation with respect to those state parameters.

This is true because the first term is calculated using the state parameters of the power network and is independent of the squared pressures and molar fractions. Hence:

$$\frac{\partial PB_{GT}}{\partial \theta} = \frac{\partial p_{inj}}{\partial \theta} \tag{7-8}$$

and:

$$\frac{\partial PB_{GT}}{\partial V} = \frac{\partial p_{inj}}{\partial V} \tag{7-9}$$

Formulations for calculation of the partial derivatives of power injection with respect to voltage magnitudes and voltage angles were presented in Chapter 2. Partial derivative of the power balance equation of the gas turbines with respect to the squared pressures is:

$$\frac{\partial PB_{GT}}{\partial PS} = -\eta_{GT} \times GCV_{mix} \times \frac{\partial q_l}{\partial PS} \tag{7-10}$$

where the partial derivative of the flow of the node with respect to squared pressure was calculated using the equations presented in Chapter 5. Also, the partial derivative of the power balance equation of the gas turbines with respect to the molar fractions is:

$$\frac{\partial PB_{GT}}{\partial y} = -\eta_{GT} \times \left\{ q_l \times \frac{\partial GCV_{mix}}{\partial y} + GCV_{mix} \times \frac{\partial q_l}{\partial y} \right\} \tag{7-11}$$

Since the calorific value of a gas mixture is calculated using:

$$GCV_{mix} = \frac{\sum_{i=1}^{N_C} (y_i . GCV_i)}{\mathrm{Z}_{mix}} \tag{7-12}$$

the partial derivative of calorific value of the gas mixture with respect to the molar fraction of the components at the coupling component node will be equal to:

$$\frac{\partial GCV_{mix}}{\partial y_j} = \frac{1}{Z_{mix}} \times \frac{\partial\left(\sum_{i=1}^{N_C}(y_i . GCV_i)\right)}{\partial y_j} - \frac{\sum_{i=1}^{N_C}(y_i . GCV_i)}{{Z_{mix}}^2} \times \frac{\partial Z_{mix}}{\partial y_j} \tag{7-13}$$

The partial derivative in the first term of Equation (7-13) is calculated as follows:

$$\frac{\partial\left(\sum_{i=1}^{N_C}(y_i . GCV_i)\right)}{\partial y_j} = GCV_j \tag{7-14}$$

where y_j represents the molar fraction of component j at the coupling component node. The partial derivative of the calorific value at the coupling component node with respect to the molar fractions of all the components at all the rest of the nodes is equal to zero.

The compressibility of the gas mixture is calculated as follows:

$$Z_{mix} = 1 - \left(\sum_{i=1}^{N_C}(y_i . c_i)\right)^2 \tag{7-15}$$

Hence, the partial derivative of it with respect to the molar fractions of the gas at the coupling component node is calculated using:

$$\frac{\partial Z_{mix}}{\partial y_j} = -2 \times c_j \times \sum_{i=1}^{N_C}(y_i . c_i) \tag{7-16}$$

where y_j represents the molar fraction of component j at the coupling component node. The partial derivative of the compressibility of the gas mixture at the coupling component node with respect to all the components at all the rest of the nodes is equal to zero.

The partial derivative of the flow at the node with respect to the molar fractions ($\frac{\partial q_l}{\partial y}$) was already explained in Chapter 5.

Calculating the values for the partial derivative terms of Equation (7-11) as just explained, the value for the partial derivative of the power balance equation at the gas turbine with respect to molar fractions is calculated and placed in the measurement Jacobian matrix.

- Power to gas units:

Partial derivatives of the power balance equation of power to gas units, i.e. Equation (7-6), with respect to the state parameters of the integrated network are as follows:

$$\frac{\partial PB_{P2G}}{\partial \theta} = -\eta_{P2G} \times \frac{\partial p_{inj}}{\partial \theta} \tag{7-17}$$

$$\frac{\partial PB_{P2G}}{\partial V} = -\eta_{P2G} \times \frac{\partial p_{inj}}{\partial V} \tag{7-18}$$

$$\frac{\partial PB_{P2G}}{\partial PS} = GCV_{mix} \times \frac{\partial q_l}{\partial PS} \tag{7-19}$$

$$\frac{\partial PB_{P2G}}{\partial y} = \left\{ q_l \times \frac{\partial GCV_{mix}}{\partial y} + GCV_{mix} \times \frac{\partial q_l}{\partial y} \right\} \tag{7-20}$$

where the calculation of the terms is carried out similar to the method explained for calculation of partial derivatives of the power balance equation of gas turbines.

In this way, the elements of the measurement Jacobian matrix are calculated and the whole matrix is used for the WLS-based state estimation of integrated power and gas distribution networks.

7.3.3 The algorithm of the simulation model developed in MATLAB

A simulation model was developed in MATLAB in order to perform state estimation of integrated power and gas networks in steady state conditions. The inputs of the simulation model include:

- Specific parameters for power flow analysis of the integrated network:
    - Power network:
        - Network topology
        - Demands and generations
    - Gas network:
        - Network topology
        - Demands and injections
    - Coupling components:
        - Efficiency of gas turbine(s)
        - Efficiency of power to gas unit(s)
- Accuracy and confidence level of all the networks measurements
- Variance of power balance at the coupling components
- Acceptable tolerance of estimation (ε)

Firstly, the power flow analysis of the integrated network was performed using the simulation model developed in MATLAB (see section 7.2) in order to obtain the true values of all the operation parameters of the integrated network including the values for the state parameters and the power flows in all the branches of both networks. Then, the values of standard deviations were calculated using Equation (2-13). Afterwards, the values of the available measurements were produced using the normrnd(ψ,σ) function of MATLAB. In this way, the input parameters for the WLS state estimation algorithm were provided.

The inputs of the WLS state estimation algorithm include the values of measurements, the standard deviations, the topology and specifications of the integrated network and the acceptable tolerance of estimation (ε). The weights matrix, W, was formed using Equation (2-6) and by squaring the values of standard deviations. Also, the values of variance of zero injections in both network and the values of variances of power balance at the coupling components were placed in the matrix.

The solution process starts by guessing some values for the state vector x. Flat start was considered as guess values for the values of the state parameters in the power network, i.e. voltage magnitudes and voltage angles. Unlike the power systems there is not a straightforward clue for the guess values for the state parameters in gas systems, unfortunately. However, in this research the values of nodal pressures were distributed in the range of approximately 80%-100% of the source absolute pressure in a way that the nodal pressures are all different from one another. Regarding the molar fraction of the components, the guess values of them at all the nodes were very close to the molar fraction of the components at the main source.

Once the values of the state parameters of the integrated network were guessed, the values of the measurement function, $h\left(x^{(1)}\right)$, the measurement Jacobian, $H\left(x^{(1)}\right)$, the derivative function $g\left(x^{(1)}\right)$ and the gain matrix $G\left(x^{(1)}\right)$ at iteration number 1 was calculated using equations in sections 7.3.1 and 7.3.2 and equations (2-19) and (2-20), respectively. Afterwards, the values of the state parameters were updated using (2-18). This process was iterated until the change in the values of the state parameters, which is calculated using (2-21), is less than ε. The process is presented in Figure 7.2.

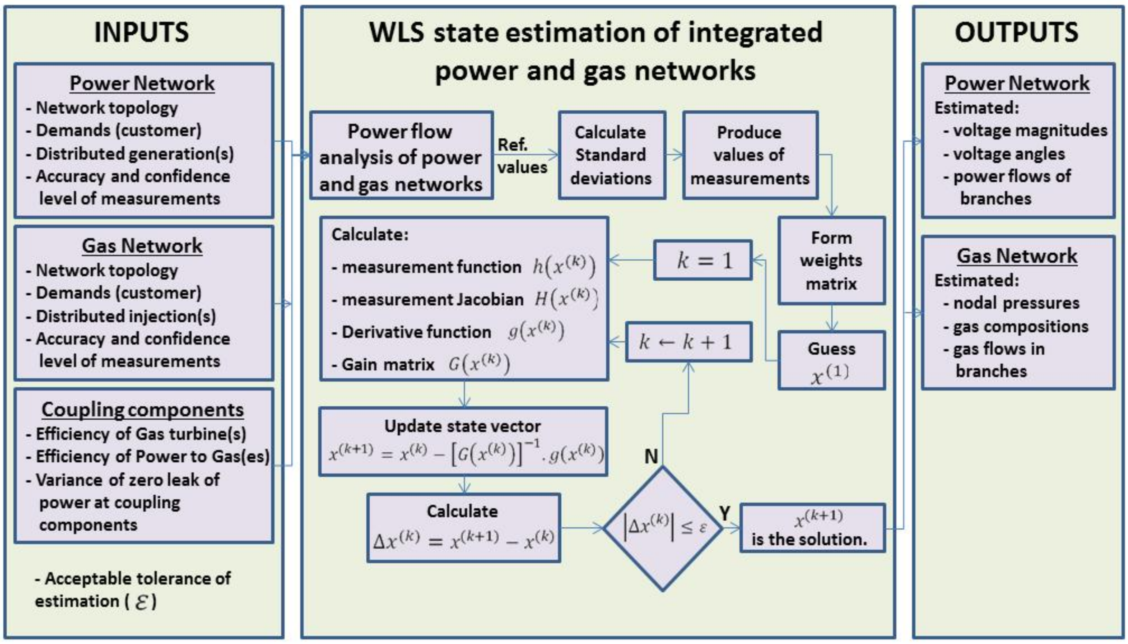

Figure 7.2: The schematic of the WLS-based state estimation of integrated power and gas networks

7.4 Case study

The test integrated power and gas network along with the assumptions of the measurements and of the algorithm of WLS state estimation are described in this section.

7.4.1 The test network

In order to study the state estimation of integrated power and gas distribution networks a test integrated network was created since no real case study integrated networks having both gas turbine and power to gas units in the distribution level were found. The schematic of the test integrated power and gas distribution network is shown in Figure 7.3. It is assumed the 100 MVA$_{base}$ power network operates at 11kV. Also, the power to gas unit consists of an electrolyser and a methanation process, hence Hydrogen, the product of the electrolysation, is converted to methane and an upgraded natural gas with a high methane content is injected into the gas network. The specifications of the networks including the topology, demands, generations and injections are presented in the Appendix III.

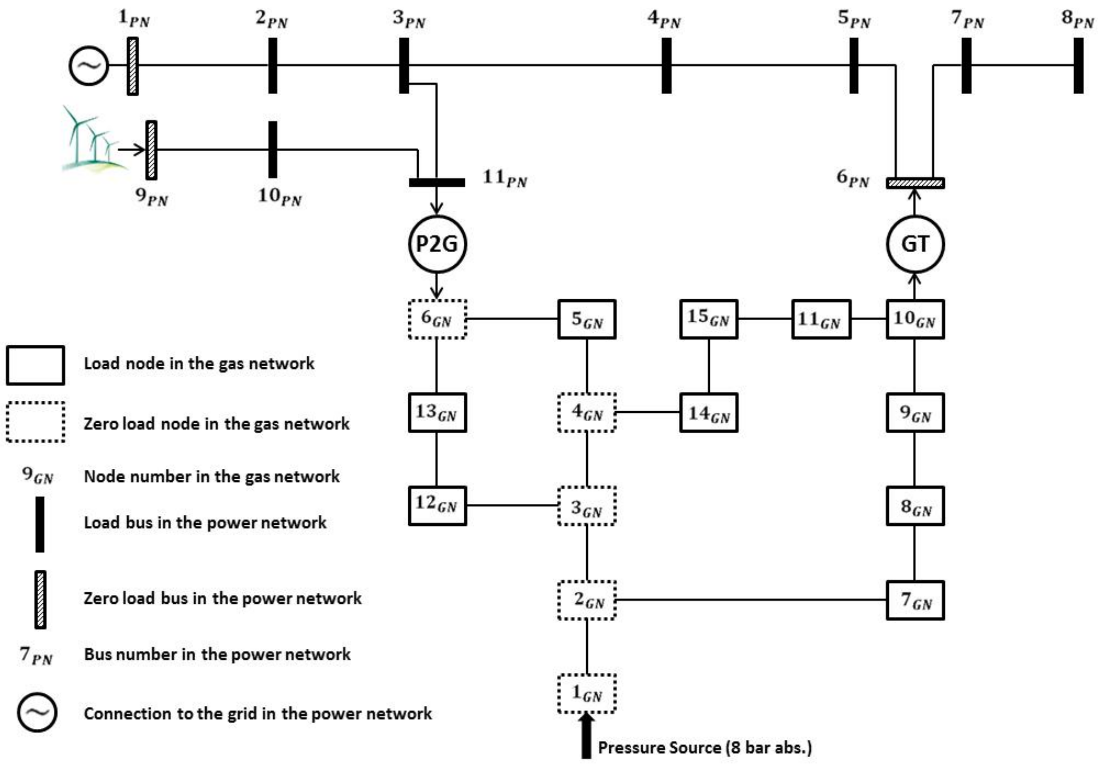

Figure 7.3: The schematic of the integrated power and gas distribution test network

7.4.2 Measurements assumptions

The available measurements of the integrated network along with their accuracies are shown in Tables 7.1 and 7.2. Variances of load measurements at the zero load nodes (zero injection measurements) and the variances of the power balance at the coupling components are all assumed to be 1.0×10^{-8}. The values of accuracies are assumed for the purpose of study of state estimation of integrated networks although they do not have significant difference with the realistic values in realistic networks.

Table 7.1: Accuracies of the available measurements of the power network

Measured Parameter*	Measurement location	Measurement type	Accuracy
Voltage magnitude	Buses# 1(slack), 6(GT), 9(WF**), 11(P2G)	Real time	1 %
Power flow	Branches: 1-2, 6-5, 6-7, 9-10, 11-3, 11-10	Real time	1 %
Power injection	All the load buses	Pseudo measurement	50 %

*: Power measurements refer to both real and reactive parts.

**: WF denotes wind farm

Table 7.2: Accuracies of the available measurements of the gas network

Measured Parameter	Measurement location	Measurement type	Accuracy
Pressure	Nodes# 1(source), 6(P2G), 10(GT)	Real time	1 %
Branch flow	Branches: 1-2, 6-5, 6-13, 10-9, 10-11	Real time	1 %
Node flow	Nodes# 1(source), 6(P2G), 10(GT)	Real time	1 %
	All the node loads	Pseudo	50 %
Molar fraction	Nodes# 1(source), 6(P2G), 10(GT)	Real time	1 %
	All the nodes except nodes# 1, 6, 10	Pseudo	10 %

7.4.3 Designed case studies

In order to study impact of deployment of smart meters in one of the networks on state estimation of the other coupled network three case studies were designed:

- *Case 1: State estimation of the base integrated network*

  In this case the base network with the measurement configuration as shown in Tables 7.1 for the power network and in Table 7.2 for the gas network was considered. The state estimation of the integrated network was performed in two approaches as follows with the same set of the measurement values in Monte Carlo simulations in both approaches in order to compare the results of estimation of the state parameters of the networks between these two approaches:

- Separated state estimation

  In this approach the state estimation of each network was performed separated from the state estimation of the other network. In other words, two separated networks were considered in this approach and the formulations presented for state estimation of power and gas networks in Chapters 2 and 5 were implemented separately to each network. In separated state estimation the real time measurements of each side of the coupling components were included in the state estimation of the network which the component is connected to.

- Integrated state estimation

  In this approach the integrated state estimation with the formulations and the algorithm explained in this Chapter (section 7.3) was applied to the integrated power and gas network.

- *Case 2: Smart meters in the power network*

In this case it was assumed all the load nodes in the power network are equipped with smart meters that measure real time values of voltage magnitude and (real and reactive) power injection of the nodes with an accuracy of 1%.

- *Case 3: Smart meters in the gas network*

In this case it was assumed all the load nodes in the gas network are equipped with smart meters that measure real time values of pressure and gas flow of the load nodes with an accuracy of 1%.

7.5 Results and discussion

7.5.1 Validation of the simulation model for SE of integrated power and gas networks

7.5.1.1 SE with perfect measurements

The performance of the simulation model developed in MATLAB for state estimation of integrated power and gas networks was first evaluated using perfect measurements, i.e. noise- or error-free measurements. In other words, the algorithm of integrated state estimation of the integrated network was fed with the true values of the available measurements presented in Table 7.1 for the power network and in Table 7.2 for the gas network. The true values of the measurements were obtained from the power flow analysis of the integrated network (section 7.2).

Figure 7.4 shows the comparison of the results of estimation of the state parameters of the power network, i.e. the values of voltage magnitudes and voltage angles at all the buses, with the true values of the parameters. Figure 7.5 demonstrates the comparison of the results of estimation of the state parameters of the gas network, i.e. the values of pressures and molar fractions of all the components at all the nodes, with the true values of the parameters.

As can be seen from Figures 7.4 and 7.5 and as was expected all the results of state estimation with perfect measurements coincide and follow the results obtained in the power flow analysis of the integrated network.

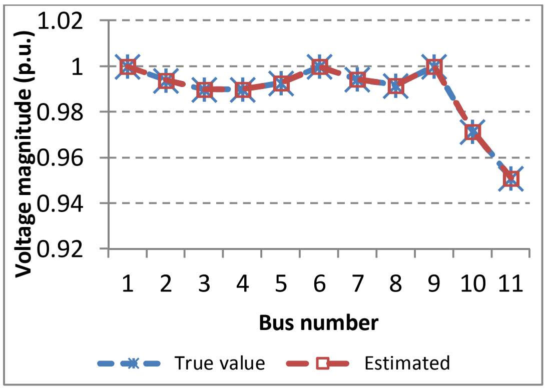

(a) Voltage magnitudes

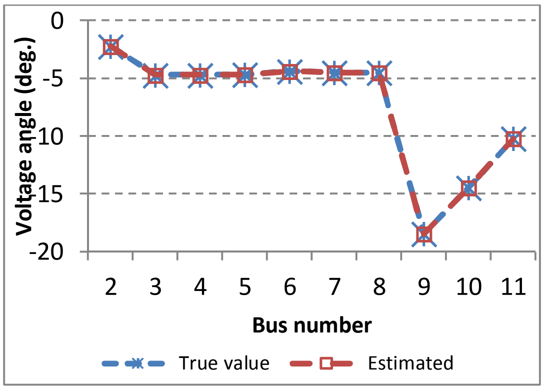

(b) Voltage angles

Figure 7.4: Comparison of the estimated and true values of the state parameters of the power network

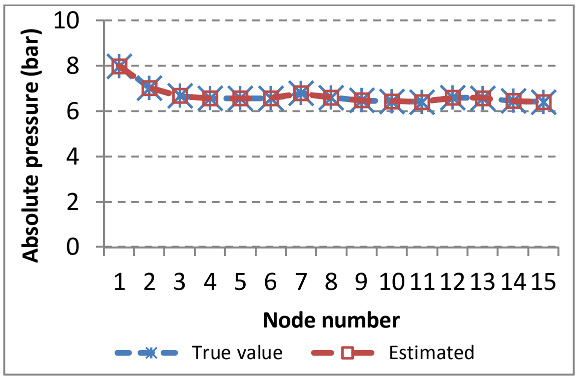

(a) Nodal pressures

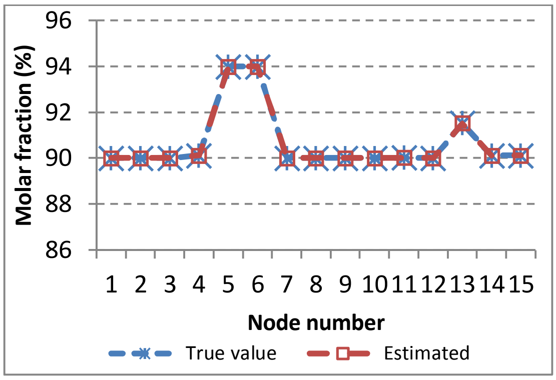

(b) Molar fraction of CH_4 at nodes after mixing

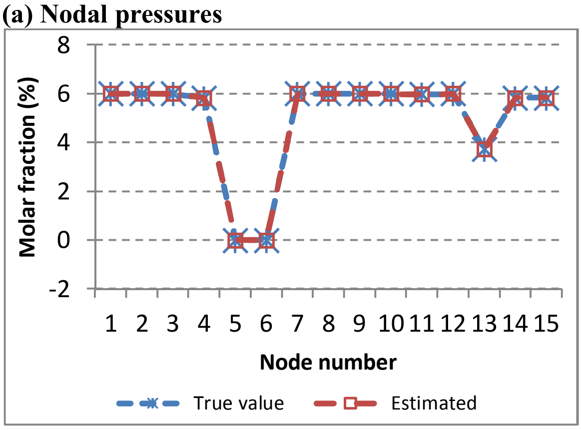

(c) Molar fraction of C_2H_6 at nodes after mixing

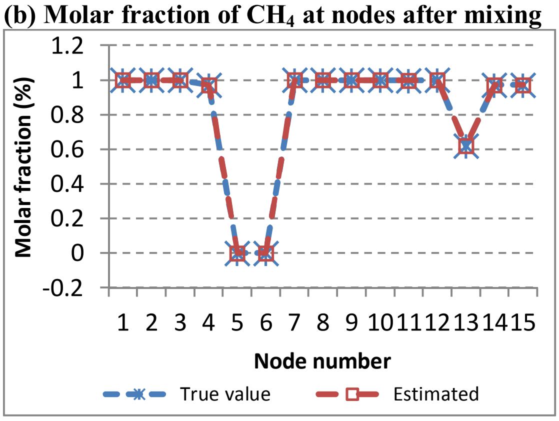

(d) Molar fraction of C_3H_8 at nodes after mixing

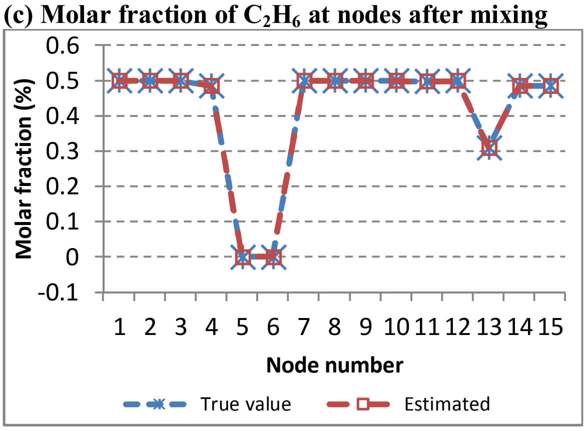

(e) Molar fraction of C_4H_{10} at nodes after mixing

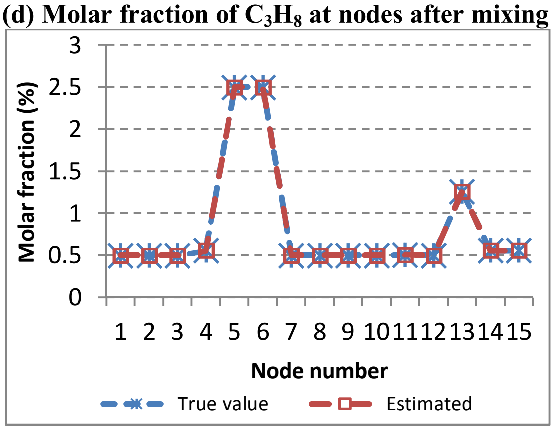

(f) Molar fraction of CO_2 at nodes after mixing

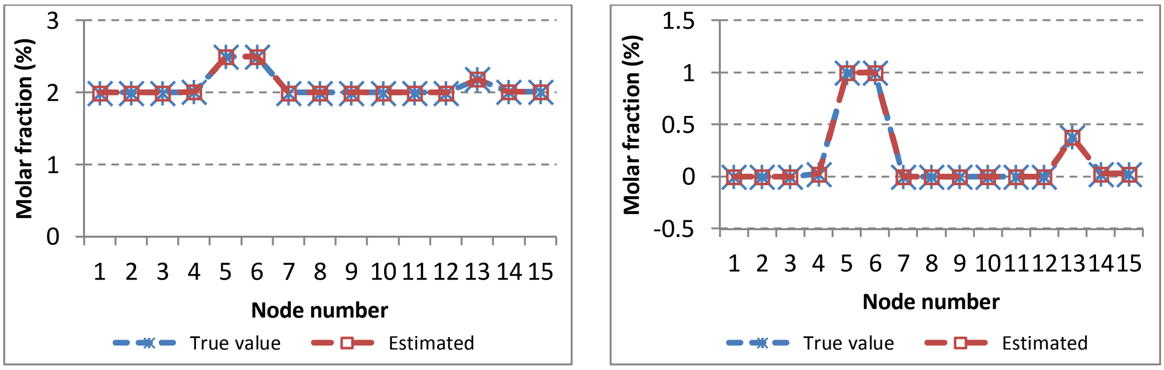

(g) Molar fraction of N_2 at nodes after mixing **(h) Molar fraction of H_2 at nodes after mixing**

Figure 7.5: Comparison of the estimated and true values of the state parameters of the gas network

7.5.1.2 Monte Carlo simulation of state estimation of the integrated network

In the next step 20,000 Monte Carlo simulations were performed on the integrated network in order to observe performance of the simulation model as well as the distribution of the estimated state parameters of the integrated network. The available measurements of the power and gas network as well as the assumed values of their accuracies were shown in Table 7.1 for the power network and in Table 7.2 for the gas network. The set of measurement values for each Monte Carlo simulation was produced using the normrnd function of MATLAB. This function produces random numbers that follow Normal distribution. The standard deviation of the distribution was calculated using Equation (2-13) with the “True values” obtained in the power flow analysis of the integrated network (section 7.2).

The distribution of the values of the state parameters of the power and gas network is shown in Figure 7.6 for the power network and in Figure 7.7 for the gas network in boxplots. In all the plots of Figures 7.6 and 7.7, 25 and 75 percentile of the data are put in the boxes and approximately 0.7% of the data are considered as the outliers, which are shown by pluses. Also, true values are shown by stars in the plots, which almost coincide with the 50 percentile of the data.

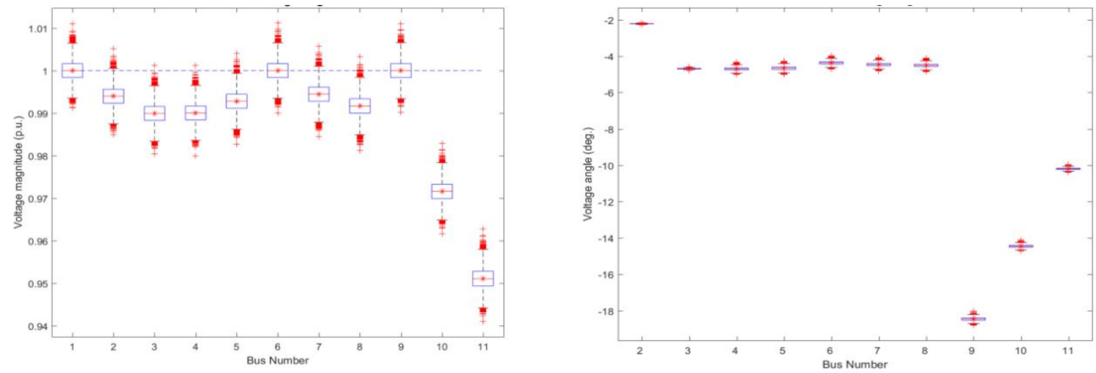

(a) Voltage magnitudes **(b) Voltage angles**

Figure 7.6: Distribution of the estimated values of the state parameters of the power network

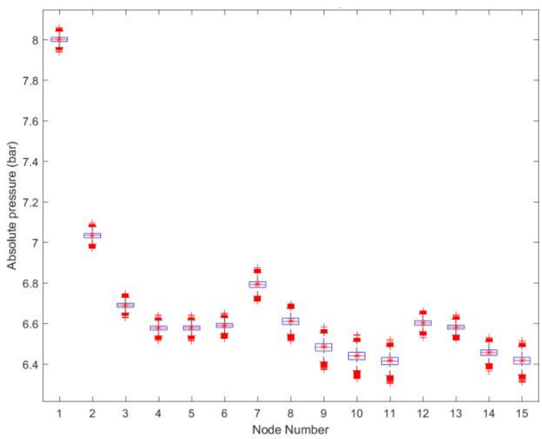

(a) Nodal pressures

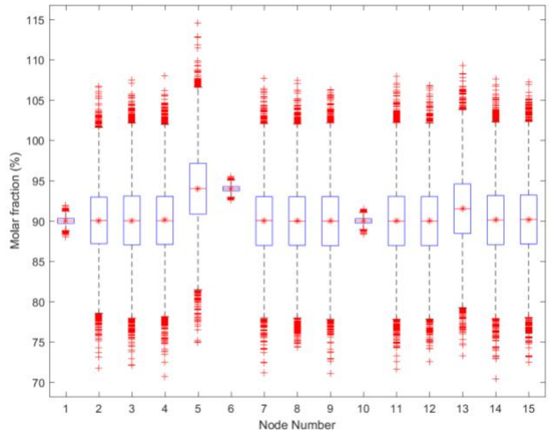

(b) Molar fraction of CH_4 at nodes after mixing

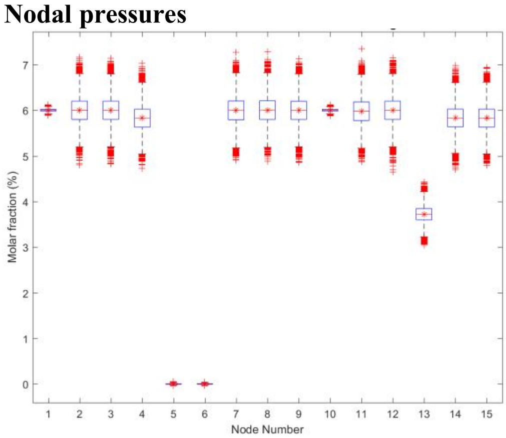

(c) Molar fraction of C_2H_6 at nodes after mixing

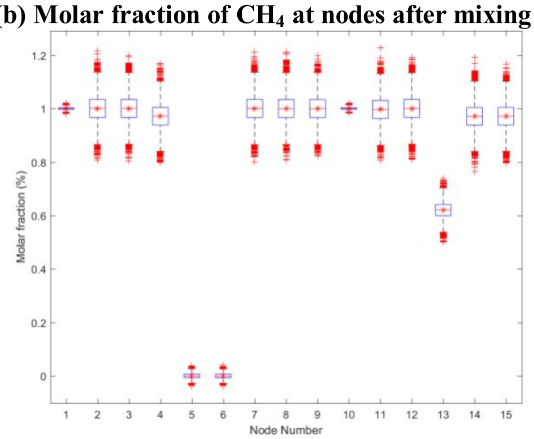

(d) Molar fraction of C_3H_8 at nodes after mixing

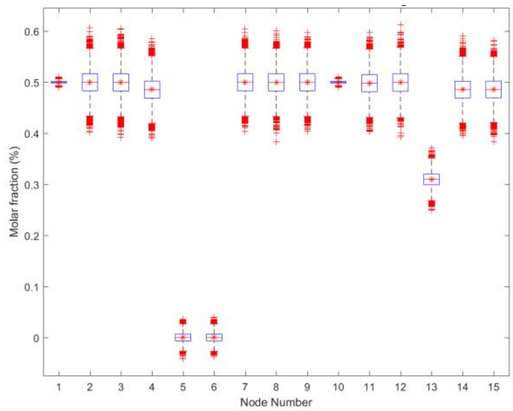

(e) Molar fraction of C_4H_{10} at nodes after mixing

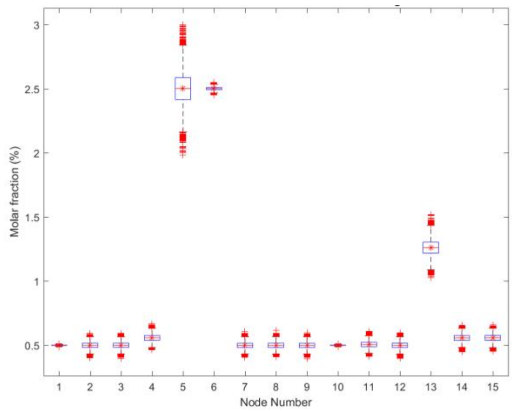

(f) Molar fraction of CO_2 at nodes after mixing

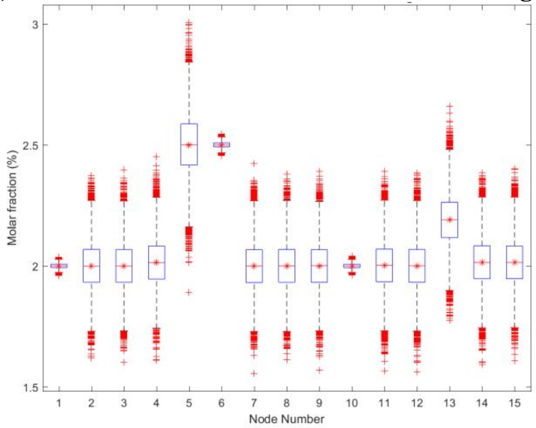

(g) Molar fraction of N_2 at nodes after mixing

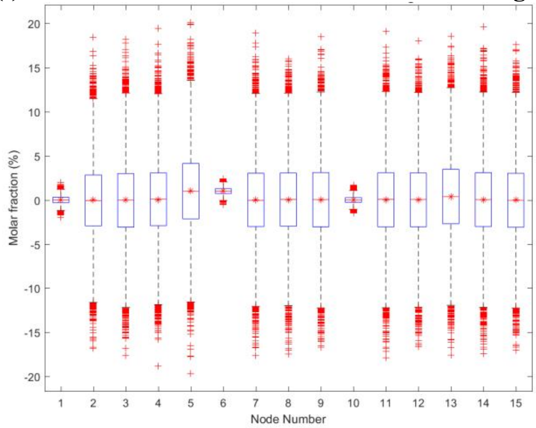

(h) Molar fraction of H_2 at nodes after mixing

Figure 7.7: Distribution of the estimated values of the state parameters of the gas network

As can be seen from Figure 7.6 the average values of the estimated state parameters of the power network, i.e. the voltage magnitudes and voltage angles, coincide with the true values presented in Figure 7.4. Also, Figure 7.7 shows that the average values of the estimated state parameters of the gas network, i.e. the nodal pressures and the molar fractions of the gas components at the nodes, coincide with the true values depicted in Figure 7.5.

Additionally, the values of the estimated state parameters of both networks have a Normal distribution with an expected or mean value, which is the true value of the state parameter. This behaviour was also expected and is due to the fact that the measurement model is linearised in the formulations of the WLS state estimation. Therefore, the estimated state parameters follow a Normal distribution provided the WLS state estimator is fed with normally distributed measurements.

7.5.2 Case 1: State estimation of the base integrated network

In all the cases the results of 20,000 Monte Carlo simulations of state estimation of the integrated network are presented. The suitability of this number of Monte Carlo simulations is discussed in section 7.5.5.

The values of MAPE of estimation of the state parameters of the power and the gas network are presented in Figures 7.8 and 7.9, respectively. As can be seen the values of MAPE are all identical for the separated and integrated state estimation of the network. This can be due to the fact that the real time measurements at the coupling components were considered in separated state estimation. Hence, the equations of power balance at the coupling components with the weights equal to the weights of the virtual measurements did not have a significant impact in the case of integrated state estimation.

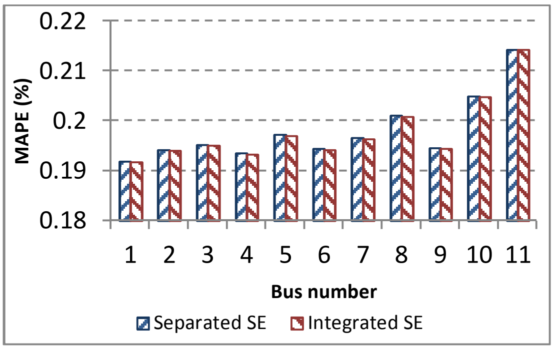

(a) Voltage magnitudes

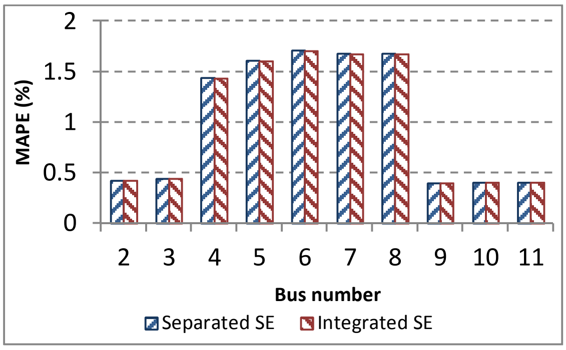

(b) Voltage angles

Figure 7.8: The MAPE values of the state parameters of the power network in Case 1

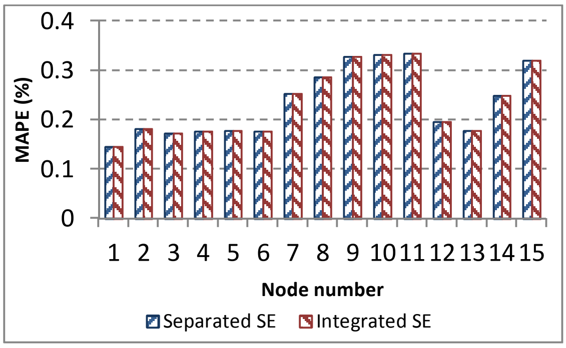

(a) Nodal pressures

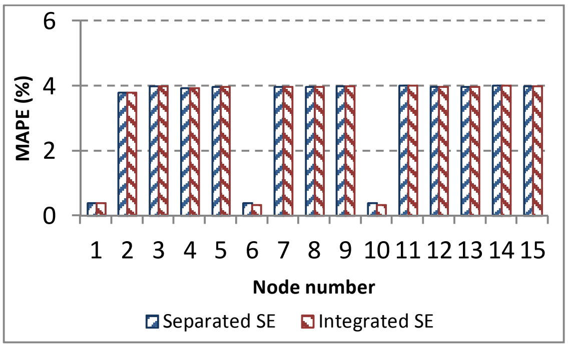

(b) Molar fraction of CH_4 at nodes after mixing

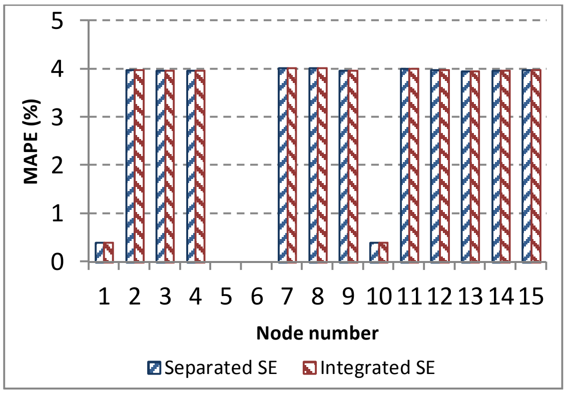

(c) Molar fraction of C_2H_6 at nodes after mixing

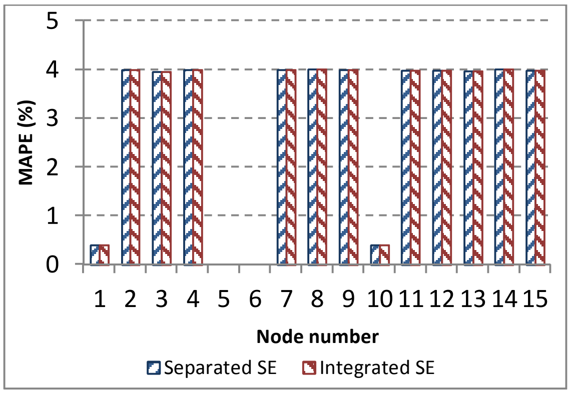

(d) Molar fraction of C_3H_8 at nodes after mixing

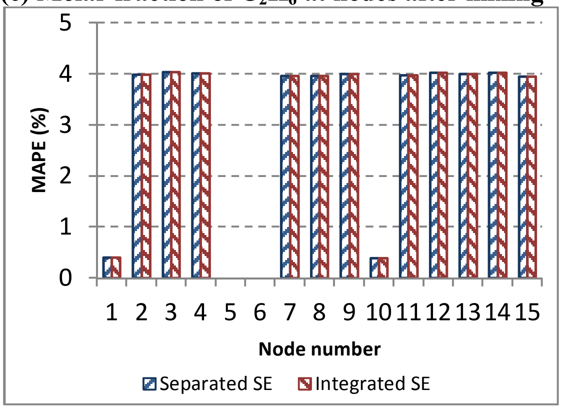

(e) Molar fraction of C_4H_{10} at nodes after mixing

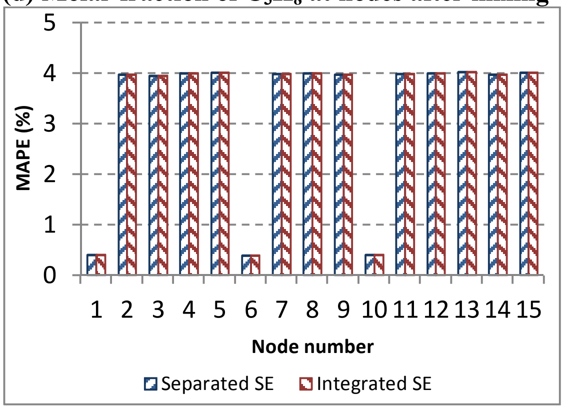

(f) Molar fraction of CO_2 at nodes after mixing

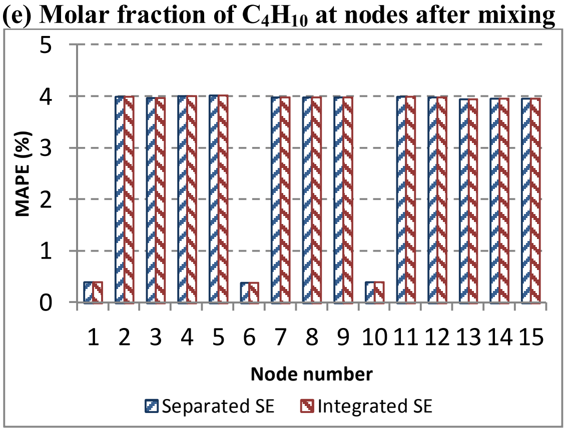

(g) Molar fraction of N_2 at nodes after mixing

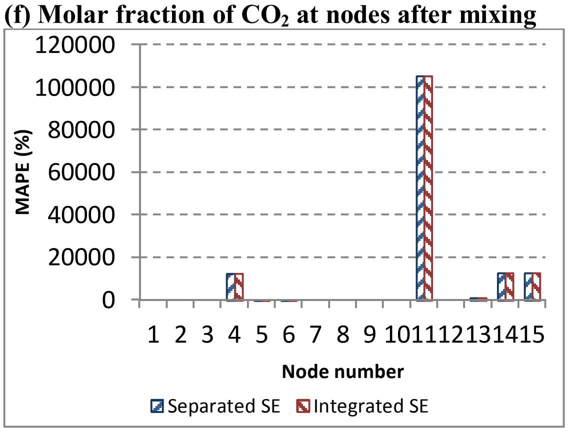

(h) Molar fraction of H_2 at nodes after mixing

Figure 7.9: The MAPE values of the state parameters of the gas network in Case 1

7.5.3 Case 2: Smart meters in the power network

The values of MAPE of estimation of the state parameters of the power and the gas network are compared against the values of MAPE in Case 1 in Figures 7.10 and 7.11, respectively. For the purpose of brevity the values of MAPE of molar fractions of a few of the components of the natural gas are presented since the same trend was observed for the rest of the components.

As can be seen from Figure 7.10 and was expected the values of MAPE of estimation of the state parameters of the power network have reduced due to the deployment of smart meters in that network. However, Figure 7.11 shows that the values of MAPE of estimation of the state parameters of the gas network are all identical to the values in Case 1, meaning that information from the power network, i.e. the deployment of smart meters in the network, does not have impact on state estimation of the gas network. This was also deduced from the results of Case 1 since having the same results from either the separated or the integrated state estimation means that the information from each network has no impact on state estimation of the other.

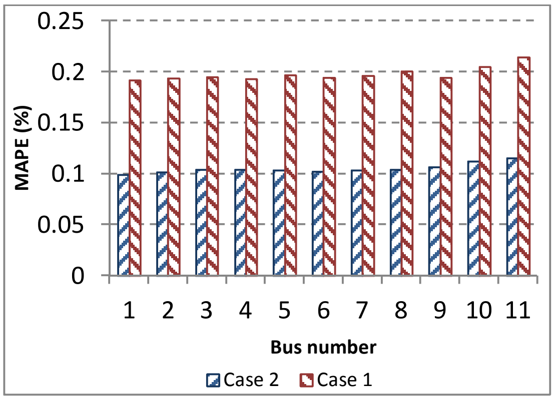

(a) Voltage magnitudes

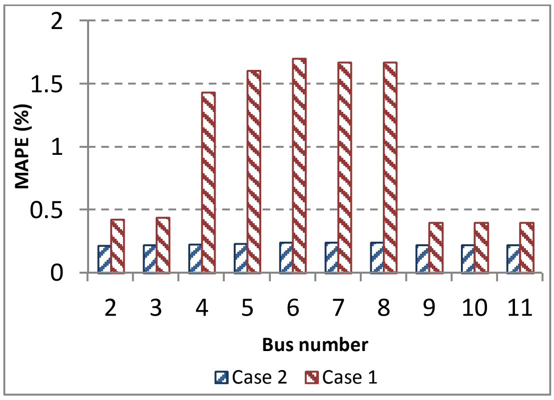

(b) Voltage angles

Figure 7.10: The MAPE values of the state parameters of the power network in Case 2

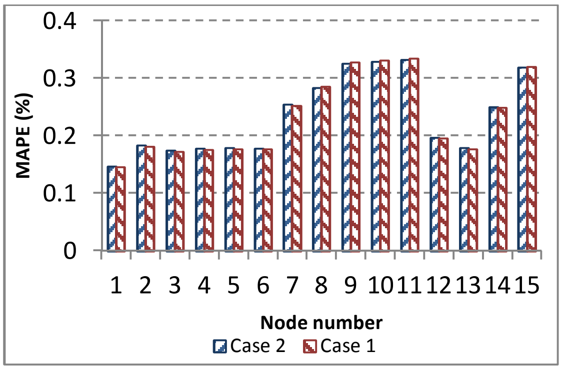

(a) Nodal pressures

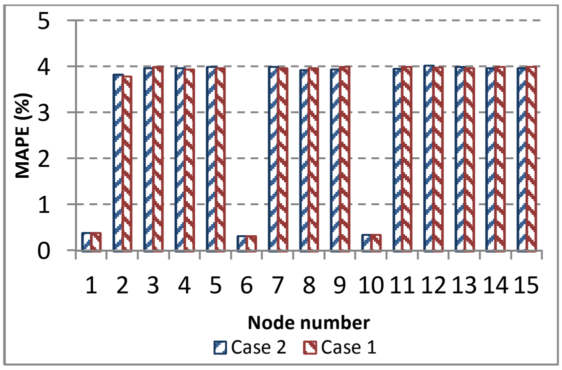

(b) Molar fraction of CH_4 at nodes after mixing

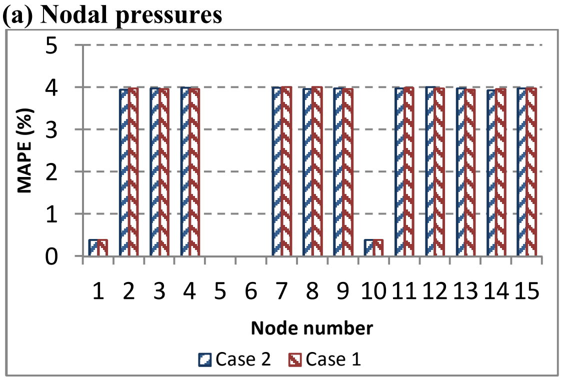

(c) Molar fraction of C_2H_6 at nodes after mixing

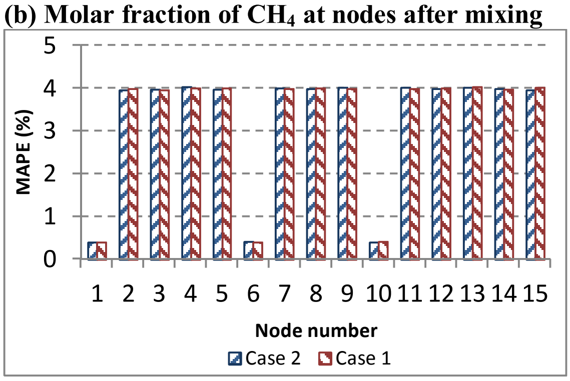

(d) Molar fraction of CO_2 at nodes after mixing

Figure 7.11: The MAPE values of the state parameters of the gas network in Case 2

7.5.4 Case 3: Smart meters in the gas network

The values of MAPE of estimation of the state parameters of the power and the gas network are compared against the MAPE values in Case 1 in Figures 7.12 and 7.13, respectively. For the purpose of brevity the values of MAPE of molar fractions of a few of the components of the natural gas are presented since the same trend was observed for the rest of the components.

As can be seen from Figure 7.13 and was expected the values of MAPE of estimation of the nodal pressures of the gas network have reduced due to having the real time measurements of pressure at all the load nodes. Also, as was expected from Chapter 6, pressure measurements do not have significant impact on estimation of molar fractions of all the gas components except the methane, which has the highest fractions among all the components, at some of the nodes. Therefore, the MAPE values of estimation of molar fractions are almost unchanged relative to Case 1.

Comparing the values of MAPE of estimation of the state parameters of the power network in Figure 7.12 shows that a slight decrease in the values of MAPE of estimation of the voltage magnitudes is observed (Figure 7.12(a)); however, deployment of smart meters in the gas network had almost no impact on estimation of the voltage angles (Figure 7.12(b)). Therefore, it can be concluded that information from the gas network, i.e. deployment of smart meters in the network, has insignificant impact on improvement of state estimation of the power network. This was already expected based on the results of Cases 1 and 2.

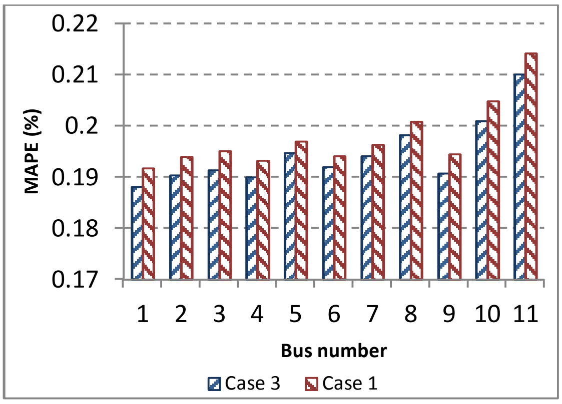

(a) Voltage magnitudes

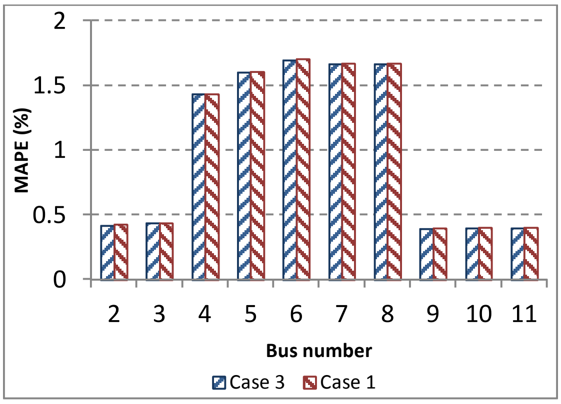

(b) Voltage angles

Figure 7.12: The MAPE values of the state parameters of the power network in Case 3

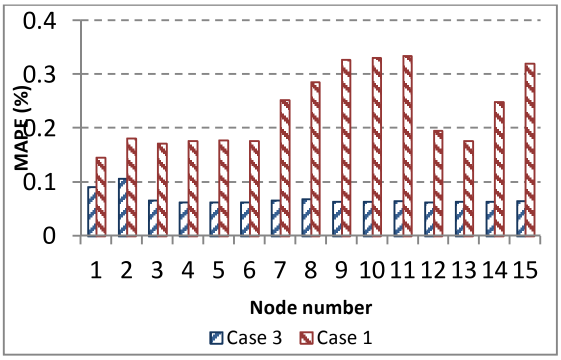

(a) Nodal pressures

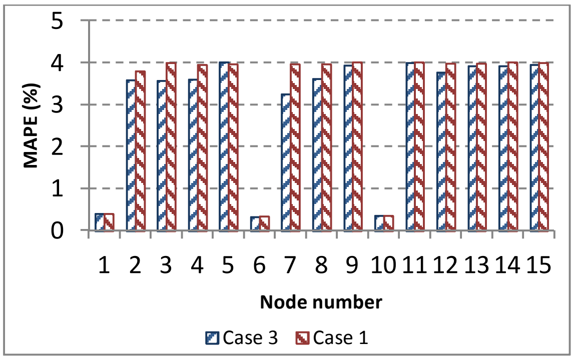

(b) Molar fraction of CH_4 at nodes after mixing

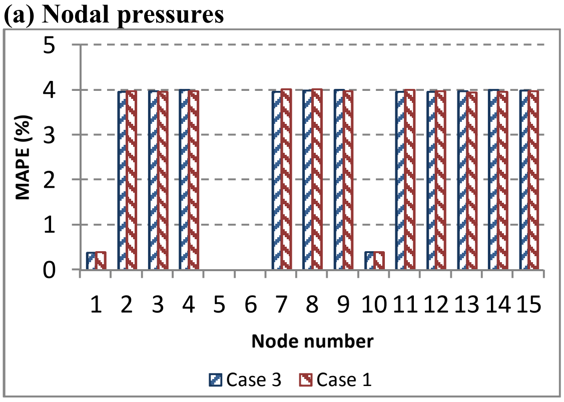

(c) Molar fraction of C_2H_6 at nodes after mixing

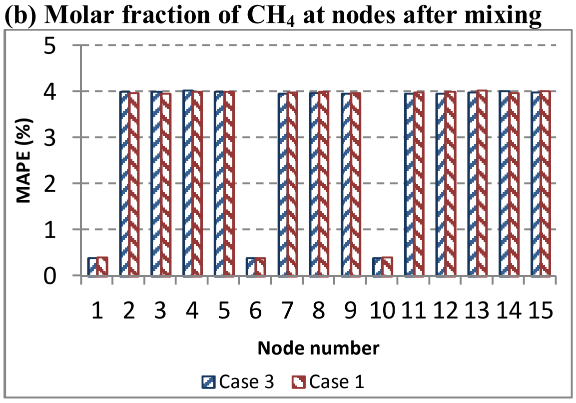

(d) Molar fraction of CO_2 at nodes after mixing

Figure 7.13: The MAPE values of the state parameters of the gas network in Case 3

According to the results of the case studies and as was observed in (Liu 2013), it can be concluded that the operation point of an integrated system especially in the steady state conditions is a unique point. This unique point can be achieved independent of the form of mathematical formulations, whether each system is simulated and analysed separately from one another or all the systems are considered in an integrated approach.

7.5.5 Suitability of the selected number of Monte Carlo simulations

In order to ensure that a suitable number of Monte Carlo simulations, i.e. 20,000, is selected the following criterion, which is the sum of MAPE of estimation of all the state parameters of the integrated network, was defined:

$$Criterion = \sum_{i=1}^{N_B} \left(MAPE_{V_i} + MAPE_{\theta_i}\right) + \sum_{i=1}^{N_N} \left(MAPE_{p_i} + \sum_{j=1}^{N_C - 1} \left(MAPE_{y_{j,i}}\right) \right) \quad (7\text{-}21)$$

where:

N_B Number of buses of the power network

N_N Number of nodes of the gas network

N_C Number of components of the gas mixture

$y_{j,i}$ Molar fraction of component j at node i

After the Monte Carlo simulation stabilised and converged, the number of Monte Carlo simulations started from 15,000 and was increased with steps of 1,000 up to 20,000. The change in the value of the criterion relative to the previous number of Monte Carlo simulations is presented in Figure 7.14 for all the three cases.

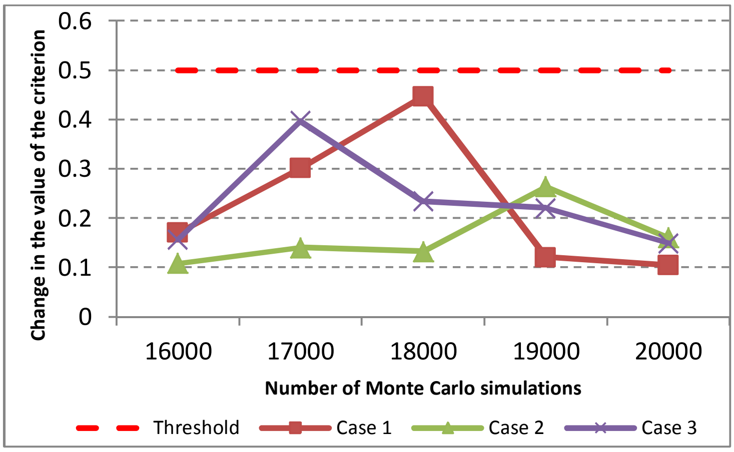

Figure 7.14: The change in the value of the criterion over Monte Carlo simulations

As can be observed the change in the value of the criterion is less than 0.5 after several consecutive times for all the cases, which means a proper number of Monte Carlo simulations is selected and the results are reliable.

7.6 Summary and conclusions

In this Chapter state estimation of integrated power and gas distribution networks with decentralised injection in both networks was studied. Based on the lessons learnt from the state estimation of power and gas networks in Chapters 2 and 5, respectively, an algorithm was developed for integrated state estimation of the integrated networks based on the weighted least squares estimation technique. Then, a simulation model was developed in MATLAB based on the algorithm and a case test integrated network was considered in order to study the state estimation of the integrated network.

The simulation model developed for integrated state estimation of integrated power and gas networks was validated through two scenarios:

- SE with perfect measurements

  The algorithm was first fed with perfect measurements, i.e. the values of the measurements were equal to the true values of the parameters that were obtained from the steady state power flow analysis of the integrated networks. It was observed and as was expected the values of the state parameters of both networks that were estimated by the algorithm were all equal to the true values that were obtained by the power flow analysis of the networks (Figures 7.4 and 7.5).

- Monte Carlo simulation of state estimation of the integrated networks

  A Monte Carlo simulation of state estimation of the integrated networks was performed with 20,000 populations using normally distributed measurements in order to observe the performance of the algorithm. It was observed and as was expected the state parameters of the network that were estimated by the algorithm have also a Normal distribution with the mean values equal to the true values that were obtained in the power flow analysis of the integrated networks (Figures 7.6 and 7.7).

Afterwards, three case studies were designed in order to address the research questions. The description of the cases as well as the results obtained in each is as follows:

- Case 1: State estimation of the base integrated network

  In this case the aim was to compare the performance of separated and integrated state estimation of the integrated network using the same set of measurements in order to investigate the possibility of obtaining more accurate results through integrated state estimation.

It was observed that the MAPE of estimation of all the state parameters of the networks were identical for the separated and integrated state estimation. This means that the integrated state estimation did not improve the estimation of the state parameters compared to the estimation of the networks in the separated approach. This can be due to the fact that the real time measurements at the coupling components were already considered in the separated state estimation of each network. Also, adding the power balance equations at the coupling components adds no more information and constraints for improvement of the accuracy of the solution in the integrated state estimation approach.

- Case 2: Smart meters in the power network

In this case all the load nodes in the power network were equipped with real time measurements of voltage magnitude and (real and reactive) power injection. The aim of this case was to study the impact of information of the power network on the state estimation of the coupled gas network.

It was observed that the information of the power network, i.e. the more real time measurements, did not improve the estimation of the coupled network, i.e. the gas network. This was already expected from the results of Case 1.

- Case 3: Smart meters in the gas network

In this case all the load nodes in the gas network were equipped with the real time measurements of pressure and gas flow of the node. The aim of this case was to investigate the impact of the information of the gas network on the state estimation of the power network.

It was observed that having more real time measurements in the gas network results in insignificant decrease in the MAPE values of estimation of voltage magnitudes in the power network. However, the deployment of smart meters in the gas network had no impact on improvement of estimation of the voltage angles of the power network.

8 Conclusions and future work

8.1 Conclusions

The research addressed in state estimation of integrated power and gas distribution networks was fulfilled through the following steps:

- State estimation of power distribution networks;
- Optimal placement of additional measurements in power distribution networks;
- Simulation of operation of gas distribution networks with decentralised injection;
- State estimation of gas distribution networks with decentralised injection;
- Optimal placement of additional measurements in gas distribution networks with decentralised injection;
- State estimation of integrated power and gas distribution networks.

8.1.1 State estimation of power distribution networks

As the first step of the work, state estimation of power distribution networks was investigated. A simulation model was developed in MATLAB, which estimates the values of the voltage magnitudes and voltage angles as the state parameters of a power network using the Weighted Least Squares (WLS) estimation technique.

The performance of the simulation model was evaluated using the UKGDS 95-bus test distribution network. The simulation model was validated through state estimation of the network using perfect measurements and the Monte Carlo simulation of state estimation of the network.

8.1.2 Optimal placement of additional measurements in power

distribution networks

Measurements and their location within a power network have a great impact on the performance of the state estimation of the network. An algorithm for placement of a given number of additional measurements at possible measurement locations within the network was developed in order to improve the accuracy of estimation of the state parameters of the network. Two simulation models were developed in MATLAB, which both are based on the algorithm, for the purpose of placement of additional individual measurements (Simulation model 1) and for placement of additional measurement units (Simulation model 2). Also, a new probability formula for the probability of the estimated state parameters of a power distribution network falling within the desired ranges was developed and validated.

The performance of the results of Simulation model 1 and Simulation model 2, which was evaluated using the UKGDS 95-bus test distribution network, shows that they are capable of optimal placement of given number of additional measurements within the power distribution network.

8.1.3 Simulation of operation of gas distribution networks with decentralised injection

Simulation of operation of gas distribution networks with decentralised injection is the basis for state estimation of them since the measurements are simulated by adding a random noise to the values of the parameters obtained from gas power flow analysis. A simulation model was developed in MATLAB for this purpose, which calculates the values of nodal pressures, flows of the branches, flows at nodes and molar fraction of the components of the gas mixture at the nodes.

The performance of the simulation model was validated against the results obtained from the commercial software Synergi Gas using a test gas distribution network operating at low pressure. The impact of decentralised injection on the operation of the network was also studied.

8.1.4 State estimation of gas distribution networks with

decentralised injection

Based on the lessons learnt from state estimation of power networks an algorithm was developed for performing state estimation of gas distribution networks with decentralised injection. A simulation model was developed in MATLAB based on the algorithm, which estimates the values of the nodal pressures and the molar fraction of the gas components at nodes using the WLS estimation technique.

The performance of the simulation model was evaluated using an example gas distribution network operating in medium pressure level. The simulation model was validated through state estimation of the test network using the perfect measurements and the Monte Carlo simulation of state estimation of the network.

8.1.5 Optimal placement of additional measurements in gas distribution networks with decentralised injection

Measurements and their placement within a gas distribution network with decentralised injection affect the performance of the estimation of the state parameters of the network. The impact of different real time measurements, i.e. measurements of pressure, gas flow and molar fraction, on the state estimation of an example gas distribution network with a decentralised injection operating in medium pressure level was investigated.

Also, an algorithm was developed for placement of additional measurements subject to a limited budget of the operator of a gas distribution network with decentralised injection. A simulation model was developed in MATLAB based on the algorithm, which ranks the best measurements designs (number, type and place of measurements) based on the accuracy index of molar fraction. This was considered as the decision criterion since the operator of a gas distribution network needs to have a proper estimation of the state of the gas mixture across the network at the times that decentralised injection occur.

The performance of the simulation model shows satisfactory results. Also, a sensitivity analysis of the state estimation of the best measurement designs for different values of error of pseudo measurements of loads and pseudo measurements of molar fractions at the nodes was also carried out.

8.1.6 State estimation of integrated power and gas distribution networks

In order to investigate transfer of information from one energy network to another energy network, which are connected to each other through several coupling components, integrated state estimation of power and gas distribution networks was performed. An algorithm was developed for this purpose based on the lessons learnt from the formulation of the problem of state estimation of power and gas distribution networks. A simulation model was developed in MATLAB based on the algorithm, which performs the integrated state estimation of integrated power and gas distribution networks with decentralised generation and injection in both networks using the WLS estimation technique.

The performance of the simulation model was evaluated through example integrated power and gas distribution networks, which both have decentralised generation and injection and are coupled to each other. The simulation model was validated through state estimation with perfect measurements and the Monte Carlo simulation of state estimation of the integrated networks.

Afterwards, the results of the integrated state estimation of the integrated networks were compared with the results of separated state estimation. Additionally, the impact of deployment of smart meters in one of the networks on the results of state estimation of the other coupled network was studied.

It was observed that deployment of smart meters in the power distribution network had no impact on improvement of the results of state estimation of the coupled gas distribution network. Also, deployment of smart meters in the gas distribution network had an insignificant impact on improvement of the estimation of the voltage magnitudes in the coupled power distribution network. However, no impact on improvement of estimation of voltage angles was observed.

8.2 Contributions of the thesis

- ***Optimal placement of additional measurements in power distribution networks***

    - An alternative formulation for calculating the probability of the estimated state parameters of a power distribution network falling within desired ranges was developed and validated.

    - The algorithm developed for the placement of additional individual measurements was extended for the placement of additional measurement units.

- ***Simulation of operation of gas distribution networks with decentralised injection***

    - The simulation model developed for simulation of operation of gas distribution networks having several decentralised injection was validated with the commercial software Synergi Gas.

- ***State estimation of gas distribution networks with decentralised injection***

    - The simulation model developed for state estimation of gas distribution networks having several decentralised injection was validated.

- ***Optimal placement of additional measurements in gas distribution networks with decentralised injection***

    - The impact of different measurements on the state estimation of gas distribution networks with decentralised injection was investigated.

    - A simulation model was developed for placement of additional measurements within a gas distribution network with decentralised injection for improvement of estimation of the molar fractions of the gas mixture within the network. A sensitivity analysis of the best measurement designs for different errors of pseudo measurements of loads and pseudo measurements of molar fractions was also carried out.

- ***State estimation of integrated power and gas distribution networks***

  - The simulation model developed for integrated state estimation of integrated power and gas distribution networks with decentralised generation and injection in both networks was validated.

  - Impact of deployment of smart meters in one of the networks on the state estimation results of the other coupled network was studied.

8.3 Future work

8.3.1 State estimation of gas distribution networks with decentralised injection

The following are proposed for further research for studying state estimation of gas distribution networks with decentralised injection:

- To develop more robust state estimation algorithms, which are capable of estimation of the state parameters of more meshed gas distribution networks having several decentralised injection;

- To consider other realistic distributions for measurements corresponding to realistic situations, rather than the normal distribution;

- To validate the simulation model developed for state estimation of gas distribution networks with decentralised injection using realistic networks.

8.3.2 Optimal placement of additional measurements in gas distribution networks with decentralised injection

The following are suggested for better investigation of the problem of measurement placement in gas distribution networks with decentralised injection:

- To improve the algorithm for placement of flow meters at nodes to consider all the possible placements;

- To consider more packages of measurements to be placed within the network;

- To reduce the computation effort for more complex networks and more input budget of the operator, by incorporating efficient algorithms such as ordinal optimisation;

- To apply the algorithm to realistic and more meshed networks with several decentralised injection given more realistic relative costs of the metering devices;

- To investigate the performance of the algorithm for improvement of the state estimation of the realistic networks.

8.3.3 State estimation of integrated power and gas distribution networks

The following are proposed to take the research further in the area of integrated state estimation of integrated power and gas distribution networks:

- To increase the number of coupling components connected between both networks;

- To study the algorithm on realistic networks;

- To assess the impact of the faults in one of the energy networks on the whole integrated energy networks;

- To develop an algorithm for fault diagnostic of the integrated energy networks to localise the fault to recommend networks reconfigurations;

- To consider district heating network as another energy vector through a combined heat and power unit;

- To develop an algorithm for state estimation of integrated energy networks at their dynamic conditions of operation.

References

Abdel-Majeed, A. et al. 2013. Meter placement for low voltage system state estimation with distributed generation. 22nd International Conference and Exhibition on Electricity Distribution (CIRED 2013). 10-13 June 2013.

Abdelsalam, H. A. et al. 2014. Impact of distribution system reconfiguration on optimal placement of phasor measurement units. Power Systems Conference (PSC), 2014 Clemson University. 11-14 March 2014.

Abeysekera, M. 2016. COMBINED ANALYSIS OF COUPLED ENERGY NETWORKS. PhD Thesis, Cardiff University.

Abeysekera, M. et al. 2014. Simulation and Analysis of Low Pressure Gas Networks with Decentralized Fuel Injection. Energy Procedia 61, pp. 402-406.

Abeysekera, M. et al. 2016a. Integrated energy systems: An overview of benefits, analysis methods, research gaps and opportunities. HubNET position paper series.

Abeysekera, M. et al. 2016b. Steady state analysis of gas networks with distributed injection of alternative gas. Applied Energy 164, pp. 991–1002.

Abur, A. and Exposito, A. G. 2004. Power System State Estimation: Theory and Implementation. Marcel Dekker Inc.

Ahmadian Behrooz, H. and Bozorgmehry Boozarjomehry, R. 2015a. Distributed and decentralized state estimation in gas networks as distributed parameter systems. ISA Transactions 58, pp. 552–566.

Ahmadian Behrooz, H. and Bozorgmehry Boozarjomehry, R. 2015b. Modeling and state estimation for gas transmission networks. Journal of Natural Gas Science and Engineering 22(0), pp. 551-570.

Automind. 2016. SPS - Stoner Pipeline Simulator [Online]. Available at: http://www.automind.com.br/english/produtos-detalhe.php?id=204 [Accessed: 2/2/2016].

Bai, X. et al. 2016. Defining and advancing a systems approach for sustainable cities. Current Opinion in Environmental Sustainability 23, pp. 69-78.

Baran, M. E. et al. 2009a. Including voltage measurements in branch current state estimation for distribution systems. IEEE Power & Energy Society General Meeting (PES 2009). 26-30 July 2009.

Baran, M. E. et al. 2009b. Topology error identification using branch current state estimation for distribution systems. Transmission & Distribution Conference & Exposition: Asia and Pacific, 2009. 26-30 Oct. 2009.

Baran, M. E. et al. 1995. A meter placement method for state estimation. IEEE Transactions on Power Systems, 10(3), pp. 1704-1710.

Baran, M. E. et al. 1996. Meter placement for real-time monitoring of distribution feeders. IEEE Transactions on Power Systems, 11(1), pp. 332-337.

Baran, M. E. and Kelley, A. W. 1994. State estimation for real-time monitoring of distribution systems. IEEE Transactions on Power Systems, 9(3), pp. 1601-1609.

Baran, M. E. and Kelley, A. W. 1995. A branch-current-based state estimation method for distribution systems. IEEE Transactions on Power Systems, 10(1), pp. 483-491.

Bignucolo, F. and Caldon, R. 2007. Optimizing the voltage measurements location for the management of active distribution networks. 42nd International Universities Power Engineering Conference (UPEC 2007). 4-6 Sept. 2007.

Bretas, N. G. and London Jr., J. B. A. 2001. Measurement placement design and reinforcement for state estimation purposes. IEEE Power Tech Conference. Porto, Portugal,, 10-13 September.

Brown, E. P. M. 1981. Power system state estimation and probabilistic load flow analysis. PhD thesis, University of Canterbury.

Celik, M. K. and Liu, W. H. E. 1995. An incremental measurement placement algorithm for state estimation. IEEE Transactions on Power Systems, 10(3), pp. 1698-1703.

Chaudry, M. et al. 2014. Combined gas and electricity network expansion planning. Applied Energy 113, pp. 1171–1187.

Chaudry, M. et al. 2013. A sequential Monte Carlo model of the combined GB gas and electricity network. Energy Policy 62, pp. 473–483.

Choudhary, P. et al. 1985. STATE ESTIMATION AS AN AID TO GAS DISTRIBUTION CONTROL. IFAC Proceedings Series.

Choudhary, P. A. 1987. State Estimation Applied to Gas Distribution Networks. PhD Thesis, University of Manchester.

Clements, K. A. et al. 1983. Power System State Estimation with Measurement Deficiency: an Observability/Measurement Placement Algorithm. IEEE Transactions on Power Apparatus and Systems, PAS-102(7), pp. 2012-2020.

Climate Change Guide. 2016. Trace gas definition [Online]. Available at: http://www.climate-change-guide.com/trace-gas-definition.html [Accessed: 20.8.2016].

Committee on Climate Change. 2008. UK regulations: the Climate Change Act [Online]. Available at: https://www.theccc.org.uk/tackling-climate-change/the-legal-landscape/the-climate-change-act/ [Accessed: 23.1.2018].

Control & Power Research Group, I. C. L. 2015. State Estimations In Power Distribution (SEPD) [Online]. Available at: http://www.ee.ic.ac.uk/bikash.c.pal/index_files/state_space.htm [Accessed: 19.12.2015].

Davenport, R. and Bramellar, A. 1972. Optimum pressure control in gas networks for the reduction of losses. 38th Autumn Research Meeting, London,: Institute of Gas Engineers.

DECC. 2012. Smart metering implementation programme: information leaflet [Online]. Available at: https://www.gov.uk/government/publications/smart-metering-implementation-programme-information-leaflet [Accessed: 23.1.2018].

Deng, Y. et al. 2002. A branch-estimation-based state estimation method for radial distribution systems. IEEE Transactions on Power Delivery 17(4), pp. 1057-1062.

DNV.GL. 2016a. Advanced hydraulic modelling - Synergi Gas [Online]. Available at: https://www.dnvgl.com/services/advanced-hydraulic-modelling-synergi-gas-3894 [Accessed: 2/2/2016].

DNV.GL. 2016b. Analyse pipeline design and performance - Synergi Pipeline

Simulator [Online]. Available at: https://www.dnvgl.com/services/analyse-pipeline-design-and-performance-synergi-pipeline-simulator-5376 [Accessed: 2/2/2016].

E.ON. 2016. GasCalc Software [Online]. Available at: https://www.eon.com/en/business-areas/technical-services/gascalc-software.html [Accessed: 2/2/2016].

Edward Lau, T. W. and Ho, Y. C. 1997. Universal alignment probabilities and subset selection for ordinal optimization. Journal of Optimization Theory and Applications 93(3), pp. 455-489.

Emara-Shabaik, H. E. et al. 2002. A non-linear multiple-model state estimation scheme for pipeline leak detection and isolation. Proceedings of the Institution of Mechanical Engineers, Part I: Journal of Systems and Control Engineering 216(6), pp. 497-512.

EnergySolutions. 2016. PipelineStudio [Online]. Available at: http://www.energy-solutions.com/products/pipelinestudio/ [Accessed: 2/2/2016].

Erdener, B. C. et al. 2014. An integrated simulation model for analysing electricity and gas systems. International Journal of Electrical Power & Energy Systems 61, pp. 410-420.

Eusgeld, I. et al. 2011. "System-of-systems" approach for interdependent critical infrastructures. Reliability Engineering & System Safety 96(6), pp. 679-686.

Fiksel, J. 2007. Sustainability and Resilience: Toward a Systems Approach. IEEE Engineering Management Review 35(3), pp. 5-5.

Fischer-Uhrig Engineering. 2016. The essential attributes of STANET® [Online]. Available at: http://www.stafu.de/en/product/2-hydraulic-calculation-methods [Accessed: 2/2/2016].

Gabbar, H. A. et al. 2014. System Approach for Building Energy Conservation. Energy Procedia 62, pp. 666-675.

Ghasemi Damavandi, M. et al. 2015. Robust Meter Placement for State Estimation in Active Distribution Systems. IEEE Transactions on Smart Grid, 6(4), pp. 1972-1982.

Ghosh, A. K. et al. 1997. Distribution circuit state estimation using a probabilistic approach. IEEE Transactions on Power Systems, 12(1), pp. 45-51.

Grisso, R. B. et al. 2014. ENERGY SERIES: What is the Whole-House Systems Approach to Energy Efficiency? Virginia Polytechnic Institute and State University: Virginia Cooperative Extension.

Hadian, S. and Madani, K. 2015. A system of systems approach to energy sustainability assessment: Are all renewables really green? Ecological Indicators 52, pp. 194-206.

Haibin, W. and Schulz, N. N. 2004. A revised branch current-based distribution system state estimation algorithm and meter placement impact. IEEE Transactions on Power Systems, 19(1), pp. 207-213.

Haijun, L. et al. 2002. A heuristic meter placement method for load estimation. IEEE Transactions on Power Systems, 17(3), pp. 913-917.

Hall, J. W. et al. 2016. The future of national infrastructure: A system-of-systems approach. Cambridge University Press.

Hayes, B. and Prodanovic, M. 2014. State Estimation Techniques for Electric Power Distribution Systems. Modelling Symposium (EMS), 2014 European. 21-23 Oct. 2014.

Ho, Y. C. et al. 2007. Ordinal optimization: soft optimization for hard problems. New York: Springer.

Houari, M. et al. 2013. Treatment of transformers and voltage regulators in branch current state estimation for distribution networks. IEEE Power and Energy Society General Meeting (PES 2013). 21-25 July 2013.

HSE. 1996. A guide to the Gas Safety (Management) Regulations 1996, Guidance on Regulations. In: HSE ed. UK.

ISO. 1996. ISO 6976: Natural gas - Calculation of calorific values, density, relative density and Wobbe index from composition.

Jamil, E. et al. 2014. Towards optimal placement of phasor measurement units for smart distribution systems. 6th IEEE Power India International Conference (PIICON 2014). 5-7 Dec. 2014.

Janssen, P. et al. 2013. Meter placement impact on distribution system state estimation.

22nd International Conference and Exhibition on Electricity Distribution (CIRED 2013). 10-13 June 213.

Jie, W. and Miu, K. N. 2004. Meter placement for load estimation in radial power distribution systems. Proceedings of the 2004 International Symposium on Circuits and Systems, (ISCAS 2004). 23-26 May 2004.

Junqi, L. et al. 2012. Trade-Offs in PMU Deployment for State Estimation in Active Distribution Grids. IEEE Transactions on Smart Grid, 3(2), pp. 915-924.

Junqi, L. et al. 2013. Optimal placement for robust distributed measurement systems in active distribution grids. IEEE International Instrumentation and Measurement Technology Conference (I2MTC 2013). 6-9 May 2013.

Junqi, L. et al. 2014. Optimal Meter Placement for Robust Measurement Systems in Active Distribution Grids. IEEE Transactions on Instrumentation and Measurement, 63(5), pp. 1096-1105.

Khulief, Y. A. and Emara-Shabaik, H. E. 2006. Laboratory investigation of a multiple-model state estimation for detection and isolation of leaks in pipelines. Proceedings of the Institution of Mechanical Engineers, Part I: Journal of Systems and Control Engineering 220(1), pp. 1-13.

Koglin, H. J. 1975. Optimal Measuring System for State Estimation. Proc. PSCC, Cambridge, UK, Paper No 2.3/12.

Lin, W. M. and Teng, J. H. 1996. Distribution fast decoupled state estimation by measurement pairing. IEE Proceedings: Generation, Transmission and Distribution 143(1), pp. 43-48.

Liu, X. 2013. Combined Analysis of Electricity and Heat Networks. PhD Thesis, Cardiff University.

Liwacom. 2016. Simone Software [Online]. Available at: https://www.liwacom.de/simone-software/ [Accessed: 2/2/2016].

Lu, C. N. et al. 1995. Distribution system state estimation. IEEE Transactions on Power Systems, 10(1), pp. 229-240.

Mittal, S. et al. 2015. A System-of-Systems Approach for Integrated Energy Systems

Modeling and Simulation. In: Society for Modeling & Simulation International Summer Simulation Multi-Conference. Chicago, Illinois. National Renewable Energy Laboratory (NREL).

Monticelli, A. 2000. Electric power system state estimation. Proceedings of the IEEE 88(2), pp. 262-282.

Monticelli, A. and Wu, F. F. 1985. Network Observability: Identification of Observable Islands and Measurement Placement. IEEE Transactions on Power Apparatus and Systems, PAS-104(5), pp. 1035-1041.

Murray, M. A. et al. 1993. Uncertainty and state estimation in gas transmission networks. Proceedings of the 12th International Conference on Offshore Mechanical and Arctic Engineering (OMAE 1993), 20-24 June 1993. Glasgow, Scotland, Engl. ASME.

Muscas, C. et al. 2006. Optimal Placement of Measurement Devices in Electric Distribution Systems. Proceedings of the IEEE Instrumentation and Measurement Technology Conference (IMTC 2006). 24-27 April 2006.

Muscas, C. et al. 2007. Considering the uncertainty on the network parameters in the optimal planning of measurement systems for Distribution State Estimation. IEEE Instrumentation and Measurement Technology Conference Proceedings, (IMTC 2007). 1-3 May 2007.

Musulin, E. et al. 2005. Instrumentation design based on optimal Kalman filtering. Journal of Process Control 15(6), pp. 629-638.

Nichols, N. K. and Stringer, S. M. 1994. The state estimation of flow demands in gas networks from sparse pressure telemetry. Transactions of the Institute of Measurement and Control 16(2), pp. 66-74.

Nusrat, N. et al. 2012a. Novel meter placement algorithm for enhanced accuracy of distribution system state estimation. IEEE Power and Energy Society General Meeting. 22-26 July 2012.

Nusrat, N. et al. 2012b. Stochastic meter placement algorithm for active distribution networks suitable for parallel processing. 47th International Universities Power Engineering Conference (UPEC 2012). 4-7 Sept. 2012.

Osiadacz, A. J. 1987. Simulation and Analysis of Gas Networks. London: E. & F.N.

Spon Ltd.

Pal, J. K. 1991. State estimation problems in power and gas network.

Park, Y. M. et al. 1988. Design of reliable measurement system for state estimation. IEEE Transactions on Power Systems, 3(3), pp. 830-836.

Parkinson, J. S. 1984. Mathematical modelling and the application of state estimation techniques to gas distribution networks. MSc thesis, University of Manchester.

Parkinson, J. S. and Wynne, R. J. 1986. Reduced-order modeling and state estimation applied to gas distribution systems. IEEE Transactions on Automatic Control 31(8), pp. 701-709.

Parkinson, J. S. and Wynne, R. J. 1992. Systems Modelling and Control Applied to a Low-Pressure Gas Distribution Network. Proceedings of the Institution of Mechanical Engineers, Part E: Journal of Process Mechanical Engineering, 206(1), pp. 35-44.

Pegoraro, P. A. et al. 2012. PMU and smart metering deployment for state estimation in active distribution grids. IEEE International Energy Conference and Exhibition (ENERGYCON 2012). 9-12 Sept. 2012.

Pegoraro, P. A. and Sulis, S. 2012. On the robustness in distribution system state estimation. IEEE International Instrumentation and Measurement Technology Conference (I2MTC 2012). 13-16 May 2012.

Pegoraro, P. A. and Sulis, S. 2013. Robustness-Oriented Meter Placement for Distribution System State Estimation in Presence of Network Parameter Uncertainty. IEEE Transactions on Instrumentation and Measurement, 62(5), pp. 954-962.

PSI. 2016. Grid Analysis [Online]. Available at: http://www.psioilandgas.com/en/gas-management/grid-analysis/#c27583 [Accessed: 2/2/2016].

Qadrdan, M. 2012. Modelling of an Integrated Gas and Electricity Network with Significant Wind Capacity. PhD Thesis, Cardiff University.

Qadrdan, M. et al. 2015. Role of power-to-gas in an integrated gas and electricity system in Great Britain. International Journal of Hydrogen Energy 40(17), pp. 5763-5775.

Qadrdan, M. et al. 2009. Vulnerability analysis of the integrated energy infrastructure. In: Proceedings of the IEEE 44th International Universities Power Engineering Conference (UPEC 2009). 1-4 Sept. 2009.

Ramesh, L. et al. 2012. Ring main distribution state estimation through optimal meter placement. IET Chennai 3rd International on Sustainable Energy and Intelligent Systems (SEISCON 2012) . 27-29 Dec. 2012.

Reddy, H. P. et al. 2006. Simulation and state estimation of transient flow in gas pipeline networks using a transfer function model. Industrial and Engineering Chemistry Research 45(11), pp. 3853-3863.

Reddy, H. P. et al. 2011a. Leak detection in gas pipeline networks using an efficient state estimator Part I Theory and simulations. Computers and Chemical Engineering 35, pp. 651-661.

Reddy, H. P. et al. 2011b. Leak detection in gas pipeline networks using an efficient state estimator Part II Experimental and field evaluation. Computers and Chemical Engineering 35, pp. 662-670.

Schley, P. and Fiebig, C. 2014. SMARTSim - Gas Quality Tracking in Distribution Grids. E.ON Technologies, Ruhr University Bochum,.

Schweppe, F. C. and Wildes, J. 1970. Power System Static-State Estimation, Part I: Exact Model. IEEE Transactions on Power Apparatus and Systems, PAS-89(1), pp. 120-125.

Schweppe, F. C. et al. 1970. Power System Static-State Estimation, Part II: Approximate Model. IEEE Transactions on Power Apparatus and Systems, PAS-89(1), pp. 125-130.

Shafiu, A. 2005. A Distribution Management System Controller for Active Voltage Control. PhD thesis, UNIVERSITY OF MANCHESTER.

Shafiu, A. et al. 2005. Measurement location for state estimation of distribution networks with generation. IEE Proceedings- Generation, Transmission and Distribution, 152(2), pp. 240-246.

Singh, R. et al. 2009a. Choice of estimator for distribution system state estimation. IET

Generation, Transmission & Distribution, 3(7), pp. 666-678.

Singh, R. et al. 2011. Meter Placement for Distribution System State Estimation: An Ordinal Optimization Approach. IEEE Transactions on Power Systems, 26(4), pp. 2328-2335.

Singh, R. et al. 2009b. Measurement Placement in Distribution System State Estimation. IEEE Transactions on Power Systems, 24(2), pp. 668-675.

UnionGas. 2016. Chemical composition of natural gas [Online]. Available at: https://www.uniongas.com/about-us/about-natural-gas/Chemical-Composition-of-Natural-Gas [Accessed: 20.08.2016].

Unsihuay, C. et al. 2007. Modeling the Integrated Natural Gas and Electricity Optimal Power Flow. IEEE Power Engineering Society General Meeting, (PES 2007). 24-28 June 2007.

Vagenes, K. 2011. Properties of Natural Gas. NTNU:

Wang, H. et al. 2014. A robust measurement placement method in distribution system state estimation. IEEE Asia-Pacific Power and Energy Engineering Conference (APPEEC). 7-10 Dec. 2014.

Weimann, A. et al. 1990. ON-LINE SIMULATION OF GAS NETWORKS WITH CHANGING GAS QUALITIES.Advanced Information Processing in Automatic Control (AIPAC '89). Oxford: Pergamon, pp. 471-475.

Wenwu, L. et al. 2013. Distribution network state estimation based on node voltage of variable weights. Modelling, Identification & Control (ICMIC), 2013 Proceedings of International Conference on. Aug. 31 2013-Sept. 2 2013.

Wu, F. F. 1990. Power system state estimation: a survey. International Journal of Electrical Power & Energy Systems 12(2), pp. 80-87.

Yu, X. et al. 2014. Optimization of State-Estimator-Based Operation Framework Including Measurement Placement for Medium Voltage Distribution Grid. IEEE Transactions on Smart Grid, 5(6), pp. 2929-2937.

Zimmerman, R. D. et al. 2011. MATPOWER: Steady-State Operations, Planning, and Analysis Tools for Power Systems Research and Education. IEEE Transactions on

Power Systems, 26(1), pp. 12-19.

Appendix I: The data of the UKGDS 95-bus test distribution network

The data was taken from (Control & Power Research Group 2015) and the network was considered at the peak load condition with 100 MVA base power.

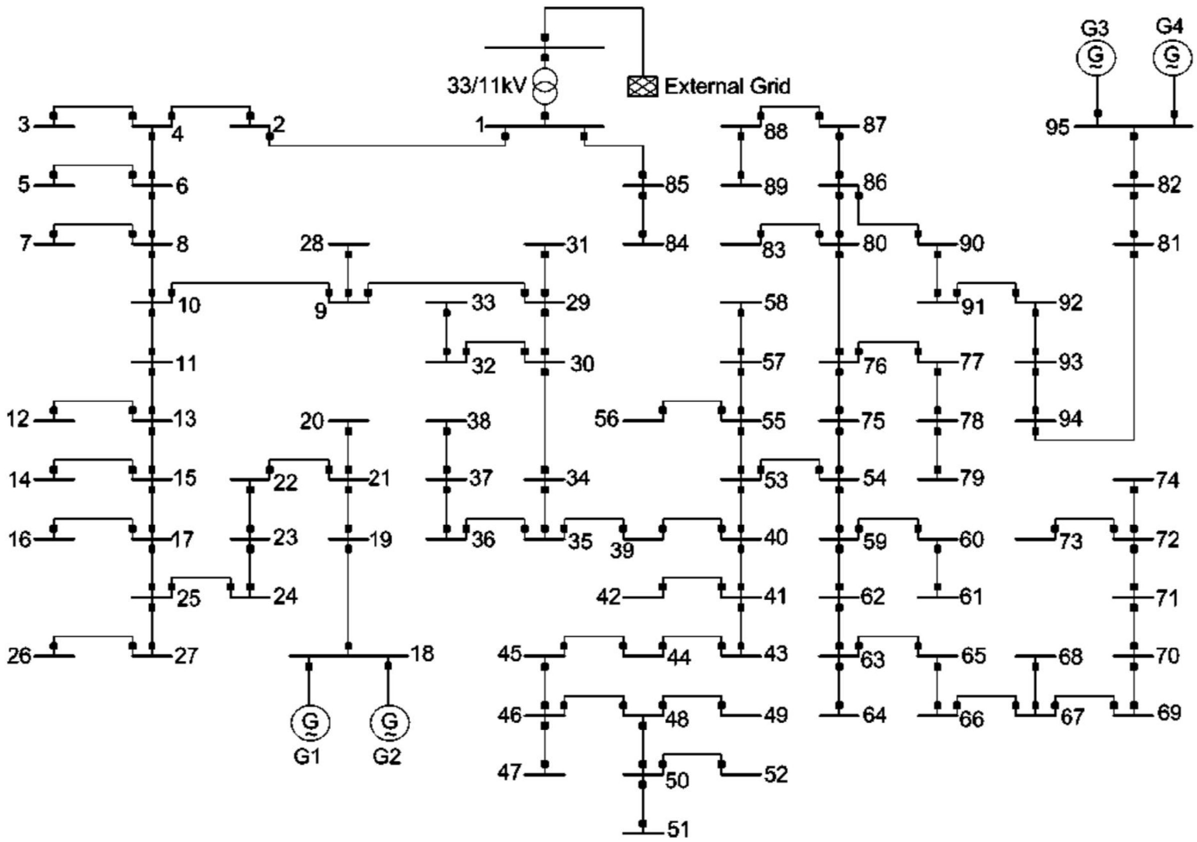

Figure AI.1: Schematic of the UKGDS 95-bus test distribution network[1]

Table AI.1: The data of the UKGDS 95-bus test distribution network

Bus data					Branch data			
Bus#	$P_d(MW)$	$Q_d(MVAr)$	$P_g(MW)$	$Q_g(MVAr)$	From	To	$R(p.u.)$	$X(p.u.)$
1	1.42985	0.38670	TBC	TBC	1	2	0.04879	0.05058
2	0.00000	0.00000	--	--	1	85	0.05489	0.05690
3	0.01486	0.00488	--	--	2	4	0.09755	0.33284
4	0.00000	0.00000	--	--	3	4	0.17322	0.07589
5	0.03433	0.00858	--	--	4	6	0.21000	0.20300
6	0.00000	0.00000	--	--	5	6	0.24251	0.10624
7	0.03410	0.00670	--	--	6	8	0.25860	0.17673
8	0.00000	0.00000	--	--	7	8	0.34645	0.15178

[1] The figure is taken from (Singh et al. 2011).

Bus data					Branch data			
Bus#	$P_d(MW)$	$Q_d(MVAr)$	$P_g(MW)$	$Q_g(MVAr)$	From	To	$R(p.u.)$	$X(p.u.)$
9	0.00000	0.00000	--	--	8	10	0.12930	0.08836
10	0.00000	0.00000	--	--	9	10	0.29500	0.15000
11	0.00495	0.00163	--	--	9	28	0.20787	0.09107
12	0.00495	0.00163	--	--	9	29	0.35400	0.18000
13	0.00000	0.00000	--	--	10	11	0.30169	0.20618
14	0.02446	0.00497	--	--	11	13	0.19395	0.13255
15	0.00000	0.00000	--	--	12	13	0.17322	0.07589
16	0.01339	0.00494	--	--	13	15	0.23705	0.16200
17	0.00000	0.00000	--	--	14	15	0.20787	0.09107
18	0.00000	0.00000	0.12000	-0.00200	15	17	0.25860	0.17673
19	0.13211	0.02683	--	--	16	17	0.13858	0.06071
20	0.01936	0.00276	--	--	17	25	0.12930	0.08836
21	0.00000	0.00000	--	--	18	19	0.12000	0.11600
22	0.02972	0.00977	--	--	19	21	0.36000	0.34800
23	0.02825	0.00983	--	--	20	21	0.13161	0.05033
24	0.06382	0.01647	--	--	21	22	0.09000	0.08700
25	0.00000	0.00000	--	--	22	23	0.30169	0.20618
26	0.06302	0.01928	--	--	23	24	0.19395	0.13255
27	0.00000	0.00000	--	--	24	25	0.21550	0.14727
28	0.02678	0.00989	--	--	25	27	0.17240	0.11782
29	0.00000	0.00000	--	--	26	27	0.10775	0.07364
30	0.00000	0.00000	--	--	29	30	0.27716	0.12142
31	0.02420	0.00345	--	--	29	31	0.24251	0.10624
32	0.05582	0.01403	--	--	30	32	0.25860	0.17673
33	0.02476	0.00814	--	--	30	34	0.11149	0.07376
34	0.02825	0.00983	--	--	32	33	0.31180	0.13660
35	0.00000	0.00000	--	--	34	35	0.34612	0.20653
36	0.06371	0.01553	--	--	35	36	0.15608	0.10326
37	0.02531	0.00995	--	--	35	39	0.34479	0.23564
38	0.00968	0.00138	--	--	36	37	0.22298	0.14752
39	0.01452	0.00207	--	--	37	38	0.21350	0.09126
40	0.00000	0.00000	--	--	39	40	0.12930	0.08836
41	0.00000	0.00000	--	--	40	41	0.11800	0.06000
42	0.03444	0.00952	--	--	40	53	0.17240	0.11782
43	0.05356	0.01978	--	--	41	42	0.20787	0.09107
44	0.00000	0.00000	--	--	41	43	0.23600	0.12000
45	0.00000	0.00000	--	--	43	44	0.17700	0.09000
46	0.00000	0.00000	--	--	44	45	0.09401	0.03595
47	0.01486	0.00488	--	--	45	46	0.17700	0.09000
48	0.00000	0.00000	--	--	46	47	0.23600	0.12000
49	0.01812	0.00470	--	--	46	48	0.35400	0.18000
50	0.00000	0.00000	--	--	48	49	0.35400	0.18000
51	0.03444	0.00952	--	--	48	50	0.27716	0.12142
52	0.05018	0.01614	--	--	50	51	0.21350	0.09126
53	0.00000	0.00000	--	--	50	52	0.53374	0.22816

Bus data					Branch data			
Bus#	$P_d(MW)$	$Q_d(MVAr)$	$P_g(MW)$	$Q_g(MVAr)$	From	To	$R(p.u.)$	$X(p.u.)$
54	0.02825	0.00983	--	--	53	54	0.30169	0.20618
55	0.00000	0.00000	--	--	53	55	0.20787	0.09107
56	0.00792	0.00260	--	--	54	59	0.36517	0.15244
57	0.00891	0.00293	--	--	54	75	0.25860	0.17673
58	0.00968	0.00138	--	--	55	56	0.27716	0.12142
59	0.00000	0.00000	--	--	55	57	0.41574	0.18213
60	0.01486	0.00488	--	--	57	58	0.27716	0.12142
61	0.01486	0.00488	--	--	59	60	0.17322	0.07589
62	0.02149	0.00545	--	--	59	62	0.14607	0.06098
63	0.00000	0.00000	--	--	60	61	0.31180	0.13660
64	0.02949	0.00789	--	--	62	63	0.25562	0.10671
65	0.02972	0.00977	--	--	63	64	0.20787	0.09107
66	0.03004	0.00970	--	--	63	65	0.18258	0.07622
67	0.00000	0.00000	--	--	65	66	0.29213	0.12195
68	0.03467	0.01140	--	--	66	67	0.25562	0.10671
69	0.01387	0.00456	--	--	67	68	0.09401	0.03595
70	0.00000	0.00000	--	--	67	69	0.43820	0.18293
71	0.00000	0.00000	--	--	69	70	0.21910	0.09146
72	0.00000	0.00000	--	--	70	71	0.07521	0.02876
73	0.01288	0.00423	--	--	71	72	0.14607	0.06098
74	0.05389	0.01971	--	--	72	73	0.29213	0.12195
75	0.00991	0.00326	--	--	72	74	0.40168	0.16768
76	0.00000	0.00000	--	--	75	76	0.12930	0.08836
77	0.00495	0.00163	--	--	76	77	0.18258	0.07622
78	0.01189	0.00391	--	--	76	80	0.21550	0.14727
79	0.05898	0.01578	--	--	77	78	0.29213	0.12195
80	0.00000	0.00000	--	--	78	79	0.43820	0.17673
81	0.00000	0.00000	--	--	80	83	0.12930	0.08836
82	0.05447	0.01502	--	--	80	86	0.19395	0.13255
83	0.00495	0.00163	--	--	81	82	0.27244	0.04012
84	0.92502	0.26839	--	--	81	94	0.15085	0.10309
85	0.00000	0.00000	--	--	95	82	0.49039	0.07222
86	0.00000	0.00000	--	--	84	85	0.03881	0.10400
87	0.10706	0.02822	--	--	86	87	0.27716	0.12142
88	0.00000	0.00000	--	--	86	90	0.25860	0.17673
89	0.10535	0.03030	--	--	87	88	0.48502	0.21249
90	0.05885	0.01385	--	--	88	89	0.22621	0.04686
91	0.00000	0.00000	--	--	90	91	0.06465	0.04418
92	0.14402	0.04881	--	--	91	92	0.27244	0.04012
93	0.00000	0.00000	--	--	92	93	0.16346	0.02407
94	0.06821	0.01341	--	--	93	94	0.08620	0.05891
95	0.00000	0.00000	0.12000	-0.04800				

Appendix II: The data of the gas distribution network with decentralised injection

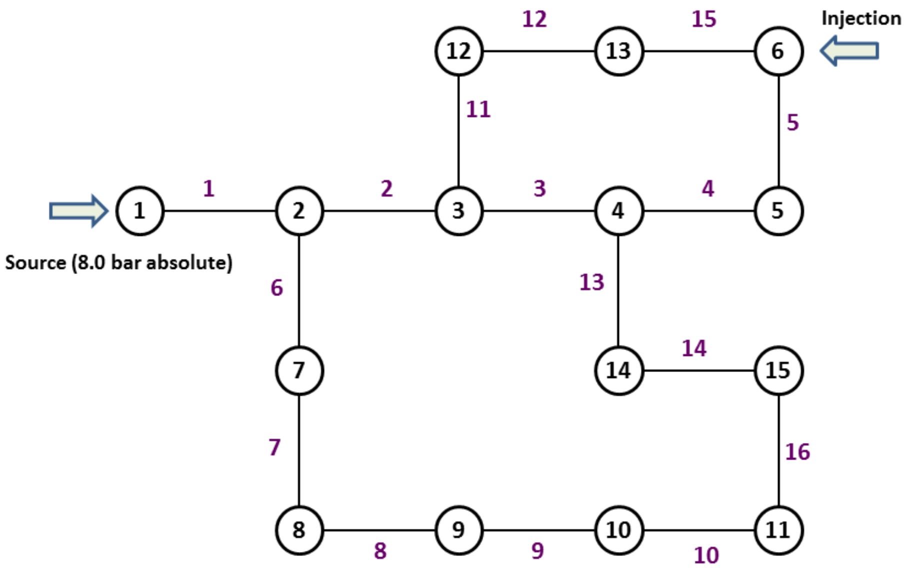

Figure AII.1: The schematic of the case study gas distribution network with decentralised injection

- ***Branch data:***

  It is assumed that all the pipes have an identical length of 20000 m, diameter of 300 mm and roughness of 0.01 mm.

Table AII.1: Node data of the test network

Node #	Load (MW)	Node #	Load (MW)	Node #	Load (MW)
1	0	6	0	11	30
2	0	7	10	12	30
3	0	8	10	13	30
4	0	9	30	14	30
5	10	10	30	15	30

Table AII.2: The composition of the injected gas at source and injection nodes

Node	Gas mix description	Molar fraction of components (%)						
		CH_4	C_2H_6	C_3H_8	C_4H_{10}	CO_2	N_2	H_2
Source (#1)	Natural gas	90.0	6.0	1.0	0.5	0.5	2.0	0.0
Injection (#6)	Upgraded biogas	94.0	0.0	0.0	0.0	2.5	2.5	1.0

Appendix III: The data of the integrated power and gas distribution network

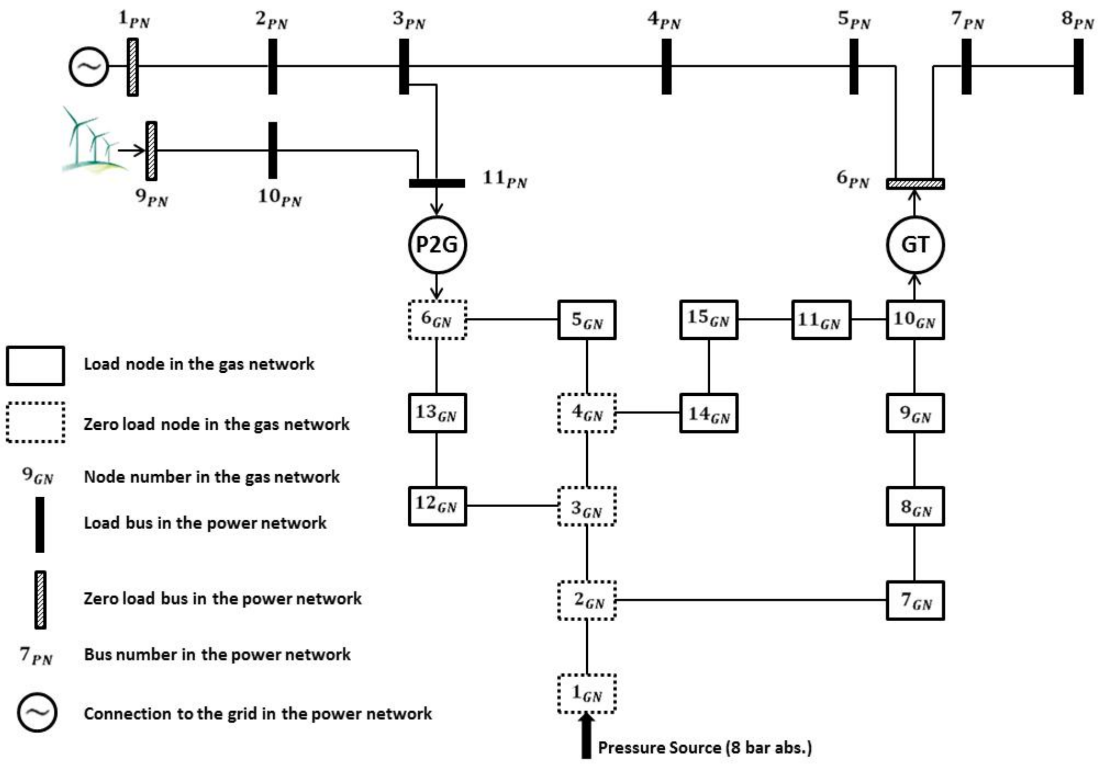

Figure AIII.1: The schematic of the integrated power and gas distribution test network

Table AIII.1: The data of the power distribution network

Bus data				Branch data			
Bus#	$P_d(MW)$	$Q_d(MVAr)$	$P_g(MW)$	From	To	$R(p.u.)$	$X(p.u.)$
1	--	--	TBC	1	2	0.04879	0.05058
2	1.5	0.2	--	2	3	0.05489	0.0569
3	1.5	0.2	--	3	4	0.09755	0.33284
4	1.5	0.2	--	4	5	0.17322	0.07589
5	1.5	0.2	--	6	5	0.21	0.203
6	--	--	6.0 (GT)	6	7	0.17322	0.07589
7	1.5	0.2	--	7	8	0.17322	0.07589
8	1.5	0.2	--	11	3	0.17322	0.07589
9	--	--	0.5	11	10	0.17322	0.07589
10	1.5	0.2	--	9	10	0.17322	0.07589
11	0	0	P2G demand				

Table AIII.2: The data of the gas distribution network

Node data		Branch data				
Node#	$d(MW)$	**From**	**To**	$L(m)$	$D(mm)$	$\epsilon(mm)$
1	--	1	2	20000	300	0.01
2	--	2	3	20000	300	0.01
3	--	3	4	20000	300	0.01
4	--	4	5	20000	300	0.01
5	10	5	6	20000	300	0.01
6	-- (P2G)	2	7	20000	300	0.01
7	10	7	8	20000	300	0.01
8	10	8	9	20000	300	0.01
9	20	9	10	20000	300	0.01
10	GT demand	10	11	20000	300	0.01
11	20	3	12	20000	300	0.01
12	20	12	13	20000	300	0.01
13	25	4	14	20000	300	0.01
14	20	14	15	20000	300	0.01
15	20	6	13	20000	300	0.01
		15	11	20000	300	0.01

Table AIII.3: The specifications of injections in the gas network

Node#	$p_{abs}(bar)$	$IP(MW)$	Molar fraction of components (%)						
			CH_4	C_2H_6	C_3H_8	C_4H_{10}	CO_2	N_2	H_2
1	8.0	TBC	90.0	6.0	1.0	0.5	0.5	2.0	0.0
6	TBC	20.0	94.0	0.0	0.0	0.0	2.5	2.5	1.0

Table AIII.4: The specifications of the coupling components

Coupling component	From	To	Efficiency (%)
Gas turbine	10 (GN)	6 (PN)	95.0
Power to gas	11 (PN)	6 (GN)	70.0